2017

RATIONAL DESIGN, SYNTHESIS, AND CHARACTERIZATION OF NOVEL mPGES-1 INHIBITORS AS NEXT GENERATION OF ANTI-INFLAMMATORY DRUGS

Ziyuan Zhou
University of Kentucky, ziyuan.zhou@uky.edu
Digital Object Identifier: https://doi.org/10.13023/ETD.2017.270

STUDENT AGREEMENT:

I represent that my thesis or dissertation and abstract are my original work. Proper attribution has been given to all outside sources. I understand that I am solely responsible for obtaining any needed copyright permissions. I have obtained needed written permission statement(s) from the owner(s) of each third-party copyrighted matter to be included in my work, allowing electronic distribution (if such use is not permitted by the fair use doctrine) which will be submitted to UKnowledge as Additional File.

I hereby grant to The University of Kentucky and its agents the irrevocable, non-exclusive, and royalty-free license to archive and make accessible my work in whole or in part in all forms of media, now or hereafter known. I agree that the document mentioned above may be made available immediately for worldwide access unless an embargo applies.

I retain all other ownership rights to the copyright of my work. I also retain the right to use in future works (such as articles or books) all or part of my work. I understand that I am free to register the copyright to my work.

REVIEW, APPROVAL AND ACCEPTANCE

The document mentioned above has been reviewed and accepted by the student's advisor, on behalf of the advisory committee, and by the Director of Graduate Studies (DGS), on behalf of the program; we verify that this is the final, approved version of the student's thesis including all changes required by the advisory committee. The undersigned agree to abide by the statements above.

Ziyuan Zhou, Student

Dr. Chang-Guo Zhan, Major Professor

Dr. David Feola, Director of Graduate Studies

RATIONAL DESIGN, SYNTHESIS, AND CHARACTERIZATION OF NOVEL mPGES-1 INHIBITORS AS NEXT GENERATION OF ANTI- INFLAMMATORY DRUGS

DISSERTATION

A dissertation submitted in partial fulfillment of the
requirements for the degree of Doctor of Philosophy in the
College of Pharmacy
at the University of Kentucky

By
Ziyuan Zhou
Lexington, KY
Director: Dr. Chang-Guo Zhan, Professor of Pharmaceutical Sciences
Lexington, KY

ABSTRACT OF DISSERTATION

RATIONAL DESIGN, SYNTHESIS, AND CHARACTERIZATION OF NOVEL mPGES-1 INHIBITORS AS NEXT GENERATION OF ANTI-INFLAMMATORY DRUGS

Aspirin and other nonsteroidal anti-inflammatory drugs (NSAIDs) are currently widely used as fever and pain relief in patients with arthritis and other inflammatory symptoms. NSAIDs effect by inhibiting cyclooxygenase-1 (COX-1) and/or cyclooxygenase-2 (COX-2). COX isozymes (COXs) are key enzymes in the biosynthesis of prostaglandin H_2 (PGH_2) from arachidonic acid (AA). It is now clear that prostaglandin E_2 (PGE_2), one of the downstream products of PGH_2, is the main mediator in both chronic and acute inflammation. Microsomal prostaglandin E synthase (mPGES-1) is the terminal enzyme of COX-2 in the PGE_2 biosynthesis pathway. Different from other two constitutively expressed PGE_2 synthase (PGES), mPGES-2 and cPGES, mPGES-1 is induced by pro-inflammatory stimuli and responsible for the production of PGE_2 related to inflammation, fever and pain. For these reasons, selective inhibition of mPGES-1 is expected to suppress inflammation induced PGE_2 production and, therefore, will exert anti-inflammatory activity while avoid the side effects of COXs inhibitors, such as gastrointestinal (GI) toxicity, and cardiovascular events.

A combination of computational and experimental approaches was used to discovery mPGES-1 inhibitors with new scaffolds. The methods used include molecular docking, molecular dynamic simulation, molecular mechanics-Poisson-

Boltzmann surface area (MM-PBSA) binding free energy calculation, and *in vitro* activity assays. Our large-scale structure-based virtual screening was performed on compounds in the NCI libraries, containing a total of ~260,000 compounds. 7 compounds have been determined for their IC_{50} values (about 300 nM to 8000 nM). What's more, these new inhibitors of mPGES-1 identified from virtual screening did not shown significant inhibition against COX isozymes even at substantially high concentrations (e.g. 100 μM).

Rational methodology for drug design and organic synthesis were applied to generate three series of mPGES-1 inhibitors with different scaffolds. In total, about 200 compounds were synthesized and tested for their *in vitro* inhibition against human mPGES-1. Compounds with high potency against human mPGES-1 were further screened for their inhibition against mouse mPGES-1 and selectivity of human mPGES-1 over COXs. Several compounds were identified as submicromolar inhibitors against human mPGES-1 with high selectivity over COXs.

In general, we have successfully identified a library of compounds as potent mPGES-1 inhibitors without significant inhibition against COXs. Structure information and *in vitro* activity evaluation data generated from the virtual screening and the library of compounds will be used to guide future design and synthesis of the mPGES-1 inhibitors.

KEWWORDS: NSAIDs; mPGES-1; anti-inflammatory drugs; PGE_2; PGH_2; COXs

Ziyuan Zhou
Student's Signature
07/22/2016
Date

RATIONAL DESIGN, SYNTHESIS, AND CHARACTERIZATION OF NOVEL mPGES-1 INHIBITORS AS NEXT GENERATION OF ANTI-INFLAMMATORY DRUGS

By

Ziyuan Zhou

Chang-Guo Zhan
Director of Dissertation

David Feola
Director of Graduate Studies

7/22/2017
Date

This dissertation is dedicated to my dear parents, whose love and support made this journey through graduate school possible.

Acknowledgments

This dissertation is based on one of the research projects throughout my graduate studies in Dr. Chang-Guo Zhan's laboratory at the College of Pharmacy, University of Kentucky. I am grateful to my advisor Professor Chang-Guo Zhan for the training opportunity in his laboratory, guiding me every step along this four years of long journey, and continually encouraging me to develop independent thinking ability, learn skills, and improve the scientific writing abilities. Through his absolute passion for science, hard work, Dr. Zhan motivates and inspires me to be a scientist in Pharmaceutical Sciences. I also would like to include a special note of appreciation to Dr. Fang Zheng who provided genuine help for me, guidance and advices at each stage of my research process and many others assistance. Thanks also to, Dr. Charles Loftin, Dr. Jan Fu, Dr. Kyung-Bo Kim and Dr. Hsin-Sheng Yang and for serving as my dissertation committee members or outside examiner, and their constructive comments, help and guidance all these years.

I am gratefully for the chance provided by the China Scholarship Counsel (CSC) for four years of support. I am also grateful for Professor Zhao-Hai Qin in China Agricultural University. He supported me during the CSC application process.

I gratefully acknowledge Dr. Hsin-Hsiung Tai with helpful discussions about the synthetic protocol of PGE_2-HRP conjugate.

I am grateful to all the past and present members of Dr. Zhan's lab for their generous assistance, scientific advice, friendship and company during my Ph.D. study, especially those who have worked together with me in this project. (Mr. Kai Ding, Mr. Shuo Zhou, Dr. Shurong Hou, Dr. Zhenyu Jin, Dr. Xiaoqin Huang, Mr. Max Zhan, Ms. Min Tong, Ms. Xirong Zheng, Ms. Ting Zhang, Dr. Jinling Zhang, Dr. Wenpeng Cui, Mr. Kyungbo Kim, Mr. Jing Deng, Dr. Yanyan Zhu) In particular, I thank Dr. Fang Zheng, Dr. Yaxia Yuan, Dr. Jianzhuang Yao, for molecular modeling and kinetic

modeling.

Finally, I am forever grateful to my parents, Hehai Zhou and Chunping Zang, for their unconditional love and support.

TABLE OF CONTENTS

List of Figures

List of Schemes

List of Tables

List of Abbreviations

AA	Arachidonic Acid
Ac	Acetyl
ACN	Acetonitrile
BEAR	Binding estimation after refinement
Bn	Benzyl
BSA	N, O-Bis (trimethylsilyl) acetamide
Bu or n-Bu	n-Butyl
CC	Column Chromatography
^{13}C NMR	Carbon-13 nuclear magnetic resonance
COX-1	Cyclooxygenase 1 or Prostaglandin G/H synthase 1
COX-2	Cyclooxygenase 2 or Prostaglandin G/H synthase 2
COXs	Cyclooxygenases
cPGES	cytosolic prostaglandin E synthase
DCM	Dichloromethane
DMF	Dimethylformamide
DMSO	Dimethyl sulfoxide
DNA	Deoxyribonucleic acid
E. coli	Escherichia coli
EC_{50}	Half maximal effective concentration
EDTA	Ethylenediaminetetraacetic acid
ELISA	Enzyme-linked immunosorbent assay
Et	Ethyl
EP_1 or PTGER1	Prostaglandin E_2 receptor 1
EP_2 or PTGER2	Prostaglandin E_2 receptor 2
EP_3 or PTGER3	Prostaglandin E_2 receptor 3
EP_4 or PTGER4	Prostaglandin E_2 receptor 4

EWG	Electron-withdrawing group
FLAP	5-LO-activating protein
GDP	guanosine diphosphate
GI	Gastrointestinal
GSSG	oxidized glutathione
GSH	reduced glutathione
GTP	guanosine monophosphate
HMBC	Heteronuclear multiple-bond correlation spectroscopy
^{1}H NMR	Proton nuclear magnetic resonance
HPLC	high performance liquid chromatography
HPMS	High performance mass spectrometry
hr	hour
HRMS	high-resolution mass spectrometry
HSQC	Heteronuclear single-quantum correlation spectroscopy
IC_{50}	half maximal inhibitory concentration
IUPAC	International Union of Pure and Applied Chemistry
k	kilo
kcat	turnover rate
kDa	kilo Dalton
KI/KO	knock-in/knock-out
Km	Michaelis-Menten constant
LB	Luria broth
LC-MS	Liquid chromatography–mass spectrometry
Lys	Lysine
MDR	Multiple drug resistant pathogens
Me	Methyl
MIC	Minimum inhibitory concentration
min	minute

mPGES-1	microsomal prostaglandin E synthase 1
mPGES-2	microsomal prostaglandin E synthase 2
NBS	B-Bromosuccinimide
NMR	Nuclear magnetic resonance spectroscopy
NOESY	nuclear overhauser effect spectroscopy
NSAIDs	Nonsteroidal anti-inflammatory drugs
MW	molecular weight
PABA	para-amino-benzoic acid
PCR	polymerase chain reaction
PEP	Phosphoenolpyruvic acid or phosphoenolpyruvate
Ph	Phenyl
PGD_2	Prostaglandin D_2
PGE_2	Prostaglandin E_2
$PGF_{2\alpha}$	Prostaglandin F2alpha
PGH_2	Prostaglandin H_2
PGG_2	Prostaglandin G_2
PGI_2	Prostaglandin I_2
PK/PD	Pharmacokinetic/Pharmacodynamic
Pr	Propyl
QSAR	Quantitative structure–activity relationship models
RNA	ribonucleic acid
rt	room temperature
SAR	Structure-activity relationship
SDS	Sodium dodecyl sulfate
SDS-PAGE	Sodium dodecyl sulfate polyacrylamide gel electrophoresis
sp.	Species
TB	Tuberculosis
TEA	Triethylamine

TFA	Trifluoroacetic acid
THF	Tetrahydrofuran
TXA_2	Thromboxane A_2
TXB_2	Thromboxane B_2
TOCSY	Total correlation spectroscopy
VRE	Vancomycin-resistant Enterococci
WT	Wild-type

Chapter 1: mPGES-1 inhibitors as next generation of anti-inflammatory drugs

1.1 PGE_2 as an inflammation mediator

Prostaglandin E_2 (PGE_2) is a crucial prostaglandin (PG) produced by most mammalian tissues and regulate in multiple biological activities under both normal physiological conditions and pathological processes.[1] The function of PGE_2 as a mediator for fever and pain in the inflammation has drawn most attentions.[2-6] The biosynthesis of PGE_2 is initiated from the release of arachidonic acid (AA) from the phospholipid membranes by phospholipase A_2 (PLA_2), followed by a serial of enzymatic transformations known as the biosynthetic pathway of PGE_2.[3] In the first step of this pathway, AA is transformed to PGH_2 by COX-1 or COX-2 *via* an unstable peroxide intermediate PGG_2. Next, PGH_2 is converted to PGE_2 by PGE synthase (PGES).[7] PGE_2 is a pro-inflammatory mediator, which can trigger fever and pain, the two main characteristics of inflammation.[8] The PGE_2 production can be induced by stimuli of pro-inflammation like TNF-α[9], interleukin-1β (1L-1β) and lipopolysaccharide (LPS).[10] Moreover, PGE_2 is also involved in multiple types of cancers. It has been found to regulate crucial steps in cancer development by decreasing the level of apoptosis, inducing metastasis, increasing angiogenesis in the tumor and stimulating tumor cells proliferation.[11] In spite of all these bad effects of PGE_2, the positive aspect of constructive PGE_2 cannot be ignored.[12] Reported studies in PGE_2-receptor-deficient mice have also revealed the role of PGE_2 in normal physiological functions, including suppressing of type I allergy, inducing bone formation, and protection against inflammatory bowel disease *etc*.[13]

1.2 Problems of current anti-inflammatory drugs

Since the synthesis of Aspirin by Bayer in 1897, non-selective cyclooxygenase (COX)-1 and COX-2 inhibitors are the mainstays to treat inflammatory symptoms.[14]

The physiological roles of COX-1 and COX-2 are different. As a constitutively expressed enzyme, COX-1 catalyzes the biosynthesis of cytoprotective PGs, whereas COX-2 is mainly responsible for the synthesis of PGs involved in the inflammation. Different from COX-1, COX-2 can be induced by inflammatory stimuli.[15] Aspirin, ibuprofen, indomethacin, and other traditional non-selective, non-steroidal anti-inflammatory drugs (NSAIDs) function by inhibiting both COX-1 and COX-2. The history of COX non-specific NSAIDs is associated with an increasing risk of gastrointestinal side effects. To cope with the limitations of traditional NSAIDs, the COX-2 selective inhibitors were developed as an attempt to eliminate the gastrointestinal toxicity as well as achieve the anti-inflammatory benefit of NSAIDs.[16] COX-2 specific inhibitors were introduced as medications for pain and fever since 1997. They were so successful that almost half of the prescriptions written for NSAIDs in the United States in 2004 were COX-2 specific inhibitors.[17] However, several COX-2 inhibitors were taken off the pharmaceutical market of U.S. and other countries in 2004 and 2005 due to multiple kinds of severe side effects.[18] These side effects include increased likelihood of cardiovascular diseases, ulcers, and bleeding within the gastrointestinal tract. The cause for these side effects is that the PGH_2 is also a precursor to a number of other prostaglandins, including PGI_2, PGJ_2 PGD_2, $PGF_{2\alpha}$ and TXA_2. Among these prostaglandins, TXA_2 and PGI_2 are pivotal in maintaining the normal functions of cardiovascular system. TXA_2 has a physiological function in vasoconstriction and pro-thrombosis. On the contrary, as the antagonist of TXA_2, PGI_2 has the effect of vasodilatation and antiplatelet. The balance between TXA_2 and PGI_2 is crucial to maintain the normal functions of cardiovascular system. COX-2 specific inhibitors like rofecoxib will disrupt this balance, consequentially resulted in disruption of the normal function of cardiovascular system.[19-22]

1.3 mPGES-1 as target for next generation of anti-inflammatory drugs

Protein mPGES-1 is a member of Membrane-Associated Proteins in Eicosanoid and Glutathione metabolism (MAPEG) superfamily. The MAPEG family includes six human proteins: microsomal glutathione transferase 1 (MGST1), MGST2, MGST3, MGST-like1 (MGST1-L1), 5-lipoxygenase-activating protein (FLAP) and leukotriene C_4 (LTC_4). All of the members from this family are small proteins with similar 3D structures and have molecular weights around 14-18 kDa.[23] mPGES-1, microsomal PGE synthase-2 (mPGES-2), and cytosolic PGE synthase (cPGES) are three enzymes in human that are involved in the biosynthesis of PGE_2.[23] Different from mPGES-1 which is induced by pro-inflammation, mPGES-2 and cPGES are constitutively expressed.[24] Distinct from mPGES-1, mPGES-2 does not need glutathione (GSH) as a cofactor.[24] mPGES-2 could couple with both COX enzymes, whereas cPGES only couples with COX-1. Taking together, mPGES-2 and cPGES provide the basal level of PGE_2 (also known as constitutive PGE_2) for physiological homeostasis. Constitutive PGE_2 is not induced by inflammatory stimulus. Protein mPGES-1 is a stimuli-dependent and pro-inflammatory enzyme. It preferentially consume PGH_2 from COX-2 as substrate to produce PGE_2 related to inflammation.[24] Moreover, the knockout studies in various animal models confirmed the involvement of mPGES-1 in diseases including pain hypersensitivity,[25] pyresis,[26] atherosclerosis,[27] arthritis,[28] cardiac ischemia,[29] Alzheimer's disease,[30] and induced hydronephrosis.[31] Increased mPGES-1 expression in human is also related to inflammatory pathologies, *e.g.* Alzheimer's disease,[32] cancer,[33] bowel inflammation,[34] atherosclerosis,[35] myositis,[36] and osteoarthritis.[37-39] Inhibition of the PGE_2 production could attenuate the inflammatory syndromes in many diseases.[40] Given the reports that mPGES-1 knockout mice have normal behavior and can reproduce normally, mPGES-1 specific inhibitors are expected to have negligible adverse side effects.[41] All of these studies indicated that mPGES1, as the terminal synthase of biosynthesis pathway of inflammatory related PGE_2, has

great potential to be a promising target for next generation of anti-inflammatory drugs.[42]

1.4 Reported mPGES-1 inhibitors and their problems

Scientific research regarding mPGES-1 inhibitors are booming in recent years because mPGES-1 inhibitors have the potential to become the next generation of anti-cancer and anti-inflammatory drugs.[43] The efforts of identifying mPGES-1 inhibitors started from structural modification of the mPGES-1 substrate (PGH_2).[43] However, the stable analogues of PGH_2 only showed minimal to moderate inhibition against human mPGES-1. LTC_4 is a weak inhibitor of mPGES-1,[44] but it can act as a strong, GSH-competitive inhibitor of MGST-1.[45] Some stable analogs of the substrate (PGH_2), such as **U-44069** and **U-46619**, show no inhibition at all, whereas another stable analog (**U-51605**) exhibits weak inhibition against human mPGES-1 with IC_{50} around 10 μM. Whereas arachidonic acid and its analogs are stronger inhibitors of mPGES-1, with IC_{50} as low as 300 nM.[44, 46] Several COX-2 inhibitors could act as weak inhibitors of mPGES-1 [43], celecoxib (IC_{50} = 22 ± 3 μM), valdecoxib (IC_{50} = 75 ± 19 μM) and lumiracoxib (IC_{50}=33±4μM), for instance. But not all the coxibs are active against mPGES-1. Etoricoxib and rofecoxib failed to inhibit mPGES-1 even at very high concentrations (up to 200μM).[47] **MK-886** is a potent 5-lipoxygenase-activating protein (FLAP) inhibitor and a moderate human mPGES-1 inhibitor synthesized by Merck.[48] Derived from **MK-886**, compound **1** depicted in Figure 1.1 is a specific inhibitor of human mPGES-1 with selectivity of at least 100-fold over recombinant human mPGES-2, TXA_2 synthase, and FLAP.[48] Andrea Wiegard *et al*. reported in 2012 that pyrazole alkalotic acid derivatives could act as inhibitors against human mPGES-1.[49] The structural optimization made around this scaffold did not lead to obvious improvement in the inhibitory activity.[49] Gianluigi Lauro *et al*. identified a group of mPGES-1 inhibitors (Compound **15**, **20** and **21** in Figure 1.1) with unprecedented chemical core by employing the fragment virtual screening.[50] However, with IC_{50} values all above 1 μM, none of these compounds was proved to be potent mPGES-1 inhibitors.[50]

In summary, although there have been an increasing number of papers reporting inhibitors against human mPGES-1, most of the reported mPGES-1 inhibitors have not shown *in vivo* activities. In particular, none of human mPGES-1 inhibitors has an equally potent inhibitory activity against mouse mPGES-1, which has impeded the usage of wild-type mouse model in preclinical studies. Hence, no mPGES-1 inhibitor has been proven clinically useful.

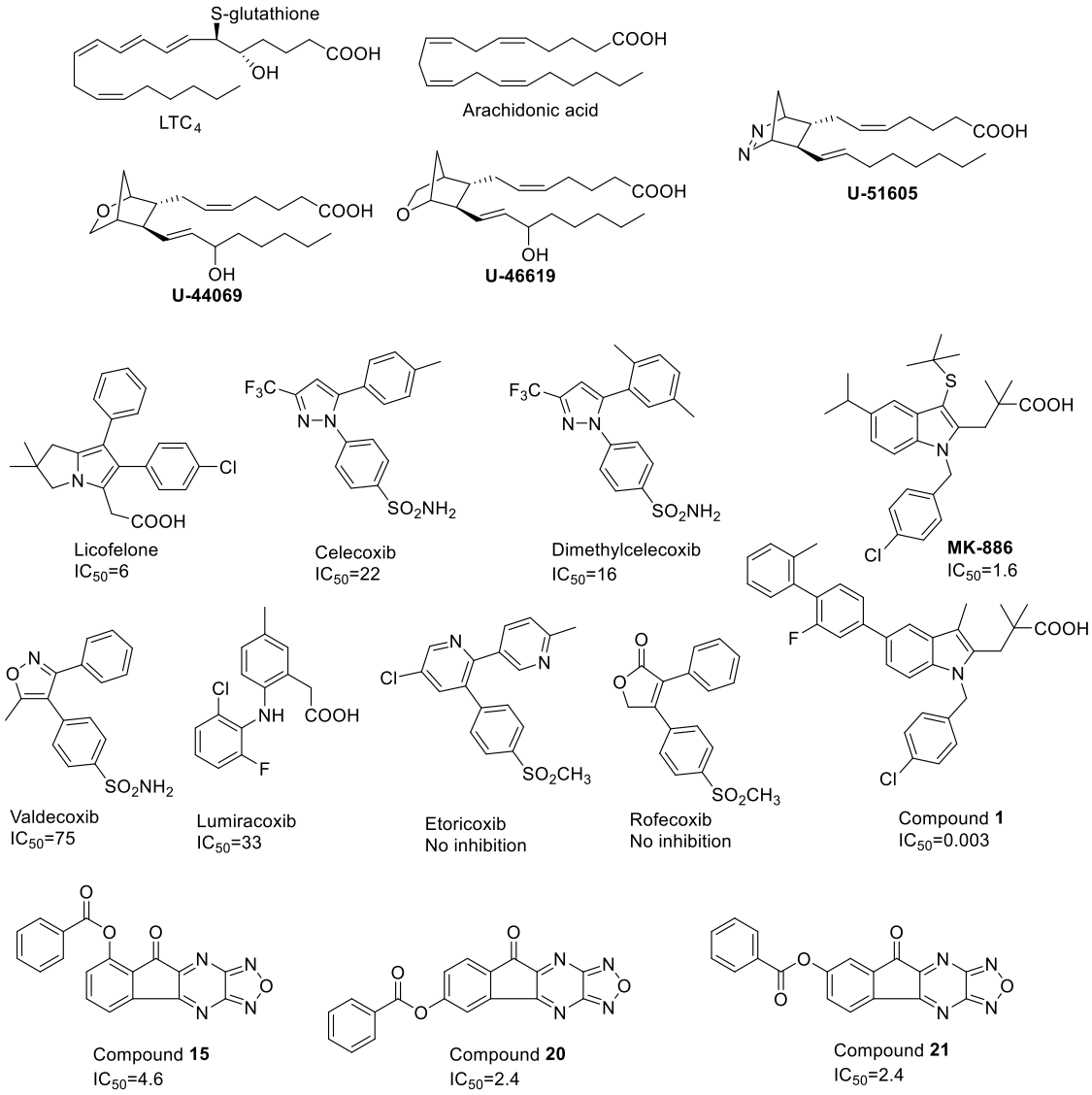

Figure 1.1 Some reported mPGES-1 inhibitors (IC_{50} / μM)

1.5 Reported animal experiments of mPGES-1 inhibitors and their problems

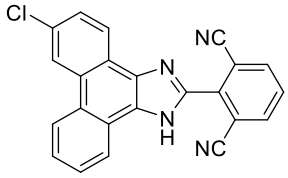

Figure 1.2 Structure of **MF63**

MF63, *2-(6-Chloro-1H-phenanthro [9, 10-d]imidazol-2-yl)-isophthalonitrile*, is a potent human mPGES-1 inhibitor identified by Merck Frosst Canada in 2008,[51] with IC_{50} = 1.3 nM against human mPGES-1. However, **MF63** did not significantly inhibit mouse or rat mPGES-1, which makes the animal study of **MF63** in wide-type mice or rats impossible. To solve this problem, Xu *et al.* performed an animal experiment using KI (knock-in) mouse.[51] They found that **MF63** can effectively reduce the PGE_2 levels in brains and air pouches of the knock-out/knock-in mice.[51] Although the technologies of knock-out/knock-in mouse provide us with valuable scientific research tools and win the Nobel Prize in physiology or medication in 2007, these technologies have their own limitations.[52] In particular, the loss/change of gene activities might result in alternation in the phenotype of the mouse[52] and the emerging of the flanking allele problems.[53] A human mPGES-1 inhibitor that can also inhibit mouse mPGES-1 will help to avoid the problems of the knock-out/knock-in mouse model in the preclinical studies.

Based on the discussion above, most currently available NSAIDs have severe side effects because they block the synthesis of all the PGH_2 downstream prostaglandins. As a downstream enzyme of prostaglandins metabolism, mPGES-1 is a promising target for the next generation of anti-inflammatory drugs. But the development of anti-inflammatory drugs targeting mPGES-1 is seriously hindered by the lack of mPGES-1 specific inhibitors that can potently inhibit both human and mouse mPGES-1 enzymes. Therefore, the identification of dual inhibitors against both human and mouse mPGES-1 with novel scaffolds is significant. Our ultimate aim is to develop mPGES-1 specific inhibitors as next generation of anti-inflammatory agents. To achieve this aim, we need

to identify human and mouse mPGES-1 dual inhibitors to make the preclinical studies more feasible.

In conclusion. The absence of feasible animal models could preclude the preclinical studies. New inhibitors that can potently inhibit both human and mouse mPGES-1 enzymes will make preclinical studies more feasible and avoid the problems occurred in the knock-in/knock-out mouse models. However, so far, no potent dual inhibitor against both human and mouse mPGES-1 enzymes has been reported. Although several compounds were reported to inhibit both human and mouse mPGES-1 enzymes, their dual inhibition was insignificant.[5, 54, 55] For these reasons, the design and synthesis of dual inhibitors against mouse and human mPGES-1 enzymes are significant. In this study, we are using a combined approach of the structure-based virtual screening, *de novo* drug design, and *in vitro* activity assays to identify dual inhibitors of human and mouse mPGES-1 enzymes with novel scaffolds.

1.6 Aims of this study

Aim 1: To identify/predict new inhibitors of human mPGES-1 by performing virtual screening

The NCI, ENZO and SPECS compound libraries were filtered by using a multistep virtual screening protocol. A recently available, more computationally expensive but more accurate method was used to estimate the binding free energy for each compound binding with human mPGES-1, and the compounds are ranked according the estimated binding free energies. The top-ranked compounds were ordered for *in vitro* activity assays in Aim 3.

Aim 2: To design and synthesize novel inhibitors of human mPGES-1 by carrying out *de novo* design and organic synthesis

In order to generate potent dual inhibitors against both human and mouse mPGES-1 enzymes, the known potent mPGES-1 inhibitors were selected as hints or leads for

further structural optimization through *de novo* design. Our *de novo* drug design was based on the 3D structures of both human and mouse mPGES-1 enzymes, particularly the common amino-acid residues.

Aim 3: To examine the compounds obtained in Aims 1 and 2 for their *in vitro* inhibitory activities against human and mouse mPGES-1 enzymes by using competitive ELISA assays

The enzyme activity assays were performed to determine the inhibitory activities of the compounds against both human and mouse mPGES-1 enzymes.

A combination of computational and experimental approaches were used to achieve our aims. The methods to be used include large-scale structure-based virtual screening, molecular dynamic simulation, molecular mechanics Poisson-Boltzmann surface area (MM-PBSA) binding free energy calculation, molecular docking, organic synthesis, and *in vitro* activity assays.

1.7 Experimental sections related to the aims

Experimental section for Aim 1: To identify/predict new inhibitors of human mPGES-1 by performing virtual screening

Our lab started to study the detailed 3D structure and mechanism of mPGES-1 and identify its inhibitors long before any of the X-ray crystal structures of human mPGES-1 was reported.[1, 40, 56-58] The very first crystal structure of mPGES-1 (PDB code 3DWW), which was determined by electron crystallography, was published by Caroline Jegerschold *et al* in 2008.[59] It was a low-resolution structure (3.5 Å resolution) representing an inactive, closed protein conformation in which the binding site is not accessible to substrate PGH_2. Recent years were marked by a burst of crystal structures of mPGES-1-GSH-inhibitor complexes. In 2013, two high-resolution structures were published: 4AL0 with no inhibitor, 4AL1 binding with 48T (a GSH-analog acting as a GSH-competitive inhibitor).[60] One year later, Li *et al*. published a 2.08 Å resolution

crystal structure (4BPM) with LVJ acting as a GSH non-competitive inhibitor. Also in 2014, another crystal structure of mPGES-1 also with LVJ as the ligand (4WAB) was released by Weinert *et al*, but their study focused on the method of crystallization of membrane proteins rather than the structure of mPGES-1.[61] Early in 2015, the crystal structures of mPGES-1 with four different ligands were published by Luz *et al*: 4DZ (4YL0), 4U8 (4YL1), 4U9 (4YL3) and 4DV (4YK5).[62] The recent development in understanding of the 3D structure will make our structure-based virtual screening possible and more reliable.

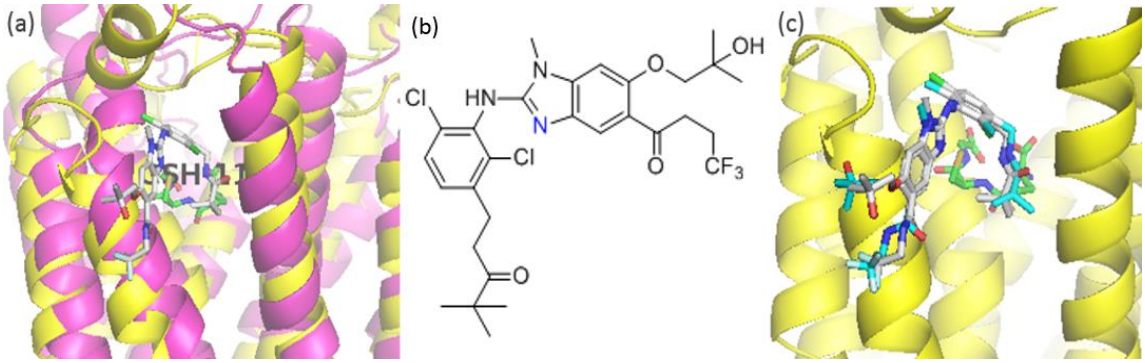

Figure 1.3 Cristal structure of human mPGES-1 (a) The binding pocket of mPGES-1 with GSH and LVJ (yellow for 4BPM; pink for 3DWW represent closed state), (b) Structure of LVJ by Chemdraw. (c) Restore docking by autodock. (GSH is in Green, crystal structure of LVJ in white. docking result in cyan)

The X-ray crystal structure of mPGES-1 with a GSH non-competitive inhibitor, 4BPM, was used for virtual screening in this study. In 4BPM, LVJ binds to the catalytic pocket by "hydrophobic effect" and hydrogen bonding between the hydroxyl group of Ser127 and the nitrogen of benzimidazole. The N (blue in Figure 1.3b) of LVJ acts as a hydrogen bond acceptor. The tertiary butyl of LVJ is inserted into a hydrophobic chamber of the binding pocket.[63] Although the AutoDock Vina program[64] was able to give a prediction of the binding conformation of the LVJ (Figure 1.3c), we failed to rank the LVJ amongst the best inhibitors of human mPGES-1 in a validation study,

indicating that the score function of the AutoDock Vina is not very accurate. Taking the limitation of capacity of wet experiment into consideration, it is only practical to take a very small fraction of the best-ranking compounds for the assays. Therefore, rather than ranking all the compounds based on the binding score generated by the AutoDock like He Shan *et al*. did [65], we used a more sophisticated and accurate approach to estimate the binding energies. Our virtual screening approach will be similar to that published previously.[1, 66] Our virtual screening first focused on compounds available in the NCI, SPECS and ENZO libraries. All of the compounds will be docked into the binding pocket one by one using the AutoDock Vina,[64] followed by energy-minimizations, molecular dynamics (MD) simulation, and MM-PBSA binding free energy calculations using the Amber 12 program suite.[67, 68]

In Chapter 2, compounds with novel scaffolds were identified to have inhibitory activities against human mPGES-1 enzyme. Some of these inhibitors could be used as lead compounds for further development of potent mPGES-1 inhibitors with novel scaffolds.

Experimental section for Aim 2: To design and synthesize novel inhibitors of human mPGES-1 by carrying out *de novo* design and organic synthesis

No X-ray crystal structure of mouse mPGES-1 is available so far. Depicted in Figure 1.4 is a homologous model of mouse mPGES-1 generated by using human mPGES-1 structure (4BPM) as a template. The reliability of the mouse mPGES-1 structure is guaranteed by the high sequence similarity (0.82)[62] between mouse and human mPGES-1 and the high GMQE (Global Model Quality Estimation) score (0.87).[69, 70] The difference in key residues, such as #52 (which is R in human and K in mouse), #53 (which is H in human and K in mouse) and #124 (which is P in human and R in mouse), may explain why some potent human mPGES-1 inhibitors like **MF63** and LVJ have very little or no inhibition towards mouse mPGES-1.

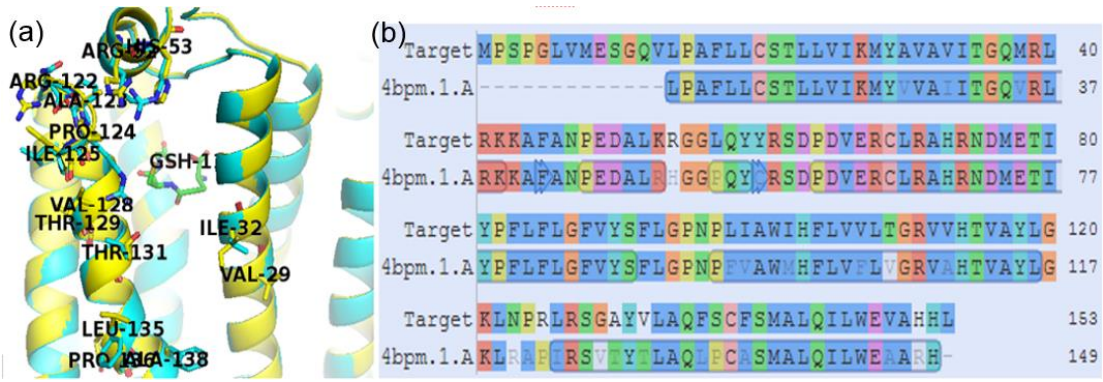

Figure 1.4 The similarity of human and mouse mPGES-1. (Mouse mPGES-1 structure was created by homologous modeling on *swissmodel.expasy.org*) (a) 3D structures of mouse mPGES-1 (cyan) and human mPGES-1 (yellow), (b) The sequence comparison: Mouse mPGES-1 as Target; Human mPGES-1 as 4bpm.1.A

Figure 1.5 Proposed Binding mode of compounds with human mPGES-1 (4BPM). (left) mPGES-1 & **v04**, (right) mPGES-1 & **py31**.

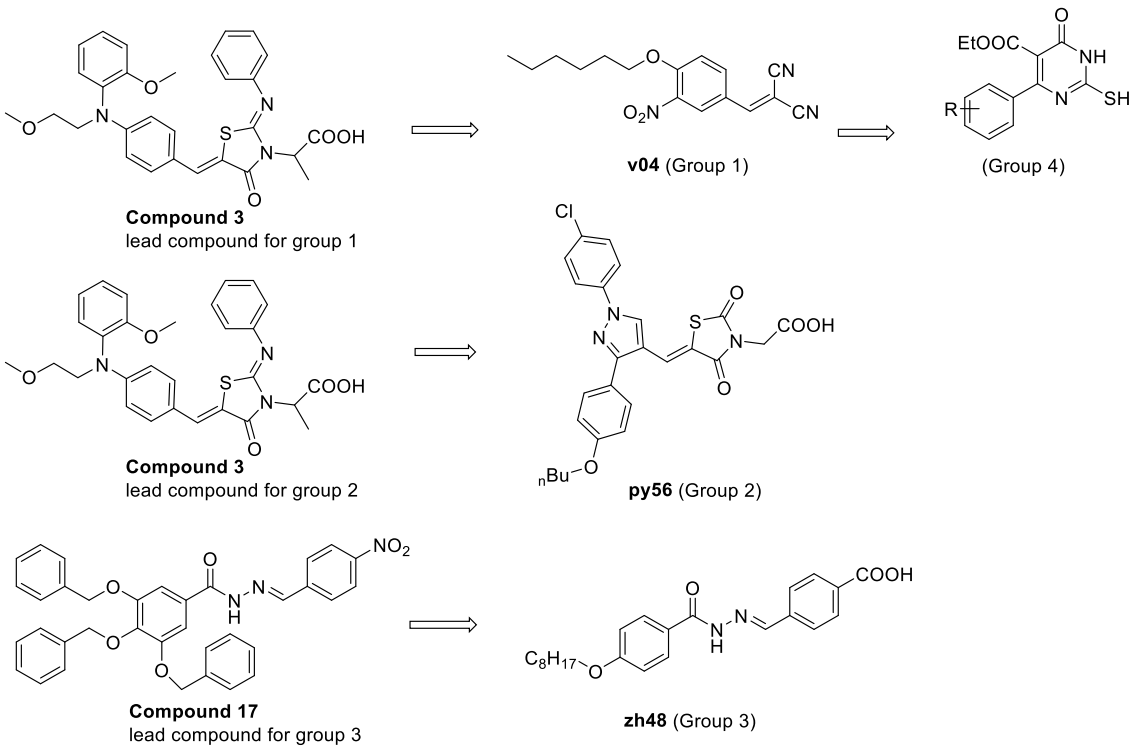

Scheme 1.1 The structural modification of representative compounds from three serials: from **compound 3**[1] to **v04** (Group 1 in Chapter 3), from **compound 3**[1] to **py56** (Group 2 in Chapter 4), from **compound 17**[65] to **zh48** (Group 3 in Chapter 5).

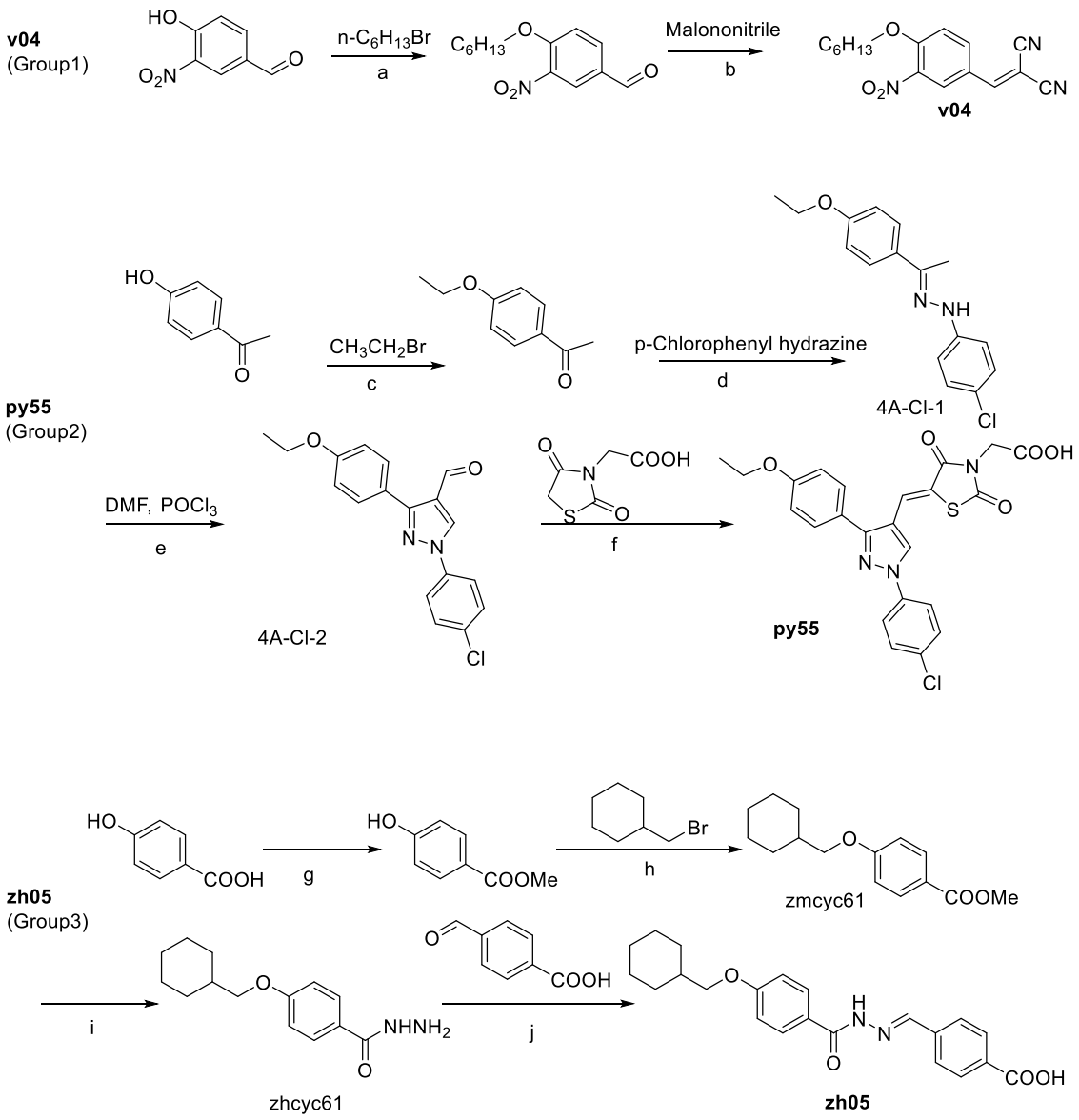

Scheme 1.2 Synthesis route for representative compounds

Reagents and conditions: (a) DMF, K_2CO_3, reflux; (b) EtOH, reflux, catalytic amount of acetic acid; (c) DMF, K_2CO_3, reflux; (d) EtOH, reflux, catalytic amount concentrate chloride acid; (e) DMF/$POCl_3$, 0℃-100℃, basified with K_2CO_3 solution; (f) EtOH or EtOH/water, reflux. (g) MeOH, reflux, catalytic amount of acetic acid; (h) DMF, K_2CO_3, reflux; (i) EtOH, reflux; (j) EtOH, acetic acid, reflux.

Group 1 (Chapter 3) was derived from **compound 3**[1], an mPGES-1 inhibitor discovered by previous lab members. **compound 3**[1] has IC_{50} values of 3.5 μM against human mPGES-1. More importantly, it is an mPGES-1 specific inhibitor, which shows

no inhibition against COX-2. Figure 4, 5 and 6 in the corresponding reference indicate the proposed binding mode: as a hydrophilic group of **compound 3**[1], the hydrophilic carboxylic acid functional group could insert into the polar cavity of the active site formed by Ser127, Thr131, Arg126 and Tyr130. The hydrophobic end could insert into the nonpolar cavity formed by Val124, Ile32 and Ala138. The "bridge" between the polar "head" and nonpolar "tail", phenyl ring, might interact by π-π stacking with the aromatic ring of Tyr130. Based on this binding model, in a preliminary study, we designed the scaffold of compounds Group 1 (Chapter3). The scaffold of these compounds is composited of a hydrophobic and hydrophilic end. The hexane ring on the hydrophobic end might have no specific effect except for "hydrophobic interaction". Therefore, we replaced it with inexpensive straight-chain paraffin. The active methylene compounds were used to substitute the 2, 4-thiazolidinedione functional group as the hydrophilic group.

Group 2 (Chapter 4) was derived from the same lead compound, **compound 3** published by our lab in 2011.[1] Vilsmeier-Haach reaction was applied to synthesis of the hydrophobic end of compounds in another serial (Group 2).[71] The reactant for the Vilsmeier-Haach reaction, *4-chloro-[2-[1-[4-(butoxy)phenyl]ethylidene]hydrazinyl*, (4A-Cl-1 in scheme 1) is unstable in solid state, its powder will deteriorate within one day in air, so it has to be dried and dissolved in DMF upon preparation. The DMF solution of 4A-Cl-1 was previously cooled with ice bath. $POCl_3$ was added dropwise to the reaction mixture which will be warmed to room temperature and then heated at 100 degree Celsius for about 3-4 hours. After cooling the reaction mixture to 0 degree Celsius, saturated K_2CO_3 solution was added slowly to the mixture with vigorous stirring. After the solution turned from acidic to basic, the precipitate was filtered and washed with water several times. The pure final product was obtained by recrystallization of the precipitate with ethanol.

Group 3 (Chapter 5) compounds were derived from the **compound 17**, which was published by Shan H, *et al.* in 2013.[65]

Group 4 was derived from Group 1 with Biginelli reaction.[72] Specifically, these compounds containing a dihydropyrimidine as a hydrophilic group were derived from the scaffold skeleton of the Group 1. However, due to low potency against human mPGES-1, we gave up the scaffold of Group 4.

So far, about 200 compounds have been synthesized (58 compounds in Chapter3, 56 compounds in Chapter4 and 91 compounds in Chapter 5). Their structures have been confirmed by ^{1}H-NMR and ^{13}C-NMR (Appendix I, table I-1, I-2 and I-3), then by HPMS (Appendix II, table II-1, II-2 and II-3). SAR was discussed based on the in vitro activity data. Possible binding modes were predicted based on the SAR and structures of the compounds. Various new compounds could be design and synthesized based on these results.[73-75]

Experimental section for Aim 3: To examine the compounds obtained in aims 1 and 2 for their in vitro inhibitory activities against human and mouse mPGES-1 enzymes by using competitive ELISA assays

The inhibitory activities of the compounds from virtual screening and organic synthesis were analyzed by *in vitro* cell-free activity assays using mPGES-1 enzymes expressed in Human Embryonic Kidney 293 (HEK293) cells.[1] Crude microsomal human or mouse enzyme and compounds were added to 1.5 ml microfuge tubes. Tubes containing only mPGES-1 were used as blank control, and tubes contain only buffer were used as negative control. The volume of reaction mixture before reaction was 96 µl, containing 100 mM potassium phosphate with pH 7.2, 5µl of 50 mM GSH, 1 µl of 100 µg/ml enzyme preparation (except for negative controls), and compound in 1 µl DMSO. To ensure that the results were comparable, we also added 1 µl DMSO without compounds to the tubes of blank controls, negative controls, and positive controls. The lipophilic compound might form colloid-like aggregates, and in turn appear to 'inhibit' human or mouse mPGES-1 without specific interaction with the enzymes. Adding detergent triton-X100 (0.1%) in the reaction buffer helps to rule out the nuisance inhibition, which is relevant for highly lipophilic compounds.[49] The substrate PGH_2

was purchased from Cayman Chemical Inc. It is stable in -80 ℃ in acetone solution for six month. The substrate was diluted with DMF into a 50 μg/ml (0.14 mM) solution before use. During the reactions, the solution of substrate was put on dry ice all the time to avoid non-enzyme degradation of the substrate. The reaction mixtures containing enzyme and compounds were incubated at room temperature for 20 minutes. Then the substrate PGH_2 (in DMF/Acetone solution, 4 μl) was added to initiate the reaction. After 60 seconds, 10 μl of $SnCl_2$ (40 mg/ml in EtOH) was added to terminate the reaction by reducing the remaining substrate PGH_2 into $PGF_{2\alpha}$. The cross reactivity of $PGF_{2\alpha}$ and PGD_2 (Product of the non-enzymatic conversion of PGH_2) with the PGE_2 antibody is less than 0.01% (manual of Prostaglandin E_2 ELISA Kit, Cayman Chemical). Therefore, the PGD_2 and $PGF_{2\alpha}$ will have little interference on the subsequent PGE_2 ELISA. The reaction mixture was put on ice, diluted by enzyme immunoassay (EIA) buffer for the determination of product concentrations. In order to eliminate the interference of the non-enzymatic conversion of PGH_2 to PGE_2, the negative control tests were performed every time under the same conditions. Tubes for the positive controls had the same enzyme concentration, but a sufficiently long reaction time (longer than 20 minutes) was used to completely convert the substrate to PGE_2. Tubes containing the same concentration of enzyme but without the inhibitor was used as the blank controls, which will also be performed every time. Mean of the PGE_2 concentrations in the blank controls was used as the standard (100%), whereas mean of the PGE_2 concentrations in negative controls will serve as 0%. The inhibition rate of the compound was calculated as a ratio, equal to the 100% minus the percentage of the remaining activity of enzyme.

A competitive Enzyme-linked Immunosorbent Assay (ELISA) was used to determine the PGE_2 level quantitatively. PGE_2-HRP (PGE_2-horseradish peroxidase conjugate) and product PGE_2 competed for a limited amount of PGE_2 antibody. One day before the ELISA, the 96-well high-binding EIA microplate was coated with protein A (Thermo Fisher Scientific, Lot number 1469040A) in order to attach PGE_2-antibody (Sigma: P5164 or a gift from Dr. Hsin-Hsiung Tai) to the microplate. As far

as we know, no commercial PGE_2-HRP conjugate is available. To solve this problem, the PGE_2-HRP conjugate synthesized by Dr. Hsin-Hsiung Tai years ago, which was used in our initial preliminary studies in this project.[76, 77] We synthesized the PGE_2-HRP conjugate according to the procedure depicted in Scheme 3.1 (with HRP from Sigma) for further studies in this project. As shown in Scheme 1.3, to activate the carboxylic group of PGE_2, the DMF solution of PGE_2 was incubated at room temperature with *1-Ethyl-3-(3-dimethylaminopropyl) carbodiimide hydrochloride* (EDC) to activate the carboxyl group of PGE_2 by converting PGE_2 to PGE_2-O-acylisourea ester, which is very reactive and unstable. The PGE_2 O-acylisourea ester then react with *N-hydroxysuccinimide* (NHS) to form the semi-stable PGE_2-NHS ester. After 2 hours, the solution of horseradish peroxidase (HRP) in a buffer with 100mM $NaHCO_3$ was added. The condensation reaction occulted between PGE_2-NHS and the naked amino groups on HRP. The mixture was incubated at 4 ℃ in the dark overnight. G-25 column equilibrated with PBS buffer was used to purify the crude mixture. The whole purification process will be performed in the 4 ℃ cold room. Phenol solution was added to the PBS buffer as antioxidant and sanitizer. The product was tested for activity before lyophilization. The lyophilized PGE_2-HRP conjugate should be a water soluble, yellow to pink powder. The powder was stored in -20 ℃ before use. According to our experiences, this conjugate could be kept active for many years under -20 ℃.

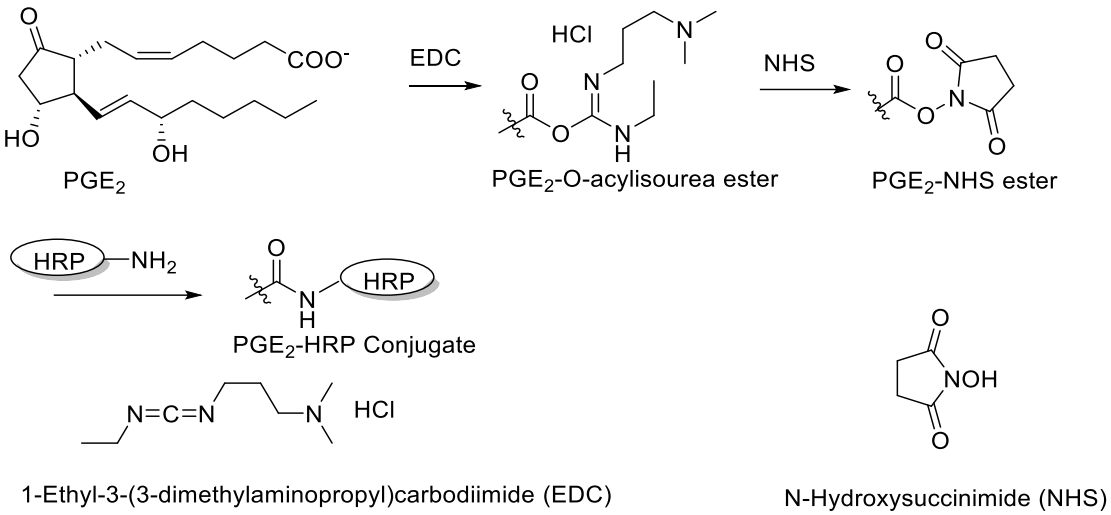

Scheme 1.3 Synthesis of PGE_2-HRP conjugate

In this dissertation, some of the compounds obtained from Aims 1 and 2 have been analyzed first at single concentrations of 10 μM and 1 μM against human mPGES-1. Then, the promising inhibitors have been assayed further for their IC_{50} values against human and mouse mPGES-1 enzymes. Tested IC_{50} curves were depicted in Figure 3.1, Figure 3.2, Figure 4.1, Figure 4.2 and Figure 5.1. Inhibition rates and IC_{50} data were summarized in Table 3.1, Table 4.1 and Table 5.1. The *in vitro* data showed that some of the compounds could potently inhibit human mPGES-1. In addition, some of them also showed potent inhibitory activity against mouse mPGES-1. These results demonstrated that our strategy for designing dual inhibitors against both human and mouse mPGES-1 enzyme is feasible.

Chapter 2: Selective Inhibitors of Human mPGES-1 from Structure-Based Computational Screening

Summary: Human mPGES-1 is recognized as a promising target for next generation of anti-inflammatory drugs. Although various mPGES-1 inhibitors have been reported in literatures, few have entered clinical trials and none has been proven clinically useful so far. There are clearly unmet demands for novel inhibitors of mPGES-1 with new scaffolds as the next generation anti-inflammatory therapeutics. Here, we report the identification of a series of new, potent and selective inhibitors of human mPGES-1 with diverse scaffolds through combined computational and experimental studies. The computationally modeled binding structures of these new inhibitors with mPGES-1 provide some interesting clues for the rational design of modified structures of the inhibitors to more favorably bind with mPGES-1. The main data discussed in this Chapter have been published.[78]

2.1 Introduction

Prostaglandin E_2 (PGE_2) is known as the principal pro-inflammatory prostanoid and plays an important role in nociception.[79] The biosynthesis of PGE_2 starts from arachidonic acid (AA) which is converted by cyclooxygenase COX-1 or COX-2 to prostaglandin H_2 (PGH_2).[80] PGH_2 is then converted to PGE_2 by the prostaglandin E synthase (PGES) enzymes,[81] including microsomal PGES-1 (mPGES-1), an inducible enzyme.[82] It is known that mPGES-1 and COX-2 together[83, 84] play a key role in a number of inflammation-related diseases.[85-91] Hence, human mPGES-1 is recognized as a promising target for next generation of drugs to treat the inflammation-related diseases.[92]

There are a number of non-steroidal anti-inflammatory drugs (NSAIDs) available for current clinical practice. The available NSAIDs inhibit COX-1 and/or COX-2.[93] All of the available COX-1/2 inhibitors have significant adverse side effects.[94] The serious

side effects led to withdrawal of rofecoxib (Vioxx), a selective COX-2 inhibitor. Therefore, people are interested in developing novel, improved anti-inflammatory drugs.[93] Through the action of the COX inhibitors, all prostaglandins downstream of PGH_2 cannot be produced, resulting in a variety of problems. For example, blocking the production of prostaglandin-I_2 (PGI_2) will cause significant cardiovascular problems.[95] Inducible enzyme mPGES-1 is a more promising target for anti-inflammatory drugs, because the mPGES-1 inhibition will only block the PGE_2 production without affecting the production of PGI_2 and other prostaglandins, as confirmed by the gene knock-out studies.[96, 97] Thus, mPGES-1 inhibitors are expected to retain the anti-inflammatory effect of COX inhibitors, but without the side effects caused by the COX inhibition.

Although various mPGES-1 inhibitors have been reported,[98-118] few have entered clinical trials[119] and none has been proven clinically useful so far due to various problems of the compounds. The development of new inhibitors of mPGES-1 with different scaffolds as the next generation therapeutics for inflammation-related diseases is in high demand. Here, we report the identification of a set of new, potent and selective inhibitors of human mPGES-1 with various scaffolds through combined computational and experimental studies.

2.2 Results and Discussion

Our virtual screening was based on the X-ray crystal structure (PDB ID: 4BPM)[120] of human mPGES-1 and performed on the Development Therapeutics Program (DTP) Release 4 compound library including ~265,000 compounds available at the National Cancer Institute (https://cactus.nci.nih.gov/download/nci/). The virtual screening procedure used to screen the compounds in the library is similar to that we previously used to identify small-molecule inhibitors of various protein targets.[121, 122] First, the ~265,000 compounds were screened by performing receptor-rigid docking using AutoDock Vina,[123] leading to identification of top-100,000 compounds. Then, each of

the top-100,000 compounds was further optimized using a four-step procedure (including 2,000 steps of energy-minimization, 20 ps of molecular dynamic simulation, 4,000 steps of energy-minimization, and then Molecular Mechanics/Poisson-Boltzmann Surface Area (MM/PBSA) binding energy calculation using AMBER 12 software package)[124, 125] similar to the known binding estimation after refinement (BEAR) protocol.[126, 127] The top-40 compounds were selected according to the ascending order of the MM/PBSA binding energies.

The computationally selected 40 compounds were tested for their inhibitory activity against human mPGES-1. Our protocol for the protein preparation and *in vitro* activity assays were the same as what we described previously.[128-130] All of the 40 compounds were assayed first for their inhibitory activity at a concentration of 10 μM. Then, the most active compounds were tested further for the dose-dependent inhibition in order to determine their IC_{50} values (Table 2.1) against mPGES-1. Finally, the most promising compounds were also assayed for their inhibitory activities against COX-1/2 (mixed COX-1 and COX-2) in order to know their selectivity for mPGES-1 over COX-1/2. The COX-1/2 assays were performed by using the COX (ovine/human) Inhibitor Screening Assay Kit (Item No. 560131) ordered from Cayman Chemical Company (Ann Arbor, MI). According to the kit, the COX activity assay utilizes the competition between prostaglandins (PGs) and a PG tracer, *i.e.* a PG-acetylcholinesterase (PG-AChE) conjugate, for a fixed amount of PG antiserum.[131, 132] Following the assay using the kit, we used a mixture of COX-1 and COX-2 (denoted as COX-1/2) with equal amount of each enzyme. The efficacies of tested compounds were determined as % inhibition against the COX enzymes at the concentration of 100 μM. All of the enzyme activity assays were carried out in triplicate.

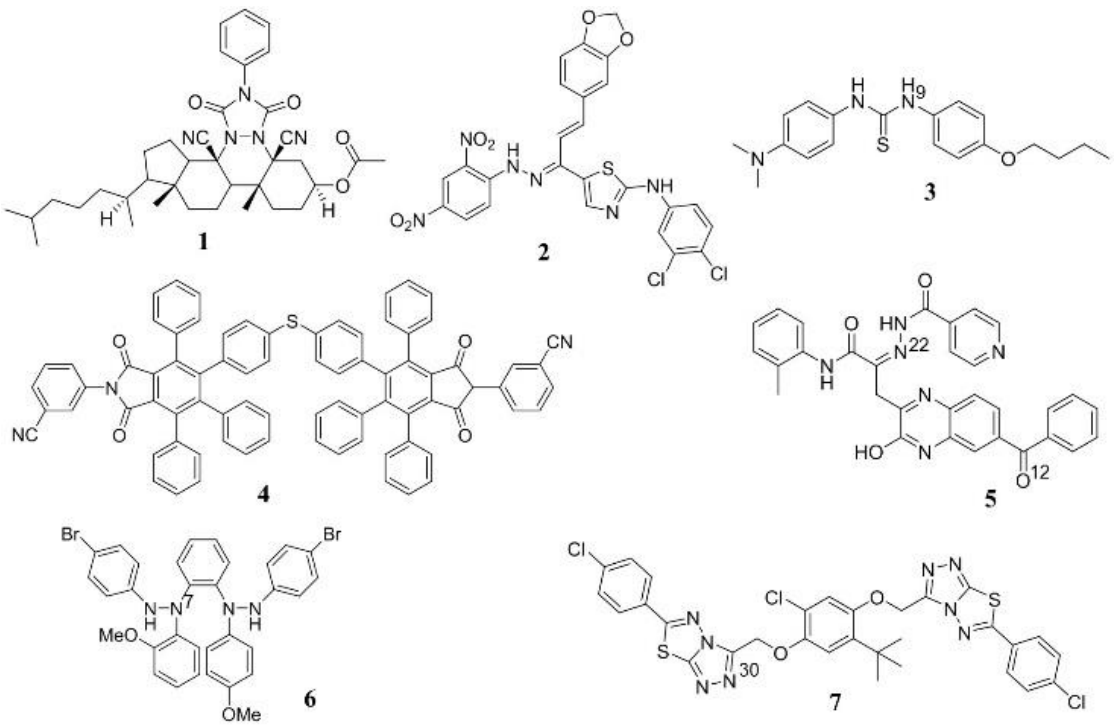

Figure 2.1 Molecular structures of the top-7 inhibitors of human mPGES-1 identified. (Some atoms with the numbering as superscripts are mentioned in the text for convenience of the discussion)

According to the activity assays, all of the computationally selected 40 compounds showed significant inhibitory activity against human mPGES-1, with 10% to 100% inhibition at a concentration of 10 μM (see Table 2.1). Molecular structures of the most active compounds (top-7) are depicted in Figure 2.1, and those of the remaining compounds are provided in Experimental Section.

Table 2.1 ***In vitro*** **inhibitory activities of the newly identified mPGES-1 inhibitors**

Compound	%Inhibition of mPGES-1 at 10 μM[a]	IC_{50} (nM) for mPGES-1[b]	%Inhibition of COX-1/2 at 100 μM[c]
1	99	276 ± 60	14 ±13
2	98	284 ± 81	8 ± 20
3	99	370 ± 79	1 ± 3

4	100	439 ± 84	9 ± 22
5	94	664 ± 106	0 ± 3
6	100	889 ± 186	37 ± 4
7	75	917 ± 99	15 ± 2
8	71	N.D.	N.D.
9	70	N.D.	N.D.
10	70	N.D.	N.D.
11	69	N.D.	N.D.
12	65	N.D.	N.D.
13	65	N.D.	N.D.
14	64	N.D.	N.D.
15	59	N.D.	N.D.
16	59	N.D.	N.D.
17	59	N.D.	N.D.
18	57	N.D.	N.D.
19	53	N.D.	N.D.
20	50	N.D.	N.D.
21	49	N.D.	N.D.
22	49	N.D.	N.D.
23	48	N.D.	N.D.
24	47	N.D.	N.D.
25	46	N.D.	N.D.
26	46	N.D.	N.D.
27	46	N.D.	N.D.
28	44	N.D.	N.D.
29	43	N.D.	N.D.
30	40	N.D.	N.D.
31	37	N.D.	N.D.

32	36	N.D.	N.D.
33	32	N.D.	N.D.
34	30	N.D.	N.D.
35	29	N.D.	N.D.
36	28	N.D.	N.D.
37	26	N.D.	N.D.
38	25	N.D.	N.D.
39	15	N.D.	N.D.
40	10	N.D.	N.D.

[a]The % inhibition of the compounds at a concentration of 10 μM against human mPGSE-1.
[b]The determined IC_{50} against human mPGES-1 based on the data depicted in Figure 2.2
[c]The % inhibition of the compound at a concentration of 100 μM against the COX-1/2 (mixed COX-1 and COX-2). The enzyme mixture contained equal amounts of COX-1 and COX-2 in terms of their enzyme activities. In this way, when a compound can significantly inhibit either COX-1 or COX-2, it will show the significant inhibitory effects against the mixed COX-1 and COX-2.

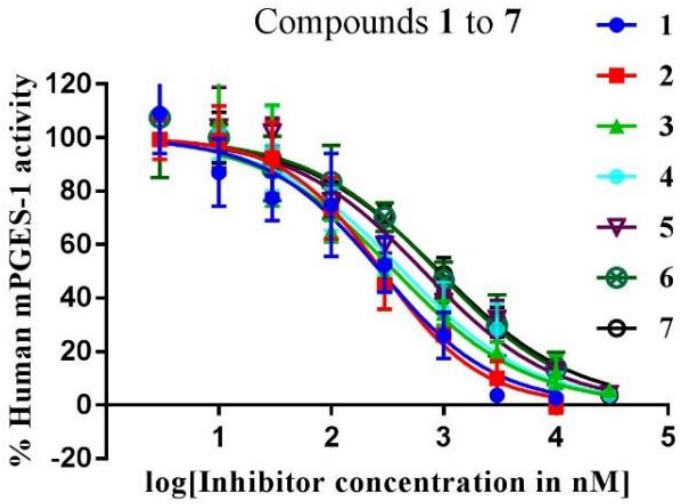

Figure 2.2 Dose-dependent inhibition of human mPGES-1 by compounds **1** to **7**: plots of the remaining enzyme activity *vs* the inhibitor concentration

Based on the activity data summarized in Table 2.1, compounds **1** to **7** at a

concentration of 10 μM inhibited the mPGES-1 activity by at least 75%. All of these compounds showed nanomolar IC_{50} values, 276 to 917 nM. Depicted in Figure 2.2 are their dose-response curves. The data in Table 2.1 also revealed that all of the top-7 compounds are highly selective for mPGES-1 over COX-1/2, as these compounds at a very high concentration (100 μM) showed no significant inhibition against COX-1 or COX-2, except for compound **6**. Even for compound **6**, the inhibition at 100 μM was only ~37%, suggesting that IC_{50} > 100 μM for compound **6** against COX-1/2.

Depicted in Figure 2.3 are the energy-minimized structures of human mPGES-1 binding with the top-7 compounds. In general, each of these compounds binds with the enzyme at the substrate-binding site and fit the binding site well. Figure 2.3(A) depicts the overall complex of the enzyme with **1**, and Figure 2.3(B) shows the structural detail of the binding site, showing that the main scaffold of **1** binds very well with the hydrophobic groove of the substrate-binding site of mPGES-1. The extended hydrocarbon side chain has hydrophobic interaction with the protein environment.

As shown in Figure 2.3(C), 2,4-dinitrobenzyl group of compound **2** stays in the bottom of the substrate-binding pocket of mPGES-1. The thiazole and dichlorobenzyl groups have the hydrophobic interaction with the protein. Compound **3** fits very well into the substrate-binding site of mPGES-1, as seen in Figure 2.3(D) showing a hydrogen bond (HB) between the NH group (including N9) and the hydroxyl oxygen on the side chain of residue T131. Compound **4** is huge in size, but it fits well in the substrate-binding site as seen in Figure 2.3(E). It is interesting to know that the binding site of the enzyme can accommodate a ligand as large as compound **4**.

As shown in Figure 2.3(F), there are two HBs between the protein and compound **5**. One HB is between N22 of **5** and the hydroxyl group of S127 side chain, and the other forms between and O12 of **5** and the hydroxyl group of T131 side chain. In addition, the benzyl rings of **5** have the hydrophobic interaction with the protein.

Figure 2.3(G) shows that, unlike the other compounds discussed above, compound **6** binds with the protein on the upper part of the substrate-binding groove of mPGES-

1, with a HB between N7 of **6** and the hydroxyl group of S127 side chain. As seen in Figure 2.3(H), compound **7** occupies the substrate-binding pocket with both of the phenyltriazolothiadiazole rings. N30 of compound **7** forms a HB with the hydroxyl group of Y130 side chain.

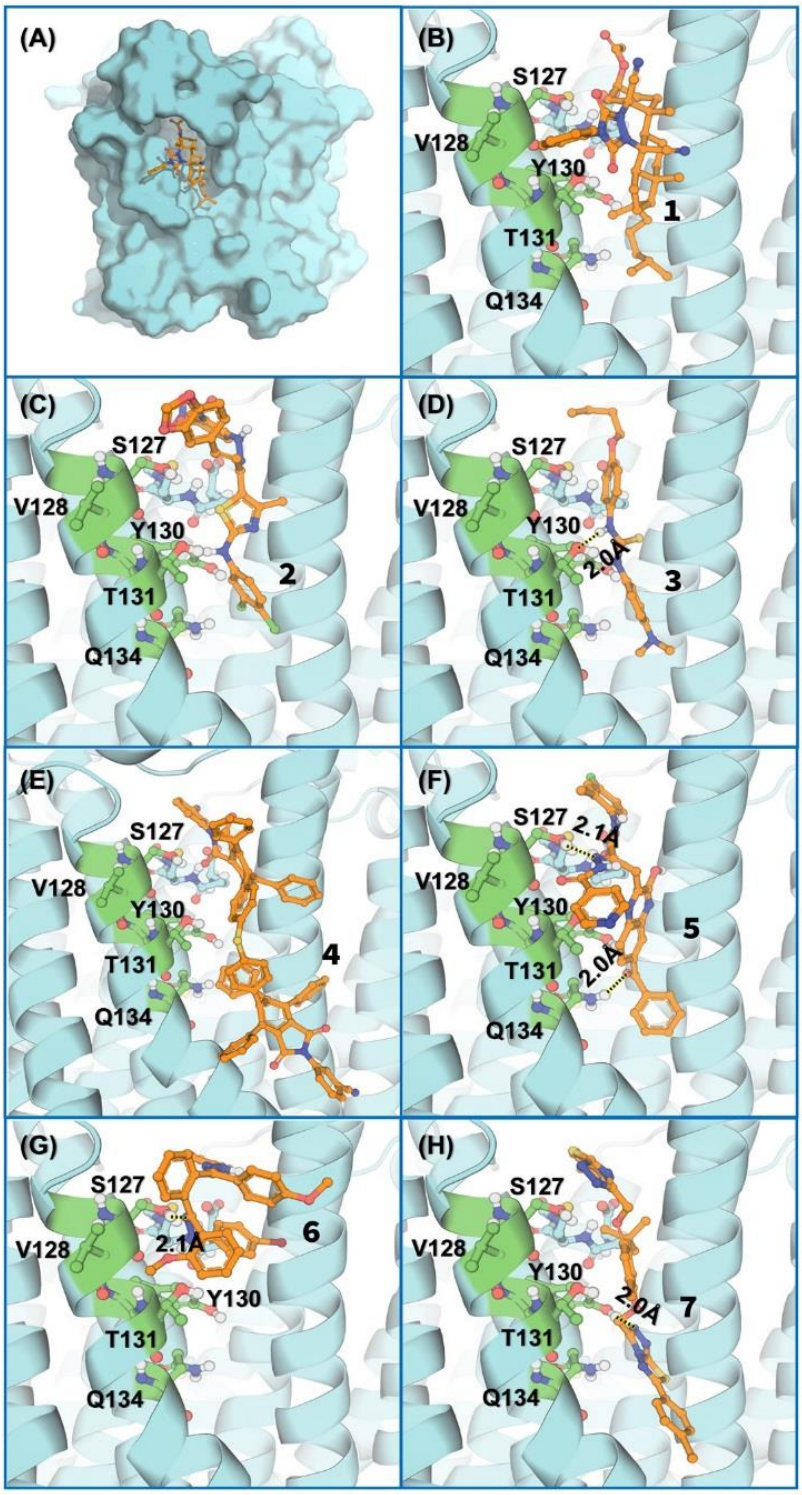

Figure 2.3 Energy-minimized structures of human mPGES-1 binding with the

identified inhibitors (1 to 7 depicted in Figure 2.1): (A) and (B) Compound 1; (C) 2; (D) 3; (E) 4; (F) 5; (G) 6; (H) 7. The protein is shown in cyan cartoon, and the key residues are shown in green ball-and-stick models. The ligand is shown in orange ball-and-stick models. Important polar interactions are shown in dashed lines.

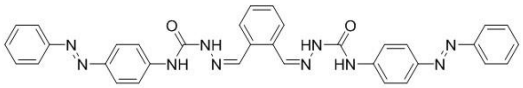

8

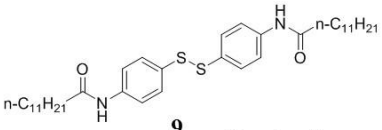

9

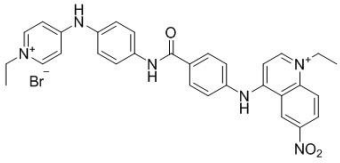

10

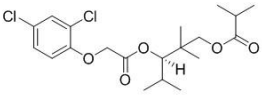

11

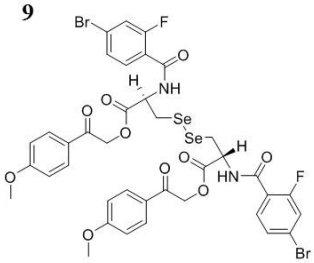

12

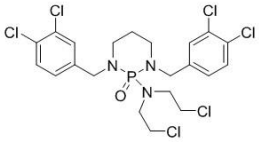

13

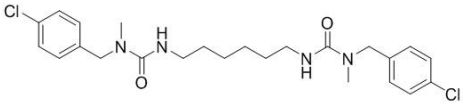

14

15

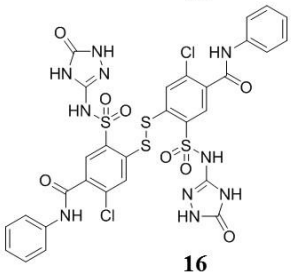

16

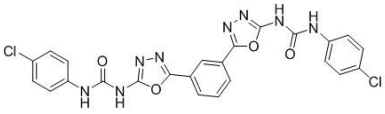

17

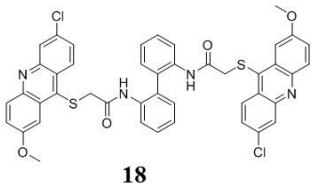

18

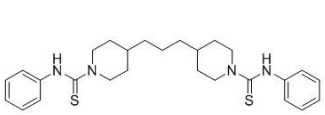

19

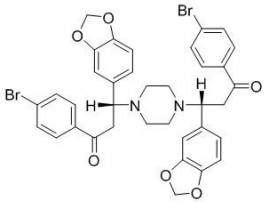

20

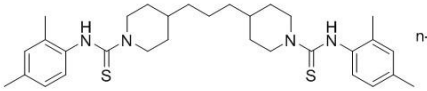

21

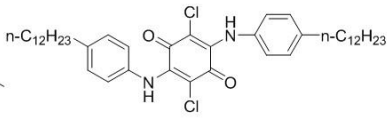

22

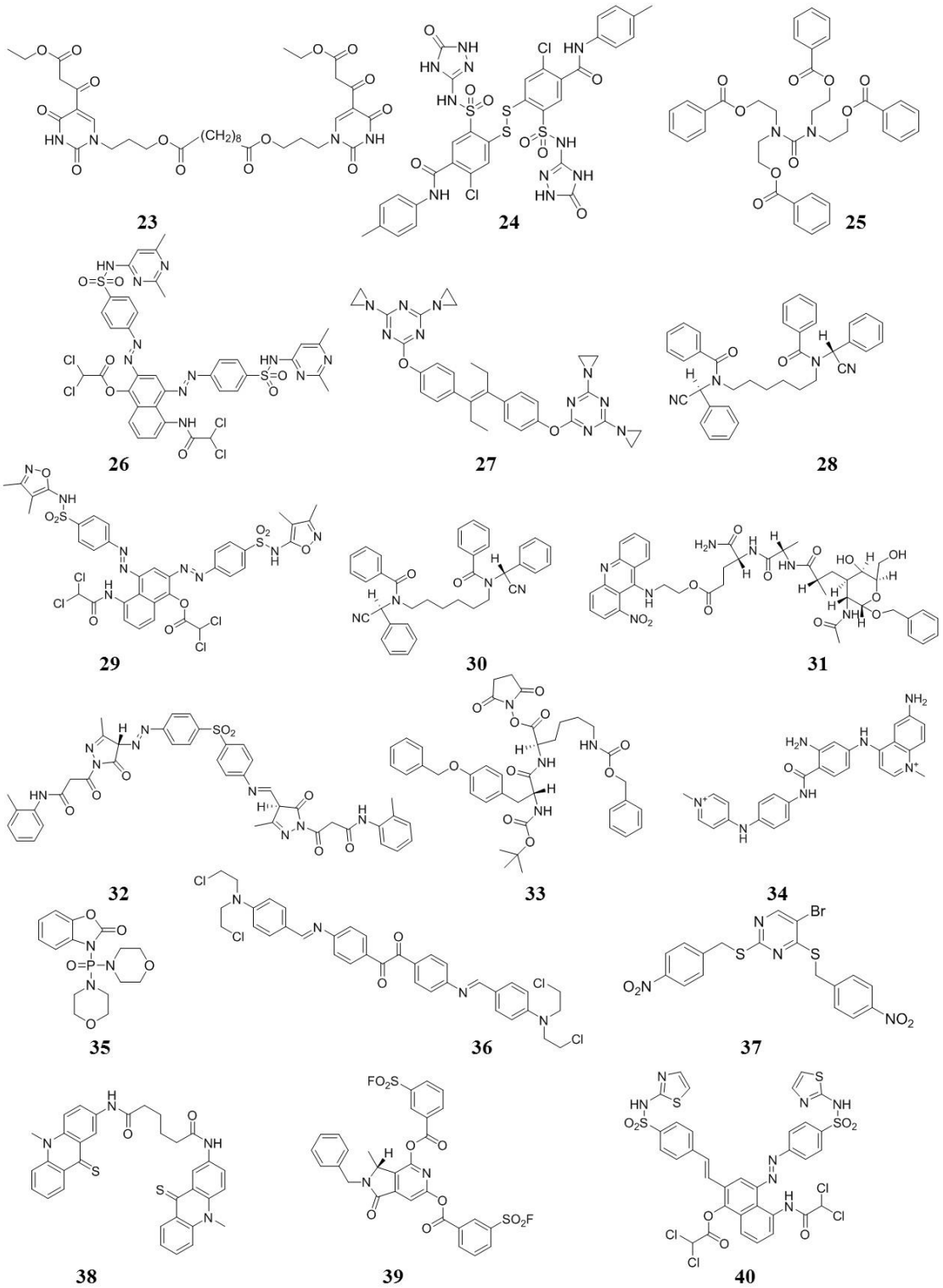

Figure 2.4 Molecular structures of remaining compounds (**8** to **40** listed in Table 2.1)

2.3 Conclusions

Overall, the diverse binding structures of these highly selective inhibitors with mPGES-1 depicted in Figure 2.3 provide some interesting clues concerning how to design modified structures of the inhibitors to more favorably bind with mPGES-1. Based on the structures in Figure 2.3, each inhibitor has some unique interaction with the protein. A more potent inhibitor/ligand could be designed to have more of these favorable protein-ligand interactions.

Chapter 3: Design, synthesis and characterization of 2-cyano-3-phenylacrylic acid derivatives as human and mouse mPGES-1 dual inhibitors

Summary: A series of 2-cyano-3-phenylacrylic acid derivatives were designed, synthesized, and evaluated as novel dual inhibitors against both human and mouse mPGES-1. Compounds **v20** and **v27** displayed IC_{50} values of 50 nM and 51 nM against human mPGES-1, respectively. The structure-activity relationship was discussed. Further binding mode analysis revealed that **v20**, as the most potent inhibitor against both human and mouse mPGES-1 of these 2-cyano-3-phenylacrylic acid derivatives, could form hydrogen bonds with Arg52 and His53 of human mPGES-1, while it will also form a hydrogen bond with Lys52 of mouse mPGES-1. These hydrogen bonds are necessary for maintaining the bioactivities of the compounds in this series. This also explains why compounds with carboxyl groups showed much higher potency than their corresponding ester derivatives. The most potent human mPGES-1 inhibitors also showed inhibition activities against mouse mPGES-1. This will make the pre-clinical experiments with wild-type mouse disease models feasible.

3.1 Introduction

So far, three PGE_2 synthases have been identified: mPGES-1, mPGES-2, cPGES. Among them, mPGES-2 and cPGES are the constitutively expressed forms of PGE_2 synthases, while mPGES-1 is an inducible membrane-bonded isoform of PGE_2 synthases.[133] Since the discovery of mPGES-1 in the late 1990s, mPGES-1 has emerged as a strategic target for the treatment of PGE_2-related acute and chronic disorders,[134, 135] for example, Hypoxia,[136] arthritis,[137-139] tendon disease,[140] myotonic dystrophy,[141] human abdominal aortic aneurysm,[142] Alzheimer's disease,[143] ischemic excitotoxicity,[144] brain ischemic injury,[144] inflammation related pain and fever.[18, 145] Interestingly, the PGE_2 inhibition was reported to be able to enhance the antiviral immunity.[146] The significance of mPGES-1 in rapidly proliferating cells such as tumor

cells makes it an ideal target for pharmacological intervention against cancer.[147-149]

The traditional anti-inflammatory drugs (or traditional NSAIDs) reduce PGE_2 level by blocking the COXs (COX isozymes).[150] However, administration of COXs inhibitors for an extended period would cause numerous adverse effects, that preventing them from being utilized widely.[151] The major concern related to the usage of traditional NSAIDs are renal, cardiovascular and gastrointestinal side effects.[152, 153] For this reason, there is an urgent need to develop alternative of traditional NSAIDs as next generation of anti-inflammatory drugs.[154] Therefore, the discovery of novel mPGES-1 inhibitors could be a valuable pharmacological approach while avoid the side effects of the traditional NSAIDs at the same time.[155]

Despite a great number of potent human mPGES-1 inhibitors have been reported, almost all of them failed to show inhibitory activity against mouse mPGES-1, which made the preclinical trials in the inflammation disease model of wild-type (WT) mice impossible.[55] The lack of mouse mPGES-1 inhibitory activity is due to the structural differences between the human and mouse mPGES-1.[156] In this Chapter, we will present a new class of human and mouse mPGES-1 dual inhibitors designed starting from a previously identified hit, *i.e.* **compound 3** (see Scheme 1.1).[1] Some of the presented 2-cyano-3-phenylacrylic acid derivatives were able to inhibit both human and mouse mPGES-1 in sub-micromole level.

3.2 Results and Discussions

3.2.1 Inhibitory activities against human and mouse mPGES-1

The experimental studies to discover mPGES-1 inhibitors in our lab were carried out by employing cell-free mPGES-1 activity assays protocol as described before.[1] The reaction was initiated by exogenous addition of the substrate PGH_2 in the reaction buffer that contains mPGES-1 and inhibitor. The direct conversion of PGE_2 from PGH_2 can be determined by ELISA. The reported mPGES-1 inhibitor **MK886** was used as

the reference compounds.[157-162]

All synthesized conjugates of 2-cyano-3-phenylacrylic acid derivatives (**v01-v58**) were evaluated for their *in vitro* human mPGES-1 inhibition activity in a concentration-dependent manner. The results of inhibitory activities (IC_{50} values) are presented in Table 3.1 in nanomolar (nM) concentrations.

Table 3.1 Structures and activities for 2-cyano-3-phenylacrylic acid analogs v01 ~ v58

ID	Structures	IC_{50} (against human mPGES-1)/nM[a]	IC_{50} (against mouse mPGES-1)/nM
v01	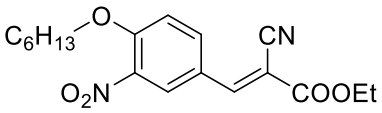	8739 ± 1169	N.D.[b]
v02	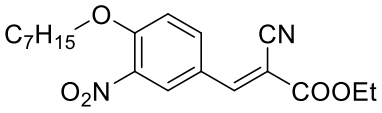	4817 ± 511	N.D.
v03	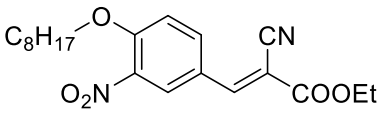	4749 ± 489	N.D.
v04	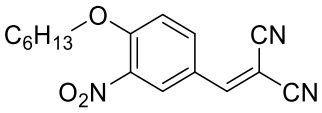	285 ± 40	754 ± 73
v05	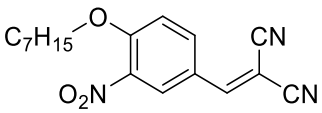	135 ± 16	776 ± 217
v06	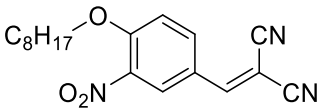	89 ± 12	716 ± 120
v07	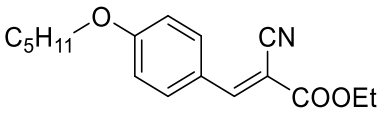	6225± 502	N.D.
v08	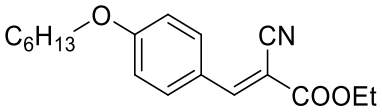	5241 ± 429	N.D.
v09	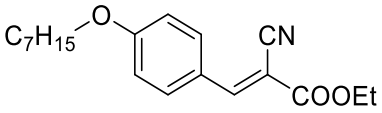	3518 ± 471	N.D.

v10	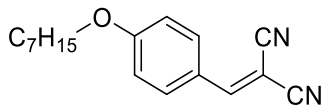	136 ± 13	1390 ± 255
v11	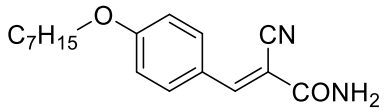	376 ± 31	N.D.
v12	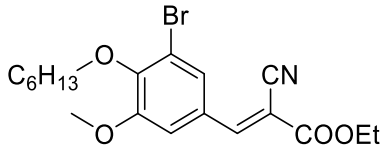	998 ± 196	N.D.
v13	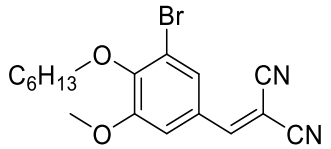	181 ± 33	1632 ± 250
v14	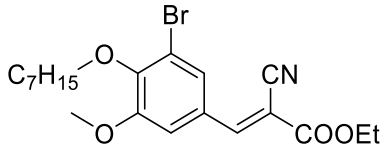	1008 ± 262	N.D.
v15	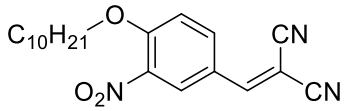	83 ± 14	357 ± 52
v16	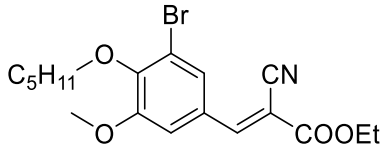	1297 ± 232	N.D.
v17	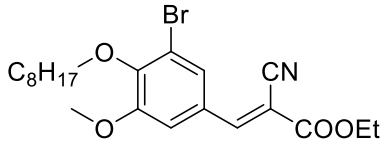	1865 ± 350	N.D.
v18	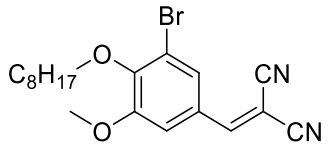	74 ± 8	572 ± 83
v19	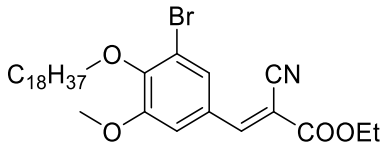	2270 ± 350	N.D.
v20	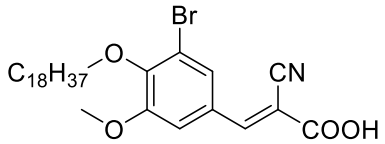	50 ± 9	270 ± 64

v21	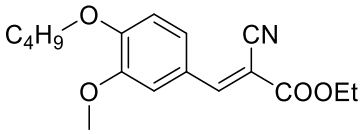	5633 ± 987	N.D.
v22	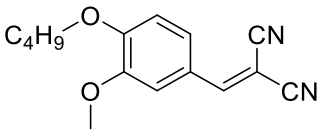	348 ± 100	1771 ± 241
v23	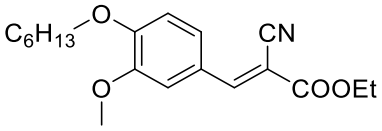	1448 ± 192	N.D.
v24	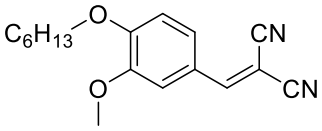	294 ± 60	N.D.
v25	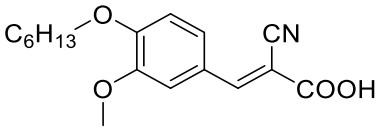	242 ± 30	N.D.
v26	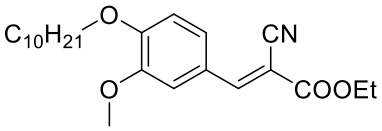	905 ± 177	N.D.
v27	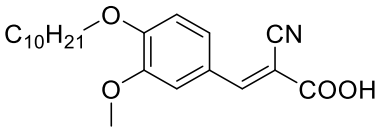	51 ± 10	390 ± 84
v28	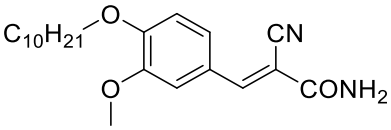	4374 ± 915	N.D.
v29	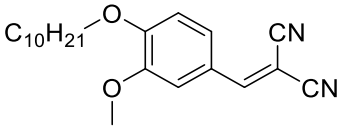	110 ± 29	3724 ± 683
v30	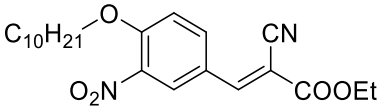	2883 ± 687	N.D.

v31	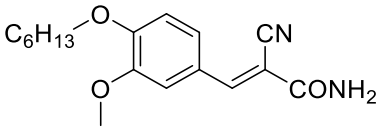	1095 ± 212	N.D.
v32	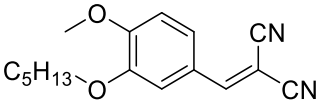	356 ± 123	N.D.
v33	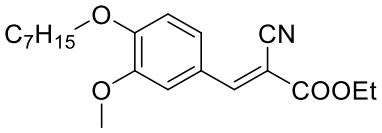	4283 ± 1404	N.D.
v34	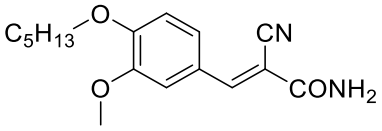	2210 ± 450	N.D.
v35	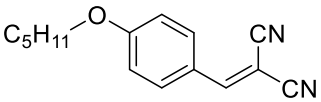	531 ± 116	N.D.
v36	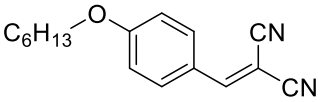	256 ± 33	7291 ± 2546
vx	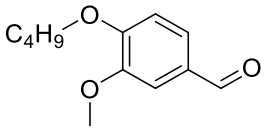	>30000	N.D.
v37	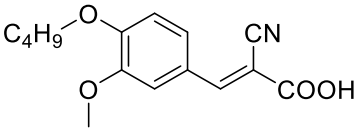	541 ± 82	N.D.
v38	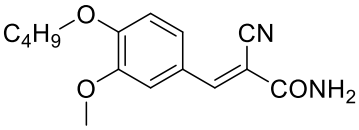	5414 ± 818	N.D.
v39	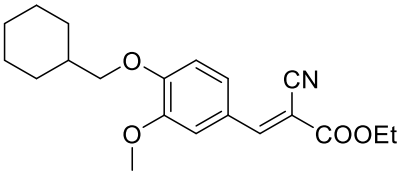	10811 ± 1038	N.D.

v40	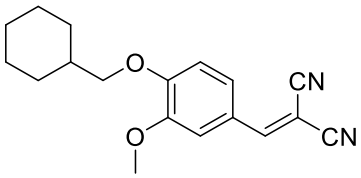	1451 ± 152	N.D.
v41	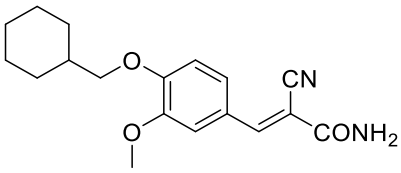	1455 ± 119	N.D.
v42	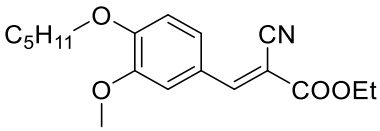	4140 ± 858	N.D.
v43	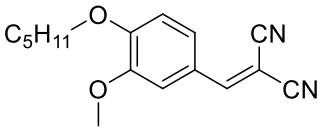	439 ± 104	N.D.
v44	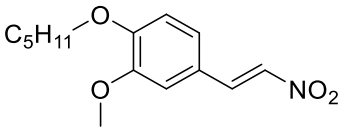	2772 ± 577	N.D.
v45	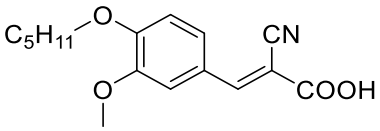	456 ± 42	N.D.
v46	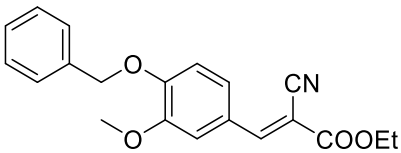	2084 ± 440	N.D.
v47	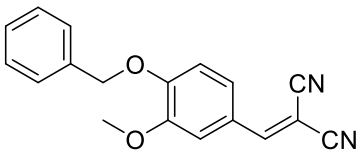	272 ± 56	N.D.
v48	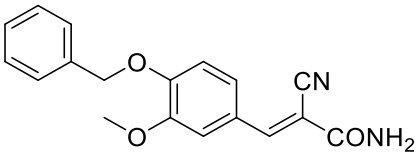	6992 ± 1190	N.D.
v49	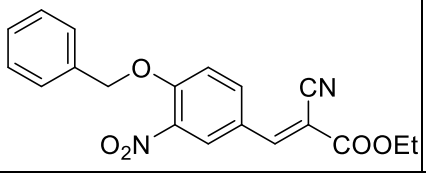	2383 ± 274	N.D.

v50	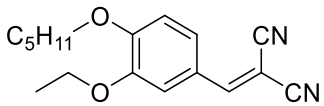	112 ± 12	6733 ± 2194
v51	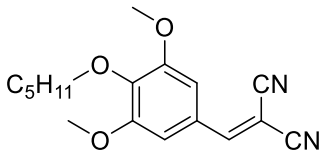	152 ± 26	1807 ± 584
v52	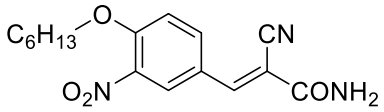	3083 ± 1203	N.D.
v53	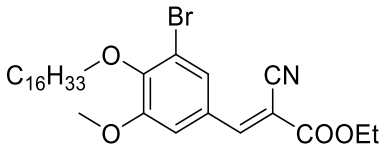	1441 ± 666	N.D.
v54	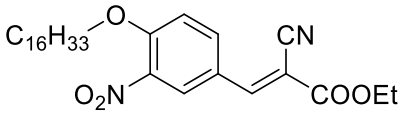	3477 ± 1428	N.D.
v55	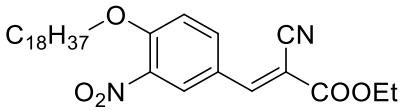	1504 ± 213	N.D.
v56	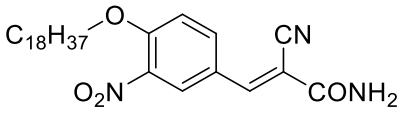	1636 ± 283	N.D.
v57	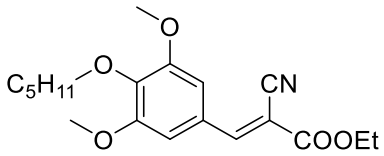	17796 ± 5680	N.D.
v58	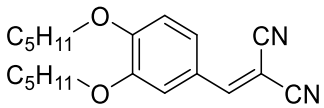	98 ± 19	1814 ± 540

[a]Data are expressed as means ± SD of single determinations obtained in triplicate.
[b]N.D. = not determined

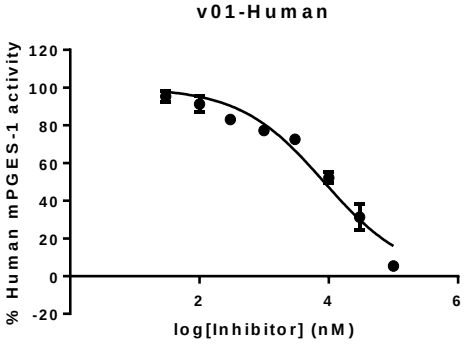
v01-Human
% Human mPGES-1 activity
log[Inhibitor] (nM)

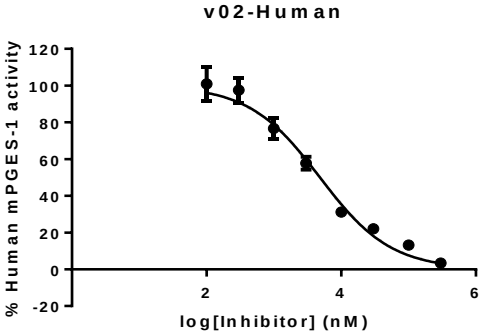
v02-Human
% Human mPGES-1 activity
log[Inhibitor] (nM)

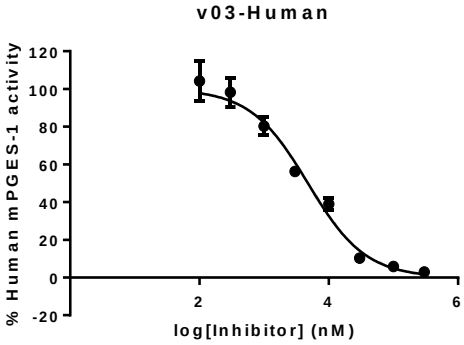
v03-Human
% Human mPGES-1 activity
log[Inhibitor] (nM)

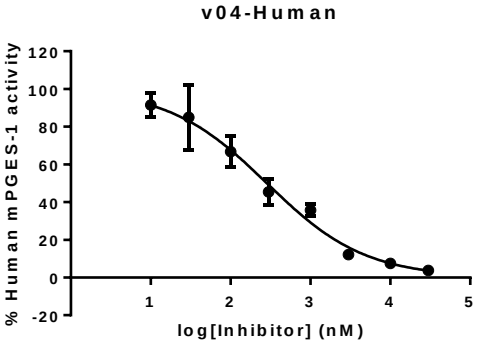
v04-Human
% Human mPGES-1 activity
log[Inhibitor] (nM)

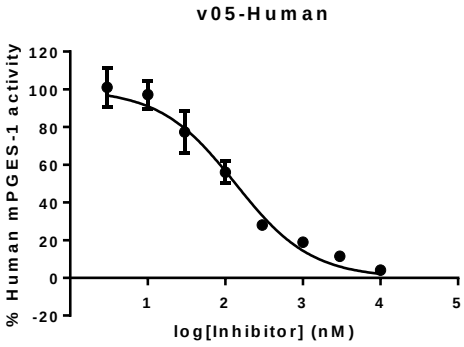
v05-Human
% Human mPGES-1 activity
log[Inhibitor] (nM)

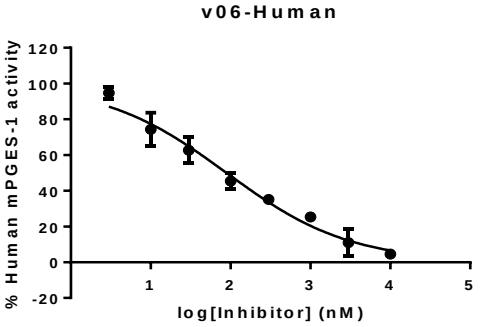
v06-Human
% Human mPGES-1 activity
log[Inhibitor] (nM)

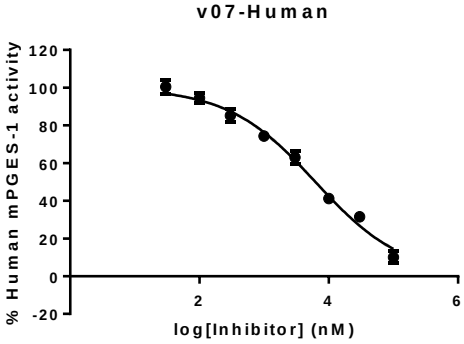
v07-Human
% Human mPGES-1 activity
log[Inhibitor] (nM)

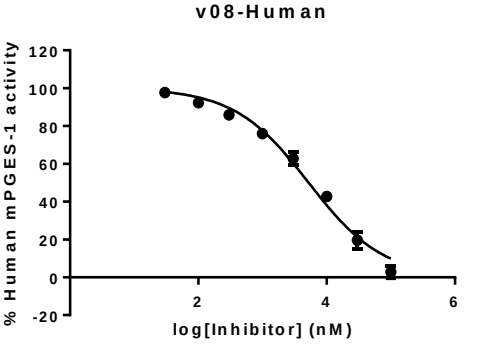
v08-Human
% Human mPGES-1 activity
log[Inhibitor] (nM)

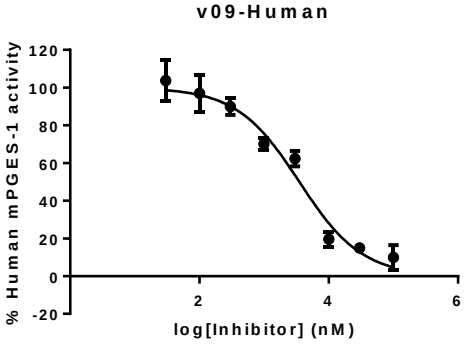
v09-Human
% Human mPGES-1 activity
log[Inhibitor] (nM)

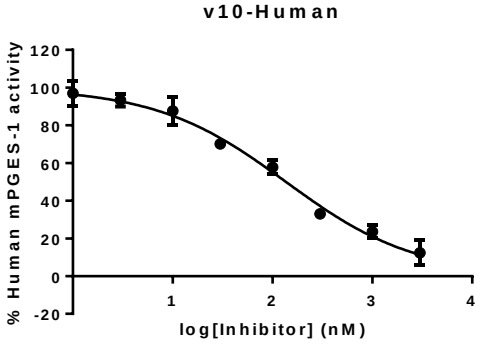
v10-Human
% Human mPGES-1 activity
log[Inhibitor] (nM)

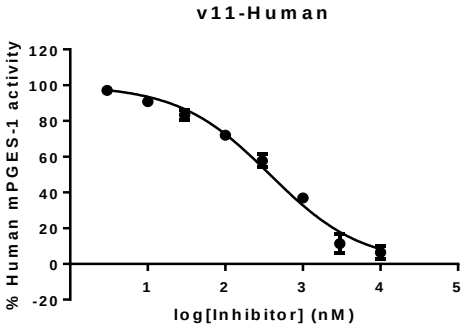
v11-Human
% Human mPGES-1 activity
log[Inhibitor] (nM)

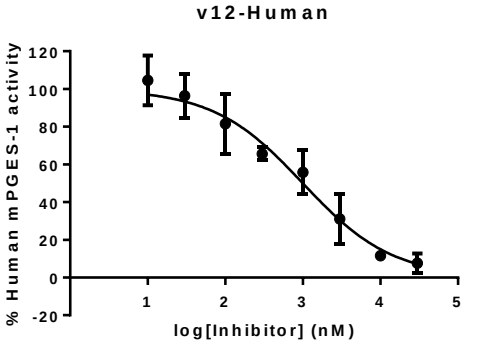
v12-Human
% Human mPGES-1 activity
log[Inhibitor] (nM)

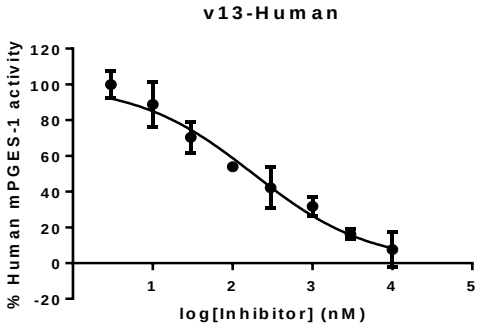
v13-Human
% Human mPGES-1 activity
log[Inhibitor] (nM)

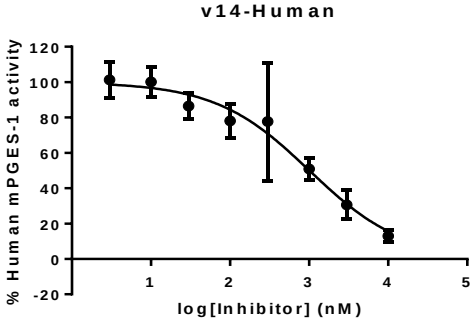
v14-Human
% Human mPGES-1 activity
log[Inhibitor] (nM)

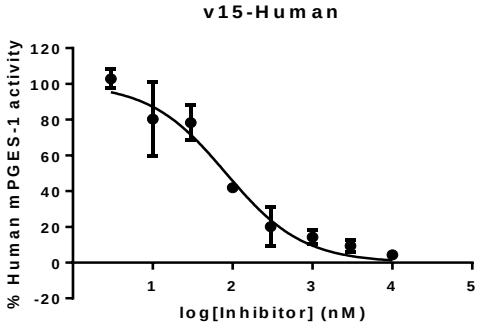
v15-Human
% Human mPGES-1 activity
log[Inhibitor] (nM)

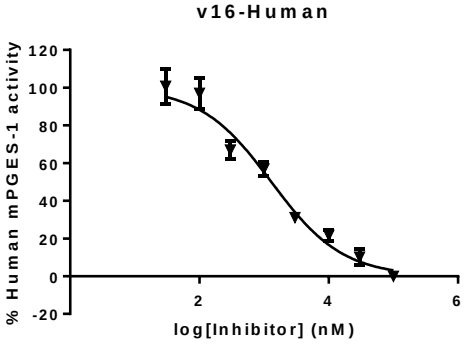
v16-Human
% Human mPGES-1 activity
log[Inhibitor] (nM)

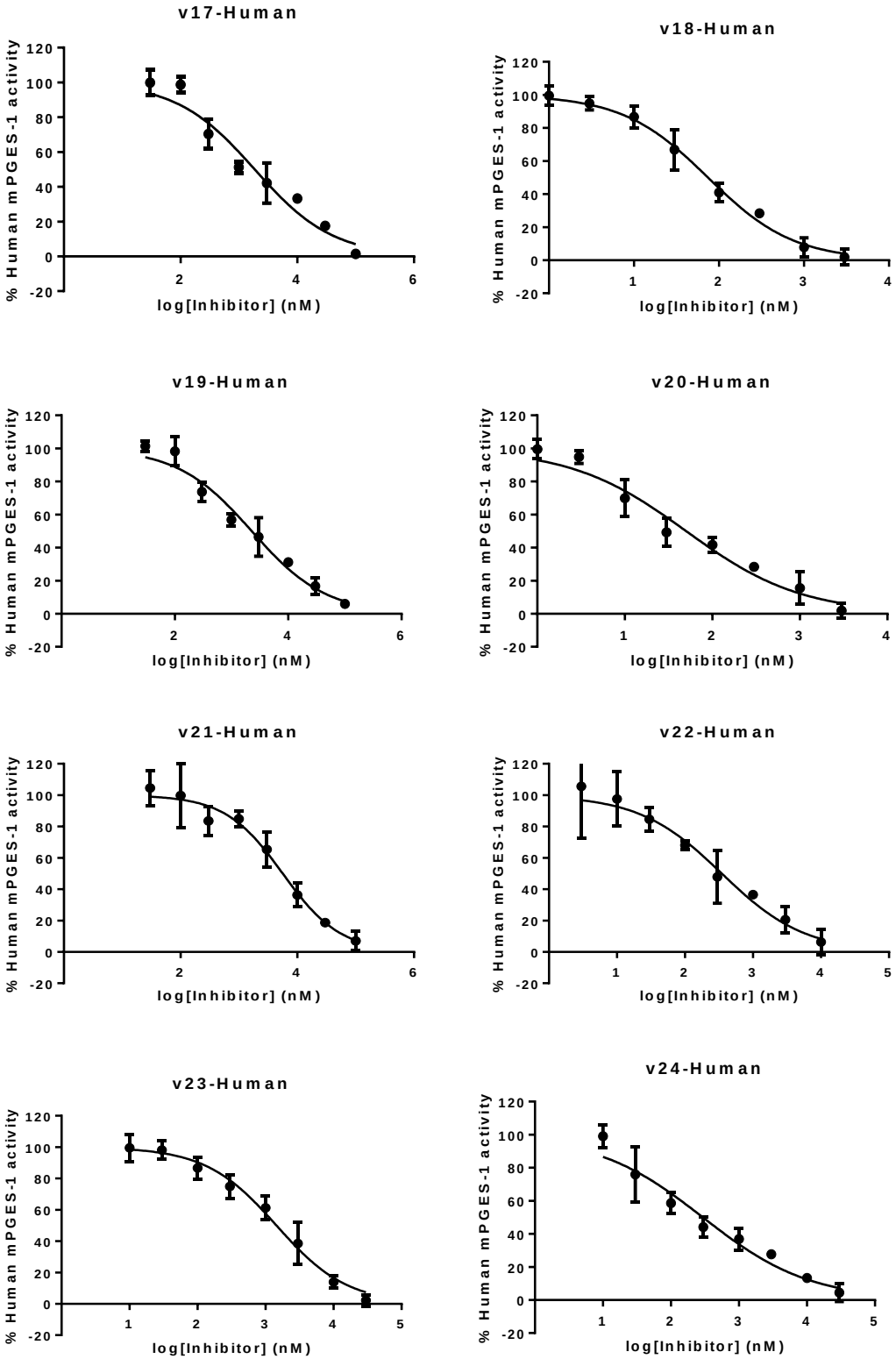
v17-Human
v18-Human
v19-Human
v20-Human
v21-Human
v22-Human
v23-Human
v24-Human
% Human mPGES-1 activity
log[Inhibitor] (nM)

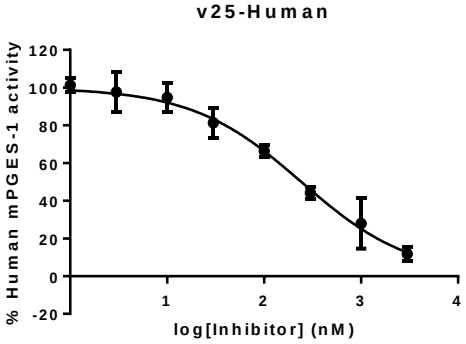
v25-Human
% Human mPGES-1 activity
log[Inhibitor] (nM)

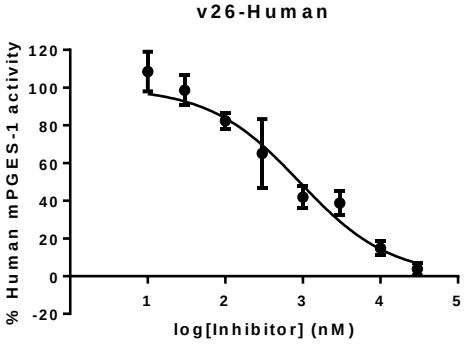
v26-Human
% Human mPGES-1 activity
log[Inhibitor] (nM)

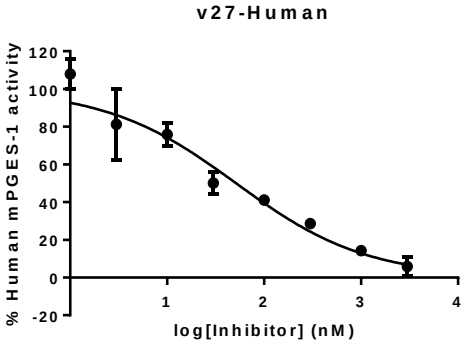
v27-Human
% Human mPGES-1 activity
log[Inhibitor] (nM)

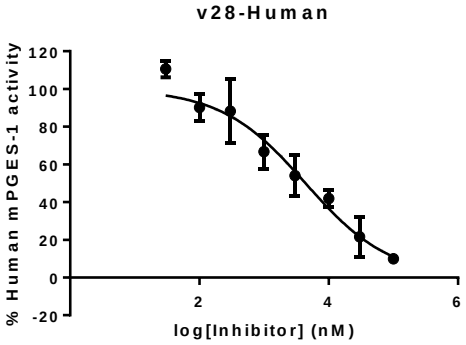
v28-Human
% Human mPGES-1 activity
log[Inhibitor] (nM)

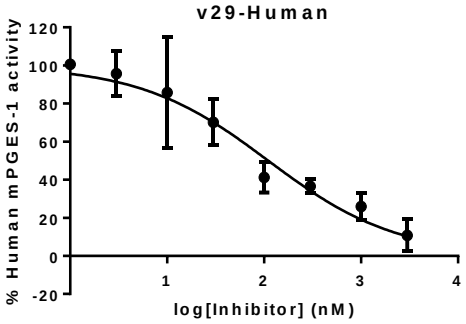
v29-Human
% Human mPGES-1 activity
log[Inhibitor] (nM)

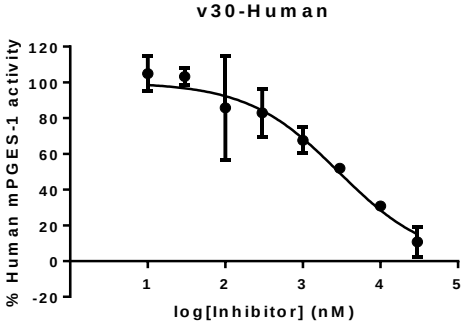
v30-Human
% Human mPGES-1 activity
log[Inhibitor] (nM)

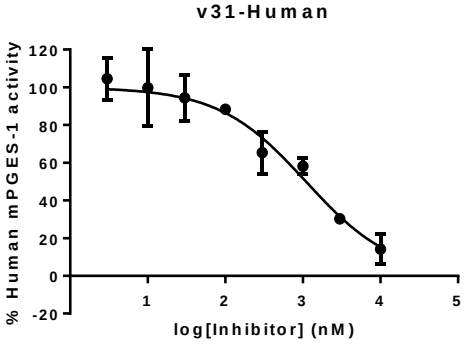
v31-Human
% Human mPGES-1 activity
log[Inhibitor] (nM)

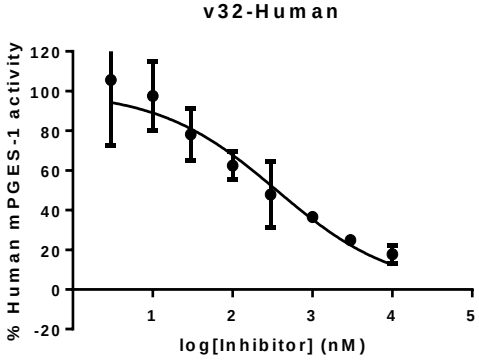
v32-Human
% Human mPGES-1 activity
log[Inhibitor] (nM)

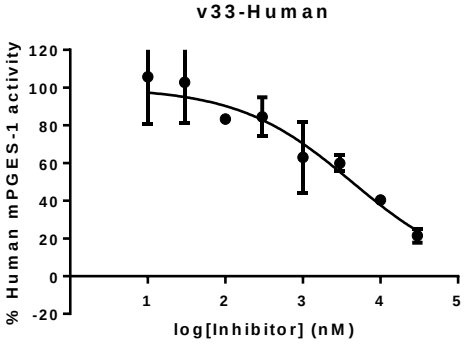
v33-Human
% Human mPGES-1 activity
120
100
80
60
40
20
0
-20
1
2
3
4
5
log[Inhibitor] (nM)

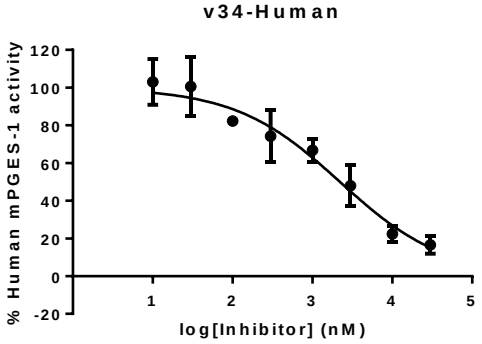
v34-Human
% Human mPGES-1 activity
120
100
80
60
40
20
0
-20
1
2
3
4
5
log[Inhibitor] (nM)

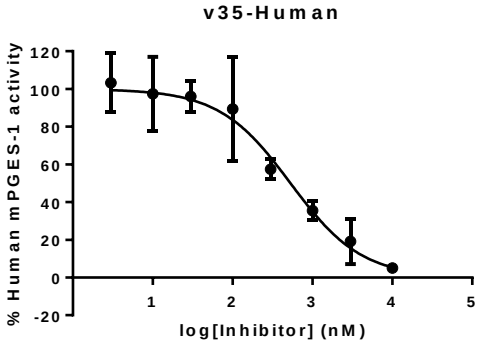
v35-Human
% Human mPGES-1 activity
120
100
80
60
40
20
0
-20
1
2
3
4
5
log[Inhibitor] (nM)

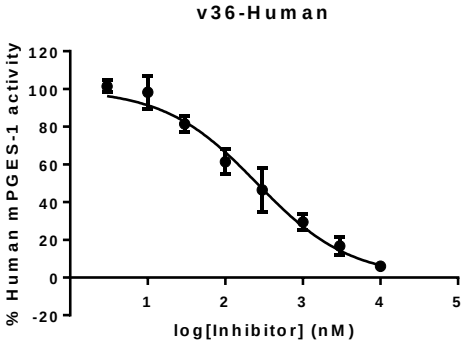
v36-Human
% Human mPGES-1 activity
120
100
80
60
40
20
0
-20
1
2
3
4
5
log[Inhibitor] (nM)

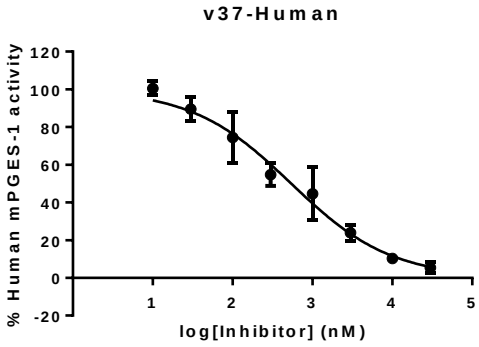
v37-Human
% Human mPGES-1 activity
120
100
80
60
40
20
0
-20
1
2
3
4
5
log[Inhibitor] (nM)

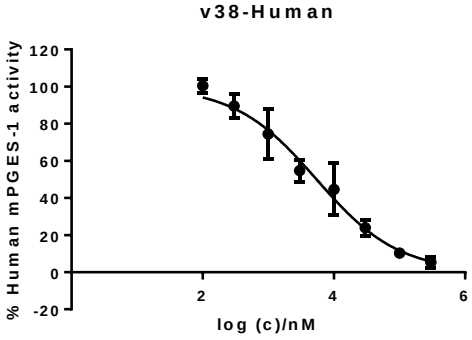
v38-Human
% Human mPGES-1 activity
120
100
80
60
40
20
0
-20
2
4
6
log (c)/nM

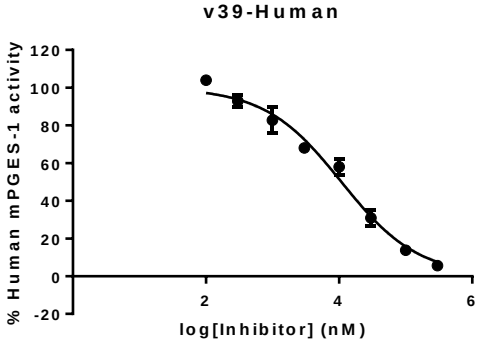
v39-Human
% Human mPGES-1 activity
120
100
80
60
40
20
0
-20
2
4
6
log[Inhibitor] (nM)

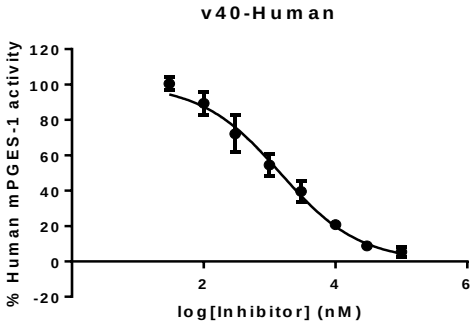
v40-Human
% Human mPGES-1 activity
120
100
80
60
40
20
0
-20
2
4
6
log[Inhibitor] (nM)

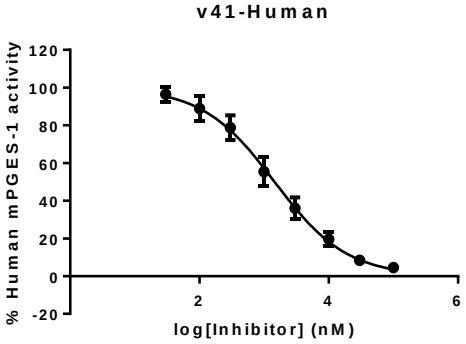
v41-Human
% Human mPGES-1 activity
log[Inhibitor] (nM)

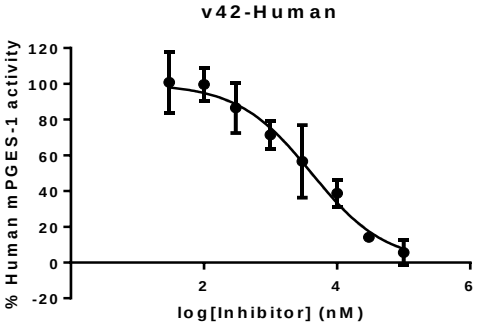
v42-Human
% Human mPGES-1 activity
log[Inhibitor] (nM)

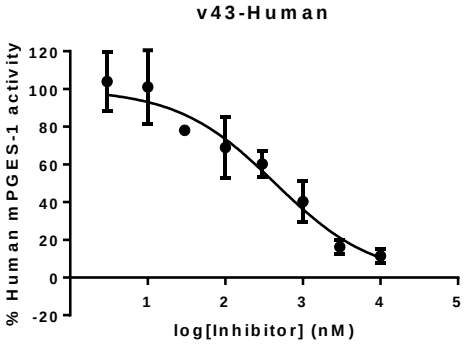
v43-Human
% Human mPGES-1 activity
log[Inhibitor] (nM)

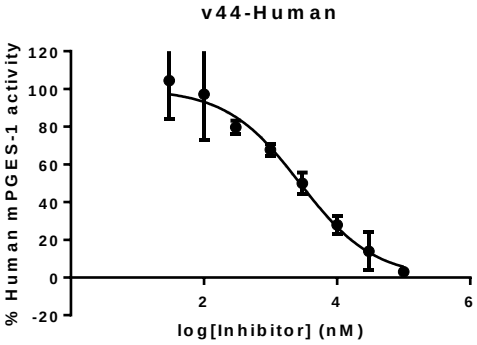
v44-Human
% Human mPGES-1 activity
log[Inhibitor] (nM)

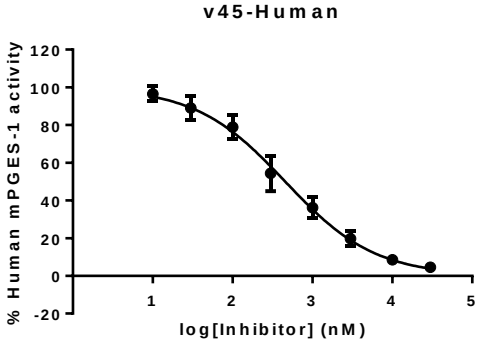
v45-Human
% Human mPGES-1 activity
log[Inhibitor] (nM)

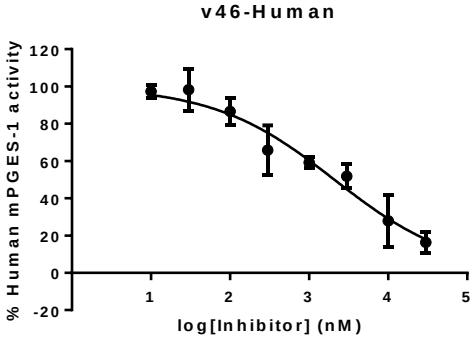
v46-Human
% Human mPGES-1 activity
log[Inhibitor] (nM)

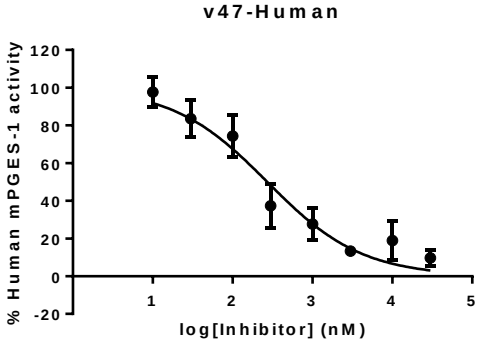
v47-Human
% Human mPGES-1 activity
log[Inhibitor] (nM)

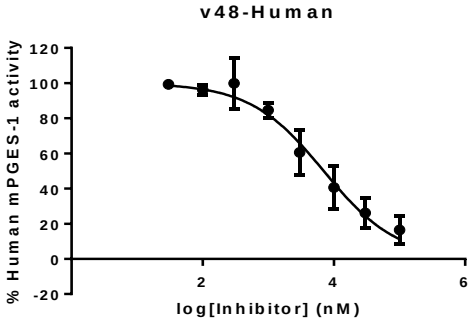
v48-Human
% Human mPGES-1 activity
log[Inhibitor] (nM)

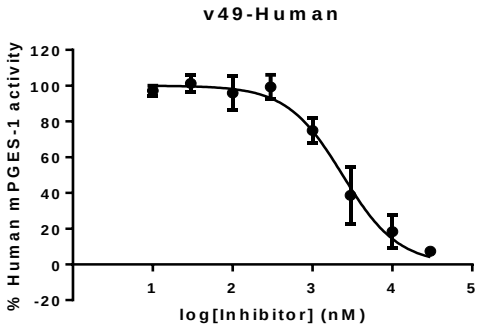
v49-Human
% Human mPGES-1 activity
log[Inhibitor] (nM)

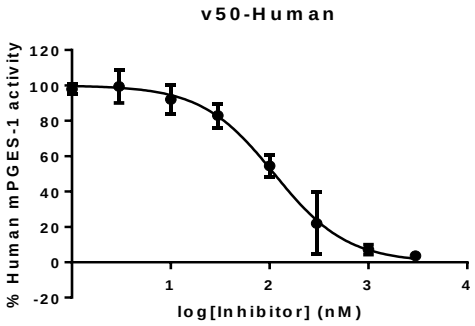
v50-Human
% Human mPGES-1 activity
log[Inhibitor] (nM)

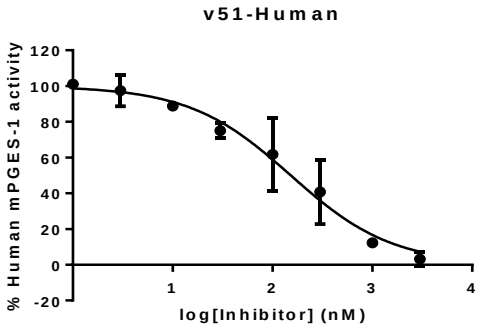
v51-Human
% Human mPGES-1 activity
log[Inhibitor] (nM)

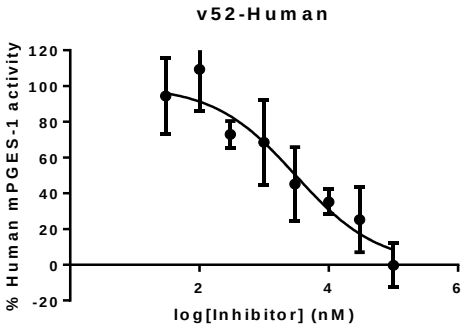
v52-Human
% Human mPGES-1 activity
log[Inhibitor] (nM)

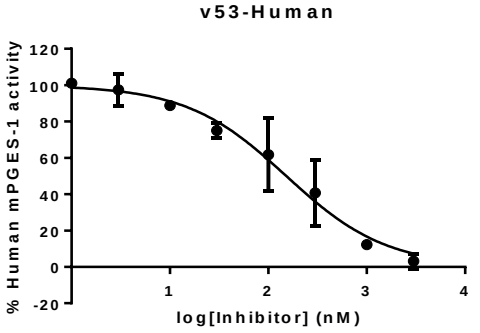
v53-Human
% Human mPGES-1 activity
log[Inhibitor] (nM)

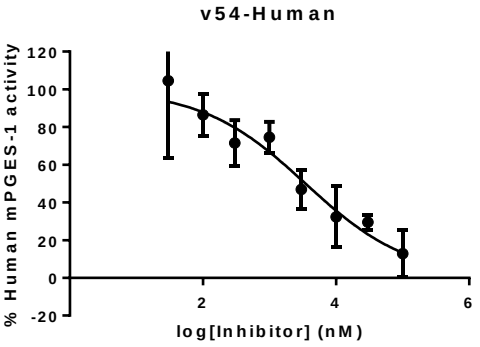
v54-Human
% Human mPGES-1 activity
log[Inhibitor] (nM)

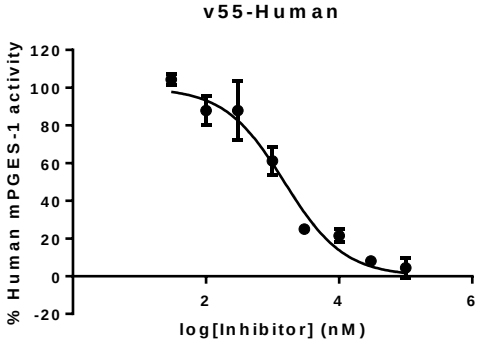
v55-Human
% Human mPGES-1 activity
log[Inhibitor] (nM)

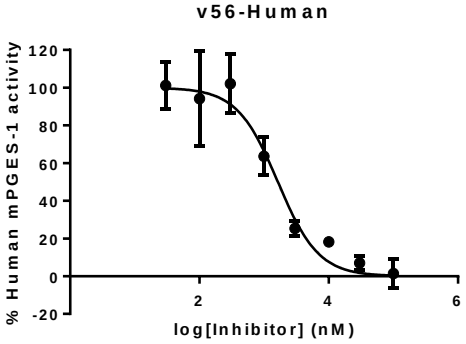
v56-Human
% Human mPGES-1 activity
log[Inhibitor] (nM)

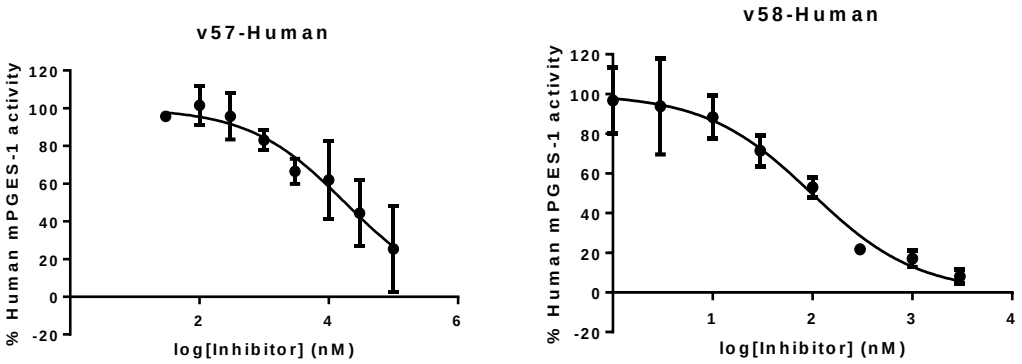

Figure 3.1 Human mPGES-1 inhibitory activity of 2-cyano-3-phenylacrylic acid derivatives. The inhibitor concentration is given in log scale.

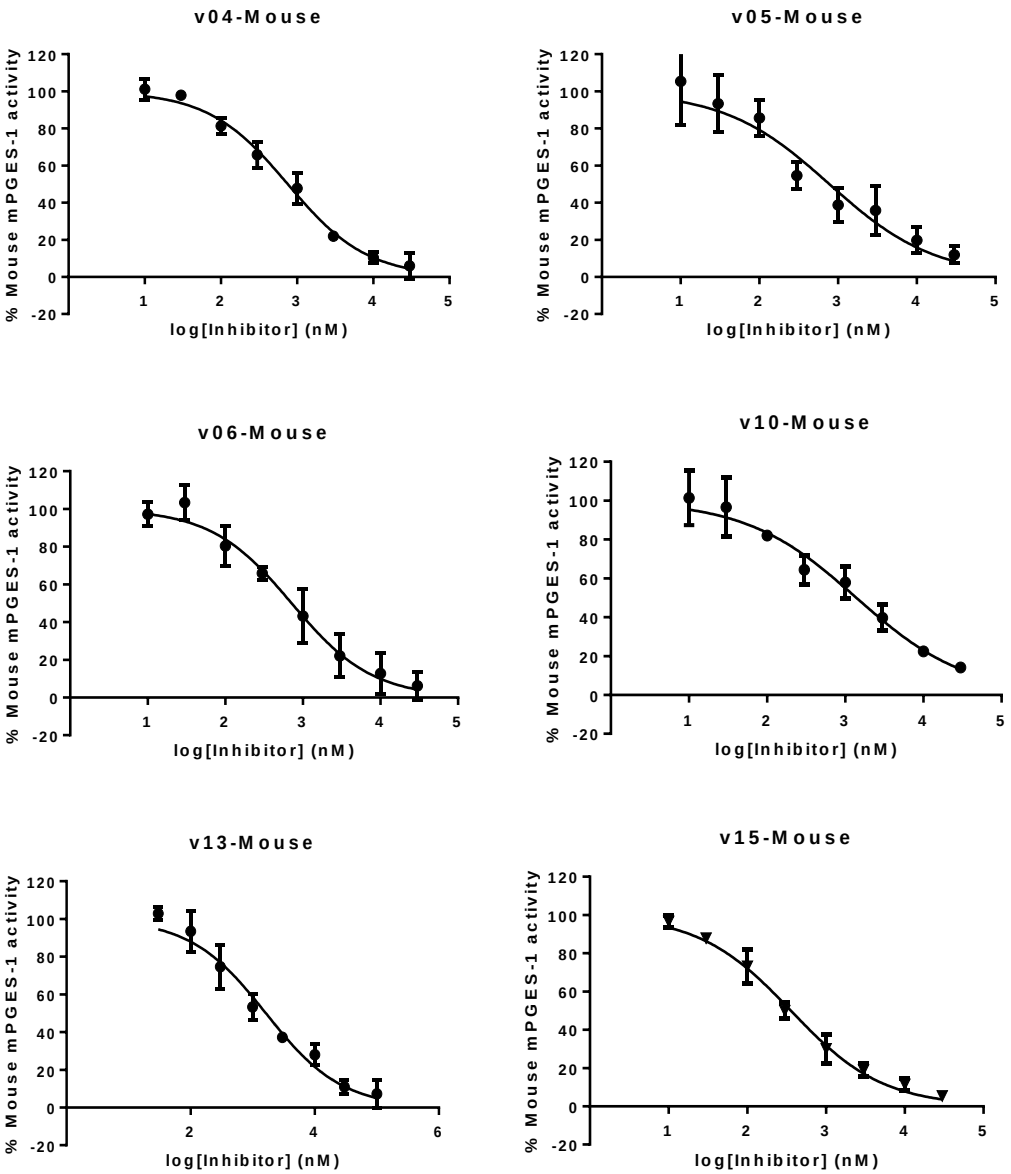

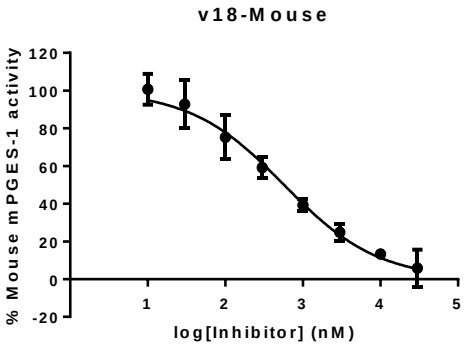
v18-Mouse
% Mouse mPGES-1 activity
120
100
80
60
40
20
0
-20
1
2
3
4
5
log[Inhibitor] (nM)

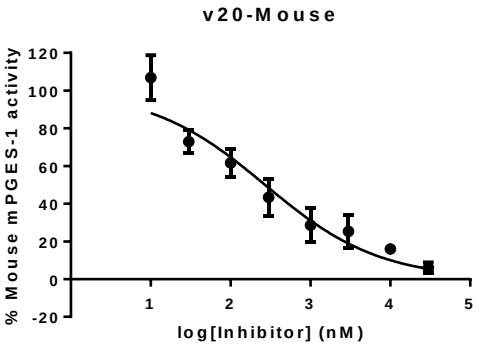
v20-Mouse
% Mouse mPGES-1 activity
120
100
80
60
40
20
0
-20
1
2
3
4
5
log[Inhibitor] (nM)

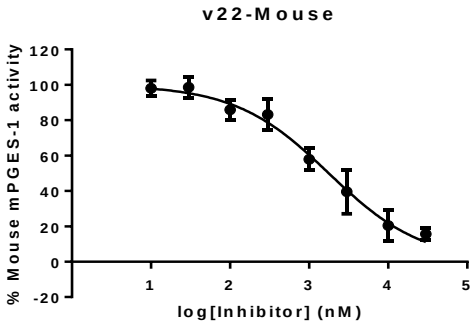
v22-Mouse
% Mouse mPGES-1 activity
120
100
80
60
40
20
0
-20
1
2
3
4
5
log[Inhibitor] (nM)

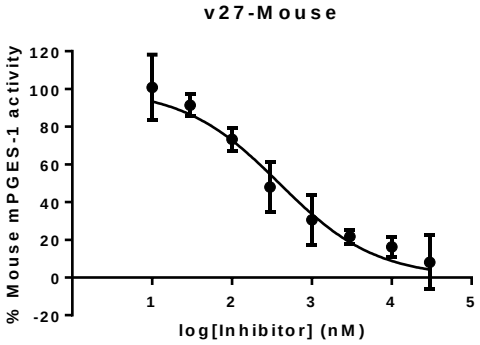
v27-Mouse
% Mouse mPGES-1 activity
120
100
80
60
40
20
0
-20
1
2
3
4
5
log[Inhibitor] (nM)

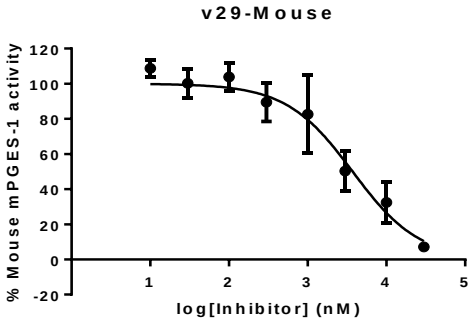
v29-Mouse
% Mouse mPGES-1 activity
120
100
80
60
40
20
0
-20
1
2
3
4
5
log[Inhibitor] (nM)

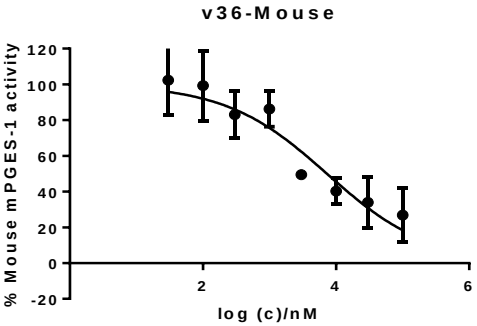
v36-Mouse
% Mouse mPGES-1 activity
120
100
80
60
40
20
0
-20
2
4
6
log (c)/nM

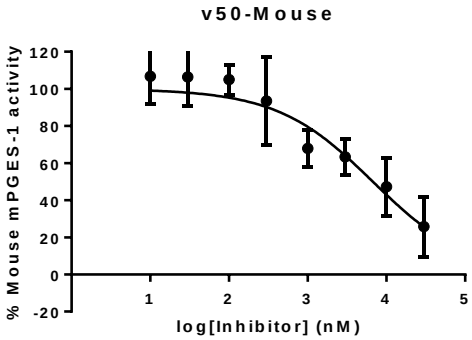
v50-Mouse
% Mouse mPGES-1 activity
120
100
80
60
40
20
0
-20
1
2
3
4
5
log[Inhibitor] (nM)

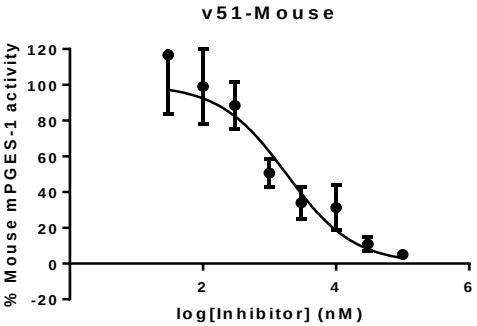
v51-Mouse
% Mouse mPGES-1 activity
120
100
80
60
40
20
0
-20
2
4
6
log[Inhibitor] (nM)

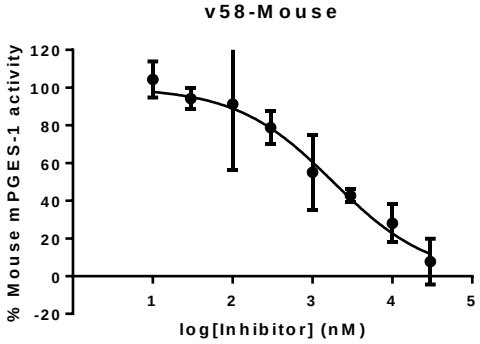

Figure 3.2 Mouse mPGES-1 inhibitory activity of screened inhibitors 2-cyano-3-phenylacrylic acid derivatives. The inhibitor concentration is given in log scale.

3.2.2 SAR study

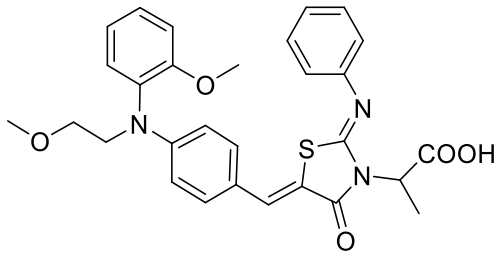

Compound 3
IC_{50}: 3.5 μM

Scheme 3.1. **Compound 3**,[1] the starting compound for 2-cyano-3-phenylacrylic acid derivatives

Compound 3[1] is the lead compound for the design and synthesis of 2-cyano-3-phenylacrylic acid derivatives as mPGES-1 inhibitors. It is a human mPGES-1 inhibitor identified by a former member in our lab with IC_{50} value of 3.5 μM against human mPGES-1.[1] In order to get compounds with more potency, derivatives of 2-cyano-3-phenylacrylic acid were then explored (Table 3.1). In the *in vitro* study, Compounds **v06** (89nM), **v15** (83nM), **v18** (74nM) and **v50** (112nM) showed similar high activities against human mPGES-1, which suggest that the substitute on the phenyl group (X position in Scheme 3.2) probably had no apparent effect on the inhibitory activity. The esters have much lower activities than their corresponding acid. A case in point is that

v26 (905 nM) is a less potent inhibitor against human mPGES-1 than its corresponding acid **v27** (51 nM).

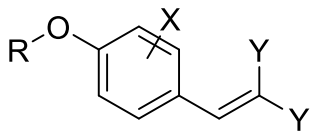

X: NO_2, OH, OMe, Br, OEt, OC_5H_{11}
Y: CN, COOEt, COOH, $CONH_2$
R: C_4H_9, C_5H_{11}, C_6H_{13}, C_7H_{15}, C_8H_{17}, $C_{10}H_{21}$, $C_{16}H_{33}$, $C_{18}H_{37}$, Bn, etc.

Scheme 3.2 The scaffold of 2-cyano-3-phenylacrylic acid derivatives

Table 3.1 highlighted the SAR for the 2-cyano-3-phenylacrylic acid derivatives moiety. These studies revealed that the inhibition activities of the 2-cyano-3-phenylacrylic acid derivatives were very dependent on the nature and position of the substituents present on the R position and Y positions. Introducing a nitro group, cyano group or carboxylic group to the Y positions will strengthen the *in vitro* activity while an ester group (COOEt) or $CONH_2$ group to the Y positions will weaken the *in vitro* activity, which implies that EWGs (electron-withdrawing groups) or electronegative groups are required at the Y positions for the activities. The above discussion indicates that for the 2-cyano-3-phenylacrylic acid scaffold, the electronegative substitutions for Y and the hydrophobic groups for R position are key factors for potent human and mouse mPGES-1 inhibitory activity.

3.2.3 Off target tests

In inflammatory responses, cyclooxygenases (COXs) are expressed in resident and infiltrating cells of the inflammatory locus and involved in the biosynthesis of prostaglandins (PGs).[163] COXs plays a significant role in the biosynthesis of PGs from arachidonic acid (AA).[164] COXs inhibition could result in various side effects, for example, the COX-2 specific inhibitors are responsible for the dramatic risks in cardiovascular toxicity.[165] For this reason, high selectivity will be important to the

success of a development candidate of next generation anti-inflammatory drugs, precluding the usage of a basic moiety mPGES-1 selective inhibitor design. mPGES-1 selective inhibitors will have the effect of anti-inflammation while avoiding the side effects of the traditional NSAIDs.[16] In our study, only inhibitors with IC_{50} values below 100 nM were assayed for their COXs inhibitions.

The 'COX (ovine / human) Inhibitor Screening Assay Kit' (Cayman Chemical, Item No. 560131)[131, 132] was used for this assay. Briefly, the compounds were incubated with purified COXs for 10 min at 37℃ on the water bath. The concentration for all the inhibitors was 100 μM. The reactions were initiated with the addition of AA. The reaction mixture was quickly vortexed and incubated for exactly two minutes at 37℃ (water bath), and then the reaction was stopped by adding saturated stannous chloride solution. The tubes were then removed from the water bath and vortexed, incubated for five minutes at room temperature. The reaction mixture should become cloudy at this time. Then the cloudy solution was diluted three thousand times. The level of prostaglandins (PGs) in the diluted solutions were then assayed by a 96-well plate, which was provided by this commercial kit. The inhibition rates were listed in Table 3.2.

Table 3.2 Inhibition of the most potent mPGES-1 inhibitors against COXs

Name	%/Inhibition against COXs at 100 μM
v06	28.6 ± 2.8
v15	9.4 ± 5.4
v18	2.0 ± 3.0
v20	59.8 ± 1.2
v27	44.1 ± 0.9
v58	0.2 ± 1.7

The six tested compounds did not show significant inhibition against COXs at 100 μM. This result indicates that these six compounds have high selectivity on mPGES-1 over COXs. Based on the structural similarity of this compound set, we expect that

these 2-cyano-3-phenylacrylic acid derivatives are not significant inhibitors of COXs.

3.2.4 Configuration analysis

To confirm that of the 2-cyano-3-phenylacrylic acid derivatives will adopt *trans*/E configuration rather than cis/Z configuration, four compounds, **v01**, **v37**, **v38** and **v44**, with four different function groups were chosen to be optimized with Gaussian09.[166] The geometries of all compounds in this dissertation were fully optimized with the density functional theory (DFT) employing the Beck's three-parameter hybrid exchange functional and the Lee-Yang-Parr correlation function (B3LYP) with the basis set of 6-31+G*. To evaluate the zero-point vibration energy and to confirm that the optimized structures were really global minima on the potential energy surface, the harmonic vibration-al were calculated at the same level of B3LYP/6-31+G* in water with SMD as solvation model. The SMD[167] model was developed more recently compared with other self-consistent reaction field (SCRF) such as IEFPCM[168] and CPCM,[169, 170]. A highlight for SMD is that it took more than two thousand experimental solvation free energies as training set for better predictions.[167, 171, 172] For these reasons, the SMD is believed to be a more accurate method than other commonly applied solation models. Therefore, we choose SMD as the solvation model in our study.

Table 3.3 Theoretical Relative Gibbs Free Energies of Z configuration to E configuration (in water)

Name	Theoretical Relative Gibbs Free Energies ($\Delta G_{Z\text{-}E}$ kcal/mole) of Z configuration in water*
v01	2.9
v37	5.6
v38	4.3
v44	7.6

$\Delta G_{Z\text{-}E}$=G(Z configuration) - G(E configuration)

In this study, we set the Gibbs free energy of the E configuration as zero point. Based on the above calculation, the E configurations are more stable than the corresponding Z configuration for the calculated compounds. Therefore, all of these 2-cyano-3-phenylacrylic acid derivatives should adapt the E configuration.

3.2.5 Binding mode analysis

In order to study the inhibition mechanism of this series of derivatives, we applied molecular docking to predict the binding mode of compounds **v20** with human and mouse mPGES-1.

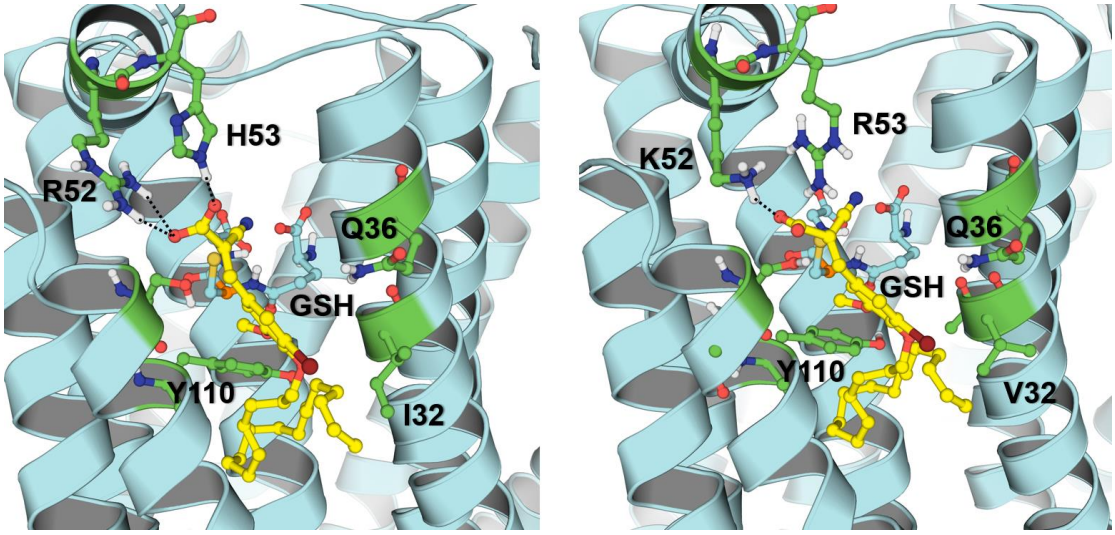

Figure 3.3 predicted binding mode of **v20** with human (left) and mouse (right) mPGES-1

The hydrogen bonds between the carboxyl group of **v20** and the residues on the loop (R52 and H53 for human mPGES-1; K52 and R53 for mouse mPGES-1) are of great importance for the inhibitory activates against human and mouse mPGES-1. Replacement of the carboxyl group with other groups such as esters will result in significant loss of inhibitory activity. Flexibility of this compound makes it possible to bind with both human and mouse mPGES-1.

3.3 Conclusions

In conclusion, a series of 2-cyano-3-phenylacrylic acid derivatives have been identified as human mPGES-1 inhibitors. Amongst them, several compounds were identified as dual inhibitors against both human and mouse mPGES-1. Six compounds showed IC_{50} less than 100 nM. The most potent human mPGES-1 inhibitors are **v20** and **v27**, with IC_{50} values of 51 and 50 nM against human mPGES-1 respectively. What's more, with IC_{50} values both below 400 nM, they are also potent mouse mPGES-1 inhibitors. Their activities against the mouse mPGES-1 will avoid the possible troubles of the KI/KO mouse and make the future animal study with mouse disease models feasible. The SAR studies and binding mode investigation demonstrate that for this 2-cyano-3-phenylacrylic acid scaffold, the cyano substitution and carboxylic substitution for Y position, the bigger hydrophobic groups are favorable for improving *in vitro* inhibitory activities. On the other hand, the ester structure and the amide group at Y position and the phenyl group for R are not favorable for high activities. The presented SAR indicates that further decoration of the phenyl group in the middle may provide us more potent dual inhibitors against human and mouse.

3.4 Experimental section

3.4.1 Chemistry

^{1}H NMR and ^{13}C NMR spectra were recorded on 400 or 500 MHz spectrometers using tetramethylsilane (TMS) as the internal standard. Chemical shifts are reported in parts per million (ppm) downfield from TMS. The spin multiplicities are described as s (singlet), d (doublet), dd (double doublet), t (triplet), q (quartet), or m (multiplet). Coupling constants are calculated and reported in Hertz (Hz). Analytical thin layer chromatography (TLC) was performed on commercial available precoated silica gel 60- F254 (0.5 mm) glass plates. Visualization of the spots on TLC plates was achieved either by exposure to iodine vapor or UV light. Column chromatography was performed

using silica gel of 100–200 mesh. Moisture sensitive reactions were carried out using standard syringe septum Techniques and under inert atmosphere of nitrogen. All solvents and reagents were used without further purification. All evaporation of solvents was carried out under reduced pressure on rotary evaporator below 70 °C. The names of all the compounds given in the experimental section were taken from the ChemDraw.[173]

The high performance mass spectrometer (HPMS) used in this study was AB SCIEX triple TOFTM-5600 (AB SCIEX,Redwood City, CA, U.S.A.). All the compounds were run in positive ion and high sensitivity mode under the conditions and settings as described before.[174] The positive ions were generated in the source using nitrogen as the source gases. Source gas temperature was set at 500 °C. Ion spray voltage floating (ISVF) was set to 3000 V. The Analyst® TF 1.7 software package (AB SCIEX, Redwood City, CA, U.S.A.) was used for instrument control and HPMS data acquisition. The Multi-Quant TM3.0 software (AB SCIEX, Redwood City, CA, U.S.A.) was used for quantitative analysis.[174]

3.4.2 General method for the synthesis of target compounds

The reaction of substituted hydroxyl aldehydes and different halogenated hydrocarbons give the alkylated aldehydes, which were further converted to their corresponding target compounds (**v01** ~ **v58**). The synthesis of the starting materials and representative target compounds is illustrated in Scheme 3.3.

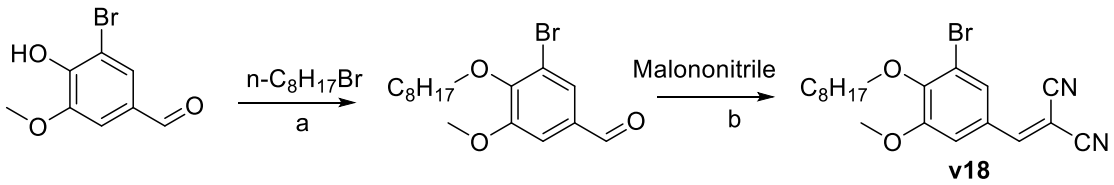

Scheme 3.3 Reagents and conditions for the synthesis of **v18**

(a) DMF, K_2CO_3, 80℃, 80% ~ 90%; (b) Malononitrile, acetic acid, EtOH, reflux, 40% ~ 80%.

3.4.3 Structural information of representative target compounds

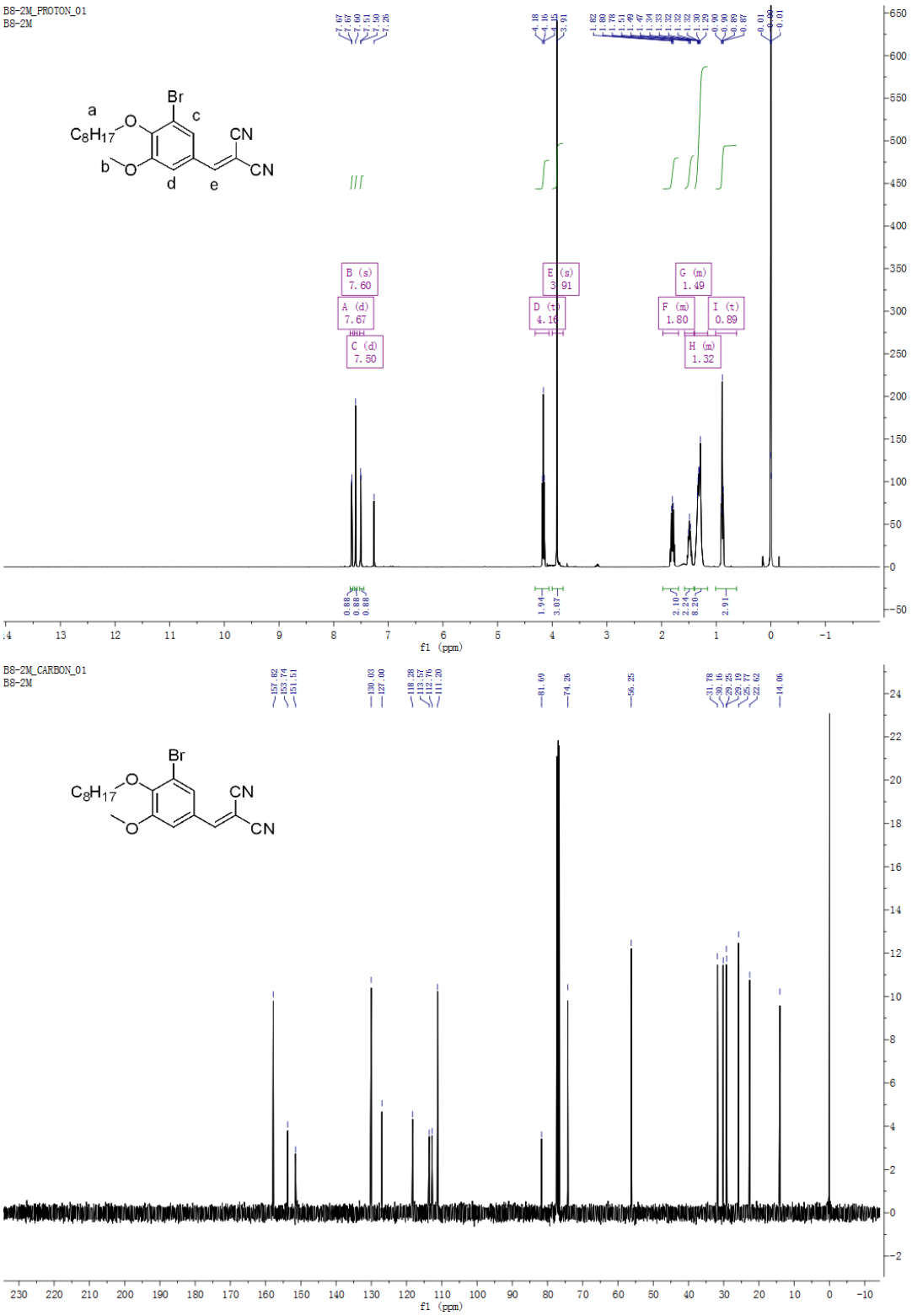

Figure 3.4 ^{1}H NMR and ^{13}C NMR for representative compound **v18**

The ^{1}H NMR and ^{13}C NMR spectrum of representative compound **v18** in $CDCl_3$ is shown in **Figure 3.4**. In this figure, all ^{1}H NMR peaks and ^{1}H-^{1}H coupling are well resolute, and could be assigned to the molecular structure. c-H: δ 7.67 (d, J = 2.1 Hz, 1H), e-H: 7.60 (s, 1H), d-H: 7.50 (d, J = 2.1 Hz, 1H), a-H: 4.16 (t, J = 6.6 Hz, 2H), b-H: 3.91 (s, 3H), a-H: 1.98 – 1.69 (m, 2H), a-H: 1.58 – 1.41 (m, 2H), a-H: 1.39 – 1.16 (m, 8H), a-H: 0.89 (t, J = 8.7, 5.0 Hz, 3H).

Structures, Names, ^{1}H NMR and ^{13}C NMR data for all of the 58 2-cyano-3-phenylacrylic acid derivatives were summarized in **Appendix I**, **Table I-1**. Calculated and found molecular weights of protonated target compounds were summarized in **Appendix II**, **Table II-1**.

Chapter 4: Design and synthesis 1, 3-Diphenylpyrazole derivatives as human mPGES-1 inhibitors

Summary: Human mPGES-1 has emerged as prospective target in the exploration of next-generation of anti-inflammatory drugs, as specific mPGES-1 inhibitors are expected to discriminatively suppress the production of induced PGE_2 without blocking the normal biosynthesis of other prostanoids including homeostatic PGE_2. Therefore, this therapeutic approach is believed to be able to reduce the adverse effects associated with the application of traditional non-steroidal anti-inflammatory drugs (tNSAIDs) and selective COX-2 inhibitors (coxibs). Identified from structure-based virtue screening, the lead was used in the design of novel inhibitors based on the binding mode with the enzyme structure. We recently developed a class of benzylidenebarbituric acid derivatives as inhibitors against both human and mouse mPGES-1. In order to further identify potent inhibitors with novel chemical scaffolds, as continued efforts, we thereby report the synthesis and in vitro evaluation of 5-((1,3-diphenyl-1*H*-pyrazol-4-yl)methylene)pyrimidine-2,4,6(1*H*,3*H*,5*H*)-trione (**py20**) and related 1, 3-Diphenylpyrazole derivatives as potent mPGES-1 inhibitors.

4.1 Introduction

In the eicosanoid pathway, arachidonic acid (AA) is converted to prostaglandin H_2 (PGH_2) by the action of cyclooxygenases (COX-1 and COX-2).[175-177] PGH_2 serves as common precursor for various biologically active prostanoids, such as thromboxane A_2 (TXA_2), PGD_2, PGI_2, $PGF_{2\alpha}$ and PGE_2, depending on different distal synthases.[19, 43, 178] Among these prostanoids, PGE_2, well recognized as an important inflammatory mediator, is isomerized from PGH_2 catalyzed by three distinct synthases (mPGES-1, mPGES-2 and cPGES).[177, 179-181] Unlike the other two constitutively expressed enzymes, the expression of mPGES-1, similar to that of COX-2, is highly inducible in response to pro-inflammatory stimuli.[177, 182]

As two generations of anti-inflammatory drugs, tNSAIDs and coxibs represent the mainstream for the treatment of inflammation-related symptoms by either non-selectively inhibiting COX isozymes or selectively inhibiting COX-2, respectively.[165, 183, 184] However, both of these two categories of drugs inhibit the biosynthesis of all downstream prostanoids and so their application is associated with considerable adverse effects.[185-189] tNSAIDs trigger gastrointestinal (GI) ulceration because of the interference with COX-1-derived protective function in GI tract.[16, 153, 190, 191] Coxibs, as a class of specific COX-2 inhibitors,[192] on the other hand, break the internal balance of vasodilative PGI_2 and vasoconstrictive TXA_2 and thus result in cardiovascular risk.[193-195] Since PGE_2 is the major inducible PG in inflammation, inhibiting mPGES-1 is recognized as a prospective candidate therapeutic approach in the development of the next generation of anti-inflammatory drugs.[26, 28, 43, 196]

We recently developed a series of benzylidenebarbituric acid derivatives as inhibitors against both human and mouse mPGES-1 enzymes. As we carefully analyzed the binding mode of these compounds with human mPGES-1 crystal structure (PDB: 4BPM)[120] it is observed that there is still substantial unoccupied area in the active pocket. We decided to introduce pyrazole core not only because of its existence in many bioactive molecules, but also its versatility for multi-functionalization.[71, 197-202] Thus, a series of *5-((1,3-diphenyl-1H-pyrazol-4-yl) methylene) pyrimidine-2,4,6(1H,3H,5H) -trione* derivatives and other structurally related compounds were designed and synthesized. A number of these compounds were active against both human and mouse mPGES-1 enzymes and selective over COX isozymes.

4.2 Results and Discussions

4.2.1 Lead compound

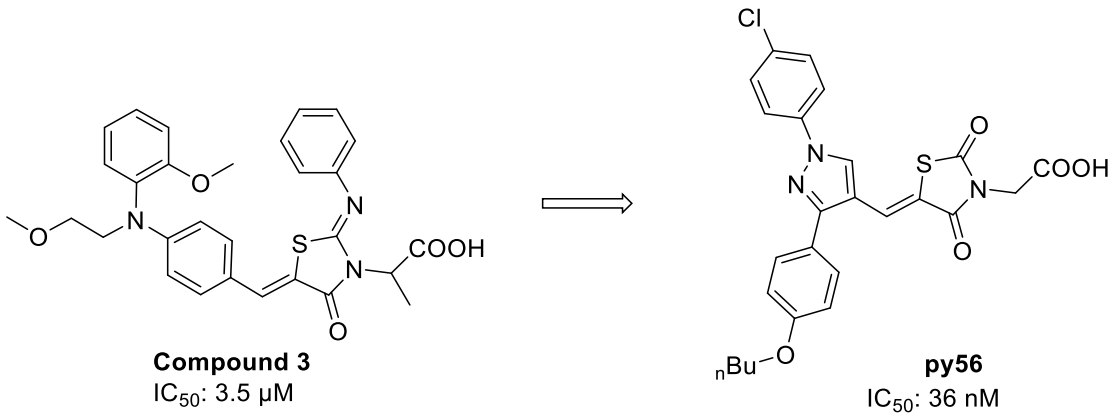

Scheme 4.1 From **Compound 3**[1] to **py56**, structural similarity between the lead compound and the most potent human mPGES-1 inhibitor in this Chapter.

Compound 3 is a human mPGES-1 inhibitor identified by Zhan *et al.* in 2011 through structure-based virtual screening.[1] With IC_{50} of 3.5 μM, it is a moderate human mPGES-1 inhibitor.

4.2.2 Inhibitory activity against human and mouse mPGES-1

The synthesized compounds were tested by employing cell-free mPGES-1 activity assays as described in Chapter 1.

Table 4.1 Structures and activities for 1, 3-Diphenylpyrazoles analogs py01-py56

ID (code)	Structures of Pyrazole compounds.	IC_{50}/nM or (%Inhibition)[c] Against human mPGES-1[a]	IC_{50}/nM or (%Inhibition) Against mouse mPGES-1
py01 (10a)	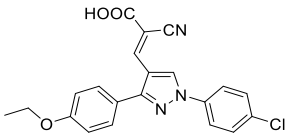	282 ± 83	(12.0 ± 2.9)

py02	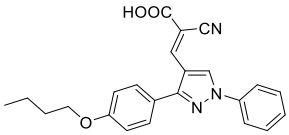	296 ± 68	(20.6 ± 4.2)
py03	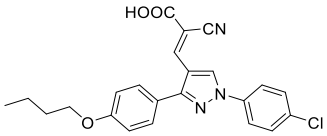	190 ± 68	(30.3 ± 3.2)
py04 (11a)	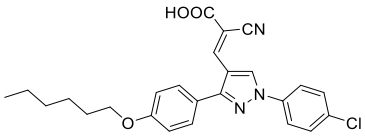	83 ± 30	(47.9 ± 5.2)
py05	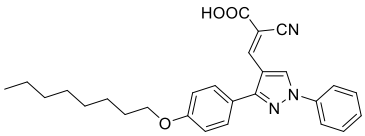	209 ± 42	(45.8 ± 8.5)
py06	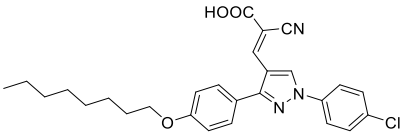	90 ± 15	(29.2 ± 2.3)
py07	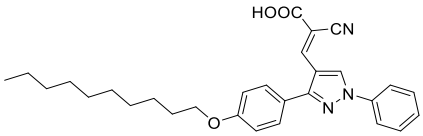	197 ± 32	(4.3 ± 20.8)
py08	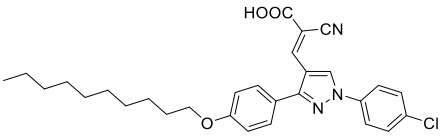	97 ± 15	(4.6 ± 21.6)
py09	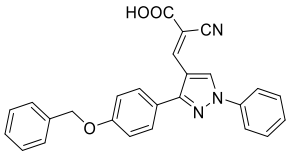	806 ± 162	(15.9 ± 22.8)
py10 (10b)	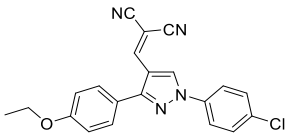	(51.0 ± 10.0)	N.D.[b]
py11	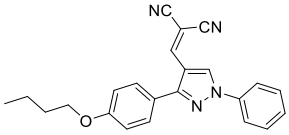	(53.9 ± 6.8)	N.D.

py12	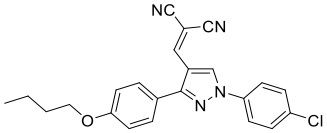	(77.1 ± 3.9)	N.D.
py13 (11b)	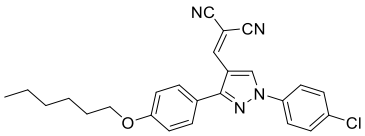	(63.7 ± 1.4)	N.D.
py14	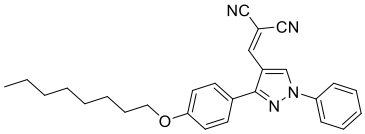	(54.9 ± 1.7)	N.D.
py15	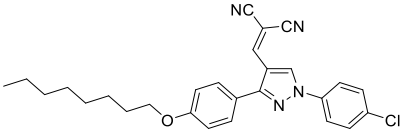	(52.2 ± 4.7)	N.D.
py16	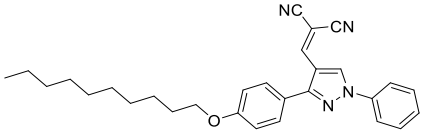	(48.8 ± 3.6)	N.D.
py17	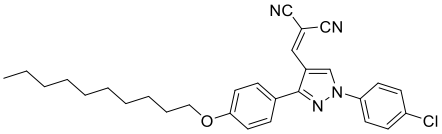	(47.3 ± 7.9)	N.D.
py18	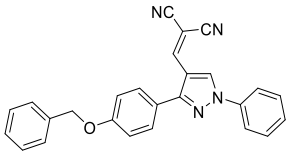	(39.0 ± 6.6)	N.D.
py19 (4b)	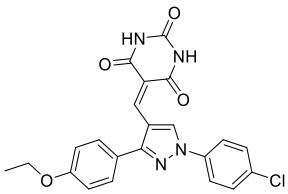	265 ± 96	(27.6 ± 4.7)
py20 (8)	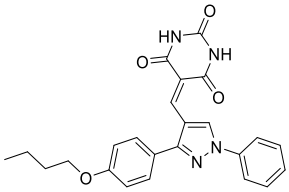	212 ± 34	2573 ± 628

py21 (4c)	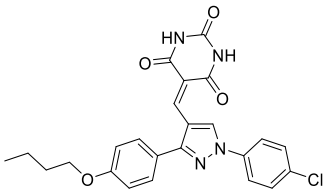	169 ± 41	357 ± 75
py22 (4d)	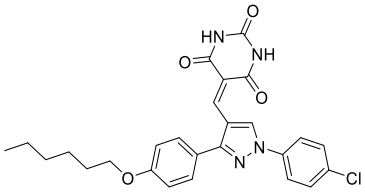	285 ± 65	(45.6 ± 2.2)
py23	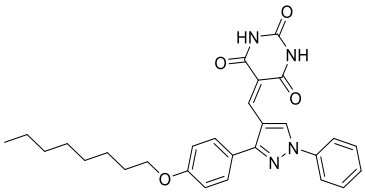	323 ± 52	2157 ± 188
py24 (4e)	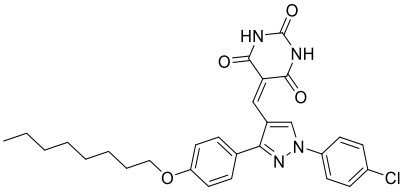	361 ± 51	740 ± 108
py25	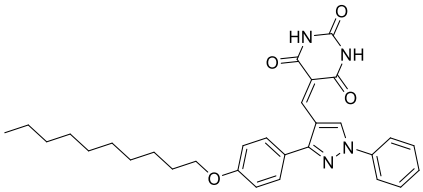	375 ± 127	(20.8 ± 4.2)
py26 (4f)	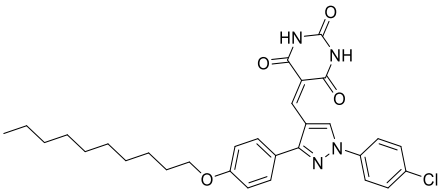	294 ± 83	(23.9 ± 9.8)
py27 (4g)	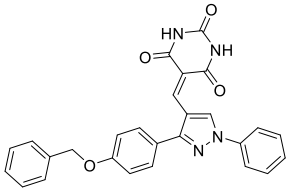	598 ± 142	(-4.4 ± 9.2)
py28 (4a)	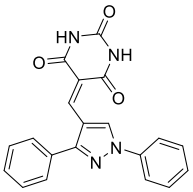	337 ± 85	(18.4 ± 9.2)

py29 (5b)	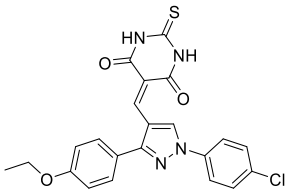	95 ± 16	(46.4 ± 8.7)
py30	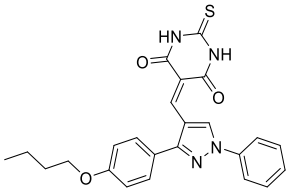	92 ± 20	1264 ± 138
py31 (5c)	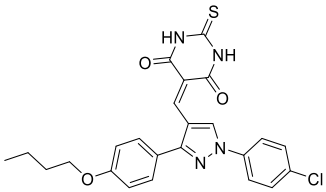	56 ± 10	445 ± 83
py32 (5d)	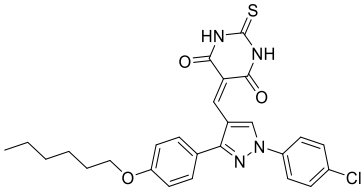	52 ± 15	1769 ± 1158
py33	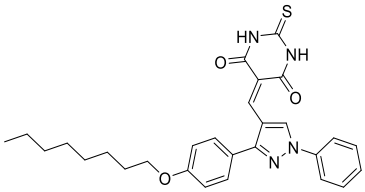	113 ± 23	1126 ± 131
py34 (5e)	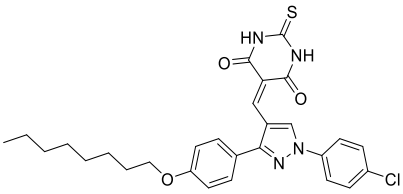	92 ± 19	316 ± 30
py35	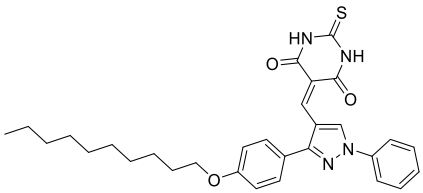	188 ± 31	(49.8 ± 14.5)
py36 (5f)	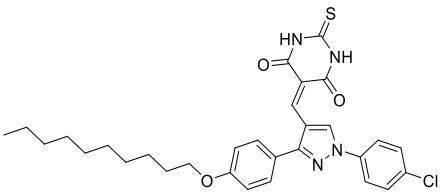	93 ± 14	(55.6 ± 25.4)

py37 (5g)	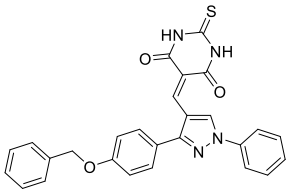	797 ± 160	(24.5 ± 5.0)
py38 (5a)	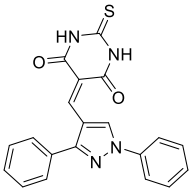	561 ± 192	(2.6 ± 5.9)
py39	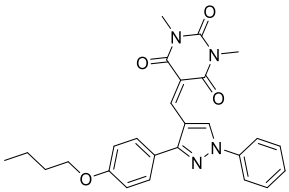	(30.3 ± 6.4)	N.D.
py40	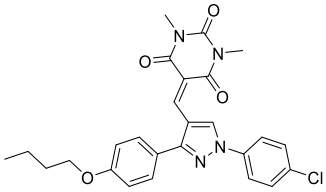	(29.1 ± 1.5)	N.D.
py41	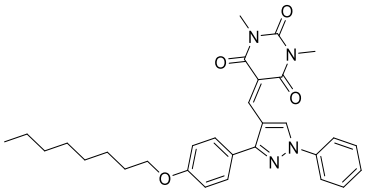	(15.5 ± 7.2)	N.D.
py42	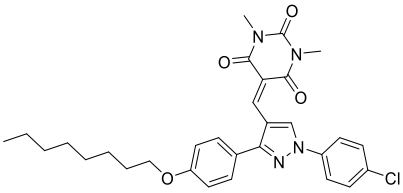	(6.8 ± 2.5)	N.D.
py43	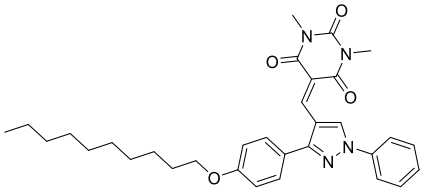	(-1.9 ± 2.5)	N.D.
py44	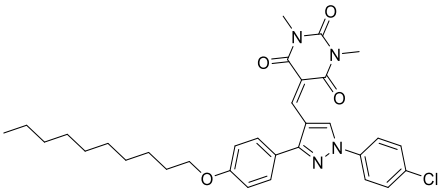	(-2.2 ± 1.1)	N.D.

py45 (10c)	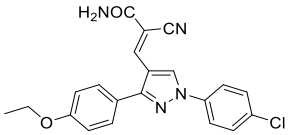	(31.9 ± 21.2)	N.D.
py46 (11c)	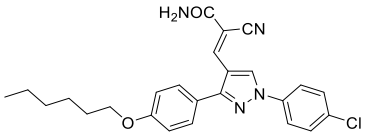	(14.1 ± 14.1)	N.D.
py47	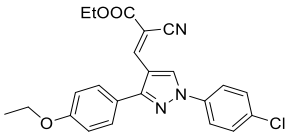	(23.5 ± 6.8)	N.D.
py48	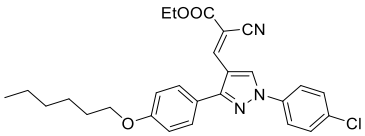	(37.1 ± 2.3)	N.D.
py49 (10d)	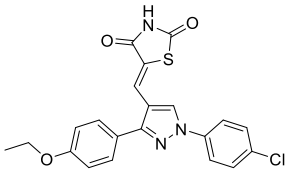	1593 ± 557	N.D.
py50 (11d)	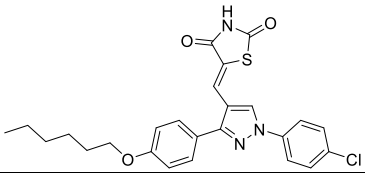	1394 ± 303	N.D.
py51	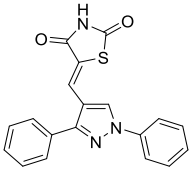	4932 ± 1161	N.D.
py52	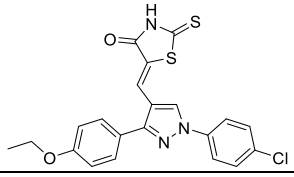	1036 ± 293	N.D.
py53 (11e)	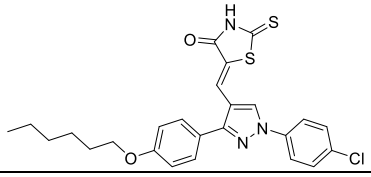	1729 ± 666	N.D.
py54	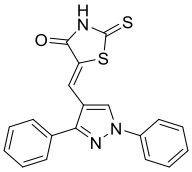	1878 ± 426	N.D.

py55	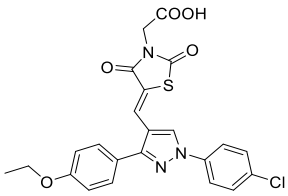	41 ± 5	(35.4 ± 3.4)
py56 (11f)	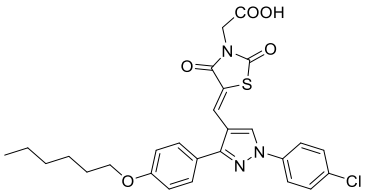	36 ± 11	(37.0 ± 16.1)

[a]Data are expressed as means ± SD of single determinations obtained in triplicate. [b]n.d. = not detected. [c]The % inhibition of the compound at a concentration of 10 µM against mPGES-1 (IC_{50} values were determined if the compounds caused in 70 % or higher inhibition).

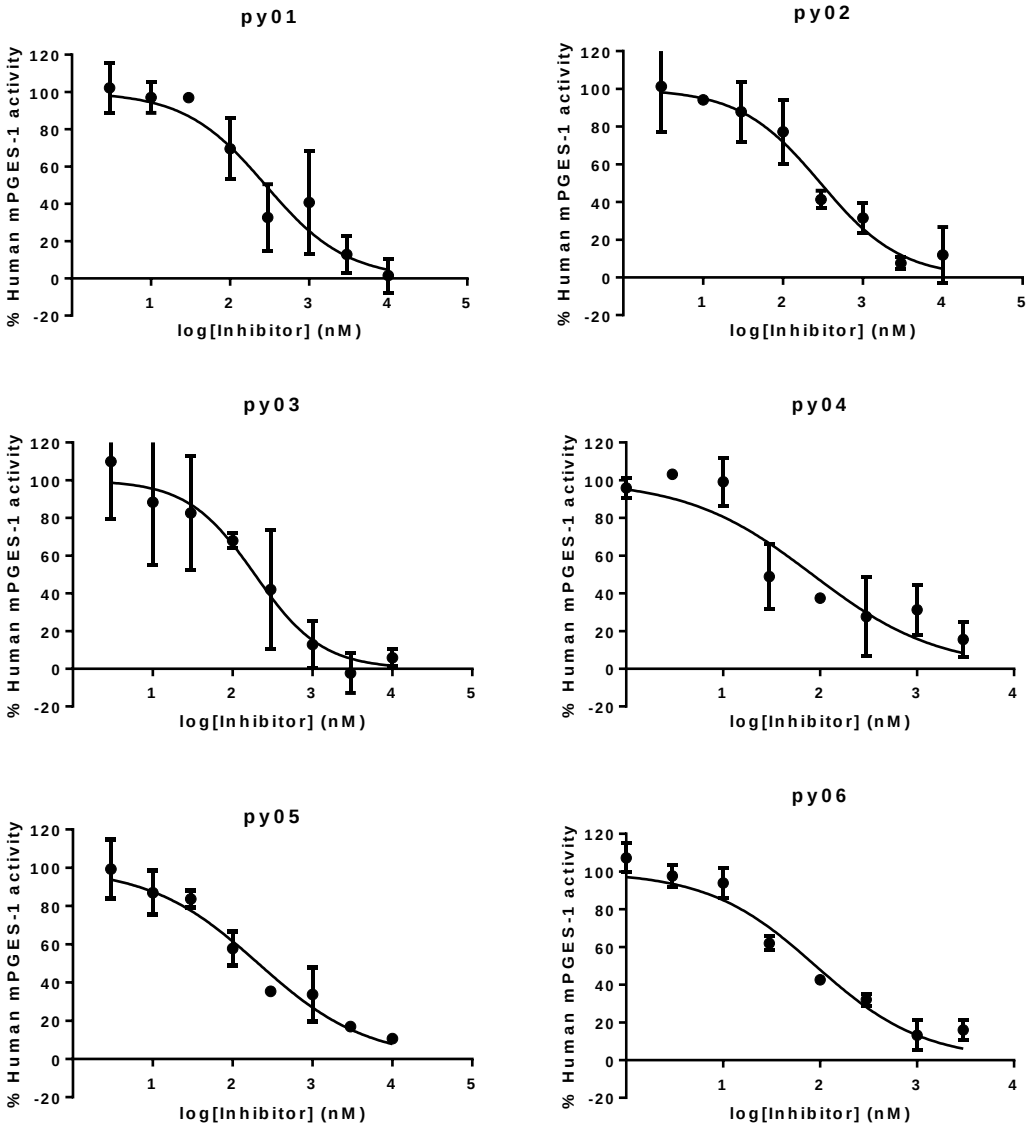

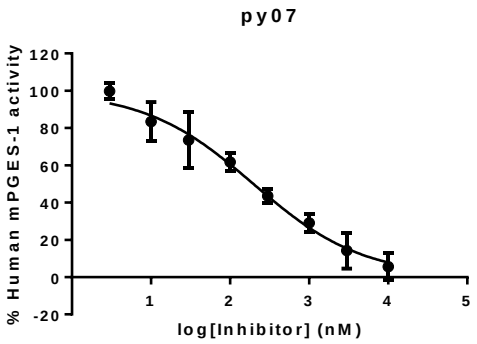
py07
% Human mPGES-1 activity
log[Inhibitor] (nM)

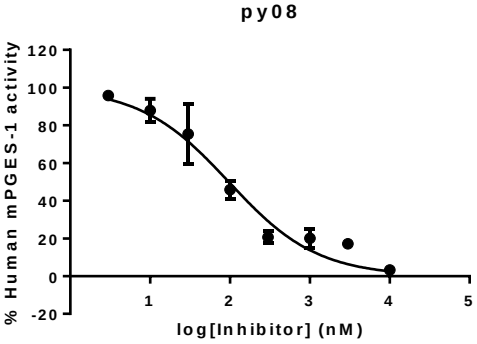
py08
% Human mPGES-1 activity
log[Inhibitor] (nM)

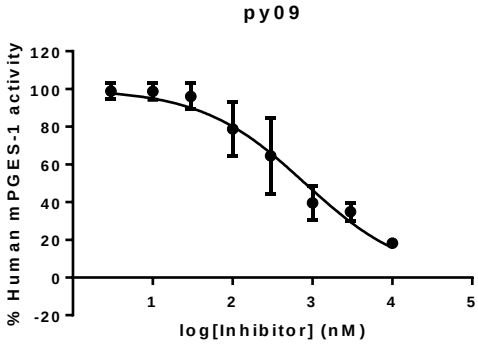
py09
% Human mPGES-1 activity
log[Inhibitor] (nM)

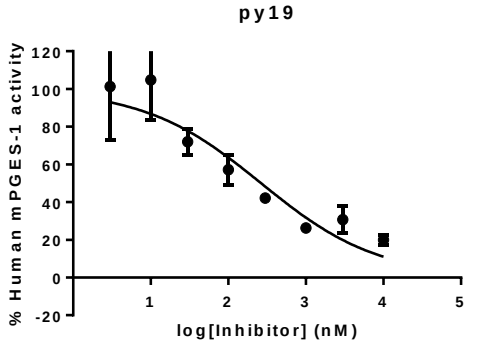
py19
% Human mPGES-1 activity
log[Inhibitor] (nM)

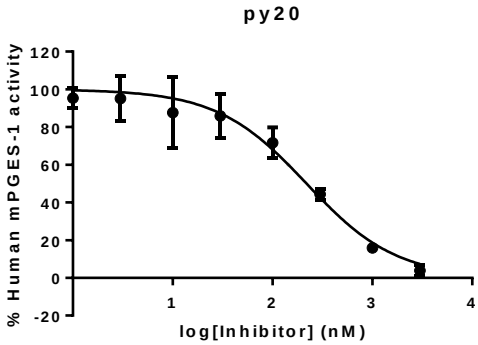
py20
% Human mPGES-1 activity
log[Inhibitor] (nM)

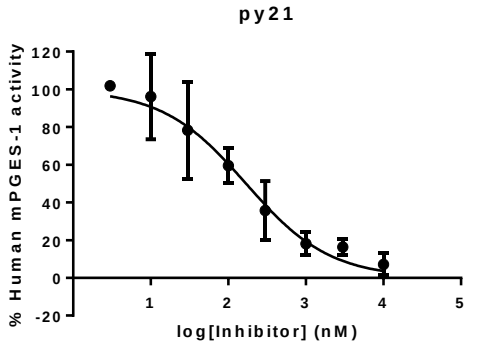
py21
% Human mPGES-1 activity
log[Inhibitor] (nM)

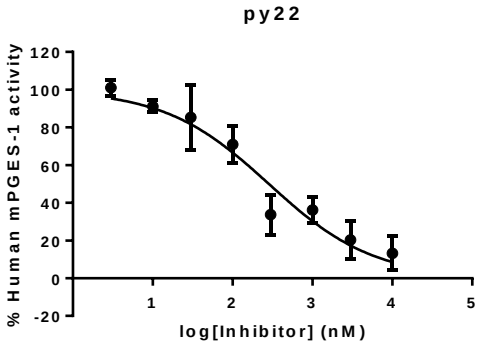
py22
% Human mPGES-1 activity
log[Inhibitor] (nM)

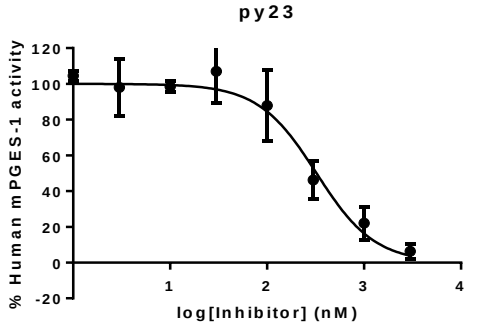
py23
% Human mPGES-1 activity
log[Inhibitor] (nM)

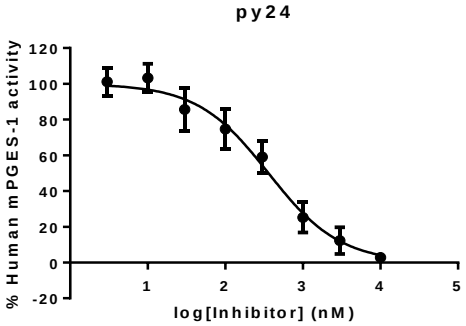
py24
% Human mPGES-1 activity
log[Inhibitor] (nM)

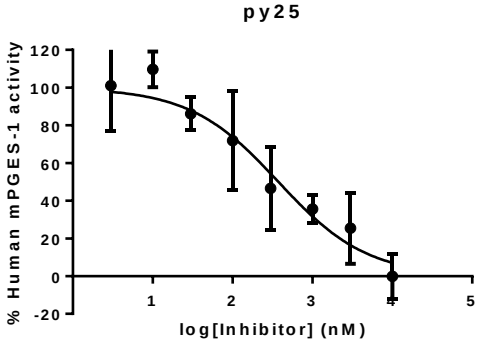
py25
% Human mPGES-1 activity
log[Inhibitor] (nM)

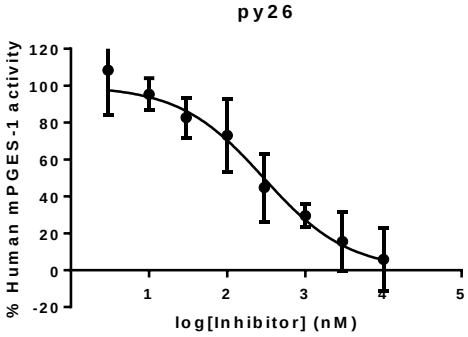
py26
% Human mPGES-1 activity
log[Inhibitor] (nM)

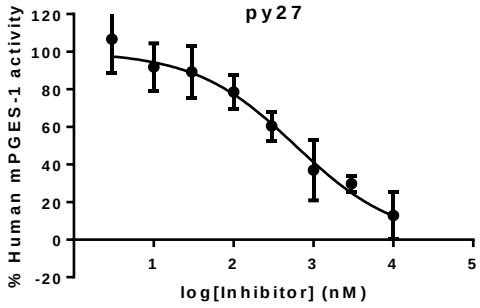
py27
% Human mPGES-1 activity
log[Inhibitor] (nM)

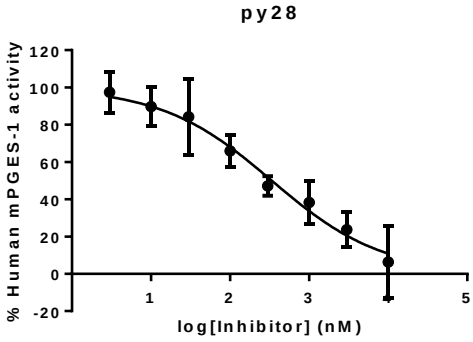
py28
% Human mPGES-1 activity
log[Inhibitor] (nM)

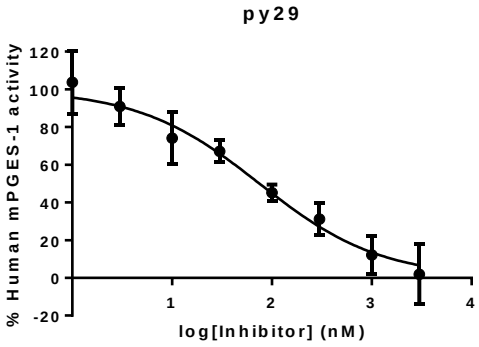
py29
% Human mPGES-1 activity
log[Inhibitor] (nM)

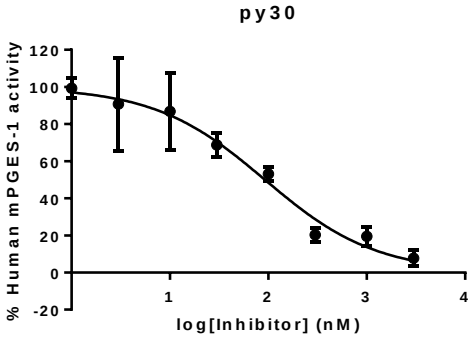
py30
% Human mPGES-1 activity
log[Inhibitor] (nM)

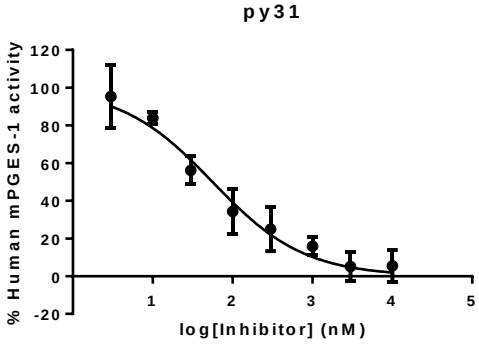
py31
% Human mPGES-1 activity
log[Inhibitor] (nM)

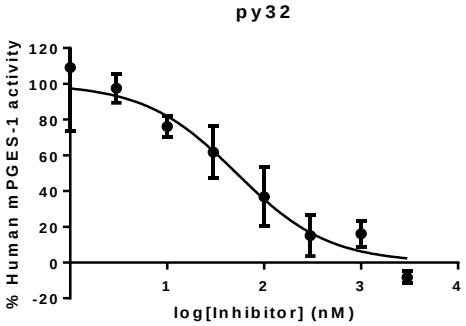
py32
% Human mPGES-1 activity
log[Inhibitor] (nM)

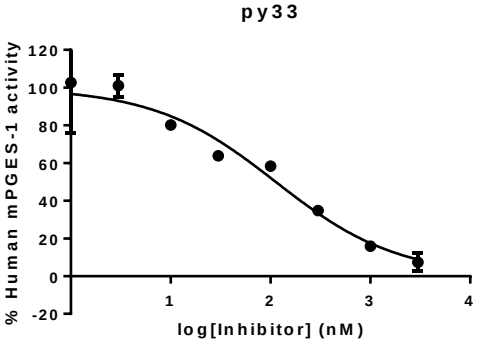
py33
% Human mPGES-1 activity
log[Inhibitor] (nM)

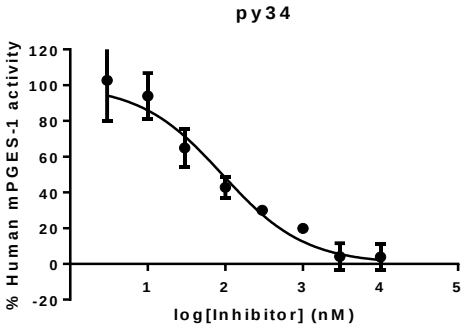
py34
% Human mPGES-1 activity
log[Inhibitor] (nM)

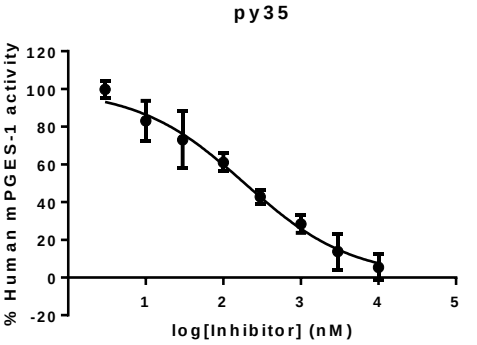
py35
% Human mPGES-1 activity
log[Inhibitor] (nM)

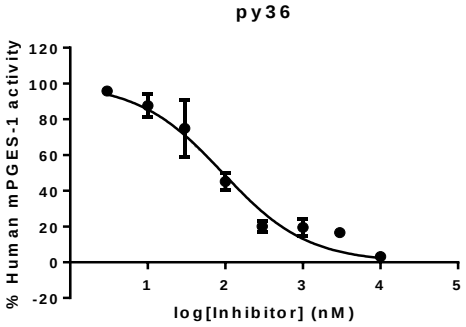
py36
% Human mPGES-1 activity
log[Inhibitor] (nM)

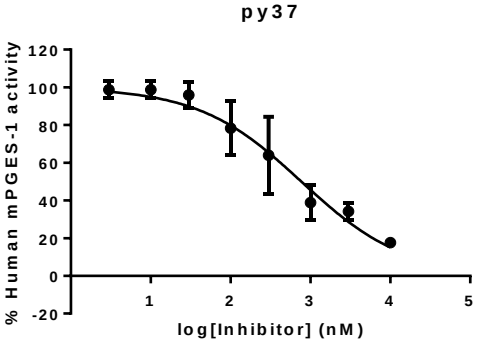
py37
% Human mPGES-1 activity
log[Inhibitor] (nM)

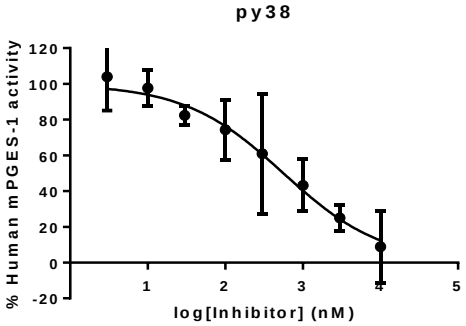
py38
% Human mPGES-1 activity
log[Inhibitor] (nM)

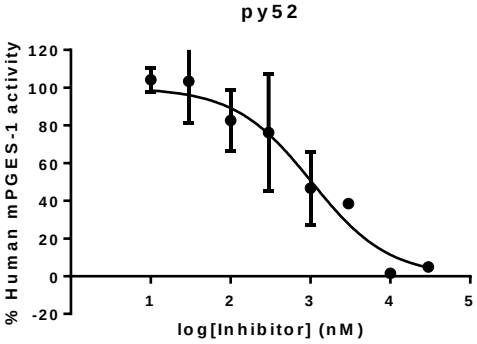
py52
% Human mPGES-1 activity
log[Inhibitor] (nM)

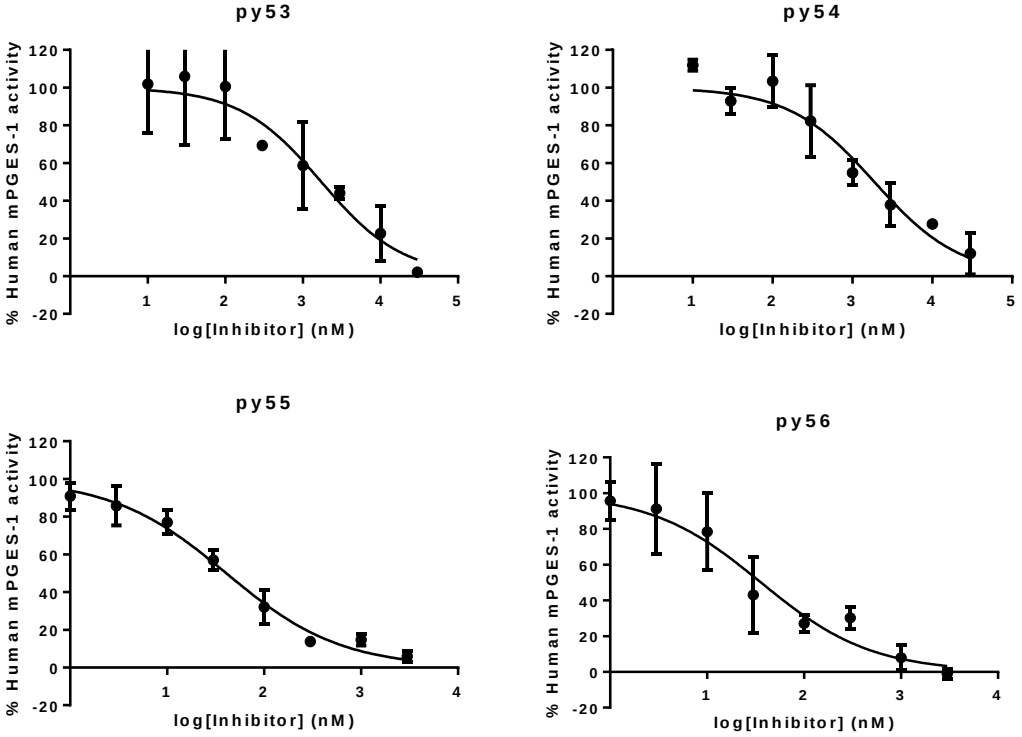

Figure 4.1 Human mPGES-1 inhibitory activity of 1, 3-Diphenylpyrazoles derivatives. The inhibitor concentration is given in log scale.

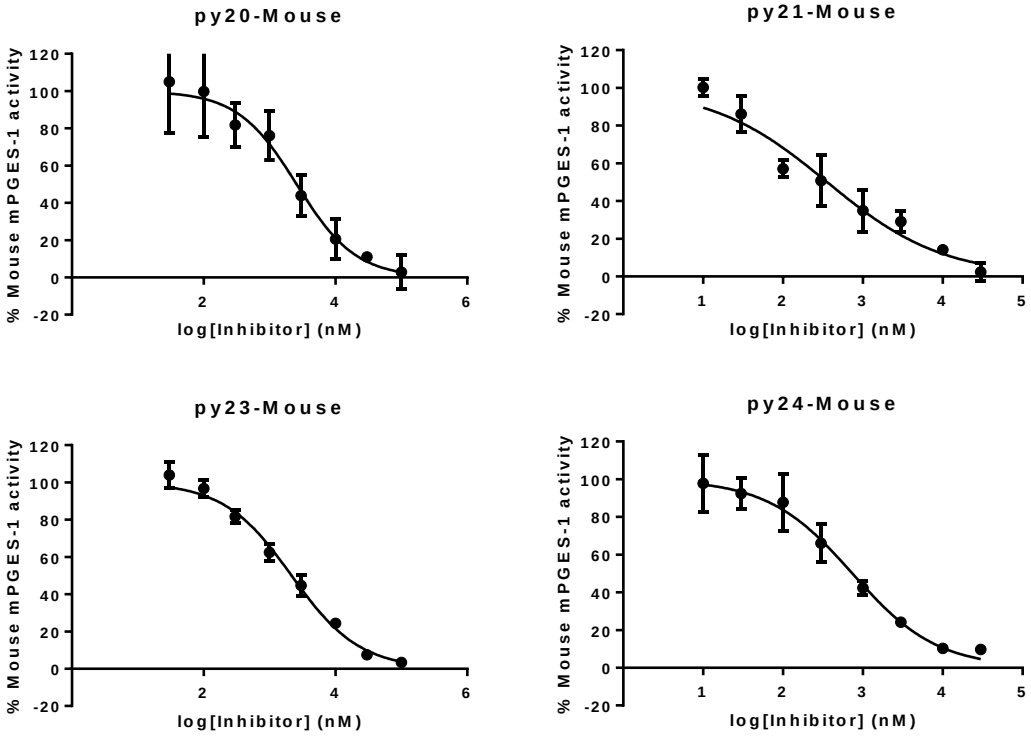

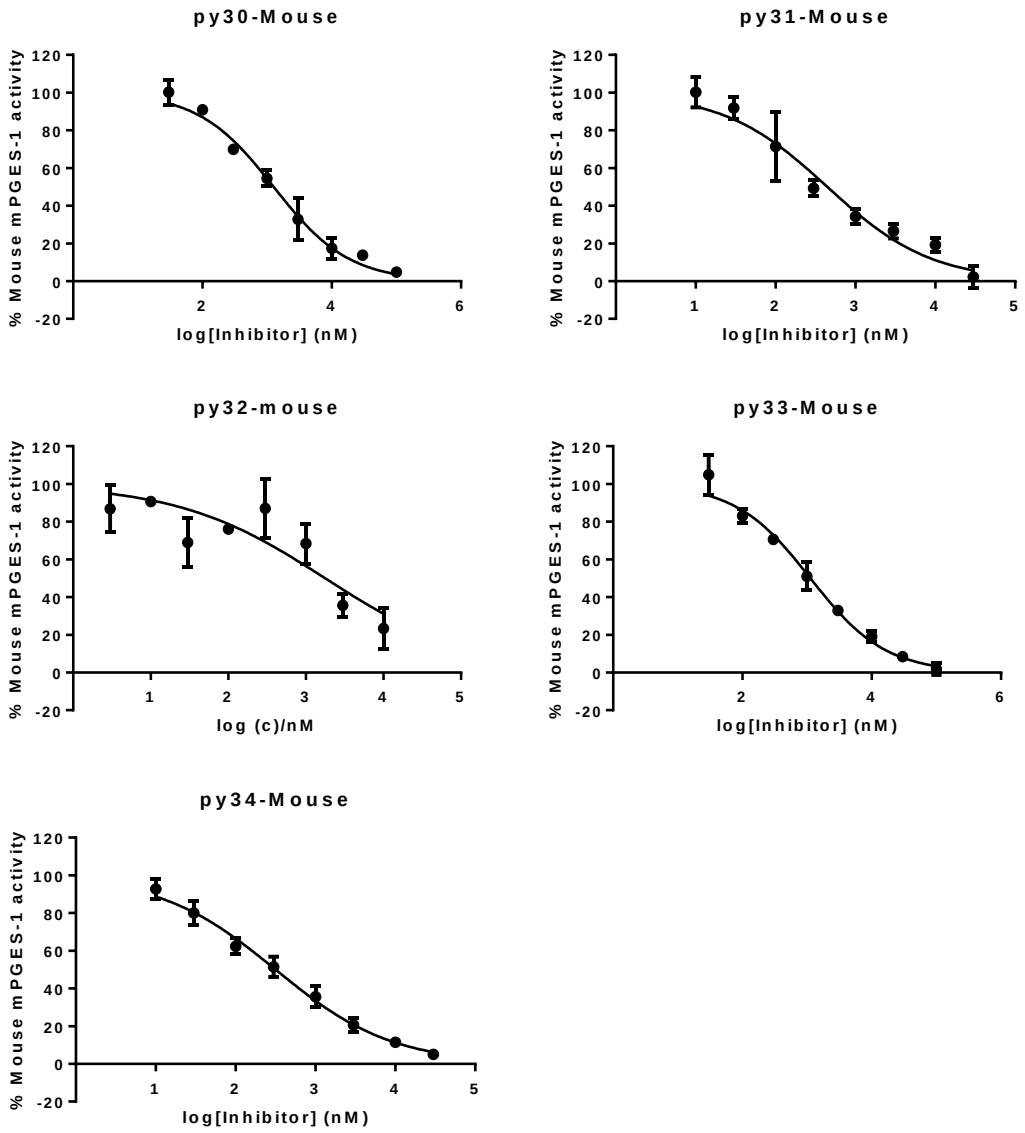

Figure 4.2 Mouse mPGES-1 inhibitory activity of 1, 3-Diphenylpyrazoles derivatives. The inhibitor concentration is given in log scale.

4.2.3 Off target testing

The selectivity of newly obtained 1,3-Diphenylpyrazoles derivatives on human mPGES-1 over COXs was tested for ten most potent compounds that showed IC_{50} values below 100 nM. The assay was carried out by employing the same protocol as described in section 3.2.3.

Table 4.2 Inhibition of the most potent mPGES-1 inhibitors against COXs

Name	%/Inhibition at 100 μM
py04	18.9 ± 0.1
py08	17.2 ± 0.0
py29	1.0 ± 4.5
py30	16.0 ± 4.1
py31	4.4 ± 8.6
py32	0.7 ± 5.4
py34	-2.0 ± 0.2
py36	11.1 ± 16.3
py55	6.8 ± 6.4
py56	1.2 ± 28.6

The six compounds tested show no significant inhibition against COXs at 100 μM. This result indicates that these six compounds have high selectivity on mPGES-1 over COXs. Based on the structural similarity of this compound set, we could expect that the presented 1, 3-Diphenylpyrazoles derivatives will show no significant inhibition against COXs.

4.2.4 SAR study

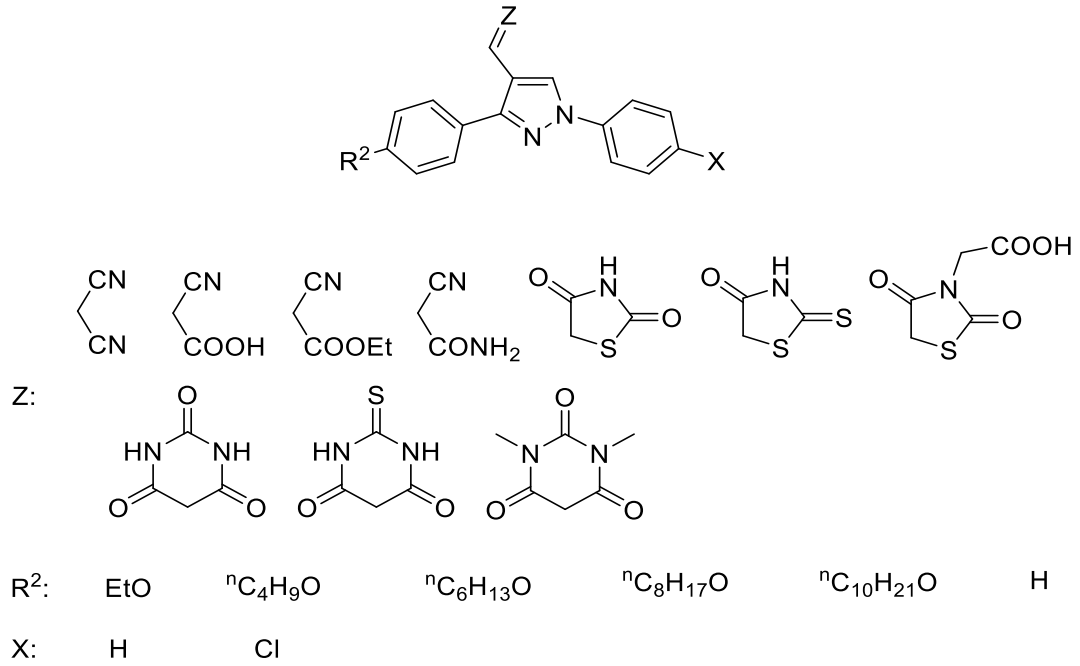

Scheme 4.2 The scaffold of 1, 3-Diphenylpyrazoles derivatives.

Table 4.3 and 4.4 highlights the SAR for the 1, 3-Diphenylpyrazoles derivatives. These studies reveal that the inhibition of the 1, 3-Diphenylpyrazoles derivatives was totally depend on the nature and position of the substituents present on the X position and Z position in Scheme 4.2.

Table 4.3 SAR on the substitution of central pyrazole ring

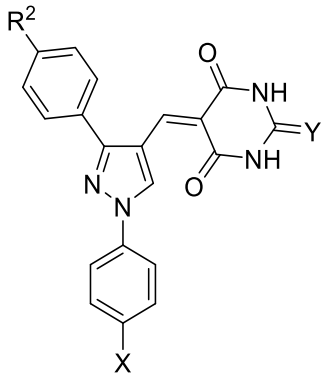

Compound	R^2	X	Y	IC_{50}[a] for human mPGES-1 (μM)	IC_{50} for mouse mPGES-1 (μM)
(4a) py28	H	Cl	O	0.337±0.085	n.d.[b] (18.4±9.2)[c]
(4b) py19	EtO	Cl	O	0.265±0.096	2.57±0.63
(4c) py21	$^nC_4H_9O$	Cl	O	0.169±0.041	0.357±0.075
(4d) py22	$^nC_6H_{13}O$	Cl	O	0.285±0.065	n.d. (45.6±2.2)
(4e) py24	$^nC_8H_{17}O$	Cl	O	0.361±0.051	0.740±0.108
(4f) py26	$^nC_{10}H_{21}O$	Cl	O	0.294±0.083	n.d. (23.9±9.8)
(4g) py27	BnO	Cl	O	0.598±0.142	n.d. (-4.4±9.2)
(5a) py38	H	Cl	S	0.561±0.192	n.d. (2.6±5.9)
(5b) py29	EtO	Cl	S	0.095±0.016	n.d. (46.4±8.7)
(5c) py31	$^nC_4H_9O$	Cl	S	0.056±0.010	0.445±0.083
(5d) py32	$^nC_6H_{13}O$	Cl	S	0.052±0.015	1.77±1.16
(5e) py34	$^nC_8H_{17}O$	Cl	S	0.092±0.019	0.316±0.030
(5f) py36	$^nC_{10}H_{21}O$	Cl	S	0.093±0.014	n.d. (55.6±25.4)
(5g) py37	BnO	Cl	S	0.797±0.160	n.d. (24.5±5.0)
(8) py20	$^nC_4H_9O$	H	O	0.212±0.034	2.57±0.63
(9) py30	$^nC_4H_9O$	H	S	0.092±0.020	1.26±0.14

[a]Data are expressed as means ± SD of single determinations obtained in triplicate. [b]n.d. = not detected. [c]The % inhibition of the compound at a concentration of 10 μM against mPGES-1 (IC_{50} values were determined if the compounds caused in 70 % or higher inhibition).

The length and shape of the aliphatic side chain were investigated in the SAR study. We fixed the substituent at pyrazole-1-position as 4-chlorophenyl and variate the side chain on 3-phenyl. From the *in vitro* data shown in **Table 4.3**, it was observed as compared to that without an side chain (**1a**), compounds with linear side chains (**4b~4f** and **5b~5f**) generally more potent against human mPGES-1, while benzyl substitution (**4g** and **5g**), however, did not improve the inhibitory efficacy. Linear side chains with 4 or 6 carbons yielded compounds with highest potency, while longer side chains, such as octyl or decyl did not give a better inhibition. Another fact was that compounds with 2-thiobarbituric acid "heads" were generally more potent as compared to those with barbituric acid ones. We also changed the substituent in pyrazole-1-position from 4-chlorophenyl to phenyl group. In this case, **1c** was used as starting substituted acetophenone. Followed the similar protocol as shown in **Scheme 2**, **8** and **9** were prepared. These compounds (**8** and **9**) were slightly less potent than those with 4-chlorophenyl substituent (**4c** and **5c**, respectively).

Table 4.4 SAR on the polar head

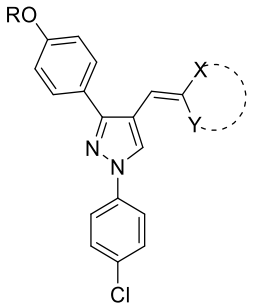

Compound	R		IC_{50}[a] for human mPGES-1 (μM)	IC_{50} for mouse mPGES-1 (μM)
(10a) py01	Et	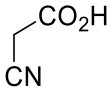	0.283±0.083	n.d.[b] (12.0±2.9)[c]
(10b) py10	Et		n.d. (51±10)	n.d.
(10c) py45	Et	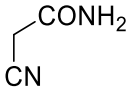	n.d. (32±21)	n.d.
(10d) py49	Et	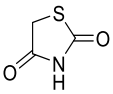	1.59±0.56	n.d.
(10e) py52	Et	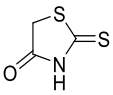	1.04±0.29	n.d.
(10f) py55	Et	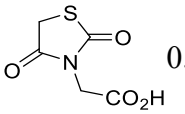	0.041±0.005	n.d. (35±3.4)
(11a) py04	^{n}Bu	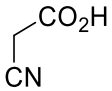	0.083±0.034	n.d. (48±5.2)
(11b) py13	^{n}Bu		n.d. (64±1.4)	n.d.
(11c) py46	^{n}Bu	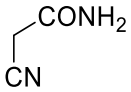	n.d. (14±14)	n.d.
(11d) py50	^{n}Bu	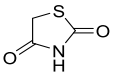	1.39±0.30	n.d.

(11e) py53	^{n}Bu	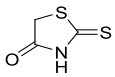	1.73±0.67	n.d. (35±3.4)
(11f) py56	^{n}Bu	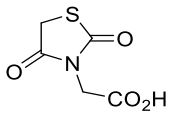	0.036±0.011	n.d. (37±16)

[a]Data are expressed as means ± SD of single determinations obtained in triplicate. [b]n.d. = not detected. [c]The % inhibition of the compound at a concentration of 10 μM against mPGES-1 (IC_{50} values were determined if the compounds caused in 70 % or higher inhibition).

With these (2-thio)barbituric acid derivatives in hand, we broadened the structural abundance with pyrazole core by coupling 1H-pyrazole-4-carbaldehyes (**3b** and **3d**) with various activated methylene compounds such as malononitrile, 2- 2-cyano-3-phenylacrylic acid and 2,4-thiazolidinedione. As shown in Table 4.4, compounds with malononitrile and 2-cyanoacetamide "heads" (**10b**, **10c** and **11b**, **11c**) were not active against human mPGES-1 while that with 2- 2-cyano-3-phenylacrylic acid (**10a** and **11a**) showed submicromolar potency. It was noted that the compounds **10f** and **11f**, obtained from the coupling of **3b** and **3d** with 2,4-thiazolidinedione acetic acid, were capable of inhibiting human mPGES-1 with low nanomolar potency (IC_{50} = 0.041 ± 0.005 μM and 0.036 ± 0.011 μM, respectively).

For the *in vitro* evaluation of these compounds, we conducted the first single concentration screening at 10 μM against human mPGES-1. Compounds caused significant inhibition (> 70 %) were tested for IC_{50} values against human mPGES-1. These compounds were than screened against the mouse enzyme at a concentration of 10 μM. Similarly, those caused an inhibition greater than 70 % was determined IC_{50} values against mouse mPGES-1. Generally, the inhibitory efficacy against mouse mPGES-1 of these compounds were lower as compared to the human enzyme. Yet some of the compounds did inhibit both enzymes with submicromolar potency, such as **5c** (IC_{50} = 0.056 ± 0.010 μM and 0.445 ± 0.083 μM for human and mouse mPGES-1, respectively) and **5e** (IC_{50} = 0.092 ± 0.019 μM and 0.316 ± 0.030 μM, respectively)
The inhibition against COX isozymes was also evaluated for some of the most potent

compounds (IC_{50} < 0.100 μM against human mPGES-1). As shown in **Table 3**, at a concentration as high as 100 μM, compounds **5b~5f**, **9**, **10f, 11a** and **11f** resulted in inhibition less than 20 %.

4.2.5 Configuration analysis

To confirm the possible 'E' 'Z' configuration of the 2-cyano-3-phenylacrylic Acid derivatives, **py01**, **py45**, **py47**, **py49**, **py52**, and **py55** were optimized by Gaussian09 at the DFT B3LYP 6-31G* level.[166] SMD[167] model was applied in this study as described in Section 3.2.4.

Table 4.5 Theoretical Relative Gibbs Free Energies of Z configuration to E configuration (in water)

Name	Theoretical Relative Gibbs Free Energies (ΔG*, kcal/mole) of Z configuration in water*
py01	2.4
py45	4.5
py47	4.6
py49	-1.3
py52	-5.7
py55	-4.8

*ΔG = G(Z configuration) - G(E configuration)

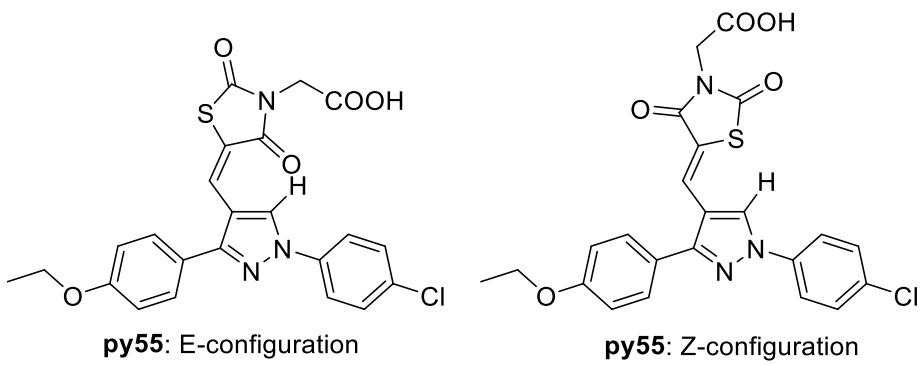

Scheme 4.3 The intro-molecular steric hindrance of **py55** (E configuration)

The E configuration is thermodynamically unstable due to the intro-molecular steric

hindrance (Scheme 4.3). This is confirmed by the calculated Gibbs free energy difference between E and Z configuration. We can speculate that all the compounds containing thiazolidine-2, 4-dione group (**py49 ~ 51**, **py55** and **py56**) or 2-thioxothiazolidin-4-one group (**py52 ~ py54**) will adapt Z configuration, otherwise, will adapt E configuration.

4.2.6 Binding mode analysis

To further study the inhibition mechanism of this series of derivatives, the binding modes of compounds **py56** and **py32** were simulated by molecular docking. The predicted binding mode are depicted in Figure 4.1

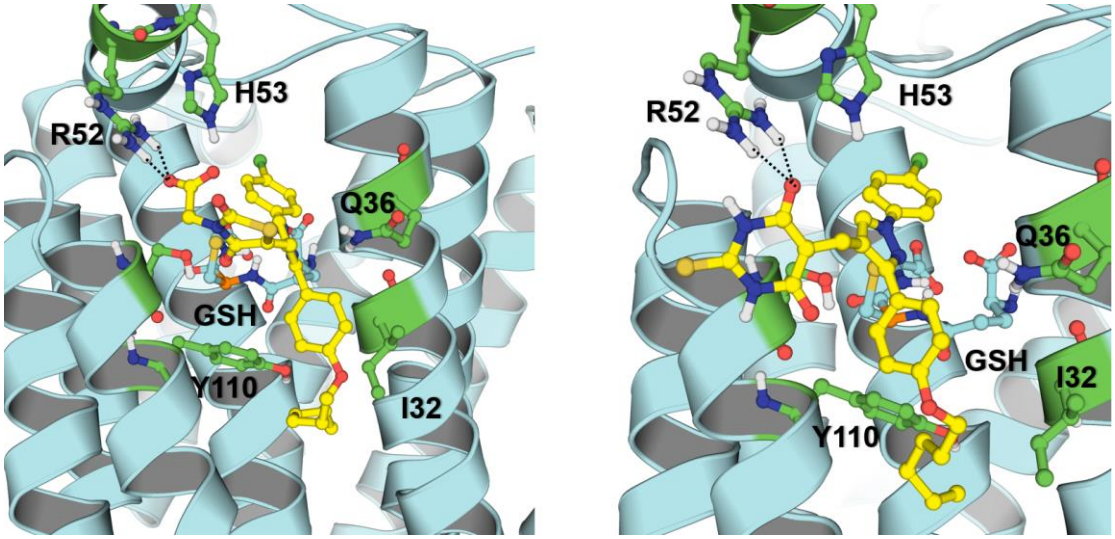

Figure 4.3 predicted binding modes of **py56** (left) and **py32** (right) with human mPGES-1

In both binding modes the substituted pyrazole scaffold are located at the same place of the enzyme, with the 4-hexoxyphenyl group located in the shallow hydrophobic groove and the chlorophenyl group inserted into the upper pocket of mPGES-1. Including the chlorine on the 1H-phenyl ring slightly improves the activity since it will have higher occupancy of the pocket. Introduction of a bulkier hydrophobic side chain

on the 3-phenyl ring also mildly increases its activity, although insignificant. Substitution of either 2-thioxothiazolidin-4-one or the 3-carboxymethylthiazolidine-2,4-dione groups are crucial for the activities. The carboxylic oxygen on **py56** can build hydrogen bonds with the NH groups on the R52 side chain while the carbonyl oxygen on **py32** can also build hydrogen bonds with the same set of atoms on R52. Any modification on the carboxyl group of **py56** will lower its activity. Swapping the sulfur with an oxygen on **py32** also lowers the activity since it will have a smaller size and less non-polar contacts with nearby residues. Introduction of methyl groups on **py32** will totally eliminate the activity of the compounds due to huge steric hindrance.

4.3 Conclusions

There is growing interest in identifying mPGES-1 inhibitors as new therapeutic agents. Herein we report the design, synthesis, and characterization a novel class of 1, 3-Diphenylpyrazole derivatives as human mPGES-1 inhibitors. In particular, compound (Z)-2-(5-((1-(4-chlorophenyl)-3-(4-(hexyloxy) phenyl)-1H-pyrazol-4-yl) methylene)-2, 4-dioxothiazolidin-3-yl) acetic acid, (**py56**) showed the most significant inhibition against human mPGES-1 with IC_{50} of 36 nM. Moreover, some of the compounds that showed inhibitions against human mPGES-1 also show inhibition against mouse mPGES-1, which indicates that further optimization based on the SAR could result in more potent duel inhibitors of human and mouse mPGES-1.

4.4 Experimental section

4.4.1 General method for the synthesis of target compounds

The reaction of substituted hydroxyl aldehydes and different halogenated hydrocarbons give the alkylating aldehydes, which were further converted to their corresponding target compounds (**py01** ~ **py56**). The synthesis of the starting materials and representative target compounds is illustrated in Scheme 4.4, Scheme 4.5 and

Scheme 4.6.

The synthesis of this series of compounds followed a straightforward multi-step protocol, as shown in Scheme 1. 4-Alkyloxyacetophenone (**1b ~ 1g**), obtained from the reaction of 4-hydroxyacetophenone and alkyl bromide, or acetophenone (**1a**) was condensed with 4-chlorophenylhydrazine in reflux ethanol containing 5 % glacial acetic acid. The ethylidene hydrazine (**2a ~ 2g**) was formed as precipitate at room temperature and filtered off. The next step was Vilsmeier-Haack-Arnold ring closing formylation, by treating **2a** ~ **2g** with $POCl_3$/DMF. The produced 1*H*-pyrazole-4-carbaldehyde intermediate (**3a** ~ **3g**) was coupled with barbituric acid or 2-thiobarbituric acid in refluxing EtOH/H_2O (4:1) to afford the final product (**4a** ~ **4g** or **5a** ~ **5g**).

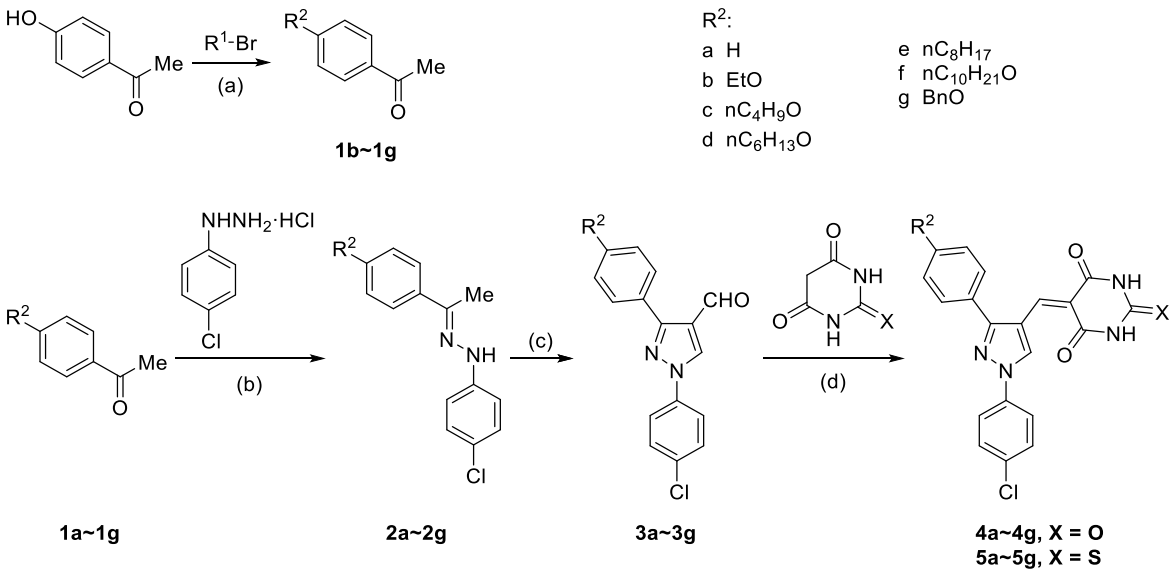

Scheme 4.4 Reagents and conditions: (a) K_2CO_3 (2.00 equiv.), DMF, 80 ºC; (b) 5 % glacial AcOH in EtOH, reflux; (c) $POCl_3$ (4.00 equiv.), DMF, 0 ºC~60 ºC; (d) EtOH/H2O (4:1, v/v), reflux.

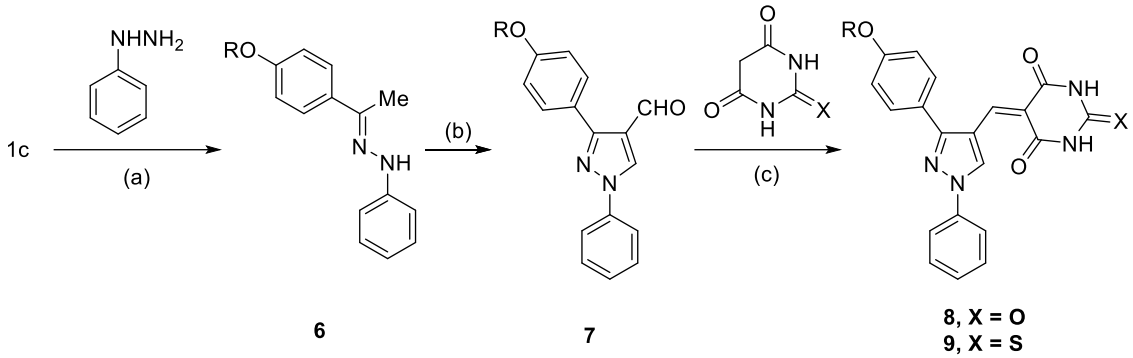

Scheme 4.5 Reagents and conditions: (a) 5 % glacial AcOH in EtOH, reflux; (b) $POCl_3$ (4.00 equiv.), DMF, 0 ºC~60 ºC; (c) EtOH/H2O (4:1, v/v), reflux.

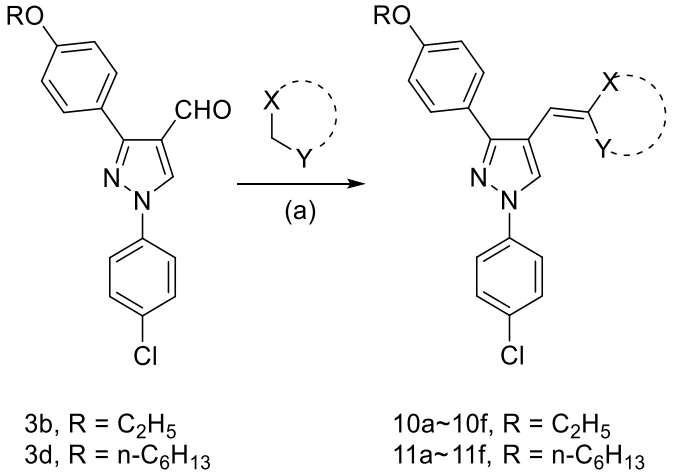

Scheme 4.6 Reagents and conditions: (a) NH_4OAc (2.00 equiv.), glacial AcOH, 100 ºC.

4.4.2 Structural information for target compounds

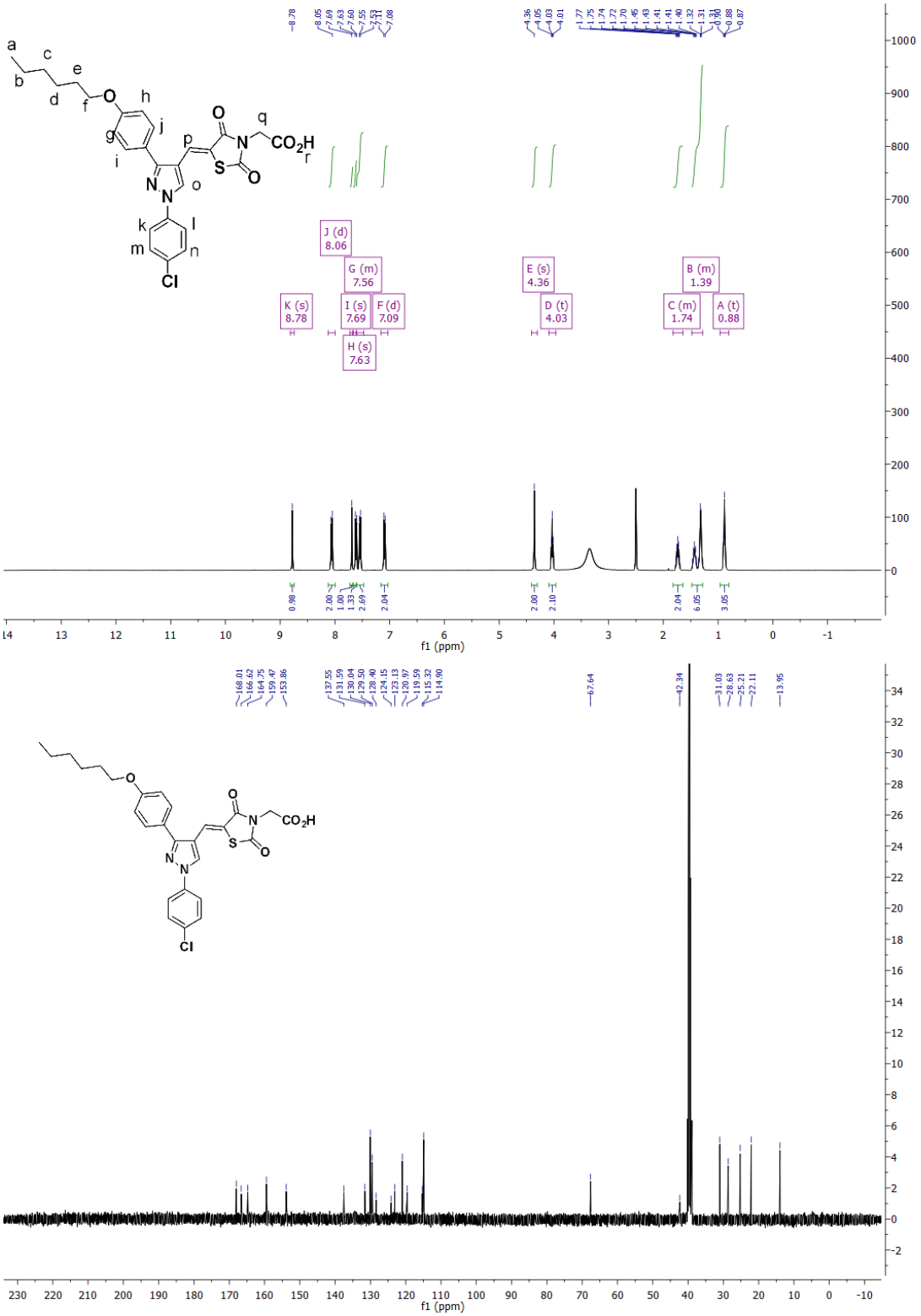

Figure 4.4 ^{1}H NMR and ^{13}C NMR for representative compound **py56**, with d6-DMSO as solvent

The ^{1}H NMR and ^{13}C NMR spectrum of representative compound **py56** in d6-DMSO for group 2 is shown in **Figure 4.4**. All ^{1}H NMR peaks and ^{1}H-^{1}H coupling are well resolved, and can be assigned to the molecular structure of **py56**. ^{1}H NMR (400 MHz, d6-DMSO) δ p-H: 8.78 (s, 1H), o-H: 7.63 (s, 1H), h, g, i, j, l, m, n-H:8.06 (d, J = 8.8 Hz, 2H), 7.69 (s, 1H), 7.61 – 7.47 (m, 3H), 7.09 (d, J = 8.7 Hz, 2H), q-H: 4.36 (s, 2H), f-H: 4.03 (t, J = 6.5 Hz, 2H), e-H: 1.82 – 1.64 (m, 2H), b, c, d-H: 1.48 – 1.28 (m, 6H), a-H: 0.88 (t, J = 6.8 Hz, 3H).

Structures, Names, ^{1}H NMR and ^{13}C NMR data for 1, 3-Diphenylpyrazole derivatives were listed in **Table I-2** of **Appendix I**. Calculated and measured molecular weights of the protonated target compounds $(MH)^{+}$ were summarized in **Appendix II**, **Table II-2**.

Chapter 5: Design, synthesis and characterization of hydrazide derivatives as a novel class of selective human mPGES-1 inhibitors

Summary: In this Chapter, we present the design, synthesis and biological evaluation of a series of hydrazide compounds as human mPGES-1 inhibitors. Some of these derivatives exhibited excellent *in vitro* mPGES-1 inhibition efficacy. Selectivity test revealed that the most potent compounds have high selectivity of human mPGES-1 over COX-1/2 enzymes. Among the 91 compounds reported in this chapter, six compounds, including the most potent human mPGES-1 inhibitor within this dissertation, showed IC_{50} values below 100 nM.

5.1 Introduction

For treating inflammation-associated symptoms, traditional NSAIDs and COX-2 selective coxibs have been developed as two generation of anti-inflammatory drugs.[203] However, as both of them shut down the production of all prostanoid downstream of PGH_2, their clinical application are associated with considerable adverse effects.[16, 189] In recent two decades, the inhibition of mPGES-1 was suggested as candidate therapeutic approach in the development of next generation of anti-inflammatory drugs.[204, 205] The mPGES-1 inhibitors block the production of only inflammation related PGE_2 and thus do not render the side effects resulted from the interference of other prostanoids.[198, 199] Therefore, great efforts have been depicted in the development and identification of novel mPGES-1 inhibitors. The hydrazide appears as pharmacophore various pharmaceutical agents such as antibiotics.[206, 207]

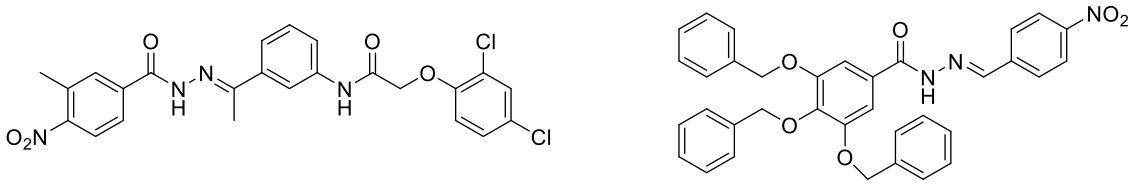

Scheme 5.1 The two reported hydrazide derivatives as human mPGES-1 inhibitors[65]

The hydrazides were first associated with human mPGES-1 in 2013.[65] By using the active conformation structural model and virtual screening, Shan H, *et al.* successfully identified two hydrazide derivatives (**compound 12** and **compound 17** in Figure 5.1) with IC_{50} value at submicromolar level (Figure 5.1).[65] However, due to the limited chemical abundance of hydrazide derivatives reported, we decided to prepare more compounds in light of the structure of **compound 17**. As selective inhibition of mPGES-1 by small-molecule inhibitors has been proved to be clinically validated as a rational and a safer alternative strategy of traditional NSAIDs for inflammations.[208, 209] Novel hydrazide derivatives capable of inhibiting mPGES-1 are synthesized and evaluated.

5.2 Results and Discussions

5.2.1 Inhibition against human mPGES-1

All newly synthesized derivatives of hydrazide were evaluated for their human mPGES-1 inhibitions in a concentration-dependent manner. The inhibitory potency (%/inhibition at 10 μM and 1 μM) are presented in Table 5.1. Ten of the compounds which showed inhibition greater than 80% at 1 μM were further determined for their IC_{50} values against human mPGES-1. Compound **zh86** in Table 5.1 is the same compound with the **compound 17** reported by Shan H *et al.*[65] Its IC_{50} determined by our *in vitro* mPGES-1 bioassay kit (170 ± 51 nM) is in the same order of magnitude with the reported IC_{50} value of 0.10 ± 0.01 μM.[65] However, the solubility of this

compound was very poor due to the amount of hydrophobic Benzyl groups. To get novel hydrazides with higher potency inhibition and possibly better aqueous solubility, we synthesize a serious of structurally related compounds. Six of the compounds were determined with IC_{50} against human mPGES-1 lower than 100 nM. Particularly, **zh89** was the most potent human mPGES-1 inhibitor, with an IC_{50} value of 27 nM.

5.2.2 Inhibition against mouse mPGES-1

The top 10 most potent human mPGES-1 inhibitors were further screened for their inhibition against mouse mPGES-1 at the concentration of 10 μM. Unfortunately, most of them failed to inhibit the mouse enzyme at 10 μM (Table 5.1). However, **zh48** was capable of inhibiting the mouse enzyme by 58.5% at 10 μM.

Table 5.1 Structures and activities against human or mouse mPGES-1 for hydrazine analogs zh01-zh91

ID	Structures	%/ Inhibition against human mPGES-1 at 10μM	%/ Inhibition against human mPGES-1 at 1μM	IC_{50} against human mPGES-1 / nM[a] (%/ Inhibition against mouse mPGES-1 at 10μM)
zh01	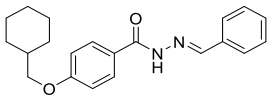	5.3 ± 4.4	-1.0 ± 6.1	N.D.[b]
zh02	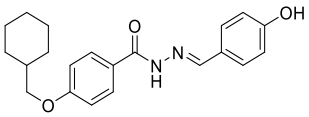	24.6 ± 18.7	11.4 ± 4.2	N.D.
zh03	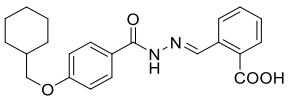	98.4 ± 0.6	82.0 ± 1.5	46.5 ± 14.9 (15.1 ± 41.1)
zh04	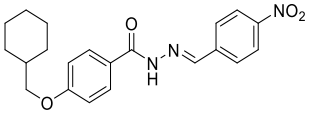	83.2 ± 2.2	42.5 ± 13.0	N.D.

zh05	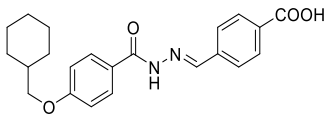	91.0 ± 1.6	71.8 ± 3.4	N.D.
zh06	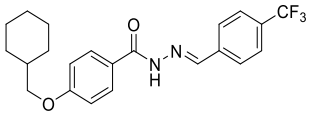	88.7 ± 1.7	66.0 ± 1.6	N.D.
zh07	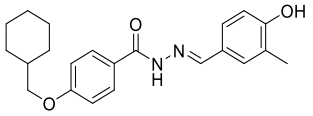	35.2 ± 20.7	2.4 ± 2.7	N.D.
zh08	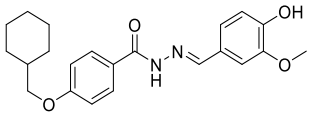	15.6 ± 3.4	4.2 ± 13.0	N.D.
zh09	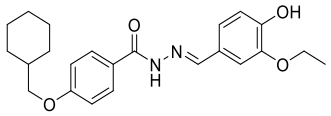	57.6 ± 3.6	20.6 ±21.6	N.D.
zh10	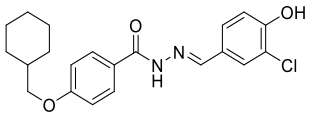	7.3 ± 4.1	5.5 ± 1.5	N.D.
zh11	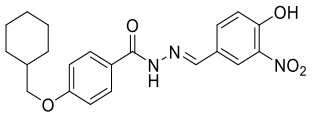	87.3 ± 0.8	68.5 ± 7.0	N.D.
zh12	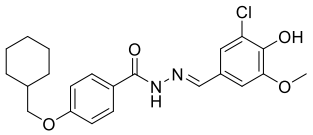	59.0 ± 1.9	21.8 ± 5.7	N.D.
zh13	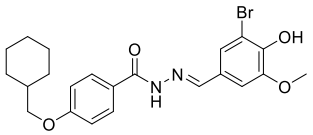	63.9 ± 14.9	6.7 ± 10.8	N.D.
zh14	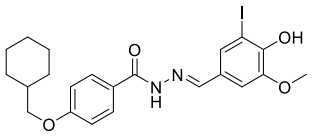	65.0 ± 12.5	19.0 ± 3.7	N.D.
zh15	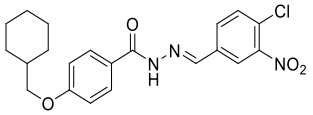	71.1 ± 3.7	50.3 ± 3.6	N.D.
zh16	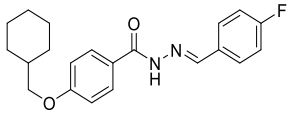	63.2 ± 11.9	38.9 ± 0.6	N.D.
zh17	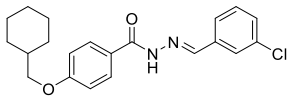	16.1 ± 6.6	10.4 ± 14.8	N.D.

zh18	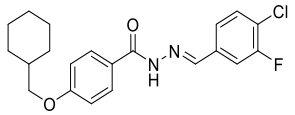	60.2 ± 15.7	19.1 ± 17.5	N.D.
zh19	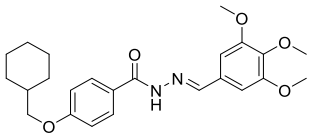	27.5 ± 9.3	1.5 ± 0.5	N.D.
zh20	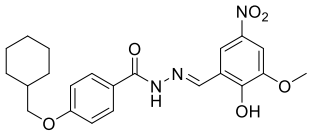	71.2 ± 7.0	44.9 ± 9.1	N.D.
zh21	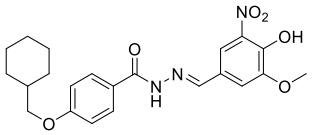	71.6 ± 5.8	33.4 ± 7.4	N.D.
zh22	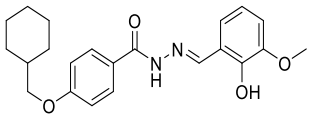	47.9 ± 9.4	8.3 ± 15.6	N.D.
zh23	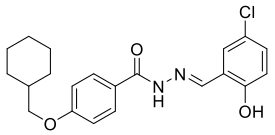	44.3 ± 14.7	3.8 ± 8.5	N.D.
zh24	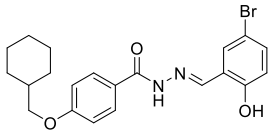	31.8 ± 15.8	2.9 ± 10.3	N.D.
zh25	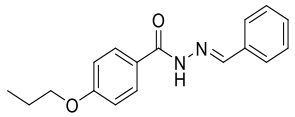	3.9 ± 9.6	5.8 ± 8.8	N.D.
zh26	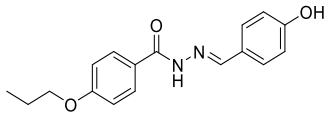	34.8 ± 4.6	10.0 ± 5.9	N.D.
zh27	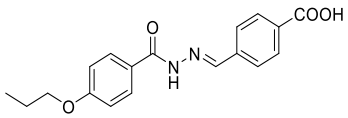	71.1 ± 6.7	55.6 ± 12.3	N.D.
zh28	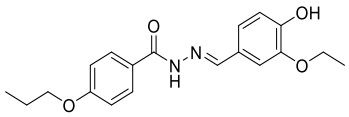	24.6 ± 9.2	6.0 ± 20.8	N.D.
zh29	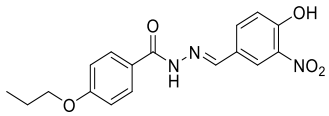	80.7 ± 9.5	47.6 ± 15.0	N.D.

zh30	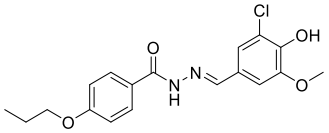	28.6 ± 4.4	1.8 ± 1.1	N.D.
zh31	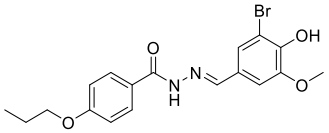	24.0 ± 6.4	-1.4 ± 13.9	N.D.
zh32	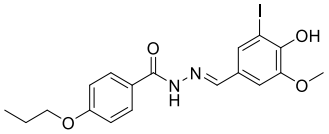	45.1 ± 3.0	5.2 ± 24.6	N.D.
zh33	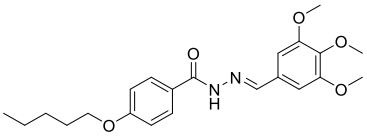	33.4 ± 4.0	9.6 ± 10.2	N.D.
zh34	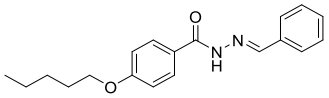	8.3 ± 15.9	5.2 ± 6.4	N.D.
zh35	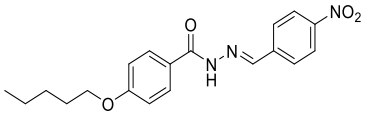	81.5 ± 8.6	57.3 ± 16.3	N.D.
zh36	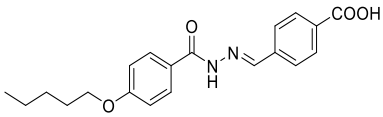	92.9 ± 11.7	52.6 ± 8.0	N.D.
zh37	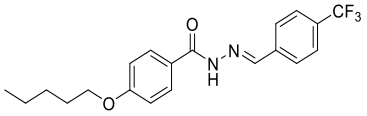	92.9 ± 1.1	81.6 ± 5.8	120.3 ± 35.2 (0 ± 27.9)
zh38	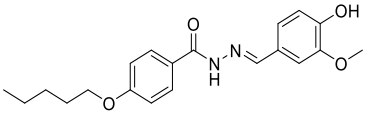	58.7 ± 3.8	7.4 ± 7.6	N.D.
zh39	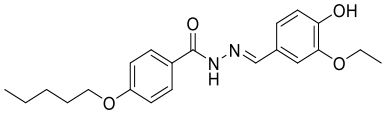	53.7 ± 2.2	5.6 ± 7.5	N.D.
zh40	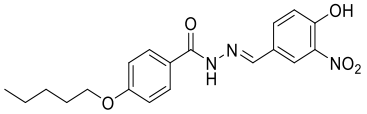	70.8 ± 10.4	51.0 ± 7.2	N.D.
zh41	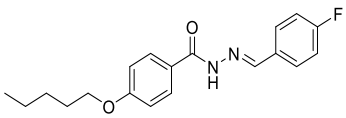	59.0 ± 0.4	27.6 ± 8.0	N.D.

zh42	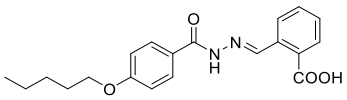	96.1 ± 2.3	87.3 ± 3.0	37.5 ± 8.8 (21.6 ± 25.4)
zh43	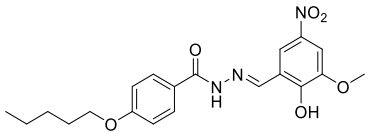	81.7 ± 1.4	67.4 ± 6.6	N.D.
zh44	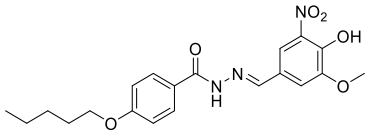	79.7 ± 4.1	67.0 ± 8.9	N.D.
zh45	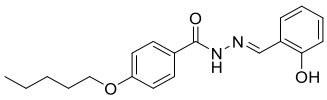	5.5 ± 9.4	4.3 ± 2.6	N.D.
zh46	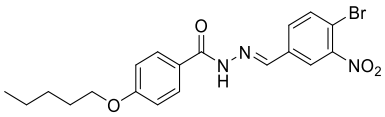	85.8 ± 8.7	72.7 ± 5.1	N.D.
zh47	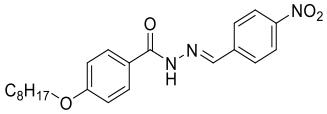	82.4 ± 5.1	59.1 ± 5.3	N.D.
zh48	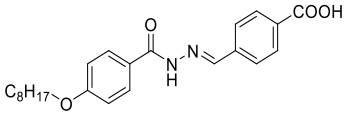	92.5 ± 6.2	81.2 ± 14.1	30.8 ± 7.0 (58.5 ± 4.4)
zh49	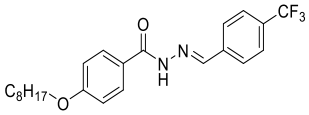	85.9 ± 3.9	80.0 ± 5.2	183.9 ± 54.1 (30.4 ± 16.9)
zh50	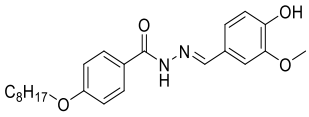	54.8 ± 5.6	13.3 ± 12.5	N.D.
zh51	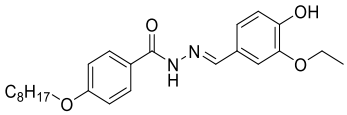	53.6 ± 3.2	7.0 ± 13.1	N.D.
zh52	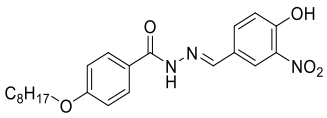	102.0 ± 0.9	72.8 ± 1.2	N.D.
zh53	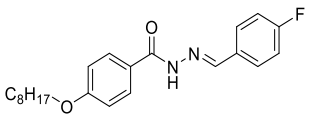	85.4 ± 9.7	61.1 ± 5.6	N.D.
zh54	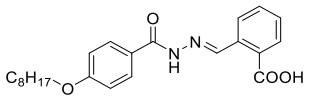	96.6 ± 2.6	75.0 ± 5.1	N.D.

zh55	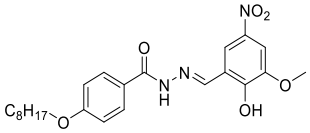	83.8 ± 7.7	68.2 ± 5.8	N.D.
zh56	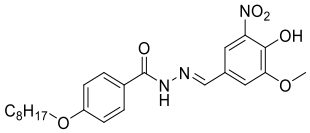	100.5 ± 2.6	66.0 ± 3.8	N.D.
zh57	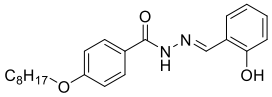	11.6 ± 10.4	-1.0 ± 4.9	N.D.
zh58	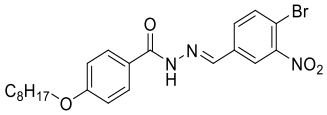	94.7 ± 9.5	66.9 ± 7.2	N.D.
zh59	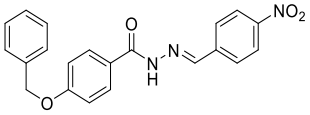	60.1 ± 6.6	34.7 ± 14.7	N.D.
zh60	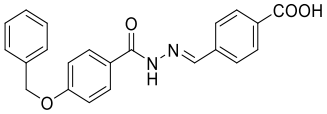	84.4 ± 4.7	81.1 ± 5.3	314.4 ± 92.3 (46.0 ± 6.7)
zh61	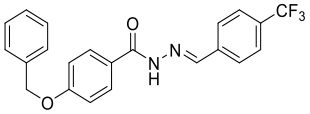	93.1 ± 7.9	61.6 ± 17.4	N.D.
zh62	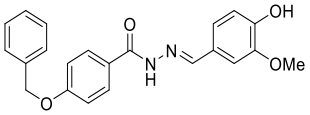	52.1 ± 23.6	23.0 ± 9.3	N.D.
zh63	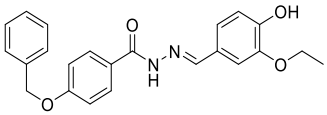	93.1 ± 6.4	61.3 ± 6.2	N.D.
zh64	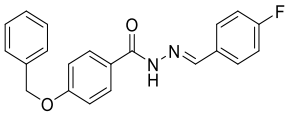	27.5 ± 20.9	9.2 ± 43.0	N.D.
zh65	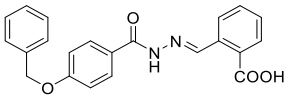	91.2 ± 10.9	77.0 ± 5.6	N.D.
zh66	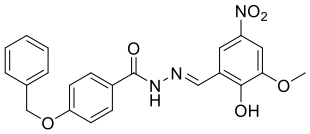	46.2 ± 15.2	16.8 ± 23.3	N.D.

zh67	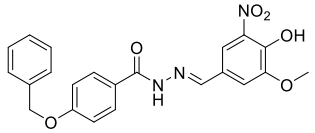	59.6 ± 13.7	9.8 ± 11.9	N.D.
zh68	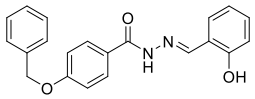	23.4 ± 10.1	3.5 ± 5.0	N.D.
zh69	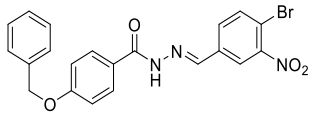	76.3 ± 1.3	20.3 ± 5.0	N.D.
zh70	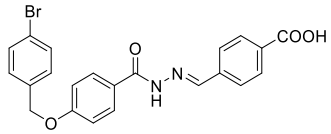	102.1 ± 0.5	78.3 ± 15.5	N.D.
zh71	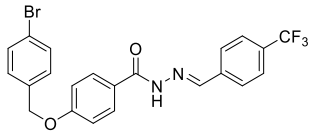	86.0 ± 13.5	77.4 ± 4.5	N.D.
zh72	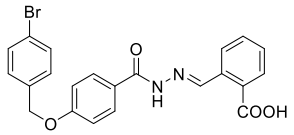	98.3 ± 11.8	72.1 ± 7.1	N.D.
zh73	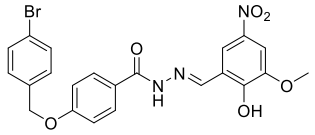	29.5 ± 7.7	13.7 ± 4.8	N.D.
zh74	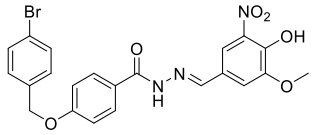	52.6 ± 7.2	17.9 ± 4.2	N.D.
zh75	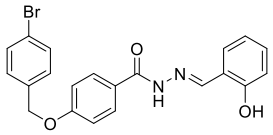	11.8 ± 7.8	2.4 ± 17.6	N.D.
zh76	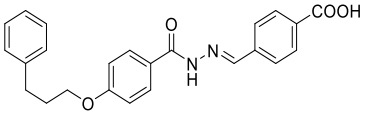	86.1 ± 14.7	67.1 ± 11.6	N.D.
zh77	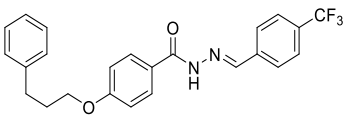	76.9 ± 10.2	52.2 ± 10.7	N.D.

zh78	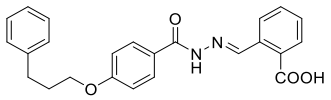	86.0 ± 2.3	70.4 ± 5.7	N.D.
zh79	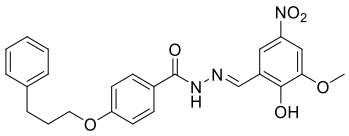	67.4 ± 11.0	51.9 ± 8.7	N.D.
zh80	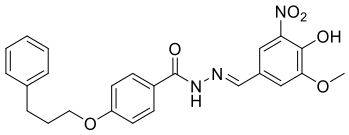	59.4 ± 22.9	53.6 ± 12.7	N.D.
zh81	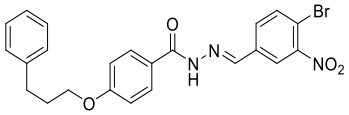	85.6 ± 11.5	47.6 ± 9.8	N.D.
zh82	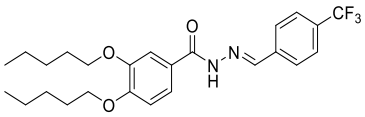	65.1 ± 19.0	39.4 ± 42.3	N.D.
zh83	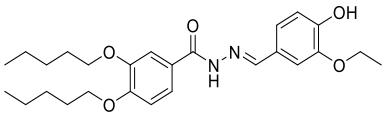	32.1 ± 23.3	11.3 ± 14.6	N.D.
zh84	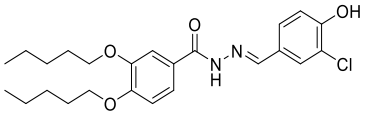	22.6 ± 5.4	8.7 ± 18.0	N.D.
zh85	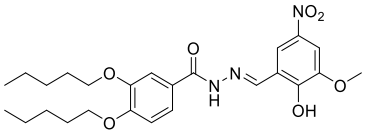	14.4 ± 21.3	48.2 ± 3.1	N.D.
zh86	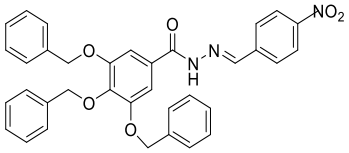	92.4 ± 3.4	75.3 ± 2.7	169.9 ± 50.6 (30.0 ± 4.5)
zh87	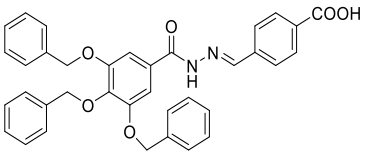	96.5 ± 1.5	83.5 ± 1.8	29.0 ± 5.8 (1.1 ± 31.9)
zh88	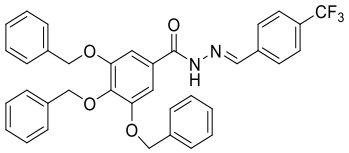	89.6 ± 5.8	80.6 ± 1.3	60.9 ± 10.1 (25.1 ± 23.3)

zh89	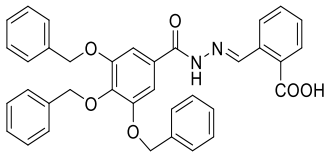	98.3 ± 5.9	95.8 ± 4.2	27.3 ± 10.1 (45.2 ± 16.2)
zh90	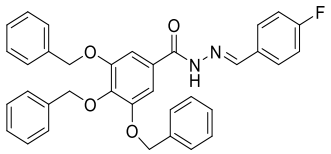	67.9 ± 2.6	20.4 ± 14.0	N.D.
zh91	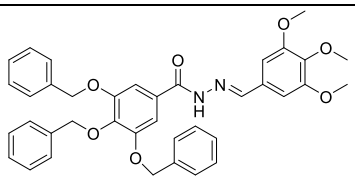	55.3 ± 3.6	4.3 ± 3.9	N.D.

[a]IC_{50} value was determined from single determination by triplet.
[b]N.D.: Not determined.

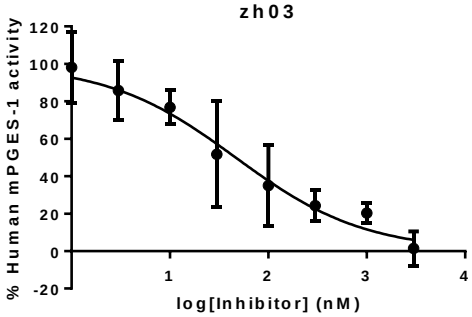

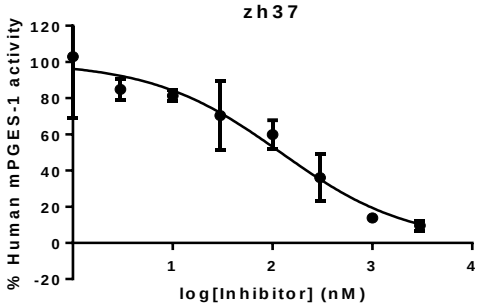

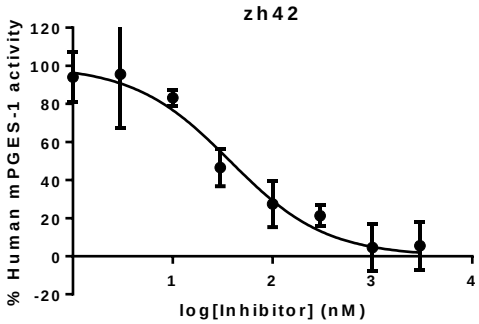

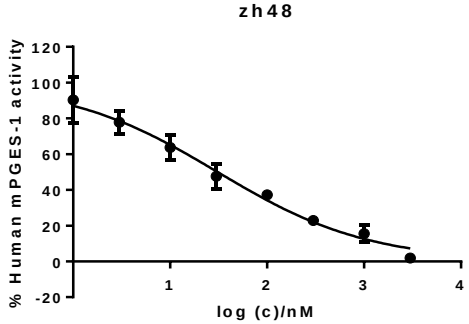

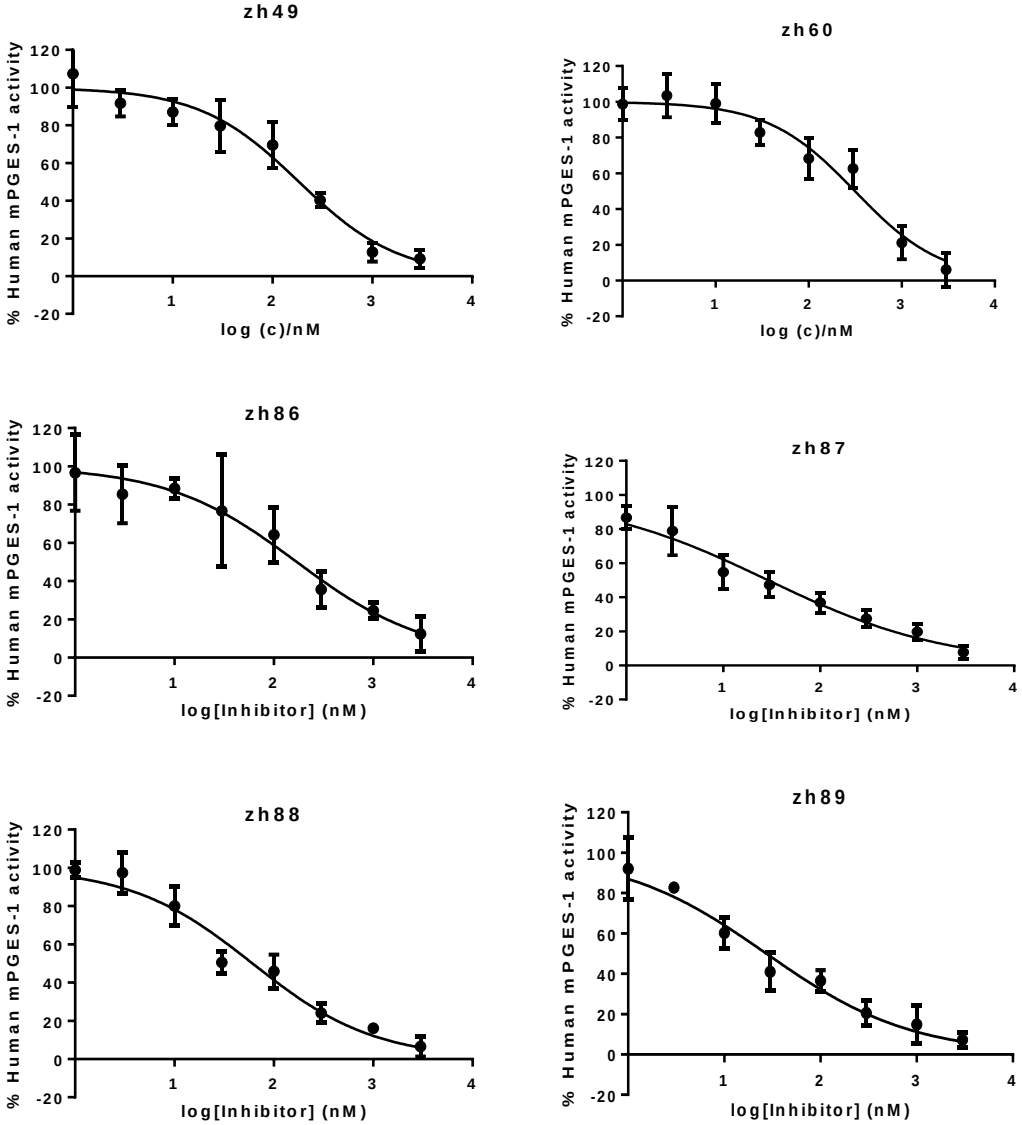

Figure 5.1 *In vitro* activity of the hydrazide derivatives against human mPGES-1. The inhibitor concentration is given in log scale.

5.2.3 Structure-activity relationships (SAR) of hydrazide derivatives

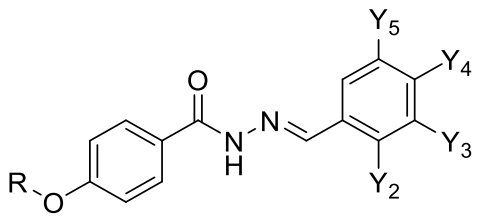

Y_2: COOH, OH
Y_3: OMe, OEt, NO_2, Me, Cl, Br, I
Y_4: COOH, OH, OMe, F, Cl, Br,
Y_5: NO_2, OMe
R: CyclohexylMethyl, nC_3H_7, nC_5H_{11}, nC_8H_{17}, Bn, BrBn, etc.

Scheme 5.2 Scaffold for the hydrazide derivatives

The above results revealed that the inhibition against human mPGES-1 was highly related to the function groups at the Y positions. Hydrogen bond acceptors such as carboxyl group or nitro group are required for the maintenance of inhibitory potency. Replacement of the nitro group or carboxyl group by other hydrophobic groups such as halogens, methoxide groups will lead to significant decreased or even caused completely loss in potency. We also changed the size and shape of the hydrophobic groups at the R position. The compound with short hydrophobic group (such as **zh25** ~ **zh32**) and the benzyl group (such as **zh59** ~ **zh81**) slightly impaired the inhibitory efficacy as compared to larger hydrophobic substitutions. On the other hand, the compounds that with three benzyl groups (**zh87** ~ **zh89**) are generally more potent human mPGES-1 inhibitors, despite their low solubility. Indicating that the compounds with multiple benzyl groups (**zh86** ~ **zh91**) might adapt a different binding mold with the rest of the compounds (**zh01** ~ **zh85**) of the hydrazide derivatives, as will be discussed later in the computational part.

5.2.4 Selectivity of human mPGES-1 over COXs

Inhibition at 100 μM was tested for six most potent compounds (IC_{50} value below 100nM) in order to investigate their cross-reactivity against COXs. The assay was carried out following the same protocol as described in Chapter 3, section 3.2.3.

Table 5.2 Inhibitions of potent mPGES-1 inhibitors against COXs

Name	%/Inhibition at 100 μM
zh03	-1.7 ± 5.5
zh42	3.8 ± 3.0
zh48	5.9 ± 3.1
zh87*	25.2 ± 5.7
zh88*	25.8 ± 0.0
zh89*	18.9 ± 9.8

*Solubility of these compounds are lower than 100 μM. Data in this table are tested at their highest aqueous solubility.

None of these potent mPGES-1 inhibitors showed significant potent inhibition against COXs, even at very high concentrations (e.g. 100 μM) or at their highest solubility in the reaction buffer. The six tested hydrazide derivatives are highly selective for mPGES-1 over COXs, as these compounds at a very high concentration (100 μM) showed no significant inhibition against COX-1 or COX-2.

5.2.5 Configuration analysis

To provide theoretical support that 'E' configuration will be more stable than the 'Z' configuration for this group of compounds, **zh01** was optimized by Gaussian09 at the DFT B3LYP 6-31+G* level,[166] and SMD[167] model was applied in this study as described in Section 3.2.4.

The calculated Gibbs free energy of Z configuration **zh01** is higher than the corresponding E configuration by 1.7 kcal/mole. None of the ninety-one hydrazide derivatives could have intro-molecular steric hindrance like the E configuration of **py49** ~ **py56** in Chapter 4. For this reason, the hydrazide derivatives should all adopt the energetic-favorable, less steric hindrance E configuration.

5.2.6 Molecular modeling study

Molecular docking studies were performed on the two selected compounds **zh89** and **zh42** to authenticate the obtained experimental *in vitro* activities against human mPGES-1. The selected compounds were successfully docked in the PGH_2 binding site of mPGES-1 (PDB ID: 4bpm) using the Autodock Vina program.[210]

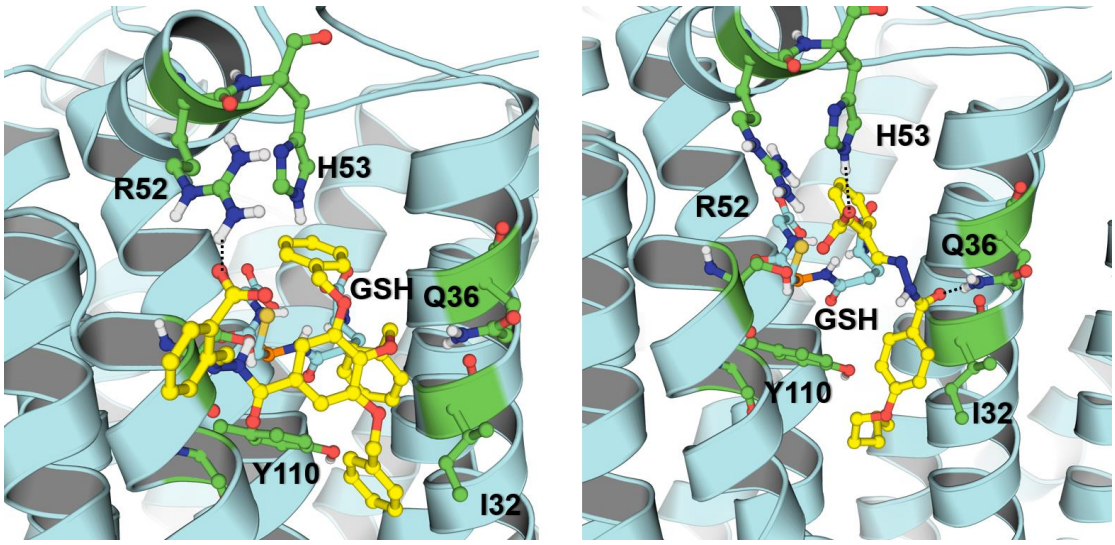

Figure 5.2 Predicted binding mode of compound **zh89** (left) and **zh42** (right) with human mPGES-1

The predicted binding models for compounds **zh89** and **zh42** is depicted in Figure 5.2. Compounds **zh89** and **zh42** adopted similar binding modes. The hydrogen bonds with the human mPGES-1 "upper reign" (R52 and H53) are crucial for the maintenance of the inhibitory efficacy. The binding mode could explain why hydrogen bond acceptor is required to maintain the activities. The hydrophobic side chains of both compounds locate in the hydrophobic pocket formed by Y110, I32, etc. Compound **zh89**, with three bulky benzyl groups, tends to interact R52 with hydrogen bonding while zh42 interacts with H53 due to the smaller size of linear side chain. Furthermore, the binding mode could also explain why compounds in this chapter shown relatively poor inhibitory activity against the mouse mPGES-1, as in mouse mPGES-1 structure, K52 and R53 are the mutant amino acid residue instead of R52 and H53 in the human enzyme. These

mutants interference the hydrogen bonding between the compounds with the corresponding pocket in the mouse enzyme structure.

5.3 Conclusions

In conclusion, based on the SAR and binding model with the crystal structure of human mPGES-1 (PDB: 4BPM), novel selective human mPGES-1 inhibitors with hydrazide scaffold have been designed, synthesized, and biologically evaluated inhibition rates (%) were determined against human mPGES-1 in a cell-free assay. In total, we synthesized 91 hydrazide derivatives. The most potent compounds against human mPGES-1 (Inhibition > 80% at 1μM) were further determined for their IC_{50} values. For the six compounds with IC_{50} values less than 100nM, inhibition against mouse mPGES-1 and the cross-reactivity against COXs were also investigated. Compound **zh89** showed IC_{50} value of 27 ± 10 nM against human mPGES-1. Furthermore, the top-six active compounds showed no significant inhibition against COXs. Overall, the results presented in this chapter suggest that hydrazide derivatives represent promising human mPGES-1 selective inhibitors for the development of next generation of NSAIDs.

5.4 Experimental Section

5.4.1 Materials and Methods

Following the same methods as described before, ^{1}H NMR and ^{13}C NMR spectra were recorded on 400 spectrometers using tetramethylsilane (TMS) as the internal standard. The HPMS protocol used in previous chapters was also successfully applied in this chapter.

5.4.2 Organic synthesis

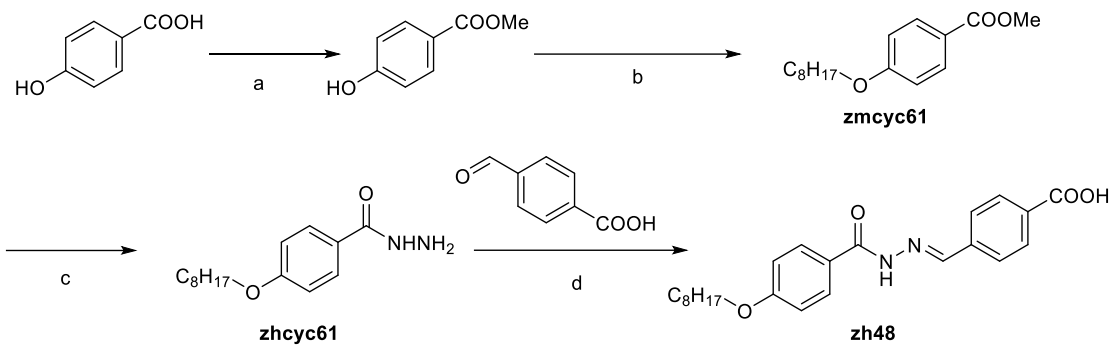

Scheme 5.3 Synthesis of compounds **zh48** Reagents and conditions:

(a) MeOH, reflux, catalytic amount of acetic acid;

(b) DMF, K_2CO_3, 80℃; (d) EtOH, reflux; (e) EtOH, acetic acid, reflux.

5.4.3 Structural information for target compounds

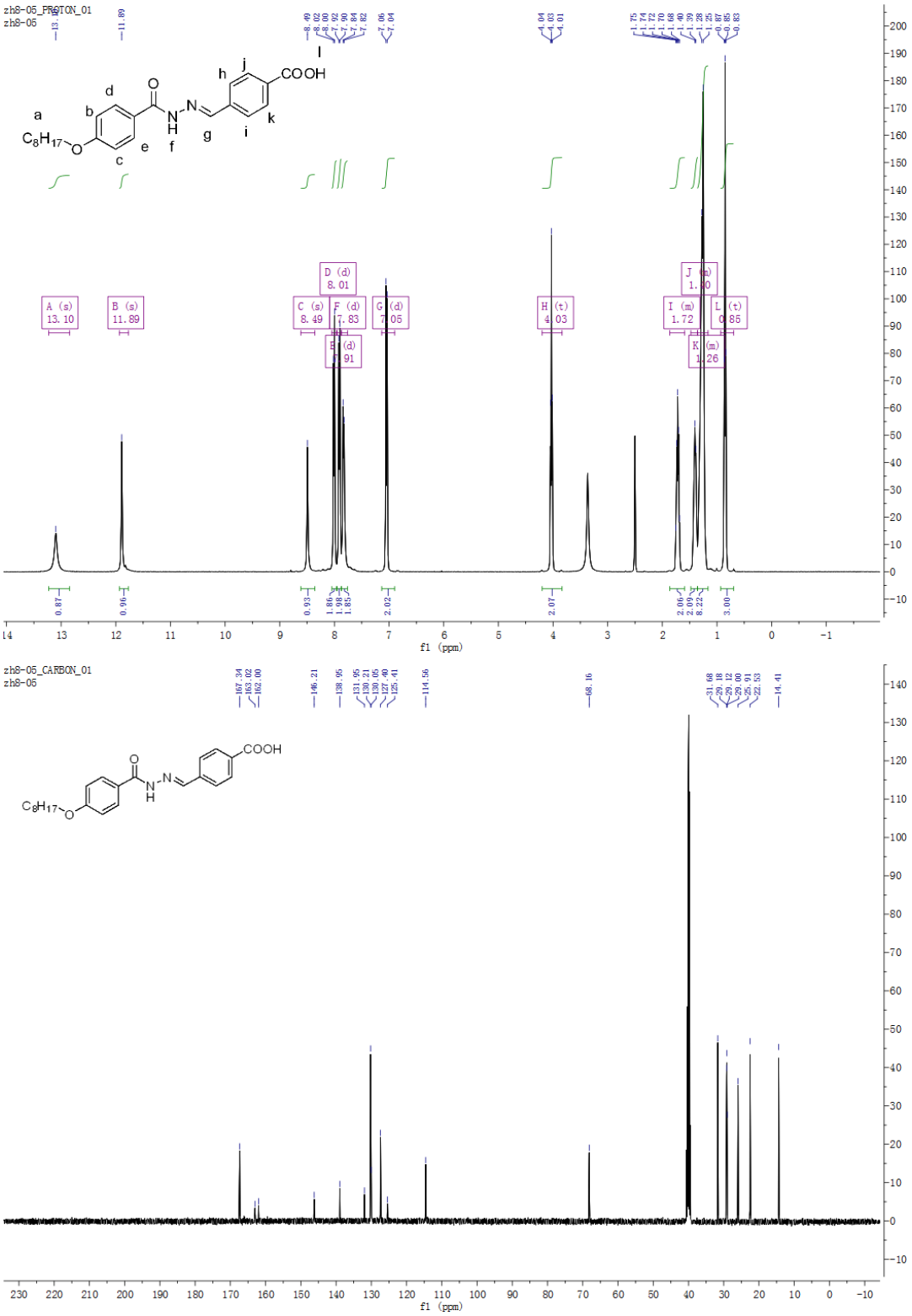

Figure 5.3 ^{1}H NMR and ^{13}C NMR for representative compound **zh48**

The ^{1}H NMR and ^{13}C NMR spectrum of representative compound **zh48** in d6-DMSO is shown in **Figure 5.3**. All ^{1}H NMR peaks and ^{1}H-^{1}H coupling are well resolved, and can be assigned to the molecular structure of **zh48**. ^{1}H NMR (400 MHz, d6-DMSO) δ 1−H: 13.10 (s, 1H), g-H: 11.89 (s, 1H), f-H: 8.49 (s, 1H), b, c, d, e, f, I j, k-H: 8.01 (d, *J* = 8.0 Hz, 2H), 7.91 (d, *J* = 8.5 Hz, 2H), 7.83 (d, *J* = 7.5 Hz, 2H), 7.05 (d, *J* = 8.7 Hz, 2H), a-H: 4.03 (t, *J* = 6.4 Hz, 2H), 1.86 – 1.59 (m, 2H), 1.48 – 1.36 (m, 2H), 1.36 – 1.16 (m, 8H), 0.85 (t, *J* = 6.6 Hz, 3H).

Structures, Names, ^{1}H NMR and ^{13}C NMR data for hydrazide derivatives are listed in **Table I-3** of **Appendix I**. Calculated and measured molecular weights of the protonated targets compounds $(MH)^{+}$ were summarized in **Appendix II**, **Table II-3**.

Chapter 6: Concluding Remarks and Future Plan

6.1 Summary of the major conclusions obtained from this investigation

Inhibition of mPGES-1 has emerged as an attractive approach for the treatment of a number of inflammation related diseases. Although many reported compounds exhibited submicromolar inhibitory concentrations against human mPGES-1, none of them have been proved clinically useful. This fact forced the scientific community to develop new mPGES-1 inhibitors with different scaffolds.

In summary, we have identified new inhibitors of human mPGES-1 by applying structure-based virtual screening. We have designed and evaluated three classes of human mPGES-1 inhibitors with different chemical scaffolds. Some of the synthesized compounds also showed potent inhibitory efficacy against mouse mPGES-1, which potently facilitate the preclinical animal studies with mouse disease models.

1) Novel human mPGES-1 inhibitors were identified by applying a virtual screening protocol and then *in vitro* assay. The protocol is a combination of flexible docking, large-scale structure-based virtual screening, energy minimization, molecular dynamics (MD) simulation, and MM/PBSA binding free energy calculation.

2) We have successfully developed about two hundred of compounds as candidates for human mPGES-1 inhibitors. They can be divided into three groups based on the scaffolds. Six compounds of Group 1 (Chapter 3), while ten compounds of Group 2 (Chapter 4) and six compounds of Group3 (Chapter 5) showed efficacy inhibitory activity against human mPGES-1 with IC_{50} values below 100nM.

3) In addition to the human mPGES-1, we also determined the inhibition against mouse mPGES-1 for the most potent human mPGES-1 inhibitors

4) Cross-activity assays with COXs demonstrated that the most potent mPGES-1 inhibitors did not cause significant inhibition against COXs.

6.2 Future plan concerning rational design of mPGES-1 inhibitors as next generation of anti-inflammatory drugs

1) To further identify mPGES-1 inhibitors with novel scaffolds as new leads by employing our virtual screening protocol to screen compounds in other libraries such as the SPECS and ZINC libraries.

2) To further characterize the detailed pharmacological and toxicological profiles of the identified mPGES-1 inhibitors, such as the *in vivo* effectiveness, selectivity of mPGES-1 over other enzymes in the AA metabolism pathway, and pharmacokinetic/pharmacodynamic (PK/PD) profiles.

3) The most potent mPGES-1 inhibitors derived from structural optimization will be used as drug candidates for appropriate animal studies.

References

1. Hamza, A., Zhao, X.-Y., Tong, M., Tai, H.-H., and Zhan, C.-G. (2011) Novel human mPGES-1 inhibitors identified through structure-based virtual screening, *Bioorg. Med. Chem. 19*, 6077-6086.
2. Olajide, O. A., Aderogba, M. A., and Fiebich, B. L. (2013) Mechanisms of anti-inflammatory property of Anacardium occidentale stem bark: Inhibition of NF-κB and MAPK signalling in the microglia, *J. Ethnopharmacol. 145*, 42-49.
3. Norberg, J. K., Sells, E., Chang, H.-H., Alla, S. R., Zhang, S., and Meuillet, E. J. (2013) Targeting inflammation: multiple innovative ways to reduce prostaglandin E2, *Pharm. Pat. Anal. 2*, 265-288.
4. Nakanishi, M., and Rosenberg, D. W. (2013) Multifaceted roles of PGE2 in inflammation and cancer, *Semin. Immunopathol. 35*, 123-137.
5. Leclerc, P., Idborg, H., Spahiu, L., Larsson, C., Nekhotiaeva, N., Wannberg, J., Stenberg, P., Korotkova, M., and Jakobsson, P.-J. (2013) Characterization of a human and murine mPGES-1 inhibitor and comparison to mPGES-1 genetic deletion in mouse models of inflammation, *Prostaglandins Other Lipid Mediators 107*, 26-34.
6. Kothavade, P. S., Nagmoti, D. M., Bulani, V. D., and Juvekar, A. R. (2013) Arzanol, a potent mPGES-1 inhibitor: novel anti-inflammatory agent, *Sci. World J.*, 986429/986421-986429/986410, 986410 pp.
7. Thoren, S., Weinander, R., Saha, S., Jegerschoeld, C., Pettersson, P. L., Samuelsson, B., Hebert, H., Hamberg, M., Morgenstern, R., and Jakobsson, P.-J. (2003) Human Microsomal Prostaglandin E Synthase-1: Purification, Functional Characterization, and Projection Structure Determination, *J. Biol. Chem. 278*, 22199-22209.
8. Funk, C. D. (2001) Prostaglandins and leukotrienes: advances in eicosanoid biology, *Science (Washington, DC, U. S.) 294*, 1871-1875.
9. Otani, T., Yamaguchi, K., Scherl, E., Du, B., Tai, H.-H., Greifer, M., Petrovic, L., Daikoku, T., Dey, S. K., Subbaramaiah, K., and Dannenberg, A. J. (2006) Levels of NAD+-dependent 15-hydroxyprostaglandin dehydrogenase are reduced in inflammatory bowel disease: evidence for involvement of TNF-α, *Am. J. Physiol. 290*, G361-G368.
10. Samad, T. A., Sapirstein, A., and Woolf, C. J. (2002) Prostanoids and pain: unraveling mechanisms and revealing therapeutic targets, *Trends Mol. Med. 8*, 390-396.
11. Wang, D., and DuBois, R. N. (2006) Prostaglandins and cancer, *Gut 55*, 115-122.
12. Smith, W. L. (1989) The eicosanoids and their biochemical mechanisms of action, *Biochem. J. 259*, 315-324.
13. Sugimoto, Y., and Narumiya, S. (2007) Prostaglandin E Receptors, *J. Biol. Chem. 282*, 11613-11617.

14. Sneader, W. (2000) The discovery of aspirin: a reappraisal, *BMJ 321*, 1591-1594.
15. Crofford, L. J. (1997) COX-1 and COX-2 tissue expression: implications and predictions, *J. Rheumatol., Suppl. 49*, 15-19.
16. Laine, L. (2002) The gastrointestinal effects of nonselective NSAIDs and COX-2-selective inhibitors, *Semin. Arthritis Rheum. 32*, 25-32.
17. Grisham, R. H. G. C. M. (2013) *Biochemistry*, 5 ed., university of virginia Mary Finch.
18. Friesen, R. W., and Mancini, J. A. (2008) Microsomal prostaglandin E2 synthase-1 (mPGES-1): a novel anti-inflammatory therapeutic target, *J. Med. Chem. 51*, 4059-4067.
19. Chen, C., and Yang, T. (2008) TXA2/PGI2 and cardiovascular disease, *Xiandai Shengwuyixue Jinzhan 8*, 2166-2168, 2172.
20. Robleto, D. O., and Herman, C. A. (1988) Cardiovascular effects of prostaglandin I2 and prostaglandin F2α in the unanesthetized bullfrog, Rana catesbeiana, *J. Exp. Zool. 246*, 10-16.
21. Saito, R., Kamiya, H., and Ono, N. (1985) Role of the central muscarinic receptor of prostaglandin I2 in cardiovascular function in rat, *Brain Res. 330*, 167-169.
22. Tegeder, I., and Geisslinger, G. (2006) Cardiovascular risk with cyclooxygenase inhibitors: general problem with substance specific differences?, *Naunyn Schmiedebergs Arch Pharmacol 373*, 1-17.
23. Jakobsson, P. J., Morgenstern, R., Mancini, J., Ford-Hutchinson, A., and Persson, B. (2000) Membrane-associated proteins in eicosanoid and glutathione metabolism (MAPEG). A widespread protein superfamily, *Am J Respir Crit Care Med 161*, S20-24.
24. Tanioka, T., Nakatani, Y., Semmyo, N., Murakami, M., and Kudo, I. (2000) Molecular identification of cytosolic prostaglandin E2 synthase that is functionally coupled with cyclooxygenase-1 in immediate prostaglandin E2 biosynthesis, *J. Biol. Chem. 275*, 32775-32782.
25. Kihara, Y., Matsushita, T., Kita, Y., Uematsu, S., Akira, S., Kira, J.-I., Ishiia, S., and Shimizu, T. (2009) Targeted lipidomics reveals mPGES-1-PGE2 as a therapeutic target for multiple sclerosis, *Proc. Natl. Acad. Sci. U. S. A. 106*, 21807-21812, S21807/21801-S21807/21811.
26. Engblom, D., Saha, S., Engstroem, L., Westman, M., Audoly, L. P., Jakobsson, P.-J., and Blomqvist, A. (2003) Microsomal prostaglandin E synthase-1 is the central switch during immune-induced pyresis, *Nat. Neurosci. 6*, 1137-1138.
27. Wang, M., Zukas, A. M., Hui, Y., Ricciotti, E., Pure, E., and FitzGerald, G. A. (2006) Deletion of microsomal prostaglandin E synthase-1 augments prostacyclin and retards atherogenesis, *Proc. Natl. Acad. Sci. U. S. A. 103*, 14507-14512.
28. Fahmi, H. (2004) mPGES-1 as a novel target for arthritis, *Curr. Opin. Rheumatol. 16*, 623-627.

29. Wu, D.-M., Mennerich, D., Arndt, K., Sugiyama, K., Ozaki, N., Schwarz, K., Wei, J.-Q., Wu, H., Bishopric, N. H., and Doods, H. (2009) Comparison of microsomal prostaglandin E synthase-1 deletion and COX-2 inhibition in acute cardiac ischemia in mice, *Prostaglandins Other Lipid Mediators 90*, 21-25.
30. Kuroki, Y., Sasaki, Y., Kamei, D., Akitake, Y., Takahashi, M., Uematsu, S., Akira, S., Nakatani, Y., Kudo, I., and Hara, S. (2012) Deletion of microsomal prostaglandin E synthase-1 protects neuronal cells from cytotoxic effects of β-amyloid peptide fragment 31-35, *Biochem. Biophys. Res. Commun. 424*, 409-413.
31. Aida-Yasuoka, K., Yoshioka, W., Kawaguchi, T., Ohsako, S., and Tohyama, C. (2014) A mouse strain less responsive to dioxin-induced prostaglandin E2 synthesis is resistant to the onset of neonatal hydronephrosis, *Toxicol. Sci. 141*, 465-474.
32. Chaudry, U. A., Zhuang, H., Crain, B. J., and Dore, S. (2008) Elevated microsomal prostaglandin-E synthase-1 in Alzheimer's disease, *Alzheimer's Dementia 4*, 6-13.
33. Radilova, H., Libra, A., Holasova, S., Safarova, M., Viskova, A., Kunc, F., and Buncek, M. (2009) COX-1 is coupled with mPGES-1 and ABCC4 in human cervix cancer cells, *Mol. Cell. Biochem. 330*, 131-140.
34. Subbaramaiah, K., Yoshimatsu, K., Scherl, E., Das, K. M., Glazier, K. D., Golijanin, D., Soslow, R. A., Tanabe, T., Naraba, H., and Dannenberg, A. J. (2004) Microsomal Prostaglandin E Synthase-1 Is Overexpressed in Inflammatory Bowel Disease. Evidence for involvement of the transcription factor Egr-1, *J. Biol. Chem. 279*, 12647-12658.
35. Gomez-Hernandez, A., Martin-Ventura, J. L., Sanchez-Galan, E., Vidal, C., Ortego, M., Blanco-Colio, L. M., Ortega, L., Tunon, J., and Egido, J. (2006) Overexpression of COX-2, Prostaglandin E Synthase-1 and Prostaglandin E Receptors in blood mononuclear cells and plaque of patients with carotid atherosclerosis: Regulation by nuclear factor-κB, *Atherosclerosis (Amsterdam, Neth.) 187*, 139-149.
36. Korotkova, M., Helmers, S. B., Loell, I., Alexanderson, H., Grundtman, C., Dorph, C., Lundberg, I. E., and Jakobsson, P. J. (2008) Effects of immunosuppressive treatment on microsomal prostaglandin E synthase 1 and cyclooxygenases expression in muscle tissue of patients with polymyositis or dermatomyositis, *Ann. Rheum. Dis. 67*, 1596-1602.
37. Lee, A. S., Ellman, M. B., Yan, D., Kroin, J. S., Cole, B. J., van, W. A. J., and Im, H.-J. (2013) A current review of molecular mechanisms regarding osteoarthritis and pain, *Gene 527*, 440-447.
38. Frolov, A., Yang, L., Dong, H., Hammock, B. D., and Crofford, L. J. (2013) Anti-inflammatory properties of prostaglandin E2: Deletion of microsomal prostaglandin E synthase-1 exacerbates non-immune inflammatory arthritis in mice, *Prostaglandins, Leukotrienes Essent. Fatty Acids 89*, 351-358.

39. Pecchi, E., Priam, S., Mladenovic, Z., Gosset, M., Saurel, A. S., Aguilar, L., Berenbaum, F., and Jacques, C. (2012) A potential role of chondroitin sulfate on bone in osteoarthritis: inhibition of prostaglandin E and matrix metalloproteinases synthesis in interleukin-1β-stimulated osteoblasts, *Osteoarthritis Cartilage 20*, 127-135.
40. Huang, X., Yan, W., Gao, D., Tong, M., Tai, H.-H., and Zhan, C.-G. (2006) Structural and functional characterization of human microsomal prostaglandin E synthase-1 by computational modeling and site-directed mutagenesis, *Bioorg. Med. Chem. 14*, 3553-3562.
41. Trebino, C. E., Stock, J. L., Gibbons, C. P., Naiman, B. M., Wachtmann, T. S., Umland, J. P., Pandher, K., Lapointe, J.-M., Saha, S., Roach, M. L., Carter, D., Thomas, N. A., Durtschi, B. A., McNeish, J. D., Hambor, J. E., Jakobsson, P.-J., Carty, T. J., Perez, J. R., and Audoly, L. P. (2003) Impaired inflammatory and pain responses in mice lacking an inducible prostaglandin E synthase, *Proc. Natl. Acad. Sci. U. S. A. 100*, 9044-9049.
42. Jakobsson, P.-J., Thoren, S., Morgenstern, R., and Samuelsson, B. (1999) Identification of human prostaglandin E synthase: a microsomal, glutathione-dependent, inducible enzyme, constituting a potential novel drug target, *Proc. Natl. Acad. Sci. U. S. A. 96*, 7220-7225.
43. Chang, H.-H., and Meuillet, E. J. (2011) Identification and development of mPGES-1 inhibitors: where we are at?, *Future Med. Chem. 3*, 1909-1934.
44. Thoren, S., and Jakobsson, P.-J. (2000) Coordinate up- and down-regulation of glutathione-dependent prostaglandin E synthase and cyclooxygenase-2 in A549 cells inhibition by NS-398 and leukotriene C4, *Eur. J. Biochem. 267*, 6428-6434.
45. Bannenberg, G., Dahlen, S.-E., Luijerink, M., Lundqvist, G., and Morgenstern, R. (1999) Leukotriene C4 is a tight-binding inhibitor of microsomal glutathione transferase-1. Effects of leukotriene pathway modifiers, *J. Biol. Chem. 274*, 1994-1999.
46. Quraishi, O., Mancini, J. A., and Riendeau, D. (2002) Inhibition of inducible prostaglandin E2 synthase by 15-deoxy-Δ12,14-prostaglandin J2 and polyunsaturated fatty acids, *Biochem. Pharmacol. 63*, 1183-1189.
47. Wobst, I., Schiffmann, S., Birod, K., Maier, T. J., Schmidt, R., Angioni, C., Geisslinger, G., and Groesch, S. (2008) Dimethylcelecoxib inhibits prostaglandin E2 production, *Biochem. Pharmacol. 76*, 62-69.
48. Riendeau, D., Aspiotis, R., Ethier, D., Gareau, Y., Grimm, E. L., Guay, J., Guiral, S., Juteau, H., Mancini, J. A., Methot, N., Rubin, J., and Friesen, R. W. (2005) Inhibitors of the inducible microsomal prostaglandin E2 synthase (mPGES-1) derived from MK-886, *Bioorg. Med. Chem. Lett. 15*, 3352-3355.
49. Wiegard, A., Hanekamp, W., Griessbach, K., Fabian, J., and Lehr, M. (2012) Pyrrole alkanoic acid derivatives as nuisance inhibitors of microsomal prostaglandin E2 synthase-1, *Eur. J. Med. Chem. 48*, 153-163.
50. Lauro, G., Terracciano, S., Bertamino, A., Riccio, R., Manfra, M., De, N. M.,

Pedatella, S., Fischer, K., Werz, O., Cantone, V., Ostacolo, C., Gomez-Monterrey, I., Novellino, E., Campiglia, P., and Bifulco, G. (2016) Identification of novel microsomal prostaglandin E2 synthase-1 (mPGES-1) lead inhibitors from Fragment Virtual Screening, *Eur J Med Chem 125*, 278-287.

51. Xu, D., Rowland, S. E., Clark, P., Giroux, A., Cote, B., Guiral, S., Salem, M., Ducharme, Y., Friesen, R. W., Methot, N., Mancini, J., Audoly, L., and Riendeau, D. (2008) MF63 [2-(6-chloro-1H-phenanthro[9,10-d]imidazol-2-yl)isophthalonitrile], a selective microsomal prostaglandin E synthase-1 inhibitor, relieves pyresis and pain in preclinical models of inflammation, *J. Pharmacol. Exp. Ther. 326*, 754-763.
52. Wolfer, D. P., Crusio, W. E., and Lipp, H.-P. (2002) Knockout mice: simple solutions to the problems of genetic background and flanking genes, *Trends in Neurosciences 25*, 336-340.
53. Crusio, W. E., Goldowitz, D., Holmes, A., and Wolfer, D. (2009) Standards for the publication of mouse mutant studies, *Genes, Brain and Behavior 8*, 1-4.
54. Leclerc, P., Pawelzik, S.-C., Idborg, H., Spahiu, L., Larsson, C., Stenberg, P., Korotkova, M., and Jakobsson, P.-J. (2013) Characterization of a new mPGES-1 inhibitor in rat models of inflammation, *Prostaglandins Other Lipid Mediators 102-103*, 1-12.
55. Hanke, T., Roersch, F., Thieme, T. M., Ferreiros, N., Schneider, G., Geisslinger, G., Proschak, E., Groesch, S., and Schubert-Zsilavecz, M. (2013) Synthesis and pharmacological characterization of benzenesulfonamides as dual species inhibitors of human and murine mPGES-1, *Bioorg. Med. Chem. 21*, 7874-7883.
56. Hamza, A., Tong, M., AbdulHameed, M. D. M., Liu, J., Goren, A. C., Tai, H.-H., and Zhan, C.-G. (2010) Understanding Microscopic Binding of Human Microsomal Prostaglandin E Synthase-1 (mPGES-1) Trimer with Substrate PGH2 and Cofactor GSH: Insights from Computational Alanine Scanning and Site-directed Mutagenesis, *J. Phys. Chem. B 114*, 5605-5616.
57. Hamza, A., AbdulHameed, M. D. M., and Zhan, C.-G. (2008) Understanding Microscopic Binding of Human Microsomal Prostaglandin E Synthase-1 with Substrates and Inhibitors by Molecular Modeling and Dynamics Simulation, *J. Phys. Chem. B 112*, 7320-7329.
58. AbdulHameed, M. D. M., Hamza, A., Liu, J., Huang, X., and Zhan, C.-G. (2008) Human Microsomal Prostaglandin E Synthase-1 (mPGES-1) Binding with Inhibitors and the Quantitative Structure-Activity Correlation, *J. Chem. Inf. Model. 48*, 179-185.
59. Jegerschoeld, C., Pawelzik, S.-C., Purhonen, P., Bhakat, P., Gheorghe, K. R., Gyobu, N., Mitsuoka, K., Morgenstern, R., Jakobsson, P.-J., and Herbert, H. (2008) Structural basis for induced formation of the inflammatory mediator prostaglandin E2, *Proc. Natl. Acad. Sci. U. S. A. 105*, 11110-11115.
60. Sjogren, T., Nord, J., Ek, M., Johansson, P., Liu, G., and Geschwindner, S. (2013) Crystal structure of microsomal prostaglandin E2 synthase provides insight into

diversity in the MAPEG superfamily, *Proc Natl Acad Sci U S A 110*, 3806-3811.
61. Weinert, T., Olieric, V., Waltersperger, S., Panepucci, E., Chen, L., Zhang, H., Zhou, D., Rose, J., Ebihara, A., Kuramitsu, S., Li, D., Howe, N., Schnapp, G., Pautsch, A., Bargsten, K., Prota, A. E., Surana, P., Kottur, J., Nair, D. T., Basilico, F., Cecatiello, V., Pasqualato, S., Boland, A., Weichenrieder, O., Wang, B.-C., Steinmetz, M. O., Caffrey, M., and Wang, M. (2015) Fast native-SAD phasing for routine macromolecular structure determination, *Nat. Methods 12*, 131-133.
62. Luz, J. G., Antonysamy, S., Kuklish, S. L., Condon, B., Lee, M. R., Allison, D., Yu, X.-P., Chandrasekhar, S., Backer, R., Zhang, A., Russell, M., Chang, S. S., Harvey, A., Sloan, A. V., and Fisher, M. J. (2015) Crystal Structures of mPGES-1 Inhibitor Complexes Form a Basis for the Rational Design of Potent Analgesic and Anti-Inflammatory Therapeutics, *J. Med. Chem. 58*, 4727-4737.
63. Li, D., Howe, N., Dukkipati, A., Shah, S. T. A., Bax, B. D., Edge, C., Bridges, A., Hardwicke, P., Singh, O. M. P., Giblin, G., Pautsch, A., Pfau, R., Schnapp, G., Wang, M., Olieric, V., and Caffrey, M. (2014) Crystallizing Membrane Proteins in the Lipidic Mesophase. Experience with Human Prostaglandin E2 Synthase 1 and an Evolving Strategy, *Crystal Growth & Design 14*, 2034-2047.
64. Morris, G. M., Huey, R., Lindstrom, W., Sanner, M. F., Belew, R. K., Goodsell, D. S., and Olson, A. J. (2009) AutoDock and AutoDockTools: Automated docking with selective receptor flexibility, *J. Comput. Chem. 30*, 2785-2791.
65. He, S., Li, C., Liu, Y., and Lai, L. (2013) Discovery of Highly Potent Microsomal Prostaglandin E2 Synthase 1 Inhibitors Using the Active Conformation Structural Model and Virtual Screen, *J. Med. Chem. 56*, 3296-3309.
66. Degliesposti, G., Portioli, C., Parenti, M. D., and Rastelli, G. (2011) BEAR, a novel virtual screening methodology for drug discovery, *J. Biomol. Screening 16*, 129-133.
67. Salomon-Ferrer, R., Case, D. A., and Walker, R. C. (2013) An overview of the amber biomolecular simulation package, *Wiley Interdiscip. Rev.: Comput. Mol. Sci. 3*, 198-210.
68. D.A. Case, T. A. D., T.E. Cheatham, III, C.L. Simmerling, J. Wang, R.E. Duke, R., Luo, R. C. W., W. Zhang, K.M. Merz, B. Roberts, S. Hayik, A. Roitberg, G. Seabra,, J. Swails, A. W. G., I. Kolossváry, K.F. Wong, F. Paesani, J. Vanicek, R.M. Wolf, J. Liu,, X. Wu, S. R. B., T. Steinbrecher, H. Gohlke, Q. Cai, X. Ye, J. Wang, M.-J. Hsieh, G., Cui, D. R. R., D.H. Mathews, M.G. Seetin, R. Salomon-Ferrer, C. Sagui, V. Babin, T., and Luchko, S. G., A. Kovalenko, and P.A. Kollman (2012). (2012) AMBER 12, (of, U., and California, S. F., Eds.).
69. Benkert, P., Biasini, M., and Schwede, T. (2011) Toward the estimation of the absolute quality of individual protein structure models, *Bioinformatics 27*, 343-350.
70. Benkert, P., Kuenzli, M., and Schwede, T. (2009) QMEAN server for protein model quality estimation, *Nucleic Acids Res. 37*, W510-W514.

71. Rathelot, P., Azas, N., El-Kashef, H., Delmas, F., Di Giorgio, C., Timon-David, P., Maldonado, J., and Vanelle, P. (2002) 1,3-Diphenylpyrazoles: synthesis and antiparasitic activities of azomethine derivatives, *European Journal of Medicinal Chemistry 37*, 671-679.
72. Stella, A., Van Belle, K., De Jonghe, S., Louat, T., Herman, J., Rozenski, J., Waer, M., and Herdewijn, P. (2013) Synthesis of a 2,4,6-trisubstituted 5-cyano-pyrimidine library and evaluation of its immunosuppressive activity in a Mixed Lymphocyte Reaction assay, *Bioorg. Med. Chem. 21*, 1209-1218.
73. Zhou, Z., Ding, K., Zhou, S., Yuan, Y., Zheng, F., and Zhan, C.-G. (2017) Computational design, synthesis and characterization of novel mPGES-1 inhibitors, pp MEDI-260, American Chemical Society.
74. Zhou, S., Zhou, Z., Yuan, Y., and Zhan, C.-G. (2017) Novel mPGES-1 inhibitors identified from structure-based virtual screening based on new acting mechanism, pp MEDI-179, American Chemical Society.
75. Ding, K., Zhou, Z., Yuan, Y., Zheng, F., and Zhan, C.-G. (2017) Rational design, synthesis, and in vitro evaluation of mPGES-1 inhibitors as next-generation of anti-inflammatory drugs, pp MEDI-104, American Chemical Society.
76. Tong, M., Ding, Y., and Tai, H.-H. (2006) Histone deacetylase inhibitors and transforming growth factor-β induce 15-hydroxyprostaglandin dehydrogenase expression in human lung adenocarcinoma cells, *Biochem. Pharmacol. 72*, 701-709.
77. Tong, M., Ding, Y., and Tai, H.-H. (2006) Reciprocal regulation of cyclooxygenase-2 and 15-hydroxyprostaglandin dehydrogenase expression in A549 human lung adenocarcinoma cells, *Carcinogenesis 27*, 2170-2179.
78. Zhou, Z., Yuan, Y., Zhou, S., Ding, K., Zheng, F., and Zhan, C.-G. (2017) Selective inhibitors of human mPGES-1 from structure-based computational screening, *Bioorganic & Medicinal Chemistry Letters 27*, 3739-3743.
79. Serhan, C. N., and Levy, B. (2003) Success of prostaglandin E-2 in structure-function is a challenge for structure-based therapeutics, *Proceedings of the National Academy of Sciences of the United States of America 100*, 8609-8611.
80. Kudo, I., and Murakami, M. (2005) Prostaglandin E synthase, a terminal enzyme for prostaglandin E-2 biosynthesis, *Journal of Biochemistry and Molecular Biology 38*, 633-638.
81. Fahmi, H. (2004) MPGES-1 as a novel target for arthritis, *Current Opinion in Rheumatology 16*, 623-627.
82. Park, J. Y., Pillinger, M. H., and Abramson, S. B. (2006) Prostaglandin E-2 synthesis and secretion: The role of PGE(2) synthases, *Clinical Immunology 119*, 229-240.
83. Murakami, M., Nakatani, Y., Tanioka, T., and Kudo, I. (2002) Prostaglandin E synthase, *Prostaglandins & Other Lipid Mediators 68-9*, 383-399.
84. Murakami, M., Naraba, H., Tanioka, T., Semmyo, N., Nakatani, Y., Kojima, F., Ikeda, T., Fueki, M., Ueno, A., Oh-ishi, S., and Kudo, I. (2000) Regulation of

prostaglandin E-2 biosynthesis by inducible membrane-associated prostaglandin E-2 synthase that acts in concert with cyclooxygenase-2, *Journal of Biological Chemistry 275*, 32783-32792.

85. Uematsu, S., Matsumoto, M., Takeda, K., and Akira, S. (2002) Lipopolysaccharide-dependent prostaglandin E-2 production is regulated by the glutathione-dependent prostaglandin E-2 synthase gene induced by the toll-like receptor 4/MyD88/NF-IL6 pathway, *Journal of Immunology 168*, 5811-5816.
86. Kamei, D., Murakami, M., Nakatani, Y., Ishikawa, Y., Ishii, T., and Kudo, I. (2003) Potential role of microsomal prostaglandin E synthase-1 in tumorigenesis, *Journal of Biological Chemistry 278*, 19396-19405.
87. Kamei, D., Yamakawa, K., Takegoshi, Y., Mikami-Nakanishi, M., Nakatani, Y., Oh-ishi, S., Yasui, H., Azuma, Y., Hirasawa, N., Ohuchi, K., Kawaguchi, H., Ishikawa, Y., Ishii, T., Uematsu, S., Akira, S., Murakami, M., and Kudo, I. (2004) Reduced pain hypersensitivity and inflammation in mice lacking microsomal prostaglandin E synthase-1, *Journal of Biological Chemistry 279*, 33684-33695.
88. Ikeda-Matsuo, Y., Ota, A., Fukada, T., Uematsu, S., Akira, S., and Sasaki, Y. (2006) Microsomal prostaglandin E synthase-1 is a critical factor of stroke-reperfusion injury, *Proceedings of the National Academy of Sciences of the United States of America 103*, 11790-11795.
89. Murakami, M., and Kudo, I. (2004) Recent advances in molecular biology and physiology of the prostaglandin E-2-biosynthetic pathway, *Progress in Lipid Research 43*, 3-35.
90. Claveau, D., Sirinyan, M., Guay, J., Gordon, R., Chan, C. C., Bureau, Y., Riendeau, D., and Mancini, J. A. (2003) Microsomal prostaglandin E synthase-1 is a major terminal synthase that is selectively up-regulated during cyclooxygenase-2-dependent prostaglandin E-2 production in the rat adjuvant-induced arthritis model, *Journal of Immunology 170*, 4738-4744.
91. Oshima, H., Oshima, M., Inaba, K., and Taketo, M. M. (2004) Hyperplastic gastric tumors induced by activated macrophages in COX-2/mPGES-1 transgenic mice, *EMBO Journal 23*, 1669-1678.
92. Friesen, R. W., and Mancini, J. A. (2008) Microsomal prostaglandin E-2 synthase-1 (mPGES-1): A novel anti-inflammatory therapeutic target, *Journal of medicinal chemistry 51*, 4059-4067.
93. Samuelsson, B., Morgenstern, R., and Jakobsson, P. J. (2007) Membrane prostaglandin E synthase-1: A novel therapeutic target, *Pharmacological Reviews 59*, 207-224.
94. Scholich, K., and Geisslinger, G. (2006) Is mPGES-1 a promising target for pain therapy?, *Trends in Pharmacological Sciences 27*, 399-401.
95. Cheng, Y., Wang, M., Yu, Y., Lawson, J., Funk, C. D., and FitzGerald, G. A. (2006) Cyclooxygenases, microsomal prostaglandin E synthase-1, and cardiovascular function, *Journal of Clinical Investigation 116*, 1391-1399.
96. Engblom, D., Saha, S., Engstrom, L., Westman, M., Audoly, L. P., Jakobsson, P.

J., and Blomqvist, A. (2003) Microsomal prostaglandin E synthase-1 is the central switch during immune-induced pyresis, *Nature Neuroscience 6*, 1137-1138.

97. Trebino, C. E., Stock, J. L., Gibbons, C. P., Naiman, B. M., Wachtmann, T. S., Umland, J. P., Pandher, K., Lapointe, J. M., Saha, S., Roach, M. L., Carter, D., Thomas, N. A., Durtschi, B. A., McNeish, J. D., Hambor, J. E., Jakobsson, P. J., Carty, T. J., Perez, J. R., and Audoly, L. P. (2003) Impaired inflammatory and pain responses in mice lacking an inducible prostaglandin E synthase, *Proceedings of the National Academy of Sciences of the United States of America 100*, 9044-9049.
98. Schiffler, M. A., Antonysamy, S., Bhattachar, S. N., Campanale, K. M., Chandrasekhar, S., Condon, B., Desai, P. V., Fisher, M. J., Groshong, C., Harvey, A., Hickey, M. J., Hughes, N. E., Jones, S. A., Kim, E. J., Kuklish, S. L., Luz, J. G., Norman, B. H., Rathmell, R. E., Rizzo, J. R., Seng, T. W., Thibodeaux, S. J., Woods, T. A., York, J. S., and Yu, X. P. (2016) Discovery and Characterization of 2-Acylaminoimidazole Microsomal Prostaglandin E Synthase-1 Inhibitors, *J. Med. Chem. 59*, 194-205.
99. Hieke, M., Greiner, C., Dittrich, M., Reisen, F., Schneider, G., Schubert-Zsilavecz, M., and Werz, O. (2011) Discovery and biological evaluation of a novel class of dual microsomal prostaglandin E2 synthase-1/5-lipoxygenase inhibitors based on 2-[(4,6-diphenethoxypyrimidin-2-yl)thio]hexanoic acid, *J. Med. Chem. 54*, 4490-4507.
100. Hanke, T., Dehm, F., Liening, S., Popella, S. D., Maczewsky, J., Pillong, M., Kunze, J., Weinigel, C., Barz, D., Kaiser, A., Wurglics, M., Lammerhofer, M., Schneider, G., Sautebin, L., Schubert-Zsilavecz, M., and Werz, O. (2013) Aminothiazole-featured pirinixic acid derivatives as dual 5-lipoxygenase and microsomal prostaglandin E2 synthase-1 inhibitors with improved potency and efficiency in vivo, *J. Med. Chem. 56*, 9031-9044.
101. Terracciano, S., Lauro, G., Strocchia, M., Fischer, K., Werz, O., Riccio, R., Bruno, I., and Bifulco, G. (2015) Structural Insights for the Optimization of Dihydropyrimidin-2(1H)-one Based mPGES-1 Inhibitors, *ACS Med. Chem. Lett. 6*, 187-191.
102. Shiro, T., Kakiguchi, K., Takahashi, H., Nagata, H., and Tobe, M. (2013) 7-Phenyl-imidazoquinolin-4(5H)-one derivatives as selective and orally available mPGES-1 inhibitors, *Bioorg. Med. Chem. 21*, 2868-2878.
103. Shiro, T., Kakiguchi, K., Takahashi, H., Nagata, H., and Tobe, M. (2013) Synthesis and biological evaluation of substituted imidazoquinoline derivatives as mPGES-1 inhibitors, *Bioorg. Med. Chem. 21*, 2068-2078.
104. Shiro, T., Takahashi, H., Kakiguchi, K., Inoue, Y., Masuda, K., Nagata, H., and Tobe, M. (2012) Synthesis and SAR study of imidazoquinolines as a novel structural class of microsomal prostaglandin E(2) synthase-1 inhibitors, *Bioorg. Med. Chem. Lett. 22*, 285-288.

105. Liedtke, A. J., Keck, P. R., Lehmann, F., Koeberle, A., Werz, O., and Laufer, S. A. (2009) Arylpyrrolizines as inhibitors of microsomal prostaglandin E2 synthase-1 (mPGES-1) or as dual inhibitors of mPGES-1 and 5-lipoxygenase (5-LOX), *J. Med. Chem. 52*, 4968-4972.
106. Shang, E., Wu, Y., Liu, P., Liu, Y., Zhu, W., Deng, X., He, C., He, S., Li, C., and Lai, L. (2014) Benzo[d]isothiazole 1,1-dioxide derivatives as dual functional inhibitors of 5-lipoxygenase and microsomal prostaglandin E(2) synthase-1, *Bioorg. Med. Chem. Lett. 24*, 2764-2767.
107. Wu, T. Y., Juteau, H., Ducharme, Y., Friesen, R. W., Guiral, S., Dufresne, L., Poirier, H., Salem, M., Riendeau, D., Mancini, J., and Brideau, C. (2010) Biarylimidazoles as inhibitors of microsomal prostaglandin E2 synthase-1, *Bioorg. Med. Chem. Lett. 20*, 6978-6982.
108. Wiegard, A., Hanekamp, W., Griessbach, K., Fabian, J., and Lehr, M. (2012) Pyrrole alkanoic acid derivatives as nuisance inhibitors of microsomal prostaglandin E2 synthase-1, *Eur. J. Med. Chem. 48*, 153-163.
109. Chini, M. G., De Simone, R., Bruno, I., Riccio, R., Dehm, F., Weinigel, C., Barz, D., Werz, O., and Bifulco, G. (2012) Design and synthesis of a second series of triazole-based compounds as potent dual mPGES-1 and 5-lipoxygenase inhibitors, *Eur. J. Med. Chem. 54*, 311-323.
110. Giroux, A., Boulet, L., Brideau, C., Chau, A., Claveau, D., Cote, B., Ethier, D., Frenette, R., Gagnon, M., Guay, J., Guiral, S., Mancini, J., Martins, E., Masse, F., Methot, N., Riendeau, D., Rubin, J., Xu, D., Yu, H., Ducharme, Y., and Friesen, R. W. (2009) Discovery of disubstituted phenanthrene imidazoles as potent, selective and orally active mPGES-1 inhibitors, *Bioorg. Med. Chem. Lett. 19*, 5837-5841.
111. Xu, D., Rowland, S. E., Clark, P., Giroux, A., Cote, B., Guiral, S., Salem, M., Ducharme, Y., Friesen, R. W., Methot, N., Mancini, J., Audoly, L., and Riendeau, D. (2008) MF63 [2-(6-chloro-1H-phenanthro[9,10-d]imidazol-2-yl)-isophthalonitrile], a selective microsomal prostaglandin E synthase-1 inhibitor, relieves pyresis and pain in preclinical models of inflammation, *J. Pharmacol. Exp. Ther. 326*, 754-763.
112. Lee, K., Pham, V. C., Choi, M. J., Kim, K. J., Lee, K. T., Han, S. G., Yu, Y. G., and Lee, J. Y. (2013) Fragment-based discovery of novel and selective mPGES-1 inhibitors Part 1: identification of sulfonamido-1,2,3-triazole-4,5-dicarboxylic acid, *Bioorg. Med. Chem. Lett. 23*, 75-80.
113. Cote, B., Boulet, L., Brideau, C., Claveau, D., Ethier, D., Frenette, R., Gagnon, M., Giroux, A., Guay, J., Guiral, S., Mancini, J., Martins, E., Masse, F., Methot, N., Riendeau, D., Rubin, J., Xu, D., Yu, H., Ducharme, Y., and Friesen, R. W. (2007) Substituted phenanthrene imidazoles as potent, selective, and orally active mPGES-1 inhibitors, *Bioorg. Med. Chem. Lett. 17*, 6816-6820.
114. Riendeau, D., Aspiotis, R., Ethier, D., Gareau, Y., Grimm, E. L., Guay, J., Guiral, S., Juteau, H., Mancini, J. A., Methot, N., Rubin, J., and Friesen, R. W. (2005)

Inhibitors of the inducible microsomal prostaglandin E2 synthase (mPGES-1) derived from MK-886, *Bioorg. Med. Chem. Lett. 15*, 3352-3355.

115. Bruno, A., Di Francesco, L., Coletta, I., Mangano, G., Alisi, M. A., Polenzani, L., Milanese, C., Anzellotti, P., Ricciotti, E., Dovizio, M., Di Francesco, A., Tacconelli, S., Capone, M. L., and Patrignani, P. (2010) Effects of AF3442 [N-(9-ethyl-9H-carbazol-3-yl)-2-(trifluoromethyl)benzamide], a novel inhibitor of human microsomal prostaglandin E synthase-1, on prostanoid biosynthesis in human monocytes in vitro, *Biochem. Pharmacol. 79*, 974-981.
116. Koeberle, A., Haberl, E. M., Rossi, A., Pergola, C., Dehm, F., Northoff, H., Troschuetz, R., Sautebin, L., and Werz, O. (2009) Discovery of benzo[g]indol-3-carboxylates as potent inhibitors of microsomal prostaglandin E(2) synthase-1, *Bioorg. Med. Chem. 17*, 7924-7932.
117. Walker, D. P., Arhancet, G. B., Lu, H. F., Heasley, S. E., Metz, S., Kablaoui, N. M., Franco, F. M., Hanau, C. E., Scholten, J. A., Springer, J. R., Fobian, Y. M., Carter, J. S., Xing, L., Yang, S., Shaffer, A. F., Jerome, G. M., Baratta, M. T., Moore, W. M., and Vazquez, M. L. (2013) Synthesis and biological evaluation of substituted benzoxazoles as inhibitors of mPGES-1: use of a conformation-based hypothesis to facilitate compound design, *Bioorg. Med. Chem. Lett. 23*, 1120-1126.
118. Wang, J., Limburg, D., Carter, J., Mbalaviele, G., Gierse, J., and Vazquez, M. (2010) Selective inducible microsomal prostaglandin E(2) synthase-1 (mPGES-1) inhibitors derived from an oxicam template, *Bioorg. Med. Chem. Lett. 20*, 1604-1609.
119. Jin, Y., Smith, C. L., Hu, L., Campanale, K. M., Stoltz, R., Huffman, L. G., Jr., McNearney, T. A., Yang, X. Y., Ackermann, B. L., Dean, R., Regev, A., and Landschulz, W. (2016) Pharmacodynamic comparison of LY3023703, a novel microsomal prostaglandin e synthase 1 inhibitor, with celecoxib, *Clin. Pharmacol. Ther. 99*, 274-284.
120. Li, D., Howe, N., Dukkipati, A., Shah, S. T., Bax, B. D., Edge, C., Bridges, A., Hardwicke, P., Singh, O. M., Giblin, G., Pautsch, A., Pfau, R., Schnapp, G., Wang, M., Olieric, V., and Caffrey, M. (2014) Crystallizing Membrane Proteins in the Lipidic Mesophase. Experience with Human Prostaglandin E2 Synthase 1 and an Evolving Strategy, *Crystal growth & design 14*, 2034-2047.
121. Yang, W., AbdulHameed, M. D. M., Hamza, A., and Zhan, C.-G. (2012) New inhibitor of 3-phosphoinositide dependent protein kinase-1 identified from virtual screening, *Bioorg. Med. Chem. Letters 22*, 1629-1632.
122. Hamza, A., Zhao, X., Tong, M., Tai, H. H., and Zhan, C. G. (2011) Novel human mPGES-1 inhibitors identified through structure-based virtual screening, *Bioorg. Med. Chem. 19*, 6077-6086.
123. Trott, O., and Olson, A. J. (2010) AutoDock Vina: improving the speed and accuracy of docking with a new scoring function, efficient optimization, and multithreading, *J. Comput. Chem. 31*, 455-461.

124. Case, D. A., Darden, T. A., Cheatham Iii, T. E., Simmerling, C. L., Wang, J., Duke, R. E., Luo, R., Walker, R. C., Zhang, W., Merz, K. M., Roberts, B., Hayik, S., Roitberg, A., Seabra, G., Swails, J., Goetz, A. W., Kolossváry, I., Wong, K. F., Paesani, F., Vanicek, J., Wolf, R. M., Liu, J., Wu, X., Brozell, S. R., Steinbrecher, T., Gohlke, H., Cai, Q., Ye, X., Wang, J., Hsieh, M. J., Cui, G., Roe, D. R., Mathews, D. H., Seetin, M. G., Salomon-Ferrer, R., Sagui, C., Babin, V., Luchko, T., Gusarov, S., Kovalenko, A., and Kollman, P. A. (2012) AMBER 12, *University of California, San Francisco*.
125. Case, D. A., Cheatham, T. E., Darden, T., Gohlke, H., Luo, R., Merz, K. M., Onufriev, A., Simmerling, C., Wang, B., and Woods, R. J. (2005) The Amber biomolecular simulation programs, *J Comput Chem 26*, 1668-1688.
126. Degliesposti, G., Portioli, C., Parenti, M. D., and Rastelli, G. (2011) BEAR, a novel virtual screening methodology for drug discovery, *J. Biomol. Screen. 16*, 129-133.
127. Rastelli, G., Degliesposti, G., Del Rio, A., and Sgobba, M. (2009) Binding estimation after refinement, a new automated procedure for the refinement and rescoring of docked ligands in virtual screening, *Chem. Biol. Drug Des. 73*, 283-286.
128. Hamza, A., Tong, M., AbdulHameed, M. D., Liu, J., Goren, A. C., Tai, H. H., and Zhan, C. G. (2010) Understanding microscopic binding of human microsomal prostaglandin E synthase-1 (mPGES-1) trimer with substrate PGH2 and cofactor GSH: insights from computational alanine scanning and site-directed mutagenesis., *J Phys Chem B. 114*, 5605-5616.
129. Huang, X. Q., Yan, W. L., Gao, D. Q., Tong, M., Tai, H.-H., and Zhan, C.-G. (2006) Structural and functional characterization of human microsomal prostaglandin E synthase-1 by computational modeling and site-directed mutagenesis, *Bioorg. Med. Chem. 14*, 3553-3562.
130. Hamza, A., Zhao, X., Tong, M., Tai, H.-H., and Zhan, C.-G. (2011) Novel human mPGES-1 inhibitors identified through structure-based virtual screening, *Bioorg. Med. Chem. 19*, 6077-6086.
131. Maclouf, J., Grassi, J., and Pradelles, P. (1987) Development of Enzyme-Immunoassay Techniques for Measurement of Eicosanoids, In *Prostaglandin and Lipid Metabolism in Radiation Injury* (Walden, T. L., and Hughes, H. N., Eds.), pp 355-364, Springer US, Boston, MA.
132. Pradelles, P., Grassi, J., and Maclouf, J. (1985) Enzyme immunoassays of eicosanoids using acetylcholine esterase as label: an alternative to radioimmunoassay, *Anal. Chem. 57*, 1170-1173.
133. Pecchi, E., Dallaporta, M., Thirion, S., Jean, A., and Troadec, J. D. (2009) mPGES-1: it makes us sick!, *Med Sci (Paris) 25*, 451-454.
134. Jia, Z., Zhang, Y., Ding, G., Heiney, K. M., Huang, S., and Zhang, A. (2015) Role of COX-2/mPGES-1/prostaglandin E2 cascade in kidney injury, *Mediators Inflammation*, 147894.

135. De Simone, R., Andres, R. M., Aquino, M., Bruno, I., Guerrero, M. D., Terencio, M. C., Paya, M., and Riccio, R. (2010) Toward the discovery of new agents able to inhibit the expression of microsomal prostaglandin E synthase-1 enzyme as promising tools in drug development, *Chem. Biol. Drug Des. 76*, 17-24.
136. Terzuoli, E., Donnini, S., Giachetti, A., Iniguez, M. A., Fresno, M., Melillo, G., and Ziche, M. (2010) Inhibition of Hypoxia Inducible Factor-1α by Dihydroxyphenylethanol, a Product from Olive Oil, Blocks Microsomal Prostaglandin-E Synthase-1/Vascular Endothelial Growth Factor Expression and Reduces Tumor Angiogenesis, *Clin. Cancer Res. 16*, 4207-4216.
137. Sano, H. (2011) The role of lipid mediators in the pathogenesis of rheumatoid arthritis, *Inflammation Regener. 31*, 151-156.
138. Korotkova, M., Daha, N. A., Seddighzadeh, M., Ding, B., Catrina, A. I., Lindblad, S., Huizinga, T. W. J., Toes, R. E. M., Alfredsson, L., Klareskog, L., Jakobsson, P.-J., and Padyukov, L. (2011) Variants of gene for microsomal prostaglandin E2 synthase show association with disease and severe inflammation in rheumatoid arthritis, *Eur. J. Hum. Genet. 19*, 908-914.
139. Korotkova, M., and Jakobsson, P.-J. (2010) Microsomal prostaglandin e synthase-1 in rheumatic diseases, *Front Pharmacol 1*, 146.
140. Dakin, S. G., Dudhia, J., Werling, N. J., Werling, D., Abayasekara, D. R. E., and Smith, R. K. W. (2012) Inflamm-aging and arachidonic acid metabolite differences with stage of tendon disease, *PLoS One 7*, e48978.
141. Beaulieu, D., Thebault, P., Pelletier, R., Chapdelaine, P., Tarnopolsky, M., Furling, D., and Puymirat, J. (2012) Abnormal prostaglandin E2 production blocks myogenic differentiation in myotonic dystrophy, *Neurobiol. Dis. 45*, 122-129.
142. Camacho, M., Dilme, J., Sola-Villa, D., Rodriguez, C., Bellmunt, S., Siguero, L., Alcolea, S., Romero, J.-M., Escudero, J.-R., Martinez-Gonzalez, J., and Vila, L. (2013) Microvascular COX-2/mPGES-1/EP-4 axis in human abdominal aortic aneurysm, *J. Lipid Res. 54*, 3506-3515.
143. Akitake, Y., Nakatani, Y., Kamei, D., Hosokawa, M., Akatsu, H., Uematsu, S., Akira, S., Kudo, I., Hara, S., and Takahashi, M. (2013) Microsomal prostaglandin E synthase-1 is induced in Alzheimer's disease and its deletion mitigates Alzheimer's disease-like pathology in a mouse model, *J. Neurosci. Res. 91*, 909-919.
144. Ikeda-Matsuo, Y., Hirayama, Y., Ota, A., Uematsu, S., Akira, S., and Sasaki, Y. (2010) Microsomal prostaglandin E synthase-1 and cyclooxygenase-2 are both required for ischaemic excitotoxicity, *Br. J. Pharmacol. 159*, 1174-1186.
145. Siljehav, V., Olsson Hofstetter, A., Jakobsson, P.-J., and Herlenius, E. (2012) mPGES-1 and prostaglandin E2: vital role in inflammation, hypoxic response, and survival, *Pediatr. Res. 72*, 460-467.
146. Coulombe, F., Jaworska, J., Verway, M., Tzelepis, F., Massoud, A., Gillard, J., Wong, G., Kobinger, G., Xing, Z., Couture, C., Joubert, P., Fritz, J. H., Powell,

W. S., and Divangahi, M. (2014) Targeted Prostaglandin E2 Inhibition Enhances Antiviral Immunity through Induction of Type I Interferon and Apoptosis in Macrophages, *Immunity 40*, 554-568.

147. Larsson, K., Kock, A., Idborg, H., Henriksson, M. A., Martinsson, T., Johnsen, J. I., Korotkova, M., Kogner, P., and Jakobsson, P.-J. (2015) COX/mPGES-1/PGE2 pathway depicts an inflammatory-dependent high-risk neuroblastoma subset, *Proc. Natl. Acad. Sci. U. S. A.*, Ahead of Print.
148. Maeng, H.-J., Lee, W.-J., Jin, Q.-R., Chang, J.-E., and Shim, W.-S. (2014) Upregulation of COX-2 in the lung cancer promotes overexpression of multidrug resistance protein 4 (MRP4) via PGE2-dependent pathway, *Eur. J. Pharm. Sci. 62*, 189-196.
149. Radilova, H., Libra, A., Holasova, S., Safarova, M., Viskova, A., Kunc, F., and Buncek, M. (2009) COX-1 is coupled with mPGES-1 and ABCC4 in human cervix cancer cells, *Mol Cell Biochem 330*, 131-140.
150. Yu, J., Liu, H., and Han, X. (2014) Research status of Wnt and COX-2 signal pathway in gastric cancer, *Xiandai Zhongliu Yixue 22*, 683-687.
151. van, d. T. J. G. B., Harkema, L., Ensink, J. M., Barneveld, A., Martens, A., van, d. L. C. H. A., van, W. P. R., and Grone, A. (2014) Expression of cyclo-oxygenases-1 and -2, and microsomal prostaglandin E synthase-1 in penile and preputial papillomas and squamous cell carcinomas in the horse, *Equine Vet J 46*, 618-624.
152. Abdel-Tawab, M., Zettl, H., and Schubert-Zsilavecz, M. (2009) Nonsteroidal anti-inflammatory drugs: a critical review on current concepts applied to reduce gastrointestinal toxicity, *Curr. Med. Chem. 16*, 2042-2063.
153. Takeda, H., Miyoshi, H., Tamai, Y., Oshima, M., and Taketo, M. M. (2004) Simultaneous expression of COX-2 and mPGES-1 in mouse gastrointestinal hamartomas, *Br. J. Cancer 90*, 701-704.
154. Korotkova, M., and Jakobsson, P.-J. (2014) Characterization of Microsomal Prostaglandin E Synthase 1 Inhibitors, *Basic Clin. Pharmacol. Toxicol. 114*, 64-69.
155. Palayoor, S. T., J-Aryankalayil, M., Makinde, A. Y., Cerna, D., Falduto, M. T., Magnuson, S. R., and Coleman, C. N. (2012) Gene Expression Profile of Coronary Artery Cells Treated With Nonsteroidal Anti-inflammatory Drugs Reveals Off-target Effects, *J. Cardiovasc. Pharmacol. 59*, 487-499.
156. Corso, G., Coletta, I., and Ombrato, R. (2013) Murine mPGES-1 3D Structure Elucidation and Inhibitors Binding Mode Predictions by Homology Modeling and Site-Directed Mutagenesis, *J. Chem. Inf. Model. 53*, 1804-1817.
157. Li, Y., Yin, S., Wang, X., Xie, S., Nie, D., Ma, L., and Wu, Y. (2013) Effect of MK886, a mPGES-1 inhibitor, on proliferation in leukemia HL-60 cells, *Xiandai Zhongliu Yixue 21*, 249-252.
158. Li, Y.-q., Yin, S.-m., Xie, S.-f., Wang, X.-j., Ma, L.-p., Nie, D.-n., and Wu, Y.-d. (2012) Effect of mPGES-1 inhibitor MK886 on cell cycle of leukemia HL-60

cells, *Zhongguo Shiyan Xueyexue Zazhi 20*, 1072-1076.

159. Li, Y.-q., Yin, S.-m., Nie, D.-n., Xie, S.-f., Ma, L.-p., Wang, X.-j., and Wu, Y.-d. (2012) Effects of mPGES-1 inhibitor MK886 on apoptosis and drug resistance of HL-60/A cells, *Zhongguo Shiyan Xueyexue Zazhi 20*, 829-834.
160. Li, Y.-q., Yin, S.-m., Ma, L.-p., Nie, D.-n., Xie, S.-f., Wang, X.-j., and Wu, Y.-d. (2012) Effects of membrane-bound prostaglandin E2 synthase 1 inhibitor MK886 on cell cycle of leukemia HL-60/A cells, *Baixuebing Linbaliu 21*, 513-516.
161. Li, Y. Q., Yin, S. M., Nie, D. N., Xie, S. F., Ma, L. P., Wang, X. J., Wu, Y. D., and Xiao, J. (2011) MK886 inhibits the proliferation of HL-60 leukemia cells by suppressing the expression of mPGES-1 and reducing prostaglandin E2 synthesis, *Int. J. Hematol. 94*, 472-478.
162. Pasha, F. A., Muddassar, M., Jung, H., Yang, B.-S., Lee, C., Oh, J. S., Cho, S. J., and Cho, H. (2008) QM and pharmacophore based 3D-QSAR of MK886 analogues against mPGES-1, *Bull. Korean Chem. Soc. 29*, 647-655.
163. Kuo, C.-L., Chi, C.-W., and Liu, T.-Y. (2004) The anti-inflammatory potential of berberine in vitro and in vivo, *Cancer Letters 203*, 127-137.
164. Hawkey, C. J. (2001) COX-1 and COX-2 inhibitors, *Best Practice & Research Clinical Gastroenterology 15*, 801-820.
165. Seibert, K., Zhang, Y., Leahy, K., Hauser, S., Masferrer, J., Perkins, W., Lee, L., and Isakson, P. (1994) Pharmacological and biochemical demonstration of the role of cyclooxygenase 2 in inflammation and pain, *Proc. Natl. Acad. Sci. U. S. A. 91*, 12013-12017.
166. Frisch, M. J., Trucks, G. W., Schlegel, H. B., Scuseria, G. E., Robb, M. A., Cheeseman, J. R., Scalmani, G., Barone, V., Mennucci, B., Petersson, G. A., Nakatsuji, H., Caricato, M., Li, X., Hratchian, H. P., Izmaylov, A. F., Bloino, J., Zheng, G., Sonnenberg, J. L., Hada, M., Ehara, M., Toyota, K., Fukuda, R., Hasegawa, J., Ishida, M., Nakajima, T., Honda, Y., Kitao, O., Nakai, H., Vreven, T., Montgomery Jr., J. A., Peralta, J. E., Ogliaro, F., Bearpark, M. J., Heyd, J., Brothers, E. N., Kudin, K. N., Staroverov, V. N., Kobayashi, R., Normand, J., Raghavachari, K., Rendell, A. P., Burant, J. C., Iyengar, S. S., Tomasi, J., Cossi, M., Rega, N., Millam, N. J., Klene, M., Knox, J. E., Cross, J. B., Bakken, V., Adamo, C., Jaramillo, J., Gomperts, R., Stratmann, R. E., Yazyev, O., Austin, A. J., Cammi, R., Pomelli, C., Ochterski, J. W., Martin, R. L., Morokuma, K., Zakrzewski, V. G., Voth, G. A., Salvador, P., Dannenberg, J. J., Dapprich, S., Daniels, A. D., Farkas, Ö., Foresman, J. B., Ortiz, J. V., Cioslowski, J., and Fox, D. J. (2009) Gaussian 09, Gaussian, Inc., Wallingford, CT, USA.
167. Chamberlin, A. C., Cramer, C. J., and Truhlar, D. G. (2008) Performance of SM8 on a Test To Predict Small-Molecule Solvation Free Energies, *The Journal of Physical Chemistry. B 112*, 8651-8655.
168. Scalmani, G., and Frisch, M. J. (2010) Continuous surface charge polarizable continuum models of solvation. I. General formalism, *J. Chem. Phys. 132*,

114110/114111-114110/114115.
169. Cammi, R., Mennucci, B., and Tomasi, J. (2003) Chapter 1: Computational modelling of the solvent effects on molecular properties: An overview of the polarizable continuum model (PCM) approach, *Comput. Chem. (Singapore, Singapore) 8*, 1-79.
170. Cossi, M., Rega, N., Scalmani, G., and Barone, V. (2003) Energies, structures, and electronic properties of molecules in solution with the C-PCM solvation model, *J. Comput. Chem. 24*, 669-681.
171. Marenich, A. V., Cramer, C. J., and Truhlar, D. G. (2009) Universal Solvation Model Based on Solute Electron Density and on a Continuum Model of the Solvent Defined by the Bulk Dielectric Constant and Atomic Surface Tensions, *The Journal of Physical Chemistry B 113*, 6378-6396.
172. Chamberlin, A. C., Levitt, D. G., Cramer, C. J., and Truhlar, D. G. (2008) Modeling Free Energies of Solvation in Olive Oil, *Molecular pharmaceutics 5*, 1064-1079.
173. Cousins, K. R. (2011) Computer Review of ChemDraw Ultra 12.0, *Journal of the American Chemical Society 133*, 8388-8388.
174. Chen, X., Zheng, X., Ding, K., Zhou, Z., Zhan, C.-G., and Zheng, F. (2017) A quantitative LC-MS/MS method for simultaneous determination of cocaine and its metabolites in whole blood, *J. Pharm. Biomed. Anal. 134*, 243-251.
175. Liu, S. Z., Jemiolo, B., Lavin, K. M., Lester, B. E., Trappe, S. W., and Trappe, T. A. (2016) Prostaglandin E2/cyclooxygenase pathway in human skeletal muscle: influence of muscle fiber type and age, *J. Appl. Physiol. 120*, 546-551.
176. Muthukaman, N., Deshmukh, S., Sarode, N., Tondlekar, S., Tambe, M., Pisal, D., Shaikh, M., Kattige, V. G., Honnegowda, S., Karande, V., Kulkarni, A., Jadhav, S. B., Mahat, M. Y. A., Gudi, G. S., Khairatkar-Joshi, N., and Gharat, L. A. (2016) Discovery of 2-((2-chloro-6-fluorophenyl)amino)-N-(3-fluoro-5-(trifluoromethyl)phenyl)-1-methyl-7,8-dihydro-1H-[1,4]dioxino[2',3':3,4]benzo[1,2-d]imidazole-5-carboxamide as potent, selective and efficacious microsomal prostaglandin E2 synthase-1 (mPGES-1) inhibitor, *Bioorg. Med. Chem. Lett. 26*, 5977-5984.
177. Li, S., Sun, Z., Zhang, Y., Chen, Q., Gong, W., Yu, J., Xia, W., Huang, S., Zhang, A., Ding, G., Jia, Z., Li, S., Sun, Z., Zhang, Y., Chen, Q., Gong, W., Yu, J., Xia, W., Huang, S., Zhang, A., Ding, G., Jia, Z., Li, S., Sun, Z., Zhang, Y., Chen, Q., Gong, W., Yu, J., Xia, W., Huang, S., Zhang, A., Ding, G., Jia, Z., Ruan, Y., and He, J. C.-J. (2017) COX-2/mPGES-1/PGE2 cascade activation mediates uric acid-induced mesangial cell proliferation, *Oncotarget 8*, 10185-10198.
178. Gomez, I., Foudi, N., Longrois, D., and Norel, X. (2013) The role of prostaglandin E2 in human vascular inflammation, *Prostaglandins, Leukotrienes Essent. Fatty Acids 89*, 55-63.
179. Millanta, F., Asproni, P., Canale, A., Citi, S., and Poli, A. (2016) COX-2, mPGES-1 and EP2 receptor immunohistochemical expression in canine and

feline malignant mammary tumours, *Vet. Comp. Oncol. 14*, 270-280.

180. Gudis, K., Tatsuguchi, A., Wada, K., Futagami, S., Nagata, K., Hiratsuka, T., Shinji, Y., Miyake, K., Tsukui, T., Fukuda, Y., and Sakamoto, C. (2005) Microsomal prostaglandin E synthase (mPGES)-1, mPGES-2 and cytosolic PGES expression in human gastritis and gastric ulcer tissue, *Lab. Invest. 85*, 225-236.
181. Mattila, S., Tuominen, H., Koivukangas, J., and Stenback, F. (2009) The terminal prostaglandin synthases mPGES-1, mPGES-2, and cPGES are all overexpressed in human gliomas, *Neuropathology 29*, 156-165.
182. Scholich, K., and Geisslinger, G. (2006) Is mPGES-1 a promising target for pain therapy?, *Trends Pharmacol. Sci. 27*, 399-401.
183. Hamalainen, M., Nieminen, R., Asmawi, M. Z., Vuorela, P., Vapaatalo, H., and Moilanen, E. (2011) Effects of flavonoids on prostaglandin E2 production and on COX-2 and mPGES-1 expressions in activated macrophages, *Planta Med. 77*, 1504-1511.
184. Bezugla, Y., Kolada, A., Kamionka, S., Bernard, B., Scheibe, R., and Dieter, P. (2006) COX-1 and COX-2 contribute differentially to the LPS-induced release of PGE2 and TxA2 in liver macrophages, *Prostaglandins Other Lipid Mediators 79*, 93-100.
185. Dev, I. K., and Ajmani, A. K. (2015) Methods and compositions for the mediation of NSAID-induced reactions, p 16pp., NubioPharma, LLC, USA .
186. Chen, Y., Liu, H., Xu, S., Wang, T., and Li, W. (2015) Targeting microsomal prostaglandin E2 synthase-1 (mPGES-1): the development of inhibitors as an alternative to non-steroidal anti-inflammatory drugs (NSAIDs), *MedChemComm 6*, 2081-2123.
187. Dai, H.-x., Zhang, X.-y., Xu, K.-j., and Chen, J.-h. (2012) Recent research advances of nonsteroidal anti-inflammatory drugs (nsaids), *Yaowu Shengwu Jishu 19*, 90-94.
188. Koeberle, A., and Werz, O. (2009) Inhibitors of the microsomal prostaglandin E2 synthase-1 as alternative to non steroidal anti-inflammatory drugs (NSAIDs) - a critical review, *Curr. Med. Chem. 16*, 4274-4296.
189. Alvarez-Soria, M. A., Herrero-Beaumont, G., Moreno-Rubio, J., Calvo, E., Santillana, J., Egido, J., and Largo, R. (2008) Long-term NSAID treatment directly decreases COX-2 and mPGES-1 production in the articular cartilage of patients with osteoarthritis, *Osteoarthritis Cartilage 16*, 1484-1493.
190. Yan, M., Rerko, R. M., Platzer, P., Dawson, D., Willis, J., Tong, M., Lawrence, E., Lutterbaugh, J., Lu, S., Willson, J. K. V., Luo, G., Hensold, J., Tai, H.-H., Wilson, K., and Markowitz, S. D. (2004) 15-hydroxyprostaglandin dehydrogenase, a COX-2 oncogene antagonist, is a TGF-β-induced suppressor of human gastrointestinal cancers, *Proc. Natl. Acad. Sci. U. S. A. 101*, 17468-17473.
191. Lazzaroni, M., and Porro, G. B. (2004) Gastrointestinal side-effects of

traditional non-steroidal anti-inflammatory drugs and new formulations, *Aliment. Pharmacol. Ther. 20*, 48-58.
192. Shi, S., and Klotz, U. (2008) Clinical use and pharmacological properties of selective COX-2 inhibitors, *Eur. J. Clin. Pharmacol. 64*, 233-252.
193. Wang, M., and FitzGerald, G. A. (2010) Cardiovascular Biology of Microsomal Prostaglandin E Synthase-1, *Trends Cardiovasc. Med. 20*, 189-195.
194. Hawkey, C. J. (1999) COX-2 inhibitors, *The Lancet 353*, 307-314.
195. Bresalier, R. S., Sandier, R. S., Quan, H., Bolognese, J. A., Oxenius, B., Horgan, K., Lines, C., Riddell, R., Morton, D., Lanas, A., Konstam, M. A., and Baron, J. A. (2005) Cardiovascular events associated with rofecoxib in a colorectal adenoma chemoprevention trial, *N. Engl. J. Med. 352*, 1092-1102.
196. Claveau, D., Sirinyan, M., Guay, J., Gordon, R., Chan, C.-C., Bureau, Y., Riendeau, D., and Mancini, J. A. (2003) Microsomal Prostaglandin E Synthase-1 Is a Major Terminal Synthase That Is Selectively Up-Regulated During Cyclooxygenase-2-Dependent Prostaglandin E2 Production in the Rat Adjuvant-Induced Arthritis Model, *J. Immunol. 170*, 4738-4744.
197. Miller, Z., Kim, K.-S., Lee, D.-M., Kasam, V., Baek, S. E., Lee, K. H., Zhang, Y.-Y., Ao, L., Carmony, K., Lee, N.-R., Zhou, S., Zhao, Q., Jang, Y., Jeong, H.-Y., Zhan, C.-G., Lee, W., Kim, D.-E., and Kim, K. B. (2015) Proteasome Inhibitors with Pyrazole Scaffolds from Structure-Based Virtual Screening, *J. Med. Chem. 58*, 2036-2041.
198. Miller, Z., Lee, D., Lee, N.-R., Ao, L., Zhan, C.-G., Lee, W., Kim, D.-E., and Kim, K.-B. (2014) Development of non-peptide pyrazole-based proteasome inhibitors as anticancer agents, pp MEDI-179, American Chemical Society.
199. Hu, J., Zhu, W., Meng, H., Liu, Y., Wang, X., and Hu, C. (2014) Identification of 1,4-Dihydrothieno[3',2':5,6]thiopyrano[4,3-c]pyrazole Derivatives as Human 5-Lipoxygenase Inhibitors, *Chem. Biol. Drug Des. 84*, 642-647.
200. Rozot, R., and Boulle, C. (2004) Hair composition containing a pyrazole carboxamide to stimulate hair growth and/or slow hair loss, p 32 pp., L'oreal, Fr. US 9107847 B2.
201. Boulle, C., and Rozot, R. (2004) Hair composition containing styryl-pyrazole derivatives for stimulation of hair growth and/or prevention of hair loss, p 30 pp., L'Oreal, Fr. US 20040242665 A1.
202. Boulle, C., and Rozot, R. (2004) Hair treatment composition containing a styryl-pyrazole compound, and use of said composition in order to stimulate or induce hair or eyelash growth and/or to stop hair loss, p 63 pp., L'oreal, Fr. EP 1558203 A2.
203. Suleyman, H., Demircan, B., and Karagoz, Y. (2007) Anti-inflammatory and side effects of cyclooxygenase inhibitors, *Pharmacol. Rep. 59*, 247-258.
204. Yuan, C., and Smith, W. L. (2015) A Cyclooxygenase-2-dependent Prostaglandin E2 Biosynthetic System in the Golgi Apparatus, *J. Biol. Chem. 290*, 5606-5620.

205. Samuelsson, B., Morgenstern, R., and Jakobsson, P.-J. (2007) Membrane prostaglandin E synthase-1: a novel therapeutic target, *Pharmacol. Rev. 59*, 207-224.
206. Heindel, N. D., Zhao, H., Leiby, J., VanDongen, J. M., Lacey, C. J., Lima, D. A., Shabsoug, B., and Buzby, J. H. (1990) Hydrazide pharmaceuticals as conjugates to polyaldehyde dextran: syntheses, characterization, and stability, *Bioconjugate Chemistry 1*, 77-82.
207. Ronald, B., Suat, L. G. C., and Jeffrey, D. C. (2012) Small Molecule Hydrazide Agents to Inhibit Growth and Proliferation of Mycobacterium Tuberculosis, *Medicinal Chemistry 8*, 273-280.
208. Murakami, M., Nakashima, K., Kamei, D., Masuda, S., Ishikawa, Y., Ishii, T., Ohmiya, Y., Watanabe, K., and Kudo, I. (2003) Cellular prostaglandin E2 production by membrane-bound prostaglandin E synthase-2 via both cyclooxygenases-1 and -2, *J. Biol. Chem. 278*, 37937-37947.
209. Kamei, D., Murakami, M., Nakatani, Y., Ishikawa, Y., Ishii, T., and Kudo, I. (2003) Potential Role of microsomal prostaglandin E synthase-1 in tumorigenesis, *J. Biol. Chem. 278*, 19396-19405.
210. Trott, O., and Olson, A. J. (2010) AutoDock Vina: Improving the speed and accuracy of docking with a new scoring function, efficient optimization, and multithreading, *J. Comput. Chem. 31*, 455-461.

Appendix I. Structures, Names, ^{1}H NMR and ^{13}C NMR data for synthesized compounds

Table I-1. Structures, Names, ^{1}H NMR and ^{13}C NMR data for 2-cyano-3-phenylacrylic acid derivatives (Chapter 3)

V	Structure.	^{1}H NMR	^{13}C NMR
v01	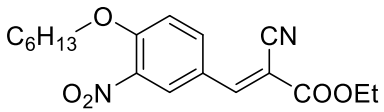 (E)-ethyl 2-cyano-3-(4-(hexyloxy)-3-nitrophenyl)acrylate	^{1}H NMR (400 MHz, cdcl$_3$) δ 8.42 – 8.21 (m, 2H), 8.14 (s, 1H), 7.19 (d, *J* = 9.6 Hz, 1H), 4.36 (q, *J* = 7.1 Hz, 2H), 4.19 (t, *J* = 6.4 Hz, 2H), 1.90 – 1.76 (m, 2H), 1.53 – 1.42 (m, 2H), 1.42 – 1.27 (m, 7H), 0.89 (t, *J* = 7.0 Hz, 3H).	^{13}C NMR (101 MHz, cdcl$_3$) δ 162.06, 155.60, 151.70, 139.77, 135.45, 129.04, 123.48, 115.22, 114.90, 102.78, 70.35, 62.85, 31.28, 28.62, 25.35, 22.44, 14.10, 13.91.
v02	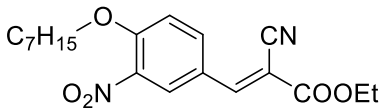 (E)-ethyl 2-cyano-3-(4-(heptyloxy)-3-nitrophenyl)acrylate	^{1}H NMR (400 MHz, cdcl$_3$) δ 8.43 – 8.25 (m, 2H), 8.15 (s, 1H), 7.23 – 7.08 (m, 1H), 4.57 – 4.31 (m, 2H), 4.20 (t, *J* = 6.4 Hz, 2H), 2.01 – 1.72 (m, 2H), 1.55 – 1.10 (m, 11H), 0.89 (t, *J* = 6.5 Hz, 3H).	^{13}C NMR (101 MHz, cdcl$_3$) δ 162.07, 155.62, 151.70, 139.80, 135.36, 129.13, 123.49, 115.23, 114.88, 102.82, 70.36, 62.87, 31.61, 28.81, 28.68, 25.66, 22.52, 14.11, 14.01.
v03	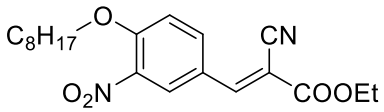 (E)-ethyl 2-cyano-3-(3-nitro-4-(octyloxy)phenyl)acrylate	^{1}H NMR (400 MHz, cdcl$_3$) δ 8.51 – 8.25 (m, 2H), 8.15 (s, 1H), 7.19 (d, *J* = 8.7 Hz, 1H), 4.38 (q, *J* = 7.2 Hz, 2H), 4.20 (t, *J* = 6.4 Hz, 2H), 1.96 – 1.72 (m, 2H), 1.55 – 1.14 (m, 13H), 0.88 (t, *J* = 6.9 Hz, 3H).	^{13}C NMR (101 MHz, cdcl$_3$) δ 162.08, 155.62, 151.70, 139.80, 135.35, 129.14, 123.49, 115.23, 114.88, 102.82, 70.36, 62.87, 31.71, 29.11, 29.08, 28.67, 25.70, 22.59, 14.11, 14.04.
v04	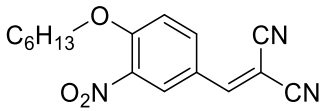 2-(4-(hexyloxy)-3-nitrobenzylidene)	^{1}H NMR (400 MHz, cdcl$_3$) δ 8.29 (d, *J* = 2.4 Hz, 1H), 8.23 (dd, *J* = 8.9, 2.4 Hz, 1H), 7.71 (s, 1H), 7.23 (d, *J* = 9.0 Hz, 1H), 4.23 (t, *J* = 6.4 Hz, 2H), 1.87 (dt, *J* = 14.3, 6.4 Hz, 2H), 1.55 – 1.42 (m,	^{13}C NMR (101 MHz, cdcl$_3$) δ 156.62, 156.60, 139.80, 135.23, 128.91, 122.82, 115.25, 113.35, 112.41, 82.33, 70.69, 31.26, 28.57, 25.32, 22.44, 13.92.

	malononitrile	2H), 1.42 – 1.23 (m, 4H), 0.90 (t, *J* = 7.1 Hz, 3H).	
v05	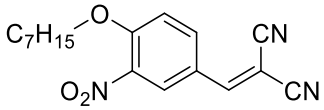 2-(4-(heptyloxy)-3-nitrobenzylidene) malononitrile	^{1}H NMR (400 MHz, cdcl$_3$) δ 8.28 (d, *J* = 2.4 Hz, 1H), 8.24 (dd, *J* = 8.9, 2.4 Hz, 1H), 7.70 (s, 1H), 7.23 (d, *J* = 9.0 Hz, 1H), 4.23 (t, *J* = 6.4 Hz, 2H), 1.94 – 1.82 (m, 2H), 1.54 – 1.42 (m, 2H), 1.42 – 1.23 (m, 6H), 0.89 (t, *J* = 6.9 Hz, 3H).	^{13}C NMR (101 MHz, cdcl$_3$) δ 156.59, 139.80, 135.19, 128.93, 122.82, 115.24, 113.34, 112.40, 82.35, 70.69, 31.60, 28.78, 28.62, 25.62, 22.51, 14.01.
v06	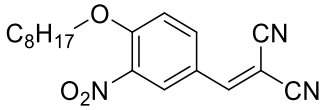 2-(3-nitro-4-(octyloxy)benzylidene) malononitrile	^{1}H NMR (400 MHz, cdcl$_3$) δ 8.51 – 8.13 (m, 2H), 7.92 – 7.54 (m, 1H), 7.43 – 7.06 (m, 1H), 4.55 – 4.04 (m, 2H), 1.92 (ddd, *J* = 24.2, 15.3, 8.5 Hz, 2H), 1.74 – 1.05 (m, 11H), 1.05 – 0.61 (m, 3H).	^{13}C NMR (101 MHz, cdcl$_3$) δ 156.60, 156.55, 139.81, 135.14, 128.96, 122.81, 115.23, 113.32, 112.38, 82.38, 70.69, 31.69, 29.07, 28.61, 25.66, 22.59, 14.05.
v07	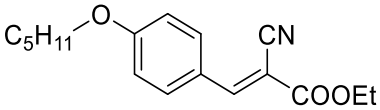 (E)-ethyl 2-cyano-3-(4-(pentyloxy)phenyl)acrylate	^{1}H NMR (400 MHz, cdcl$_3$) δ 8.15 (s, 1H), 8.07 – 7.89 (m, 2H), 7.05 – 6.72 (m, 2H), 4.36 (q, *J* = 7.2 Hz, 2H), 4.03 (t, *J* = 6.6 Hz, 2H), 1.81 (dd, *J* = 8.0, 6.8 Hz, 2H), 1.54 – 1.28 (m, 7H), 0.93 (t, *J* = 7.1 Hz, 3H).	^{13}C NMR (101 MHz, cdcl$_3$) δ 163.43, 163.15, 154.41, 133.63, 124.08, 116.25, 115.16, 99.01, 68.43, 62.35, 28.67, 28.05, 22.36, 14.18, 13.95.
v08	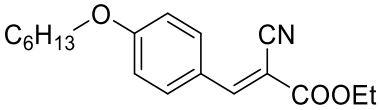 (E)-ethyl 2-cyano-3-(4-(hexyloxy)phenyl)acrylate	^{1}H NMR (400 MHz, cdcl$_3$) δ 8.14 (s, 1H), 7.97 (d, *J* = 8.8 Hz, 2H), 6.96 (d, *J* = 8.8 Hz, 2H), 4.35 (q, *J* = 7.1 Hz, 2H), 4.02 (t, *J* = 6.5 Hz, 2H), 1.96 – 1.63 (m, 2H), 1.56 – 1.16 (m, 9H), 0.90 (t, *J* = 6.7 Hz, 3H).	^{13}C NMR (101 MHz, cdcl$_3$) δ 163.43, 163.12, 154.38, 133.62, 124.07, 116.24, 115.15, 99.00, 68.44, 62.33, 31.47, 28.94, 25.58, 22.53, 14.17, 13.97.
v09	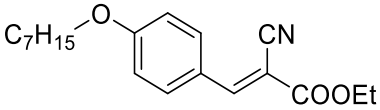	^{1}H NMR (400 MHz, cdcl$_3$) δ 8.13 (s, 1H), 7.96 (d, *J* = 9.0 Hz, 2H), 6.95 (d, *J* = 8.9 Hz, 2H), 4.34 (qd, *J* = 7.1, 0.9 Hz, 2H), 4.01 (t, *J* = 6.5 Hz, 2H),	^{13}C NMR (101 MHz, cdcl$_3$) δ 163.42, 163.10, 154.36, 133.61, 124.06, 116.22, 115.14, 98.99, 68.44, 62.32, 31.69,

	(E)-ethyl 2-cyano-3-(4-(heptyloxy)phenyl)acrylate	1.90 – 1.70 (m, 2H), 1.57 – 1.17 (m, 11H), 0.88 (t, *J* = 7.0, 6.0 Hz, 3H).	28.97, 28.95, 25.86, 22.54, 14.16, 14.02.
v10	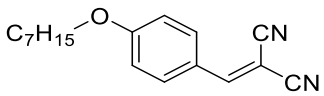 2-(4-(heptyloxy)benzylidene) malononitrile	^{1}H NMR (400 MHz, cdcl$_3$) δ 8.10 – 7.77 (m, 2H), 7.63 (s, 1H), 7.12 – 6.83 (m, 2H), 4.05 (t, *J* = 6.5 Hz, 2H), 1.97 – 1.72 (m, 2H), 1.57 – 1.13 (m, 8H), 0.89 (d, *J* = 7.0 Hz, 3H).	^{13}C NMR (101 MHz, cdcl$_3$) δ 164.51, 158.87, 133.46, 123.75, 115.52, 114.50, 113.41, 78.12, 68.73, 31.69, 28.93, 28.91, 25.83, 22.55, 14.04.
v11	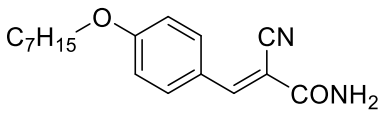 (E)-2-cyano-3-(4-(heptyloxy)phenyl)acrylamide	^{1}H NMR (400 MHz, cdcl$_3$) δ 8.22 (s, 1H), 8.01 – 7.83 (m, 2H), 7.10 – 6.84 (m, 2H), 6.65 (s, 1H), 6.43 (s, 1H), 4.01 (t, *J* = 6.6 Hz, 2H), 1.96 – 1.66 (m, 2H), 1.55 – 1.19 (m, 8H), 0.88 (t, *J* = 6.9 Hz, 3H).	^{13}C NMR (101 MHz, cdcl$_3$) δ 163.24, 162.83, 153.38, 133.31, 124.17, 117.74, 115.16, 99.15, 68.43, 31.70, 28.98, 28.96, 25.87, 22.55, 14.03.
v12	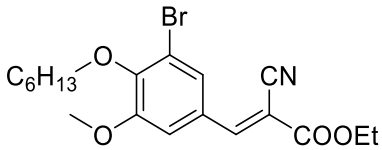 (E)-ethyl 3-(3-bromo-4-(hexyloxy)-5-methoxyphenyl)-2-cyanoacrylate	^{1}H NMR (400 MHz, cdcl$_3$) δ 8.07 (s, 1H), 7.78 (d, *J* = 2.1 Hz, 1H), 7.63 – 7.50 (m, 1H), 4.37 (q, *J* = 7.1 Hz, 2H), 4.11 (t, *J* = 6.6 Hz, 2H), 3.91 (s, 3H), 1.79 (dd, *J* = 8.3, 6.8 Hz, 2H), 1.59 – 1.26 (m, 9H), 0.97 – 0.75 (m, 3H).	^{13}C NMR (101 MHz, cdcl$_3$) δ 162.30, 153.66, 153.11, 150.24, 129.96, 127.73, 118.07, 115.56, 111.86, 102.26, 73.98, 62.73, 56.20, 31.52, 30.12, 25.47, 22.57, 14.14, 14.02.
v13	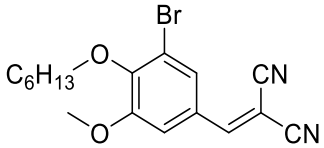 2-(3-bromo-4-(hexyloxy)-5-methoxybenzylidene) malononitrile	^{1}H NMR (400 MHz, cdcl$_3$) δ 7.67 (s, 1H), 7.59 (d, *J* = 3.8 Hz, 1H), 7.53 – 7.46 (m, 1H), 4.26 – 4.13 (m, 2H), 3.91 (s, 3H), 1.87 – 1.72 (m, 2H), 1.52 (s, 2H), 1.43 – 1.25 (m, 4H), 0.91 (t, *J* = 3.6 Hz, 3H).	^{13}C NMR (101 MHz, cdcl$_3$) δ 157.81, 153.74, 151.51, 130.04, 126.99, 118.28, 113.56, 112.75, 111.18, 81.70, 74.26, 56.24, 31.48, 30.12, 25.44, 22.55, 14.00.

v14	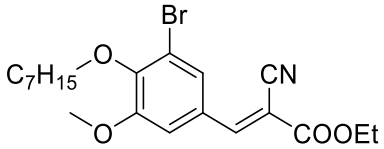 (E)-ethyl 3-(3-bromo-4-(heptyloxy)-5-methoxyphenyl)-2-cyanoacrylate	^{1}H NMR (400 MHz, cdcl$_3$) δ 8.06 (s, 1H), 7.76 (s, 1H), 7.55 (d, *J* = 1.4 Hz, 1H), 4.51 – 4.26 (m, 2H), 4.10 (t, *J* = 6.6 Hz, 2H), 3.90 (s, 3H), 1.92 – 1.70 (m, 2H), 1.57 – 1.19 (m, 11H), 0.87 (t, *J* = 6.1 Hz, 3H).	^{13}C NMR (101 MHz, cdcl$_3$) δ 162.28, 153.65, 153.08, 150.22, 129.94, 127.73, 118.06, 115.54, 111.87, 102.24, 73.96, 62.71, 56.19, 31.75, 30.16, 28.99, 25.76, 22.58, 14.13, 14.05.
v15	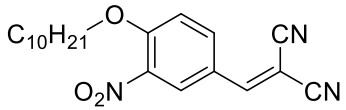 2-(4-(decyloxy)-3-nitrobenzylidene) malononitrile	^{1}H NMR (400 MHz, cdcl$_3$) δ 8.28 (d, *J* = 2.2 Hz, 1H), 8.26 – 8.18 (m, 1H), 7.70 (s, 1H), 7.23 (d, *J* = 8.9 Hz, 1H), 4.23 (t, *J* = 6.4 Hz, 2H), 1.94 – 1.78 (m, 2H), 1.56 – 1.42 (m, 2H), 1.42 – 1.15 (m, 13H), 0.87 (t, *J* = 6.7 Hz, 3H).	^{13}C NMR (101 MHz, cdcl$_3$) δ 156.60, 156.58, 139.81, 135.17, 128.93, 122.82, 115.24, 113.33, 112.39, 82.36, 70.69, 31.83, 29.45, 29.41, 29.24, 29.12, 28.62, 25.66, 22.63, 14.07.
v16	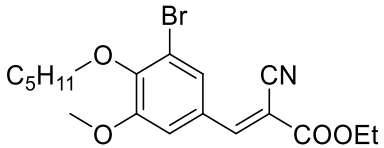 (E)-ethyl 3-(3-bromo-5-methoxy-4-(pentyloxy)phenyl)-2-cyanoacrylate	^{1}H NMR (400 MHz, cdcl$_3$) δ 8.09 (s, 1H), 7.79 (d, *J* = 2.1 Hz, 1H), 7.63 – 7.49 (m, 1H), 4.38 (q, *J* = 7.1 Hz, 2H), 4.12 (t, *J* = 6.7 Hz, 2H), 3.92 (s, 3H), 1.94 – 1.69 (m, 2H), 1.54 – 1.32 (m, 7H), 0.93 (t, *J* = 7.2 Hz, 3H).	^{13}C NMR (101 MHz, cdcl$_3$) δ 162.33, 153.69, 153.14, 150.26, 129.99, 127.75, 118.10, 115.57, 111.86, 102.29, 73.98, 62.74, 56.22, 29.84, 27.95, 22.40, 14.15, 14.00.
v17	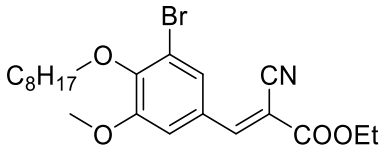 (E)-ethyl 3-(3-bromo-5-methoxy-4-(octyloxy)phenyl)-2-cyanoacrylate	^{1}H NMR (400 MHz, cdcl$_3$) δ 8.08 (s, 1H), 7.79 (d, *J* = 1.3 Hz, 1H), 7.57 (dd, *J* = 1.6, 0.5 Hz, 1H), 4.47 – 4.26 (m, 2H), 4.11 (t, *J* = 6.6 Hz, 2H), 3.92 (d, *J* = 0.5 Hz, 3H), 1.97 – 1.68 (m, 2H), 1.55 – 1.12 (m, 13H), 0.88 (t, *J* = 6.6 Hz, 3H).	^{13}C NMR (101 MHz, cdcl$_3$) δ 162.32, 153.68, 153.13, 150.26, 129.99, 127.74, 118.09, 115.57, 111.86, 102.27, 74.00, 62.73, 56.21, 31.79, 30.16, 29.29, 29.21, 25.81, 22.62, 14.14, 14.07.

v18	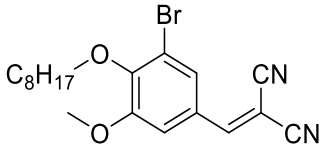 2-(3-bromo-5-methoxy-4-(octyloxy)benzylidene) malononitrile	^{1}H NMR (400 MHz, cdcl$_3$) δ 7.67 (d, *J* = 2.1 Hz, 1H), 7.60 (s, 1H), 7.50 (d, *J* = 2.1 Hz, 1H), 4.16 (t, *J* = 6.6 Hz, 2H), 3.91 (s, 3H), 1.98 – 1.69 (m, 2H), 1.58 – 1.41 (m, 2H), 1.39 – 1.16 (m, 8H), 0.89 (t, *J* = 8.7, 5.0 Hz, 3H).	^{13}C NMR (101 MHz, cdcl$_3$) δ 157.82, 153.74, 151.51, 130.03, 127.00, 118.28, 113.57, 112.76, 111.20, 81.69, 74.26, 56.25, 31.78, 30.16, 29.25, 29.19, 25.77, 22.62, 14.06.
v19	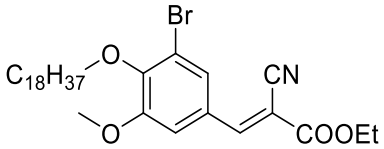 (E)-ethyl 3-(3-bromo-5-methoxy-4-(octadecyloxy)phenyl)-2-cyanoacrylate	^{1}H NMR (400 MHz, cdcl$_3$) δ 8.09 (s, 1H), 7.80 (d, *J* = 1.8 Hz, 1H), 7.58 (d, *J* = 1.9 Hz, 1H), 4.38 (q, *J* = 7.1 Hz, 2H), 4.12 (t, *J* = 6.6 Hz, 2H), 3.92 (s, 3H), 1.98 – 1.69 (m, 2H), 1.54 – 1.44 (m, 2H), 1.40 (t, *J* = 7.1 Hz, 3H), 1.37 – 1.16 (m, 28H), 0.88 (t, *J* = 6.7 Hz, 3H).	^{13}C NMR (101 MHz, cdcl$_3$) δ 162.33, 153.69, 153.13, 150.28, 130.01, 127.74, 118.09, 115.56, 111.84, 102.28, 74.01, 62.73, 56.21, 31.89, 30.16, 29.67, 29.63, 29.59, 29.55, 29.33, 25.81, 22.66, 14.14, 14.08.
v20	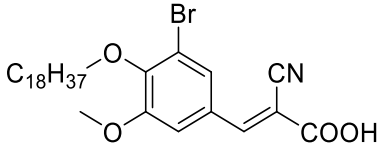 (E)-3-(3-bromo-5-methoxy-4-(octadecyloxy)phenyl)-2-cyanoacrylic acid	^{1}H NMR (400 MHz, dmso) δ 8.11 (s, 1H), 7.85 (s, 1H), 7.73 (s, 1H), 7.24 (s, 1H), 4.01 (t, *J* = 6.2 Hz, 2H), 3.84 (s, 3H), 1.81 – 1.57 (m, 2H), 1.42 (s, 2H), 1.21 (s, 28H), 0.83 (t, *J* = 6.6 Hz, 3H).	^{13}C NMR (101 MHz, dmso) δ 163.37, 153.53, 150.31, 148.33, 129.38, 126.91, 117.53, 114.54, 73.46, 56.57, 31.75, 30.05, 29.50, 29.47, 29.44, 29.40, 29.35, 29.17, 29.12, 25.76, 22.54, 14.33.
v21	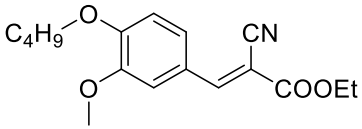	^{1}H NMR (400 MHz, cdcl$_3$) δ 8.14 (s, 1H), 7.78 (d, *J* = 2.1 Hz, 1H), 7.45 (dd, *J* = 8.4, 2.2 Hz, 1H), 6.92 (d, *J* = 8.5 Hz, 1H), 4.37 (q, *J* = 7.2 Hz, 2H), 4.11 (t, *J* = 6.8 Hz, 2H), 3.93 (s, 3H), 1.86	^{13}C NMR (101 MHz, cdcl$_3$) δ 163.14, 154.71, 153.41, 149.46, 127.81, 124.27, 116.39, 111.99, 111.85, 99.02, 68.81, 62.36, 56.05, 30.88, 19.10, 14.19, 13.77.

	(E)-ethyl 3-(4-butoxy-3-methoxyphenyl)-2-cyanoacrylate	(dt, *J* = 14.6, 6.8 Hz, 2H), 1.51 (dq, *J* = 14.8, 7.4 Hz, 2H), 1.39 (t, *J* = 7.1 Hz, 3H), 0.99 (t, *J* = 7.4 Hz, 3H).	
v22	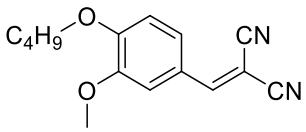 2-(4-butoxy-3-methoxybenzylidene) malononitrile	^{1}H NMR (400 MHz, cdcl$_3$) δ 7.68 (d, *J* = 2.1 Hz, 1H), 7.63 (s, 1H), 7.37 (dd, *J* = 8.5, 2.2 Hz, 1H), 6.95 (d, *J* = 8.5 Hz, 1H), 4.13 (t, *J* = 6.7 Hz, 2H), 3.93 (s, 3H), 2.13 – 1.70 (m, 2H), 1.57 – 1.44 (m, 2H), 1.00 (t, *J* = 7.4 Hz, 3H).	^{13}C NMR (101 MHz, cdcl$_3$) δ 159.08, 154.65, 149.72, 128.13, 123.95, 114.47, 113.61, 111.89, 111.07, 78.05, 69.03, 56.08, 30.81, 19.08, 13.75.
v23	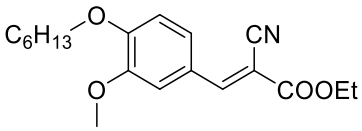 (E)-ethyl 2-cyano-3-(4-(hexyloxy)-3-methoxyphenyl)acrylate	^{1}H NMR (400 MHz, cdcl$_3$) δ 8.13 (s, 1H), 7.78 (d, *J* = 1.8 Hz, 1H), 7.44 (dd, *J* = 8.4, 2.0 Hz, 1H), 6.91 (d, *J* = 8.4 Hz, 1H), 4.46 – 4.28 (m, 2H), 4.09 (t, *J* = 6.8 Hz, 2H), 3.92 (s, 3H), 2.01 – 1.70 (m, 2H), 1.54 – 1.26 (m, 9H), 0.89 (t, *J* = 6.8 Hz, 3H).	^{13}C NMR (101 MHz, cdcl$_3$) δ 163.01, 154.58, 153.31, 149.36, 127.69, 124.18, 116.27, 111.90, 111.77, 98.92, 69.01, 62.23, 55.92, 31.35, 28.69, 25.39, 22.39, 14.06, 13.85.
v24	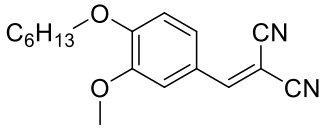 2-(4-(hexyloxy)-3-methoxybenzylidene) malononitrile	^{1}H NMR (400 MHz, cdcl$_3$) δ 7.67 (d, *J* = 1.9 Hz, 1H), 7.62 (s, 1H), 7.35 (dd, *J* = 8.4, 2.1 Hz, 1H), 6.93 (d, *J* = 8.5 Hz, 1H), 4.11 (t, *J* = 6.8 Hz, 2H), 3.92 (s, 3H), 1.94 – 1.72 (m, 2H), 1.53 – 1.40 (m, 2H), 1.40 – 1.25 (m, 4H), 0.91 (t, *J* = 6.8 Hz, 3H).	^{13}C NMR (101 MHz, cdcl$_3$) δ 159.07, 154.64, 149.72, 128.12, 123.95, 114.46, 113.61, 111.90, 111.08, 69.35, 56.07, 31.45, 28.75, 25.49, 22.50, 13.96.

v25	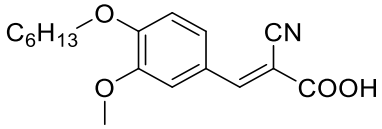 (E)-2-cyano-3-(4-(hexyloxy)-3-methoxyphenyl)acrylic acid	^{1}H NMR (400 MHz, dmso) δ 8.04 (s, 1H), 7.70 (d, *J* = 2.1 Hz, 1H), 7.51 (dd, *J* = 8.5, 2.1 Hz, 1H), 7.25 (s, 1H), 7.05 (d, *J* = 8.5 Hz, 1H), 4.05 (t, *J* = 6.6 Hz, 2H), 3.83 (s, 3H), 1.80 – 1.69 (m, 2H), 1.49 – 1.38 (m, 2H), 1.38 – 1.22 (m, 4H), 0.89 (t, *J* = 7.1 Hz, 3H).	^{13}C NMR (101 MHz, dmso) δ 165.49, 164.46, 151.99, 151.04, 149.17, 125.73, 125.32, 118.61, 117.19, 112.81, 112.78, 79.56, 79.23, 78.90, 68.76, 55.90, 31.48, 31.42, 28.96, 26.27, 25.68, 25.56, 22.50, 14.26.
v26	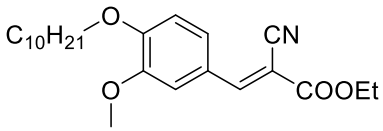 (E)-ethyl 2-cyano-3-(4-(decyloxy)-3-methoxyphenyl)acrylate	^{1}H NMR (400 MHz, cdcl$_3$) δ 8.10 (s, 1H), 7.76 (s, 1H), 7.42 (s, 1H), 6.90 (s, 1H), 4.34 (s, 2H), 4.06 (s, 2H), 3.90 (s, 3H), 1.84 (s, 2H), 1.58 – 1.07 (m, 17H), 0.85 (s, 3H).	^{13}C NMR (101 MHz, cdcl$_3$) δ 162.95, 154.50, 153.27, 149.29, 127.66, 124.11, 116.22, 111.83, 111.72, 98.86, 68.98, 62.17, 55.86, 31.69, 29.34, 29.14, 28.72, 25.69, 22.49, 14.03, 13.92.
v27	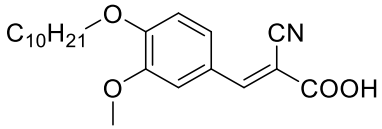 (E)-2-cyano-3-(4-(decyloxy)-3-methoxyphenyl)acrylic acid	^{1}H NMR (400 MHz, cdcl$_3$) δ 8.21 (s, 1H), 7.84 (d, *J* = 1.8 Hz, 1H), 7.49 (dd, *J* = 8.5, 1.8 Hz, 1H), 6.95 (d, *J* = 8.5 Hz, 1H), 6.13 (s, 1H), 4.12 (t, *J* = 6.8 Hz, 2H), 3.95 (s, 3H), 2.01 – 1.71 (m, 2H), 1.59 – 1.13 (m, 14H), 0.88 (t, *J* = 6.8 Hz, 3H).	^{13}C NMR (101 MHz, cdcl$_3$) δ 170.53, 167.83, 156.43, 154.11, 149.56, 128.73, 123.97, 115.91, 112.03, 111.86, 97.65, 69.24, 56.08, 31.84, 29.48, 29.28, 29.26, 28.80, 25.82, 22.63, 14.07.
v28	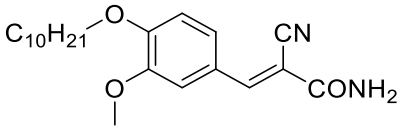 (E)-2-cyano-3-(4-(decyloxy)-3-methoxyphenyl)acrylamide	^{1}H NMR (400 MHz, cdcl$_3$) δ 8.22 (s, 1H), 7.66 (t, *J* = 8.2 Hz, 1H), 7.44 (dd, *J* = 8.4, 2.1 Hz, 1H), 6.88 (dd, *J* = 23.6, 8.6 Hz, 1H), 6.26 (s, 1H), 5.79 (s, 1H), 4.07 (q, *J* = 7.1 Hz, 2H), 3.90 (d, *J* = 8.1 Hz, 3H), 1.99 – 1.81 (m, 2H), 1.54 – 1.05 (m, 14H), 0.86 (t, *J* = 6.8 Hz, 3H).	^{13}C NMR (101 MHz, cdcl$_3$) δ 162.58, 153.82, 153.25, 149.45, 127.44, 124.31, 117.89, 111.95, 111.85, 109.99, 98.99, 69.15, 56.01, 31.85, 29.49, 29.30, 29.26, 28.85, 25.84, 22.64, 14.08.

v29	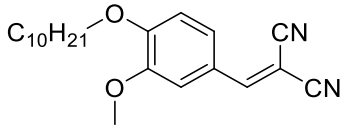 2-(4-(decyloxy)-3-methoxybenzylidene) malononitrile	^{1}H NMR (400 MHz, cdcl$_3$) δ 7.66 (s, 1H), 7.62 (s, 1H), 7.43 – 7.32 (m, 1H), 6.93 (d, *J* = 8.5 Hz, 1H), 4.23 – 4.02 (m, 2H), 3.92 (s, 3H), 2.03 – 1.77 (m, 2H), 1.54 – 1.10 (m, 14H), 0.88 (t, *J* = 6.0 Hz, 3H).	^{13}C NMR (101 MHz, cdcl$_3$) δ 159.07, 154.65, 149.71, 128.13, 123.94, 114.47, 113.61, 111.90, 111.07, 69.36, 56.07, 31.85, 29.48, 29.46, 29.26, 28.78, 25.81, 22.64, 14.07.
v30	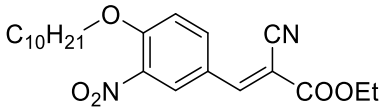 (E)-ethyl 2-cyano-3-(4-(decyloxy)-3-nitrophenyl)acrylate	^{1}H NMR (400 MHz, cdcl$_3$) δ 8.33 (dd, *J* = 7.5, 2.1 Hz, 2H), 8.15 (s, 1H), 7.23 – 7.08 (m, 1H), 4.48 – 4.27 (m, 2H), 4.20 (t, *J* = 6.4 Hz, 2H), 2.01 – 1.72 (m, 2H), 1.52 – 1.10 (m, 17H), 0.86 (t, *J* = 6.9 Hz, 3H).	^{13}C NMR (101 MHz, cdcl$_3$) δ 162.06, 155.61, 151.70, 139.78, 135.39, 129.09, 123.49, 115.22, 114.89, 102.80, 70.36, 62.86, 31.83, 29.46, 29.42, 29.24, 29.14, 28.67, 25.69, 22.63, 14.11, 14.06.
v31	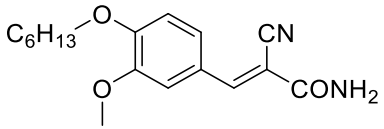 (E)-2-cyano-3-(4-(hexyloxy)-3-methoxyphenyl) acrylamide	^{1}H NMR (400 MHz, cdcl$_3$) δ 8.24 (s, 1H), 7.70 (s, 1H), 7.59 – 7.39 (m, 1H), 6.94 (dd, *J* = 8.4, 2.6 Hz, 1H), 6.29 (s, 1H), 5.85 (s, 1H), 4.11 (d, *J* = 2.5 Hz, 2H), 4.01 – 3.86 (m, 3H), 1.88 (d, *J* = 4.9 Hz, 2H), 1.48 (s, 2H), 1.35 (s, 4H), 1.04 – 0.73 (m, 3H).	^{13}C NMR (101 MHz, cdcl$_3$) δ 162.56, 153.79, 153.22, 149.42, 127.42, 124.30, 117.89, 111.92, 111.82, 99.00, 69.13, 56.00, 31.47, 28.81, 25.51, 22.51, 13.96.
v32	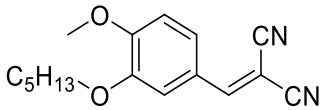 2-(4-methoxy-3-(pentyloxy)benzylidene) malononitrile	^{1}H NMR (400 MHz, cdcl$_3$) δ 7.66 (s, 1H), 7.62 (s, 1H), 7.36 (d, *J* = 8.3 Hz, 1H), 6.94 (d, *J* = 8.2 Hz, 1H), 4.07 (d, *J* = 6.3 Hz, 2H), 3.97 (s, 3H), 2.11 – 1.76 (m, 2H), 1.54 – 1.28 (m, 4H), 0.94 (t, *J* = 6.8 Hz, 3H).	^{13}C NMR (101 MHz, cdcl$_3$) δ 159.13, 155.21, 149.08, 127.86, 124.19, 114.44, 113.54, 111.99, 111.19, 78.25, 69.19, 56.25, 28.57, 28.01, 22.39, 13.95.

v33	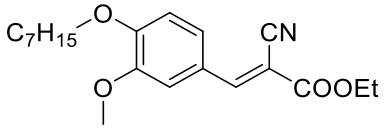 (E)-ethyl 2-cyano-3-(4-(heptyloxy)-3-methoxyphenyl) acrylate	^{1}H NMR (400 MHz, cdcl$_3$) δ 8.12 (s, 1H), 7.77 (d, *J* = 1.9 Hz, 1H), 7.52 – 7.34 (m, 1H), 6.91 (d, *J* = 8.5 Hz, 1H), 4.46 – 4.20 (m, 2H), 4.08 (t, *J* = 6.8 Hz, 2H), 3.92 (s, 3H), 2.07 – 1.76 (m, 2H), 1.56 – 1.14 (m, 11H), 0.87 (t, *J* = 6.6 Hz, 3H).	^{13}C NMR (101 MHz, cdcl$_3$) δ 163.01, 154.55, 153.31, 149.35, 127.68, 124.15, 116.25, 111.87, 111.76, 98.90, 69.00, 62.21, 55.90, 31.54, 28.83, 28.72, 25.68, 22.41, 14.05, 13.89.
v34	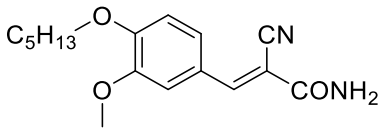 (E)-2-cyano-3-(3-methoxy-4-(pentyloxy)phenyl) acrylamide	^{1}H NMR (400 MHz, cdcl$_3$) δ 8.22 (s, 1H), 7.68 (s, 1H), 7.44 (d, *J* = 8.6 Hz, 1H), 7.07 – 6.83 (m, 1H), 6.26 (d, *J* = 45.8 Hz, 2H), 4.09 (t, *J* = 6.6 Hz, 2H), 3.92 (d, *J* = 0.9 Hz, 3H), 2.01 – 1.75 (m, 2H), 1.57 – 1.28 (m, 4H), 0.93 (t, *J* = 7.2, 6.3 Hz, 3H).	^{13}C NMR (101 MHz, cdcl$_3$) δ 162.84, 153.72, 153.20, 149.42, 127.40, 124.32, 117.86, 111.94, 111.87, 99.13, 69.11, 56.00, 28.57, 27.97, 22.38, 13.94.
v35	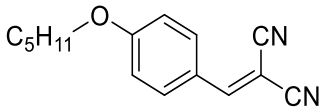 2-(4-(pentyloxy)benzylidene) malononitrile	^{1}H NMR (400 MHz, cdcl$_3$) δ 7.89 (d, *J* = 8.6 Hz, 2H), 7.63 (s, 1H), 7.10 – 6.88 (m, 2H), 4.24 – 3.96 (m, 2H), 2.03 – 1.73 (m, 2H), 1.52 – 1.30 (m, 4H), 0.94 (t, *J* = 6.8 Hz, 3H).	^{13}C NMR (101 MHz, cdcl$_3$) δ 164.50, 158.88, 133.46, 123.75, 115.51, 114.50, 113.41, 78.10, 68.71, 28.60, 28.01, 22.35, 13.94.
v36	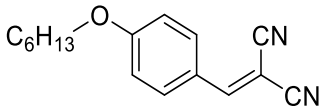 2-(4-(hexyloxy)benzylidene)malononitrile	^{1}H NMR (400 MHz, cdcl$_3$) δ 7.95 – 7.77 (m, 2H), 7.63 (d, *J* = 4.0 Hz, 1H), 7.11 – 6.86 (m, 2H), 4.06 (d, *J* = 5.8 Hz, 2H), 1.93 – 1.64 (m, 2H), 1.49 – 1.09 (m, 6H), 1.00 – 0.66 (m, 3H).	^{13}C NMR (101 MHz, cdcl$_3$) δ 163.80, 158.15, 132.75, 123.05, 114.81, 113.78, 112.70, 77.44, 68.03, 30.75, 28.18, 24.85, 21.82, 13.28.

--	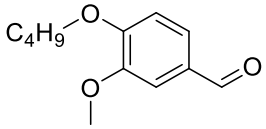 4-butoxy-3-methoxybenzaldehyde	^{1}H NMR (400 MHz, cdcl$_3$) δ 9.72 (t, *J* = 1.9 Hz, 1H), 7.45 – 7.23 (m, 2H), 6.94 – 6.59 (m, 1H), 4.20 – 3.91 (m, 2H), 3.81 (s, 3H), 1.86 – 1.65 (m, 2H), 1.57 – 1.24 (m, 2H), 0.99 – 0.75 (m, 3H).	^{13}C NMR (101 MHz, cdcl$_3$) δ 190.70, 154.09, 149.72, 129.75, 126.63, 111.28, 109.16, 68.70, 55.85, 30.87, 19.05, 13.70.
v37	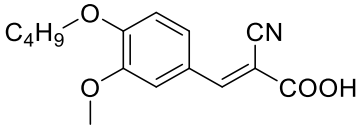 (E)-3-(4-butoxy-3-methoxyphenyl)-2-cyanoacrylic acid	^{1}H NMR (400 MHz, cdcl$_3$) δ 8.22 (s, 1H), 7.82 (t, *J* = 14.3 Hz, 1H), 7.49 (dd, *J* = 8.4, 2.1 Hz, 1H), 7.11 – 6.81 (m, 1H), 4.26 – 4.04 (m, 2H), 3.95 (s, 3H), 1.98 – 1.81 (m, 2H), 1.69 – 1.39 (m, 2H), 1.00 (t, *J* = 7.4 Hz, 3H).	^{13}C NMR (101 MHz, cdcl$_3$) δ 156.46, 154.14, 149.58, 128.75, 123.99, 115.91, 112.05, 111.87, 97.66, 68.92, 56.09, 30.85, 19.10, 13.77.
v38	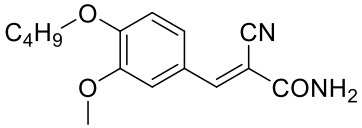 (E)-3-(4-butoxy-3-methoxyphenyl)-2-cyanoacrylamide	^{1}H NMR (400 MHz, cdcl$_3$) δ 8.20 (s, 1H), 7.65 (t, *J* = 10.1 Hz, 1H), 7.54 – 7.36 (m, 1H), 6.87 (dd, *J* = 27.9, 8.1 Hz, 1H), 6.22 (d, *J* = 57.7 Hz, 2H), 4.24 – 4.02 (m, 2H), 4.02 – 3.84 (m, 3H), 2.01 – 1.65 (m, 2H), 1.65 – 1.34 (m, 2H), 0.96 (dd, *J* = 7.7, 7.1 Hz, 3H).	^{13}C NMR (101 MHz, cdcl$_3$) δ 162.79, 153.72, 153.21, 149.43, 127.39, 124.32, 117.87, 111.94, 111.87, 99.13, 68.80, 56.00, 30.89, 19.10, 13.77.
v39	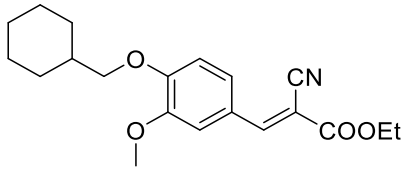 (E)-ethyl 2-cyano-3-(4-(cyclohexylmethoxy)-3-methoxyphenyl)acrylate	^{1}H NMR (400 MHz, cdcl$_3$) δ 8.13 (s, 1H), 7.77 (d, *J* = 2.2 Hz, 1H), 7.44 (dd, *J* = 8.5, 2.2 Hz, 1H), 6.90 (d, *J* = 8.5 Hz, 1H), 4.36 (q, *J* = 7.1 Hz, 2H), 3.91 (d, *J* = 3.9 Hz, 3H), 3.87 (d, *J* = 6.2 Hz, 2H), 1.99 – 1.63 (m, 6H), 1.38 (t, *J* = 7.1 Hz, 3H), 1.33 – 0.93 (m, 5H).	^{13}C NMR (101 MHz, cdcl$_3$) δ 163.16, 154.72, 153.66, 149.54, 127.83, 124.19, 116.40, 112.09, 111.96, 98.92, 74.41, 62.34, 56.09, 37.25, 29.79, 26.39, 25.63, 14.19.

v40	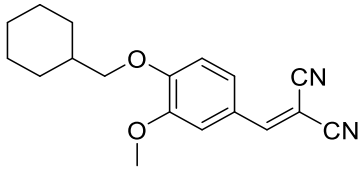 2-(4-(cyclohexylmethoxy)-3-methoxybenzylidene) malononitrile	^{1}H NMR (400 MHz, cdcl$_3$) δ 7.65 (d, *J* = 2.1 Hz, 1H), 7.61 (s, 1H), 7.35 (dd, *J* = 8.5, 2.2 Hz, 1H), 6.92 (d, *J* = 8.5 Hz, 1H), 3.89 (d, *J* = 8.4 Hz, 5H), 2.20 – 1.43 (m, 6H), 1.40 – 0.27 (m, 5H).	^{13}C NMR (101 MHz, cdcl$_3$) δ 158.94, 154.74, 149.62, 127.98, 123.69, 114.33, 113.48, 111.84, 111.00, 77.67, 74.38, 55.91, 37.07, 29.56, 26.16, 25.42.
v41	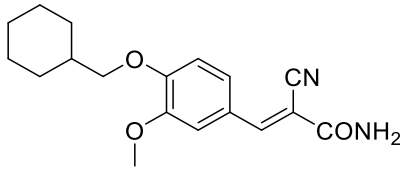 (E)-2-cyano-3-(4-(cyclohexylmethoxy)-3-methoxyphenyl)acrylamide	^{1}H NMR (400 MHz, dmso) δ 8.06 (s, 1H), 7.73 (s, 1H), 7.62 (d, *J* = 2.1 Hz, 2H), 7.50 (dd, *J* = 8.5, 2.1 Hz, 1H), 7.07 (d, *J* = 8.6 Hz, 1H), 3.81 (d, *J* = 6.3 Hz, 2H), 3.77 (s, 3H), 1.92 – 1.48 (m, 6H), 1.29 – 1.05 (m, 3H), 1.05 – 0.85 (m, 2H).	^{13}C NMR (101 MHz, dmso) δ 163.52, 152.55, 151.01, 149.23, 125.98, 124.70, 117.67, 113.02, 112.96, 103.04, 73.87, 55.99, 37.33, 29.59, 26.43, 25.60.
v42	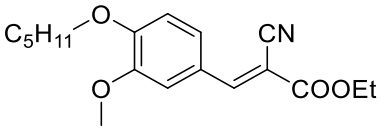 (E)-ethyl 2-cyano-3-(3-methoxy-4-(pentyloxy)phenyl)acrylate	^{1}H NMR (400 MHz, cdcl$_3$) δ 8.11 (s, 1H), 7.76 (d, *J* = 2.0 Hz, 1H), 7.52 – 7.36 (m, 1H), 7.00 – 6.72 (m, 1H), 4.50 – 4.22 (m, 2H), 4.07 (t, *J* = 6.8 Hz, 2H), 3.91 (s, 3H), 2.02 – 1.78 (m, 2H), 1.56 – 1.27 (m, 7H), 0.91 (t, *J* = 7.1 Hz, 3H).	^{13}C NMR (101 MHz, cdcl$_3$) δ 162.77, 154.32, 153.07, 149.11, 127.46, 123.93, 116.03, 111.64, 111.52, 98.66, 68.77, 62.00, 55.70, 28.23, 27.63, 22.03, 13.84, 13.59.
v43	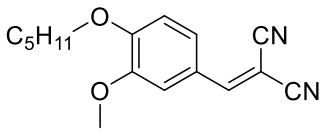 2-(3-methoxy-4-	^{1}H NMR (400 MHz, cdcl$_3$) δ 7.67 (d, *J* = 2.1 Hz, 1H), 7.62 (s, 1H), 7.35 (dd, *J* = 8.4, 2.2 Hz, 1H), 6.99 – 6.88 (m, 1H), 4.11 (t, *J* = 6.8 Hz, 2H), 3.92 (s, 3H), 2.08 – 1.81 (m, 2H), 1.54 – 1.31 (m, 4H), 0.94 (t, *J* = 7.1 Hz, 3H).	^{13}C NMR (101 MHz, cdcl$_3$) δ 159.08, 154.64, 149.71, 128.13, 123.95, 114.47, 113.61, 111.89, 111.07, 69.33, 56.08, 28.50, 27.94, 22.36, 13.93.

	(pentyloxy)benzylidene) malononitrile		
v44	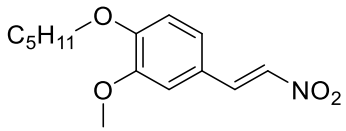 (E)-2-methoxy-4-(2-nitrovinyl)-1-(pentyloxy)benzene	^{1}H NMR (400 MHz, cdcl$_3$) δ 8.06 – 7.89 (m, 1H), 7.60 – 7.48 (m, 1H), 7.21 – 7.10 (m, 1H), 7.00 (s, 1H), 6.94 – 6.85 (m, 1H), 4.07 (td, *J* = 6.8, 2.1 Hz, 2H), 3.95 – 3.53 (m, 3H), 2.00 – 1.74 (m, 2H), 1.51 – 1.25 (m, 4H), 0.94 (t, *J* = 6.0 Hz, 3H).	^{13}C NMR (101 MHz, cdcl$_3$) δ 152.51, 149.74, 139.39, 134.95, 124.59, 122.45, 112.35, 110.60, 69.07, 56.06, 28.60, 27.98, 22.38, 13.93.
v45	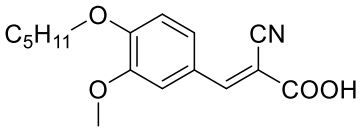 (E)-2-cyano-3-(3-methoxy-4-(pentyloxy)phenyl)acrylic acid	^{1}H NMR (400 MHz, cdcl$_3$) δ 8.22 (s, 1H), 7.84 (d, *J* = 1.1 Hz, 1H), 7.49 (d, *J* = 8.6 Hz, 1H), 6.95 (d, *J* = 8.5 Hz, 1H), 4.12 (t, *J* = 6.8 Hz, 2H), 3.95 (s, 2H), 2.02 – 1.77 (m, 2H), 1.62 – 1.26 (m, 3H), 0.94 (t, *J* = 7.0 Hz, 2H).	^{13}C NMR (101 MHz, cdcl$_3$) δ 168.20, 156.47, 154.12, 149.55, 128.76, 123.97, 115.88, 112.03, 111.85, 97.67, 69.21, 56.08, 28.52, 27.94, 22.37, 13.93.
v46	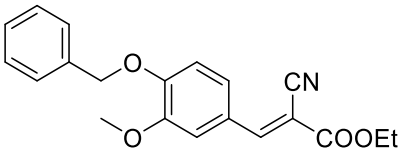 (E)-ethyl 3-(4-(benzyloxy)-3-methoxyphenyl)-2-cyanoacrylate	^{1}H NMR (400 MHz, cdcl$_3$) δ 8.12 (s, 1H), 7.80 (d, *J* = 2.1 Hz, 1H), 7.48 – 7.29 (m, 6H), 6.96 – 6.91 (m, 1H), 5.23 (s, 2H), 4.36 (q, *J* = 7.2 Hz, 2H), 3.94 (s, 3H), 1.38 (t, *J* = 7.1 Hz, 3H).	^{13}C NMR (101 MHz, cdcl$_3$) δ 163.03, 154.59, 152.77, 149.68, 135.87, 128.71, 128.69, 128.22, 127.50, 127.19, 124.76, 116.31, 112.87, 112.12, 99.44, 70.81, 62.42, 56.07, 14.19.
v47	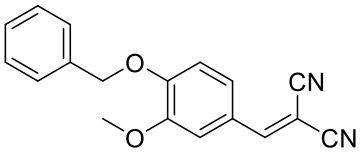	^{1}H NMR (400 MHz, cdcl$_3$) δ 7.68 (s, 1H), 7.61 (s, 1H), 7.47 – 7.28 (m, 6H), 6.96 (d, *J* = 6.9 Hz, 1H), 5.26 (s, 2H), 3.94 (d, *J* = 1.2 Hz, 3H).	^{13}C NMR (101 MHz, cdcl$_3$) δ 159.04, 153.97, 149.93, 135.48, 128.79, 128.39, 127.81, 127.21, 124.40, 114.37, 113.52, 112.89, 111.23, 78.52, 70.97, 56.10.

	2-(4-(benzyloxy)-3-methoxybenzylidene) malononitrile		
v48	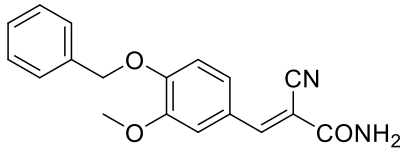 (E)-3-(4-(benzyloxy)-3-methoxyphenyl)-2-cyanoacrylamide	^{1}H NMR (400 MHz, cdcl$_3$) δ 8.22 (s, 1H), 7.71 (d, *J* = 2.0 Hz, 1H), 7.47 – 7.28 (m, 6H), 6.95 (d, *J* = 8.5 Hz, 1H), 6.29 (s, 1H), 6.03 (s, 1H), 5.24 (s, 2H), 3.95 (s, 3H).	^{13}C NMR (101 MHz, cdcl$_3$) δ 162.56, 153.65, 152.56, 149.64, 135.87, 128.73, 128.24, 127.19, 127.10, 124.81, 117.79, 112.92, 111.95, 99.50, 70.82, 56.02.
v49	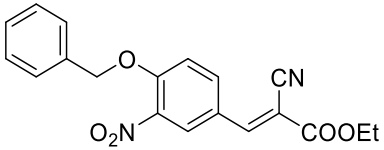 (E)-ethyl 3-(4-(benzyloxy)-3-nitrophenyl)-2-cyanoacrylate	^{1}H NMR (400 MHz, dmso) δ 8.65 (d, *J* = 2.2 Hz, 1H), 8.42 (s, 1H), 8.36 (dd, *J* = 9.0, 2.3 Hz, 1H), 7.69 (d, *J* = 9.0 Hz, 1H), 7.52 – 7.15 (m, 5H), 5.43 (s, 2H), 4.31 (q, *J* = 7.1 Hz, 2H), 1.30 (t, *J* = 7.1 Hz, 3H).	^{13}C NMR (101 MHz, dmso) δ 162.09, 154.66, 152.89, 139.79, 136.81, 135.72, 129.03, 128.76, 128.46, 128.01, 124.29, 116.77, 115.98, 102.58, 71.56, 62.85, 14.41.
v50	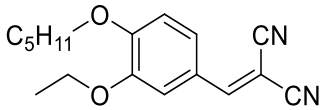 2-(3-ethoxy-4-(pentyloxy)benzylidene) malononitrile	^{1}H NMR (400 MHz, cdcl$_3$) δ 7.64 (d, *J* = 2.1 Hz, 1H), 7.59 (s, 1H), 7.32 (dd, *J* = 8.5, 2.2 Hz, 1H), 6.91 (d, *J* = 8.5 Hz, 1H), 4.14 – 4.04 (m, 4H), 1.94 – 1.79 (m, 2H), 1.51 – 1.15 (m, 7H), 0.92 (t, *J* = 7.1 Hz, 3H).	^{13}C NMR (101 MHz, cdcl$_3$) δ 159.16, 154.98, 149.06, 128.10, 123.93, 114.53, 113.62, 112.38, 112.12, 69.30, 64.73, 28.46, 27.98, 22.35, 14.53, 13.96.
v51	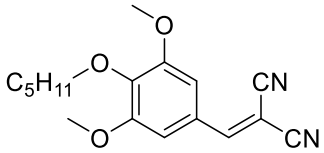	^{1}H NMR (400 MHz, cdcl$_3$) δ 7.64 (s, 1H), 7.18 (s, 2H), 4.12 (t, *J* = 5.6 Hz, 2H), 3.89 (s, 6H), 1.76 (s, 2H), 1.51 – 1.20 (m, 4H), 0.92 (d, *J* = 5.1 Hz, 3H).	^{13}C NMR (101 MHz, cdcl$_3$) δ 159.45, 153.62, 143.56, 125.75, 114.06, 113.25, 108.33, 80.18, 73.99, 56.29, 29.79, 27.83, 22.38, 14.01.

	2-(3,5-dimethoxy-4-(pentyloxy)benzylidene) malononitrile		
v52	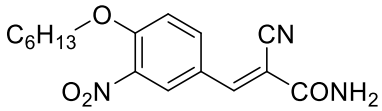 (E)-2-cyano-3-(4-(hexyloxy)-3-nitrophenyl) acrylamide	^{1}H NMR (400 MHz, cdcl$_3$) δ 8.37 (d, *J* = 2.2 Hz, 1H), 8.26 (s, 1H), 8.21 (dd, *J* = 8.9, 2.2 Hz, 1H), 7.19 (d, *J* = 8.9 Hz, 1H), 6.36 (s, 1H), 6.07 (s, 1H), 4.20 (t, *J* = 6.4 Hz, 2H), 2.05 – 1.76 (m, 2H), 1.59 – 1.41 (m, 2H), 1.41 – 1.28 (m, 4H), 0.90 (t, *J* = 6.9 Hz, 3H).	^{13}C NMR (101 MHz, cdcl$_3$) δ 161.45, 155.46, 150.89, 139.87, 135.51, 128.48, 123.62, 116.67, 114.82, 102.82, 70.32, 31.30, 28.64, 25.37, 22.46, 13.94.
v53	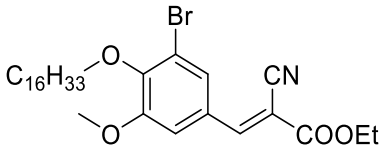 (E)-ethyl 3-(3-bromo-4-(hexadecyloxy)-5-methoxyphenyl)-2-cyanoacrylate	^{1}H NMR (400 MHz, cdcl$_3$) δ 8.09 (s, 1H), 7.80 (d, *J* = 2.0 Hz, 1H), 7.58 (d, *J* = 2.0 Hz, 1H), 4.38 (q, *J* = 7.1 Hz, 2H), 4.12 (t, *J* = 6.6 Hz, 2H), 3.92 (s, 3H), 1.96 – 1.67 (m, 2H), 1.56 – 1.08 (m, 30H), 0.88 (t, *J* = 6.8 Hz, 3H).	^{13}C NMR (101 MHz, cdcl$_3$) δ 162.36, 153.72, 153.18, 150.29, 130.05, 127.77, 118.13, 115.61, 111.85, 102.28, 74.03, 62.77, 56.24, 31.94, 30.20, 29.71, 29.67, 29.63, 29.60, 29.38, 25.85, 22.71, 14.18, 14.14, -0.00.
v54	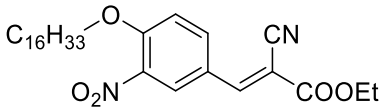 (E)-ethyl 2-cyano-3-(4-(hexadecyloxy)-3-nitrophenyl) acrylate	^{1}H NMR (400 MHz, cdcl$_3$) δ 8.43 – 8.25 (m, 2H), 8.15 (s, 1H), 7.19 (d, *J* = 8.8 Hz, 1H), 4.47 – 4.27 (m, 2H), 4.20 (t, *J* = 6.4 Hz, 2H), 1.97 – 1.72 (m, 2H), 1.57 – 1.06 (m, 32H), 0.87 (dd, *J* = 6.9, 6.5 Hz, 3H).	^{13}C NMR (101 MHz, cdcl$_3$) δ 162.07, 155.62, 151.69, 139.81, 135.34, 129.15, 123.50, 115.22, 114.88, 102.83, 70.36, 62.87, 31.89, 29.65, 29.62, 29.60, 29.52, 29.44, 29.32, 29.16, 28.68, 25.70, 22.65, 14.11, 14.08.

v55	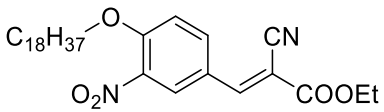 (E)-ethyl 2-cyano-3-(3-nitro-4-(octadecyloxy)phenyl) acrylate	^{1}H NMR (400 MHz, cdcl$_3$) δ 8.40 – 8.25 (m, 2H), 8.15 (s, 1H), 7.23 – 7.12 (m, 1H), 4.45 – 4.27 (m, 2H), 4.20 (t, *J* = 6.4 Hz, 2H), 2.03 – 1.74 (m, 2H), 1.54 – 1.13 (m, 34H), 0.87 (t, *J* = 6.9 Hz, 3H).	^{13}C NMR (101 MHz, cdcl$_3$) δ 162.06, 155.62, 151.69, 139.80, 135.34, 129.14, 123.50, 115.22, 114.88, 102.82, 70.36, 62.86, 31.89, 29.67, 29.62, 29.60, 29.52, 29.44, 29.33, 29.16, 28.68, 25.70, 22.65, 14.11, 14.08.
v56	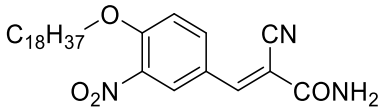 (E)-2-cyano-3-(3-nitro-4-(octadecyloxy)phenyl) acrylamide	^{1}H NMR (400 MHz, cdcl$_3$) δ 8.18 (s, 1H), 7.63 (dd, *J* = 10.4, 2.0 Hz, 2H), 6.33 (s, 1H), 6.09 (s, 1H), 4.11 (t, *J* = 6.6 Hz, 2H), 3.91 (s, 3H), 1.96 – 1.70 (m, 2H), 1.57 – 1.41 (m, 2H), 1.41 – 1.12 (m, 26H), 0.87 (t, *J* = 6.8 Hz, 3H).	^{13}C NMR (101 MHz, cdcl$_3$) δ 161.74, 153.67, 152.25, 150.08, 129.38, 127.86, 118.27, 117.04, 111.98, 102.35, 73.99, 56.15, 31.90, 30.16, 29.67, 29.64, 29.63, 29.60, 29.56, 29.34, 25.82, 22.67, 14.10..
v57	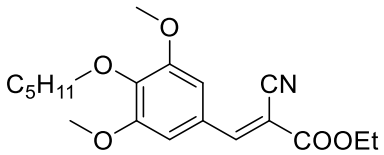 (E)-ethyl 2-cyano-3-(3,5-dimethoxy-4-(pentyloxy)phenyl)acrylate	^{1}H NMR (400 MHz, cdcl$_3$) δ 8.13 (s, 1H), 7.75 (d, *J* = 2.1 Hz, 1H), 7.46 (dd, *J* = 8.4, 2.1 Hz, 1H), 6.91 (d, *J* = 8.5 Hz, 1H), 4.36 (q, *J* = 7.1 Hz, 2H), 4.08 (dd, *J* = 11.9, 6.4 Hz, 4H), 1.86 (dd, *J* = 14.0, 6.4 Hz, 4H), 1.52 – 1.26 (m, 11H), 0.93 (td, *J* = 7.1, 2.2 Hz, 6H).	^{13}C NMR (101 MHz, cdcl$_3$) δ 154.84, 153.91, 127.60, 124.25, 113.71, 112.20, 98.83, 69.05, 62.34, 28.68, 28.59, 28.16, 28.08, 22.42, 22.38, 13.98.
v58	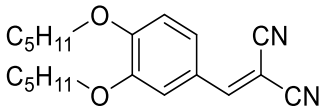 2-(3,4-bis(pentyloxy)benzylidene) malononitrile	^{1}H NMR (400 MHz, cdcl$_3$) δ 7.65 (s, 1H), 7.19 (s, 2H), 4.12 (t, *J* = 6.8 Hz, 2H), 3.89 (s, 6H), 1.84 – 1.64 (m, 2H), 1.53 – 1.23 (m, 4H), 0.92 (t, *J* = 7.2 Hz, 3H).	^{13}C NMR (101 MHz, cdcl$_3$) δ 159.45, 153.62, 143.56, 125.75, 114.06, 113.25, 108.33, 80.18, 73.99, 56.29, 29.79, 27.83, 22.38, 14.01.

Table I-2. Structures, Names, ^{1}H NMR and ^{13}C NMR data for 1, 3-Diphenylpyrazole derivatives (Chapter 4)

	Structures of Pyrazole compounds.	NMR	
		^{1}H NMR	^{13}C NMR
py01	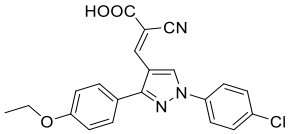 (E)-3-(1-(4-chlorophenyl)-3-(4-ethoxyphenyl)-1H-pyrazol-4-yl)-2-cyanoacrylic acid	^{1}H NMR (400 MHz, dmso) δ 13.84 (s, 1H), 9.16 (s, 1H), 8.06 (s, 1H), 7.96 (d, *J* = 8.8 Hz, 2H), 7.65 (d, *J* = 8.7 Hz, 2H), 7.55 (d, *J* = 8.5 Hz, 2H), 7.11 (d, *J* = 8.6 Hz, 2H), 4.11 (q, *J* = 13.6, 6.7 Hz, 2H), 1.36 (t, *J* = 6.8 Hz, 3H).	^{13}C NMR (101 MHz, dmso) δ 163.57, 159.73, 155.27, 145.15, 137.57, 132.34, 130.47, 129.98, 129.76, 122.82, 121.49, 116.65, 115.14, 114.63, 101.60, 63.49, 14.84.
py02	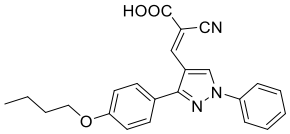 (E)-3-(3-(4-butoxyphenyl)-1-phenyl-1H-pyrazol-4-yl)-2-cyanoacrylic acid	^{1}H NMR (400 MHz, dmso) δ 13.93 – 13.33 (m, 1H), 9.13 (s, 1H), 8.06 (s, 1H), 7.90 (d, *J* = 7.5 Hz, 2H), 7.69 – 7.50 (m, 4H), 7.44 (t, *J* = 7.1 Hz, 1H), 7.10 (d, *J* = 7.7 Hz, 2H), 4.04 (t, *J* = 5.7 Hz, 2H), 1.84 – 1.35 (m, 4H), 0.94 (t, *J* = 7.1 Hz, 3H).	^{13}C NMR (101 MHz, dmso) δ 163.44, 159.63, 154.89, 144.79, 138.57, 130.23, 129.85, 129.27, 127.96, 122.80, 119.59, 116.72, 114.94, 114.25, 101.53, 67.35, 30.72, 18.76, 13.72.
py03	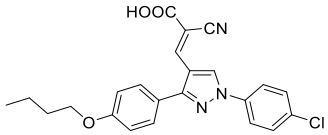 (E)-3-(3-(4-butoxyphenyl)-1-(4-chlorophenyl)-1H-pyrazol-4-yl)-2-cyanoacrylic acid	^{1}H NMR (400 MHz, dmso) δ 13.77 (s, 1H), 9.12 (s, 1H), 8.04 (s, 1H), 7.92 (d, *J* = 8.9 Hz, 2H), 7.68 – 7.58 (m, 2H), 7.51 (d, *J* = 8.6 Hz, 2H), 7.08 (d, *J* = 8.6 Hz, 2H), 4.02 (t, *J* = 6.3 Hz, 2H), 1.77 – 1.39 (m, 4H), 0.94 (t, *J* = 7.4 Hz, 3H).	^{13}C NMR (101 MHz, dmso) δ 163.37, 159.68, 155.01, 144.90, 137.30, 132.11, 130.21, 129.73, 129.42, 122.58, 121.18, 116.44, 114.92, 114.39, 101.31, 67.35, 30.72, 18.76, 13.71.

py04	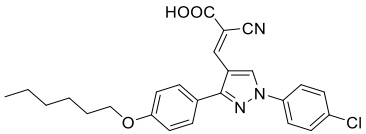 (E)-3-(1-(4-chlorophenyl)-3-(4-(hexyloxy)phenyl)-1H-pyrazol-4-yl)-2-cyanoacrylic acid	^{1}H NMR (400 MHz, dmso) δ 13.83 (s, 1H), 9.13 (s, 1H), 8.04 (s, 1H), 7.93 (d, *J* = 7.5 Hz, 2H), 7.62 (d, *J* = 7.5 Hz, 2H), 7.52 (d, *J* = 7.4 Hz, 2H), 7.08 (d, *J* = 7.4 Hz, 2H), 4.01 (t, 2H), 1.82 – 1.17 (m, 8H), 1.36 (d, *J* = 44.7 Hz, 6H), 0.87 (t, 3H).	^{13}C NMR (101 MHz, dmso) δ 163.36, 159.67, 155.01, 144.90, 137.31, 132.11, 130.20, 129.73, 129.43, 122.58, 121.19, 116.44, 114.92, 114.39, 101.32, 67.64, 31.02, 28.63, 25.20, 22.11, 13.93.
py05	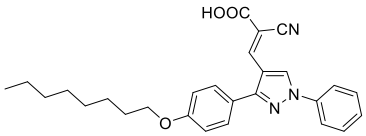 (E)-2-cyano-3-(3-(4-(octyloxy)phenyl)-1-phenyl-1H-pyrazol-4-yl)acrylic acid	^{1}H NMR (400 MHz, dmso) δ 13.74 (s, 1H), 9.15 (s, 1H), 8.08 (s, 1H), 7.91 (d, *J* = 7.4 Hz, 2H), 7.66 – 7.55 (m, 3H), 7.48 (dd, *J* = 24.4, 17.1 Hz, 2H), 7.11 (d, *J* = 7.5 Hz, 2H), 4.04 (d, *J* = 5.0 Hz, 2H), 1.82 – 1.67 (m, 2H), 1.63 – 1.09 (m, 10H), 0.86 (t, 3H).	^{13}C NMR (101 MHz, dmso) δ 163.42, 159.64, 154.96, 145.11, 138.56, 130.24, 129.87, 129.36, 128.01, 122.75, 119.63, 116.58, 114.96, 114.22, 101.06, 67.65, 31.26, 28.76, 28.70, 28.66, 25.53, 22.11, 13.98.
py06	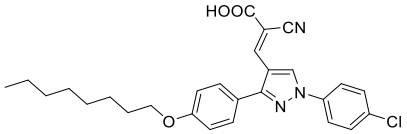 (E)-3-(1-(4-chlorophenyl)-3-(4-(octyloxy)phenyl)-1H-pyrazol-4-yl)-2-cyanoacrylic acid	^{1}H NMR (400 MHz, dmso) δ 13.84 (s, 1H), 9.16 (s, 1H), 8.06 (s, 1H), 7.95 (d, *J* = 7.2 Hz, 2H), 7.64 (d, *J* = 7.4 Hz, 2H), 7.54 (d, *J* = 7.3 Hz, 2H), 7.10 (d, *J* = 7.2 Hz, 2H), 4.03 (t, 2H), 1.77 – 1.67 (m, 2H), 1.59 – 1.22 (m, 10H), 0.86 (t, 3H).	^{13}C NMR (101 MHz, dmso) δ 163.36, 159.68, 155.04, 144.93, 137.35, 132.13, 130.23, 129.76, 129.53, 122.59, 121.26, 116.43, 114.95, 114.41, 101.36, 67.64, 31.26, 28.76, 28.69, 28.65, 25.53, 22.11, 13.98.
py07	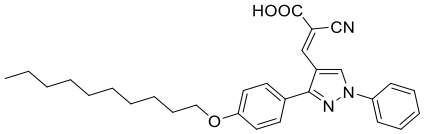	^{1}H NMR (400 MHz, dmso) δ 9.15 (s, 1H), 8.08 (s, 1H), 7.92 (d, *J* = 8.0 Hz, 2H), 7.58 (dd, *J* = 19.6, 8.1 Hz, 4H), 7.47 (d, *J* = 7.3 Hz, 1H), 7.11 (d, *J* = 7.9 Hz, 2H), 4.04 (s,	^{13}C NMR (101 MHz, dmso) δ 207.84, 163.43, 159.66, 154.98, 149.86, 145.12, 138.57, 130.26, 129.89, 128.04, 122.77, 119.66, 116.60, 114.98, 114.24, 101.11,

	(E)-2-cyano-3-(3-(4-(decyloxy)phenyl)-1-phenyl-1H-pyrazol-4-yl)acrylic acid	2H), 1.83 – 1.66 (m, 2H), 1.62 – 1.13 (m, 14H), 0.85 (t, 3H).	67.65, 31.33, 29.04, 28.98, 28.79, 28.73, 28.66, 25.52, 22.13, 13.99.
py08	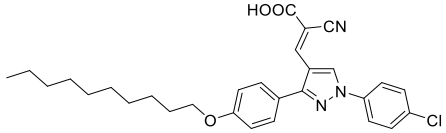 (E)-3-(1-(4-chlorophenyl)-3-(4-(decyloxy)phenyl)-1H-pyrazol-4-yl)-2-cyanoacrylic acid	^{1}H NMR (400 MHz, dmso) δ 9.16 (s, 1H), 8.06 (s, 1H), 7.96 (d, *J* = 7.3 Hz, 2H), 7.65 (d, *J* = 7.3 Hz, 2H), 7.54 (d, *J* = 7.0 Hz, 2H), 7.10 (d, *J* = 7.1 Hz, 2H), 4.03 (t, 2H), 1.73 (s, 2H), 1.45 – 1.12 (m, 14H), 0.85 (t, 3H).	^{13}C NMR (101 MHz, dmso) δ 163.37, 159.69, 155.06, 144.95, 137.36, 132.14, 130.24, 129.78, 129.56, 122.60, 121.29, 116.45, 114.97, 114.42, 101.40, 67.65, 31.32, 29.04, 28.98, 28.79, 28.72, 28.65, 25.52, 22.12, 13.98.
py09	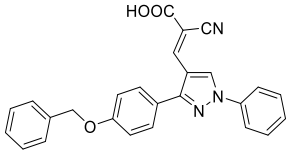 (E)-3-(3-(4-(benzyloxy)phenyl)-1-phenyl-1H-pyrazol-4-yl)-2-cyanoacrylic acid	^{1}H NMR (400 MHz, dmso) δ 13.73 (s, 1H), 9.13 (s, 1H), 8.07 (s, 1H), 7.90 (d, *J* = 7.9 Hz, 2H), 7.57 (d, *J* = 7.7 Hz, 4H), 7.51 – 7.30 (m, 6H), 7.20 (d, *J* = 7.5 Hz, 2H), 5.19 (s, 2H).	^{13}C NMR (101 MHz, dmso) δ 163.44, 159.29, 154.89, 145.08, 138.53, 136.80, 130.27, 129.85, 129.33, 128.48, 128.00, 127.94, 127.80, 123.14, 119.61, 116.59, 115.33, 114.24, 101.05, 69.39.
py10	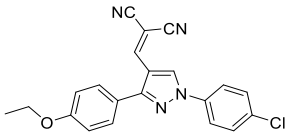 2-((1-(4-chlorophenyl)-3-(4-ethoxyphenyl)-1H-pyrazol-4-yl)methylene)malononitrile	^{1}H NMR (400 MHz, dmso) δ 9.95 (s, 1H), 9.30 (s, 1H), 7.94 (dd, *J* = 51.7, 8.7 Hz, 4H), 7.61 (d, *J* = 8.7 Hz, 2H), 7.03 (d, *J* = 8.6 Hz, 2H), 4.08 (q, *J* = 13.5, 6.6 Hz, 2H), 1.35 (t, *J* = 6.8 Hz, 3H).	^{13}C NMR (101 MHz, dmso) δ 184.54, 159.39, 152.58, 137.42, 135.17, 131.76, 130.05, 129.60, 123.29, 122.12, 121.38, 120.75, 114.89, 114.37, 63.17, 14.63.

py11	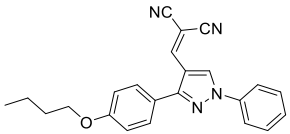 2-((3-(4-butoxyphenyl)-1-phenyl-1H-pyrazol-4-yl)methylene)malononitrile	^{1}H NMR (400 MHz, dmso) δ 9.17 (s, 1H), 8.17 (s, 1H), 7.93 (d, *J* = 7.0 Hz, 2H), 7.60 (t, *J* = 7.9 Hz, 4H), 7.47 (t, *J* = 6.9 Hz, 1H), 7.10 (d, *J* = 7.1 Hz, 2H), 4.05 (t, *J* = 4.9 Hz, 2H), 1.80 – 1.65 (m, 2H), 1.52 – 1.38 (m, 2H), 0.95 (t, *J* = 6.5 Hz, 3H).	^{13}C NMR (101 MHz, dmso) δ 159.77, 154.70, 152.63, 138.36, 130.40, 130.14, 129.88, 128.28, 122.38, 119.79, 114.96, 114.37, 113.94, 78.07, 67.34, 30.68, 18.75, 13.70.
py12	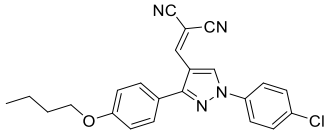 2-((3-(4-butoxyphenyl)-1-(4-chlorophenyl)-1H-pyrazol-4-yl)methylene)malononitrile	^{1}H NMR (400 MHz, dmso) δ 9.18 (s, 1H), 8.15 (s, 1H), 7.96 (d, *J* = 8.6 Hz, 2H), 7.63 (dd, *J* = 20.4, 8.6 Hz, 4H), 7.09 (d, *J* = 8.5 Hz, 2H), 4.04 (t, *J* = 6.4 Hz, 2H), 1.78 – 1.65 (m, 2H), 1.53 – 1.39 (m, 2H), 0.95 (t, *J* = 7.4 Hz, 3H).	^{13}C NMR (101 MHz, dmso) δ 159.82, 154.77, 152.48, 137.15, 132.43, 130.39, 129.78, 122.22, 121.44, 114.95, 114.54, 114.33, 113.81, 78.41, 67.34, 30.68, 18.75, 13.71.
py13	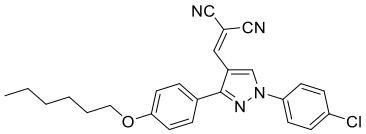 2-((1-(4-chlorophenyl)-3-(4-(hexyloxy)phenyl)-1H-pyrazol-4-yl)methylene)malononitrile	^{1}H NMR (400 MHz, dmso) δ 9.17 (s, 1H), 8.14 (s, 1H), 7.96 (d, *J* = 8.6 Hz, 2H), 7.76 – 7.43 (m, 4H), 7.08 (d, *J* = 8.4 Hz, 2H), 4.03 (t, *J* = 6.1 Hz, 2H), 1.96 – 1.56 (m, 2H), 1.37 (d, *J* = 43.8 Hz, 6H), 0.88 (s, 3H).	^{13}C NMR (101 MHz, dmso) δ 160.22, 155.16, 152.87, 137.54, 132.84, 130.79, 130.66, 130.18, 122.61, 121.82, 115.34, 114.93, 114.74, 114.21, 78.79, 68.05, 31.43, 29.02, 25.62, 22.52, 14.36.
py14	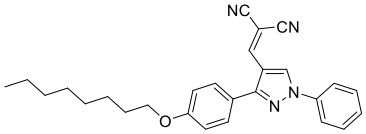	^{1}H NMR (400 MHz, dmso) δ 9.15 (s, 1H), 8.14 (s, 1H), 7.92 (d, *J* = 7.5 Hz, 2H), 7.58 (m, 4H), 7.46 (t, *J* = 6.9 Hz, 1H), 7.08 (d, *J* = 7.0 Hz, 2H), 4.02 (t, *J* = 5.5 Hz, 2H), 1.84	^{13}C NMR (101 MHz, dmso) δ 160.18, 155.10, 152.96, 138.75, 130.79, 130.57, 130.48, 130.27, 128.67, 122.77, 120.16, 119.84, 115.34, 114.79, 114.76, 114.35,

	2-((3-(4-(octyloxy)phenyl)-1-phenyl-1H-pyrazol-4-yl)methylene)malononitrile	– 1.59 (m, 2H), 1.50 – 1.00 (m, 10H), 0.86 (s, 3H).	78.43, 68.04, 31.69, 29.18, 29.12, 29.06, 25.95, 22.53, 14.40.
py15	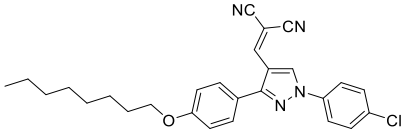 2-((1-(4-chlorophenyl)-3-(4-(octyloxy)phenyl)-1H-pyrazol-4-yl)methylene)malononitrile	^{1}H NMR (400 MHz, dmso) δ 9.18 (s, 1H), 8.15 (s, 1H), 7.96 (d, *J* = 8.5 Hz, 2H), 7.69 – 7.56 (m, 3H), 7.08 (d, *J* = 8.4 Hz, 2H), 4.03 (t, *J* = 6.1 Hz, 2H), 1.92 – 1.59 (m, 2H), 1.59 – 1.09 (m, 10H), 0.85 (s, 3H).	^{13}C NMR (101 MHz, dmso) δ 160.23, 155.18, 152.89, 137.57, 132.85, 130.80, 130.70, 130.57, 130.19, 122.63, 121.85, 121.49, 115.36, 114.95, 114.74, 114.21, 78.82, 68.06, 31.68, 29.17, 29.11, 29.05, 25.95, 22.53, 14.40.
py16	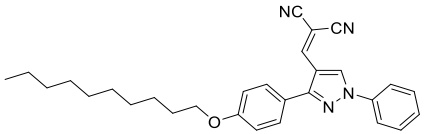 2-((3-(4-(decyloxy)phenyl)-1-phenyl-1H-pyrazol-4-yl)methylene)malononitrile	^{1}H NMR (400 MHz, dmso) δ 9.17 (s, 1H), 8.16 (s, 1H), 7.96 – 7.89 (m, 2H), 7.65 – 7.56 (m, 3H), 7.51 – 7.43 (m, 1H), 7.09 (m, 2H), 4.04 (s, 3H), 1.74 (s, 2H), 1.53 – 1.08 (m, 14H), 0.85 (t, *J* = 6.4 Hz, 3H).	^{13}C NMR (101 MHz, dmso) δ 160.19, 155.12, 153.04, 138.78, 130.81, 130.59, 130.31, 128.71, 122.79, 120.21, 119.89, 115.38, 114.79, 114.35, 79.71, 78.49, 68.05, 31.73, 29.45, 29.40, 29.19, 29.13, 29.04, 25.93, 22.54, 14.40.
py17	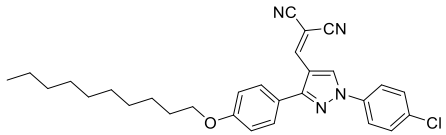 2-((1-(4-chlorophenyl)-3-(4-(decyloxy)phenyl)-1H-pyrazol-4-yl)methylene)malononitrile	^{1}H NMR (400 MHz, dmso) δ 9.20 (s, 1H), 8.17 (s, 1H), 8.02 – 7.93 (m, 2H), 7.71 – 7.64 (m, 2H), 7.64 – 7.58 (m, 2H), 7.09 (d, *J* = 8.6 Hz, 2H), 4.04 (t, *J* = 6.4 Hz, 2H), 1.86 – 1.66 (m, 2H), 1.51 – 1.18 (m, 14H), 0.85 (t, *J* = 6.3 Hz, 3H).	^{13}C NMR (101 MHz, dmso) δ 160.24, 155.21, 152.94, 137.60, 132.86, 130.82, 130.59, 130.22, 122.65, 121.90, 121.54, 115.39, 114.97, 114.75, 114.22, 78.86, 68.06, 31.73, 29.45, 29.39, 29.19, 29.13, 29.03, 25.93, 22.53, 14.40.

py18	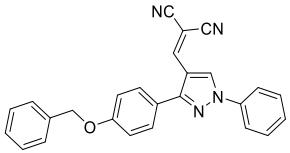 2-((3-(4-(benzyloxy)phenyl)-1-phenyl-1H-pyrazol-4-yl)methylene)malononitrile	^{1}H NMR (400 MHz, dmso) δ 9.18 (s, 1H), 8.18 (s, 1H), 7.97 – 7.87 (m, 2H), 7.69 – 7.55 (m, 4H), 7.52 – 7.33 (m, 6H), 7.25 – 7.13 (m, 2H), 5.20 (s, 2H).	^{13}C NMR (101 MHz, dmso) δ 159.84, 155.03, 153.06, 138.78, 137.24, 130.84, 130.58, 130.30, 128.92, 128.71, 128.37, 128.16, 123.19, 120.22, 115.77, 114.80, 114.36, 78.55, 69.79.
py19	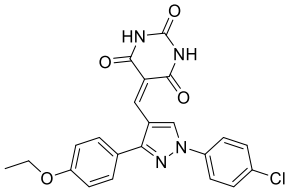 5-((1-(4-chlorophenyl)-3-(4-ethoxyphenyl)-1H-pyrazol-4-yl)methylene)pyrimidine-2,4,6(1H,3H,5H)-trione	^{1}H NMR (400 MHz, dmso) δ 11.32 (d, *J* = 9.1 Hz, 2H), 9.77 (s, 1H), 8.15 (s, 1H), 7.96 (d, *J* = 8.1 Hz, 2H), 7.65 (d, *J* = 8.1 Hz, 2H), 7.54 (d, *J* = 8.0 Hz, 2H), 7.13 (d, *J* = 7.9 Hz, 2H), 4.13 (s, 2H), 1.38 (s, 3H).	^{13}C NMR (101 MHz, dmso) δ 164.04, 163.10, 159.98, 158.39, 150.69, 146.59, 146.19, 143.96, 137.83, 134.93, 132.55, 131.29, 130.26, 123.19, 123.10, 121.73, 115.71, 115.26, 114.87, 63.73, 15.06.
py20	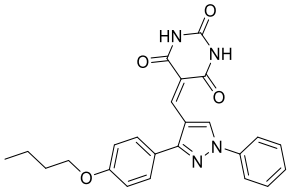 5-((3-(4-butoxyphenyl)-1-phenyl-1H-pyrazol-4-yl)methylene)pyrimidine-2,4,6(1H,3H,5H)-trione	^{1}H NMR (400 MHz, dmso) δ 11.30 (d, *J* = 10.0 Hz, 2H), 9.77 (s, 1H), 8.17 (s, 1H), 7.91 (d, *J* = 7.8 Hz, 2H), 7.70 – 7.30 (m, 5H), 7.13 (d, *J* = 8.6 Hz, 2H), 4.07 (t, *J* = 6.5 Hz, 2H), 1.88 – 1.66 (m, 2H), 1.47 (dd, *J* = 14.9, 7.4 Hz, 2H), 0.95 (t, *J* = 7.4 Hz, 3H).	^{13}C NMR (101 MHz, dmso) δ 164.09, 163.15, 160.11, 158.31, 150.68, 149.18, 144.20, 139.01, 134.84, 131.28, 130.34, 128.44, 123.24, 120.05, 115.53, 115.29, 114.55, 67.80, 31.14, 19.18, 14.14.

py21	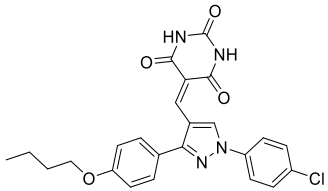 5-((3-(4-butoxyphenyl)-1-(4-chlorophenyl)-1H-pyrazol-4-yl)methylene)pyrimidine-2,4,6(1H,3H,5H)-trione	^{1}H NMR (400 MHz, dmso) δ 11.31 (d, *J* = 10.5 Hz, 2H), 9.76 (s, 1H), 8.15 (s, 1H), 7.96 (d, *J* = 8.9 Hz, 2H), 7.65 (d, *J* = 8.8 Hz, 2H), 7.53 (d, *J* = 8.6 Hz, 2H), 7.13 (d, *J* = 8.7 Hz, 2H), 4.07 (t, *J* = 6.4 Hz, 2H), 1.88 – 1.65 (m, 2H), 1.57 – 1.33 (m, 2H), 0.96 (t, *J* = 7.4 Hz, 3H).	^{13}C NMR (101 MHz, dmso) δ 164.03, 163.09, 160.15, 158.37, 150.68, 143.96, 137.83, 134.91, 132.55, 131.26, 130.25, 123.09, 121.71, 115.70, 115.29, 114.85, 67.80, 31.14, 19.17, 14.14.
py22	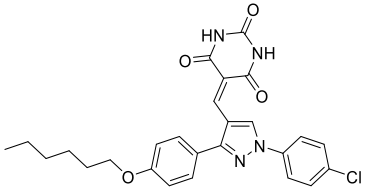 5-((1-(4-chlorophenyl)-3-(4-(hexyloxy)phenyl)-1H-pyrazol-4-yl)methylene)pyrimidine-2,4,6(1H,3H,5H)-trione	^{1}H NMR (400 MHz, dmso) δ 11.32 (d, *J* = 10.5 Hz, 2H), 9.77 (s, 2H), 8.16 (s, 1H), 7.97 (d, *J* = 7.3 Hz, 2H), 7.65 (d, *J* = 8.0 Hz, 2H), 7.54 (d, *J* = 8.3 Hz, 2H), 7.13 (d, *J* = 7.5 Hz, 2H), 4.06 (s, 2H), 1.75 (s, 2H), 1.57 – 1.23 (m, 6H), 0.89 (s, 3H).	^{13}C NMR (101 MHz, dmso) δ 164.05, 163.10, 160.15, 150.69, 146.33, 145.99, 143.95, 137.84, 132.56, 131.28, 130.26, 123.09, 121.74, 115.70, 115.30, 114.88, 68.11, 31.44, 25.62, 22.52, 14.37.
py23	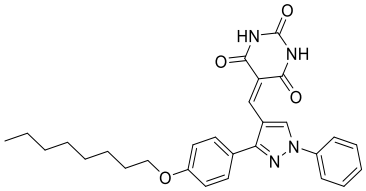 5-((3-(4-(octyloxy)phenyl)-1-phenyl-1H-pyrazol-4-	^{1}H NMR (400 MHz, dmso) δ 11.30 (d, *J* = 10.4 Hz, 2H), 9.77 (s, 1H), 8.18 (s, 1H), 7.91 (d, *J* = 7.4 Hz, 2H), 7.70 – 7.36 (m, 5H), 7.12 (d, *J* = 8.1 Hz, 2H), 4.06 (d, *J* = 5.8 Hz, 2H), 1.92 – 1.66 (m, 2H), 1.56 – 1.12 (m, 10H), 0.86 (s, 3H).	^{13}C NMR (101 MHz, dmso) δ 164.08, 163.15, 160.10, 158.29, 150.68, 144.19, 139.01, 134.83, 131.27, 130.33, 128.44, 128.42, 123.24, 120.04, 115.53, 115.27, 114.56, 68.10, 31.68, 29.18, 29.11, 29.09, 25.96, 22.52, 14.40.

	yl)methylene)pyrimidine-2,4,6(1H,3H,5H)-trione		
py24	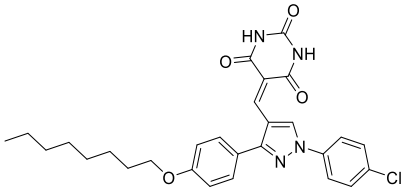 5-((1-(4-chlorophenyl)-3-(4-(octyloxy)phenyl)-1H-pyrazol-4-yl)methylene)pyrimidine-2,4,6(1H,3H,5H)-trione	^{1}H NMR (400 MHz, dmso) δ 11.31 (d, *J* = 10.4 Hz, 2H), 9.76 (s, 1H), 8.15 (s, 1H), 7.95 (d, *J* = 8.9 Hz, 2H), 7.64 (d, *J* = 8.9 Hz, 2H), 7.53 (d, *J* = 8.7 Hz, 2H), 7.12 (d, *J* = 8.7 Hz, 2H), 4.05 (t, *J* = 6.5 Hz, 2H), 1.96 – 1.63 (m, 2H), 1.43 (d, *J* = 7.8 Hz, 2H), 1.30 (dd, *J* = 13.9, 8.0 Hz, 8H), 0.87 (t, *J* = 6.8 Hz, 3H).	^{13}C NMR (101 MHz, dmso) δ 164.02, 163.08, 160.14, 158.36, 150.67, 143.97, 137.82, 134.90, 132.54, 131.25, 130.23, 123.08, 121.69, 115.69, 115.28, 114.84, 68.10, 31.67, 29.18, 29.11, 25.95, 22.52, 14.39.
py25	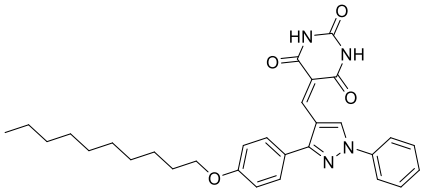 5-((3-(4-(decyloxy)phenyl)-1-phenyl-1H-pyrazol-4-yl)methylene)pyrimidine-2,4,6(1H,3H,5H)-trione	^{1}H NMR (400 MHz, dmso) δ 11.27 (s, 2H), 9.74 (d, *J* = 5.1 Hz, 1H), 8.15 (d, *J* = 5.0 Hz, 1H), 7.89 (d, *J* = 5.8 Hz, 2H), 7.63 – 7.34 (m, 5H), 7.09 (d, *J* = 6.3 Hz, 2H), 4.01 (d, *J* = 5.6 Hz, 2H), 1.83 – 1.61 (m, 2H), 1.50 – 1.03 (m, 16H), 0.82 (t, *J* = 5.2 Hz, 3H).	^{13}C NMR (101 MHz, dmso) δ 164.07, 163.14, 160.09, 158.28, 150.67, 144.21, 139.01, 134.81, 131.25, 130.32, 128.41, 123.24, 120.00, 115.53, 115.26, 114.51, 68.09, 31.73, 29.46, 29.40, 29.22, 29.14, 25.95, 22.53, 14.38.

py26	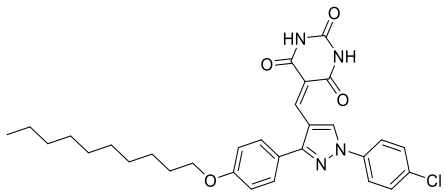 5-((1-(4-chlorophenyl)-3-(4-(decyloxy)phenyl)-1H-pyrazol-4-yl)methylene)pyrimidine-2,4,6(1H,3H,5H)-trione	^{1}H NMR (400 MHz, dmso) δ 11.31 (d, *J* = 9.5 Hz, 2H), 9.76 (s, 1H), 8.16 (s, 1H), 8.03 – 7.88 (m, 2H), 7.74 – 7.59 (m, 2H), 7.53 (d, *J* = 8.7 Hz, 2H), 7.27 – 7.01 (m, 2H), 4.05 (t, *J* = 6.5 Hz, 2H), 1.88 – 1.61 (m, 2H), 1.52 – 1.39 (m, 2H), 1.39 – 1.15 (m, 12H), 0.85 (t, *J* = 6.9 Hz, 3H).	^{13}C NMR (101 MHz, dmso) δ 164.03, 163.09, 160.15, 158.37, 150.68, 143.97, 137.83, 134.92, 132.56, 131.26, 130.25, 123.09, 121.71, 115.70, 115.29, 114.86, 68.11, 31.73, 29.45, 29.39, 29.20, 29.13, 29.07, 25.94, 22.53, 14.39.
py27	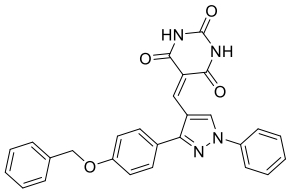 5-((3-(4-(benzyloxy)phenyl)-1-phenyl-1H-pyrazol-4-yl)methylene)pyrimidine-2,4,6(1H,3H,5H)-trione	^{1}H NMR (400 MHz, dmso) δ 11.31 (d, *J* = 10.0 Hz, 2H), 9.78 (s, 1H), 8.18 (s, 1H), 7.92 (d, *J* = 7.9 Hz, 2H), 7.68 – 7.28 (m, 9H), 7.23 (d, *J* = 8.5 Hz, 2H), 5.22 (s, 2H).	^{13}C NMR (101 MHz, dmso) δ 164.09, 163.15, 159.75, 158.23, 150.69, 144.15, 139.02, 137.24, 134.85, 131.31, 130.35, 128.92, 128.38, 128.25, 123.63, 120.06, 115.67, 115.55, 114.60, 69.83.
py28	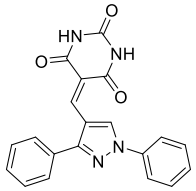 5-((1,3-diphenyl-1H-pyrazol-4-yl)methylene)pyrimidine-	^{1}H NMR (400 MHz, dmso) δ 11.34 (d, *J* = 8.6 Hz, 2H), 9.80 (s, 1H), 8.17 (s, 1H), 7.93 (d, *J* = 7.8 Hz, 2H), 7.72 – 7.52 (m, 7H), 7.48 (d, *J* = 7.4 Hz, 1H).	^{13}C NMR (101 MHz, dmso) δ 164.05, 163.13, 158.40, 150.70, 143.85, 138.98, 134.93, 131.18, 130.36, 129.96, 129.85, 129.36, 128.53, 120.10, 115.60, 114.86.

	2,4,6(1H,3H,5H)-trione		
py29	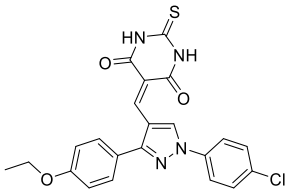 5-((1-(4-chlorophenyl)-3-(4-ethoxyphenyl)-1H-pyrazol-4-yl)methylene)-2-thioxodihydropyrimidine-4,6(1H,5H)-dione	^{1}H NMR (400 MHz, dmso) δ 12.44 (s, 2H), 9.81 (s, 1H), 8.17 (s, 1H), 7.98 (d, *J* = 8.7 Hz, 2H), 7.66 (d, *J* = 8.7 Hz, 2H), 7.55 (d, *J* = 8.5 Hz, 2H), 7.13 (d, *J* = 8.6 Hz, 2H), 4.13 (d, *J* = 7.0 Hz, 2H), 1.38 (t, *J* = 6.9 Hz, 3H).	^{13}C NMR (101 MHz, dmso) δ 178.80, 162.33, 160.90, 160.07, 158.62, 145.01, 137.74, 135.23, 132.70, 131.35, 130.28, 122.94, 121.84, 116.12, 115.29, 115.02, 63.75, 15.06.
py30	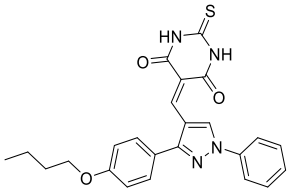 5-((3-(4-butoxyphenyl)-1-phenyl-1H-pyrazol-4-yl)methylene)-2-thioxodihydropyrimidine-4,6(1H,5H)-dione	^{1}H NMR (400 MHz, dmso) δ 12.42 (s, 2H), 9.81 (s, 1H), 8.19 (s, 1H), 7.93 (d, *J* = 7.9 Hz, 2H), 7.64 – 7.52 (m, 4H), 7.48 (d, *J* = 7.4 Hz, 1H), 7.14 (d, *J* = 8.7 Hz, 2H), 4.08 (t, *J* = 6.5 Hz, 2H), 1.87 – 1.65 (m, 2H), 1.48 (dd, *J* = 15.0, 7.4 Hz, 2H), 0.96 (t, *J* = 7.4 Hz, 3H).	^{13}C NMR (101 MHz, dmso) δ 178.77, 162.36, 160.94, 160.20, 158.55, 138.92, 135.13, 131.33, 130.36, 128.58, 123.08, 120.13, 115.96, 115.32, 114.70, 67.81, 31.14, 19.18, 14.14.

py31	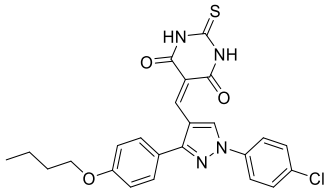 5-((3-(4-butoxyphenyl)-1-(4-chlorophenyl)-1H-pyrazol-4-yl)methylene)-2-thioxodihydropyrimidine-4,6(1H,5H)-dione	^{1}H NMR (400 MHz, dmso) δ 12.43 (s, 2H), 9.80 (s, 1H), 8.16 (s, 1H), 8.08 – 7.85 (m, 2H), 7.74 – 7.61 (m, 2H), 7.54 (d, *J* = 8.7 Hz, 2H), 7.13 (d, *J* = 8.8 Hz, 2H), 4.07 (t, *J* = 6.5 Hz, 2H), 1.88 – 1.59 (m, 2H), 1.59 – 1.33 (m, 2H), 0.96 (t, *J* = 7.4 Hz, 3H).	^{13}C NMR (101 MHz, dmso) δ 178.79, 162.31, 160.88, 160.24, 158.61, 137.73, 135.21, 132.70, 131.32, 130.27, 122.93, 121.81, 116.11, 115.33, 114.99, 67.82, 31.13, 19.17, 14.14.
py32	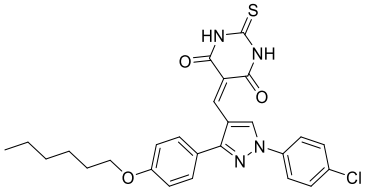 5-((1-(4-chlorophenyl)-3-(4-(hexyloxy)phenyl)-1H-pyrazol-4-yl)methylene)-2-thioxodihydropyrimidine-4,6(1H,5H)-dione	^{1}H NMR (400 MHz, dmso) δ 12.43 (s, 2H), 9.80 (s, 1H), 8.16 (s, 1H), 7.97 (d, *J* = 8.8 Hz, 2H), 7.65 (d, *J* = 8.9 Hz, 2H), 7.54 (d, *J* = 8.6 Hz, 2H), 7.13 (d, *J* = 8.7 Hz, 2H), 4.06 (t, *J* = 6.5 Hz, 2H), 1.92 – 1.63 (m, 2H), 1.59 – 1.19 (m, 6H), 0.89 (t, *J* = 6.9 Hz, 3H).	^{13}C NMR (101 MHz, dmso) δ 178.79, 162.31, 160.88, 160.23, 158.59, 145.00, 137.73, 135.20, 132.69, 131.32, 130.26, 122.93, 121.80, 116.10, 115.32, 114.99, 68.12, 31.44, 29.05, 25.62, 22.52, 14.37.
py33	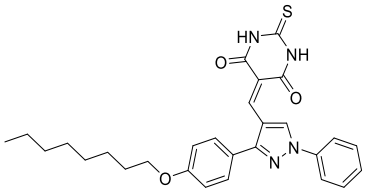	^{1}H NMR (400 MHz, dmso) δ 12.41 (s, 2H), 9.80 (s, 1H), 8.19 (s, 1H), 7.92 (d, *J* = 7.9 Hz, 2H), 7.60 (t, *J* = 7.8 Hz, 2H), 7.54 (d, *J* = 8.5 Hz, 2H), 7.47 (t, *J* = 7.4 Hz, 1H), 7.12 (d, *J* = 8.5 Hz, 2H), 4.05 (t, *J* = 6.4 Hz, 2H),	^{13}C NMR (101 MHz, dmso) δ 178.76, 162.35, 160.92, 160.18, 158.53, 145.27, 138.91, 135.11, 131.31, 130.34, 128.56, 123.07, 120.10, 115.95, 115.30, 114.66, 68.11, 31.68, 29.18, 29.11, 29.09, 25.96,

	5-((3-(4-(octyloxy)phenyl)-1-phenyl-1H-pyrazol-4-yl)methylene)-2-thioxodihydropyrimidine-4,6(1H,5H)-dione	1.86 – 1.65 (m, 2H), 1.48 – 1.38 (m, 2H), 1.38 – 1.18 (m, 8H), 0.86 (t, *J* = 6.2 Hz, 3H).	22.52, 14.40.
py34	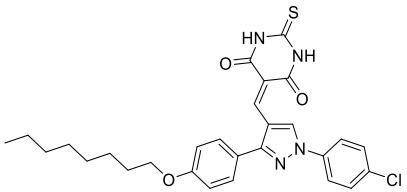 5-((1-(4-chlorophenyl)-3-(4-(octyloxy)phenyl)-1H-pyrazol-4-yl)methylene)-2-thioxodihydropyrimidine-4,6(1H,5H)-dione	^{1}H NMR (400 MHz, dmso) δ 12.43 (s, 2H), 9.80 (s, 1H), 8.17 (s, 1H), 7.97 (d, *J* = 8.9 Hz, 2H), 7.66 (d, *J* = 8.9 Hz, 2H), 7.55 (d, *J* = 8.7 Hz, 2H), 7.13 (d, *J* = 8.7 Hz, 2H), 4.06 (t, *J* = 6.5 Hz, 2H), 1.87 – 1.63 (m, 2H), 1.43 (d, *J* = 8.2 Hz, 2H), 1.39 – 1.15 (m, 8H), 0.87 (t, *J* = 6.8 Hz, 3H).	^{13}C NMR (101 MHz, dmso) δ 178.79, 162.31, 160.88, 160.24, 158.60, 144.76, 143.41, 135.23, 132.70, 131.32, 130.27, 122.93, 121.82, 116.11, 115.33, 115.01, 106.75, 68.12, 31.67, 29.17, 29.10, 25.95, 22.52, 14.40.
py35	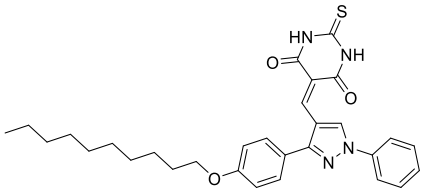 5-((3-(4-(decyloxy)phenyl)-1-phenyl-1H-pyrazol-4-yl)methylene)-2-thioxodihydropyrimidine-4,6(1H,5H)-dione	^{1}H NMR (400 MHz, dmso) δ 12.42 (s, 2H), 9.81 (s, 1H), 8.20 (s, 1H), 8.04 – 7.86 (m, 2H), 7.65 – 7.52 (m, 4H), 7.48 (t, *J* = 7.4 Hz, 1H), 7.13 (d, *J* = 8.8 Hz, 2H), 4.06 (t, *J* = 6.5 Hz, 2H), 1.98 – 1.62 (m, 2H), 1.52 – 1.38 (m, 2H), 1.38 – 1.10 (m, 12H), 0.86 (t, *J* = 6.8 Hz, 3H).	^{13}C NMR (101 MHz, dmso) δ 178.76, 162.35, 160.93, 160.19, 158.53, 145.27, 138.92, 135.12, 131.31, 130.35, 128.57, 123.08, 120.10, 115.95, 115.30, 114.67, 68.11, 31.73, 29.45, 29.40, 29.21, 29.14, 29.08, 25.94, 22.53, 14.39.

py36	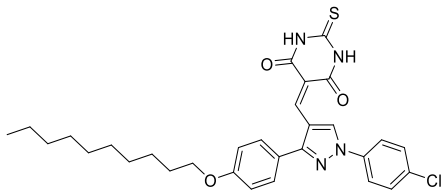 5-((1-(4-chlorophenyl)-3-(4-(decyloxy)phenyl)-1H-pyrazol-4-yl)methylene)-2-thioxodihydropyrimidine-4,6(1H,5H)-dione	^{1}H NMR (400 MHz, dmso) δ 12.43 (s, 1H), 9.80 (s, 1H), 8.17 (s, 1H), 8.00 – 7.94 (m, 1H), 7.69 – 7.63 (m, 1H), 7.58 – 7.50 (m, 1H), 7.13 (d, *J* = 8.8 Hz, 1H), 4.06 (t, *J* = 6.5 Hz, 1H), 1.88 – 1.63 (m, 1H), 1.43 (d, *J* = 7.8 Hz, 1H), 1.39 – 1.17 (m, 6H), 0.86 (t, *J* = 6.9 Hz, 2H).	^{13}C NMR (101 MHz, dmso) δ 178.80, 162.31, 160.88, 160.24, 158.60, 145.00, 137.74, 135.23, 132.70, 131.32, 130.28, 122.93, 121.82, 116.11, 115.33, 115.02, 68.11, 31.73, 29.45, 29.39, 29.20, 29.13, 29.07, 25.94, 22.53, 14.40.
py37	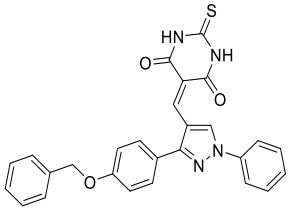 5-((3-(4-(benzyloxy)phenyl)-1-phenyl-1H-pyrazol-4-yl)methylene)-2-thioxodihydropyrimidine-4,6(1H,5H)-dione	^{1}H NMR (400 MHz, dmso) δ 12.43 (s, 2H), 9.81 (s, 1H), 8.18 (s, 1H), 7.93 (d, *J* = 6.1 Hz, 2H), 7.76 – 7.28 (m, 10H), 7.24 (d, *J* = 6.5 Hz, 2H), 5.22 (s, 2H).	^{13}C NMR (101 MHz, dmso) δ 178.78, 162.37, 160.94, 159.84, 158.48, 145.21, 138.92, 137.22, 135.15, 131.36, 130.37, 128.92, 128.61, 128.38, 128.25, 123.46, 120.15, 115.97, 115.70, 114.76, 69.84.
py38	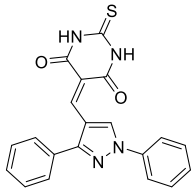 5-((1,3-diphenyl-1H-pyrazol-4-	^{1}H NMR (400 MHz, dmso) δ 12.44 (s, 2H), 9.84 (s, 1H), 8.19 (s, 1H), 8.02 – 7.90 (m, 2H), 7.70 – 7.54 (m, 7H), 7.49 (t, *J* = 7.4 Hz, 1H).	^{13}C NMR (101 MHz, dmso) δ 178.78, 162.32, 160.92, 158.65, 144.94, 138.90, 135.23, 131.02, 130.39, 129.99, 129.96, 129.39, 128.67, 120.19, 116.01, 115.01.

	yl)methylene)-2-thioxodihydropyrimidine-4,6(1H,5H)-dione		
py39	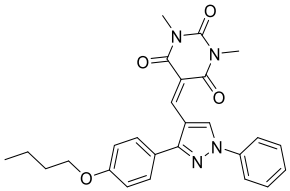 5-((3-(4-butoxyphenyl)-1-phenyl-1H-pyrazol-4-yl)methylene)-1,3-dimethylpyrimidine-2,4,6(1H,3H,5H)-trione	^{1}H NMR (400 MHz, dmso) δ 9.72 (s, 1H), 8.22 (s, 1H), 7.88 (d, *J* = 8.2 Hz, 2H), 7.60 – 7.38 (m, 5H), 7.08 (d, *J* = 8.5 Hz, 2H), 4.03 (t, *J* = 6.4 Hz, 2H), 3.22 (s, 3H), 3.17 (s, 3H), 1.81 – 1.59 (m, 2H), 1.59 – 1.32 (m, 2H), 0.93 (t, *J* = 7.4 Hz, 3H).	^{13}C NMR (101 MHz, dmso) δ 162.74, 161.68, 160.13, 158.45, 151.45, 145.17, 138.90, 134.63, 131.25, 130.31, 128.44, 123.13, 119.98, 115.57, 115.26, 114.04, 67.80, 31.15, 28.93, 28.36, 19.18, 14.14.
py40	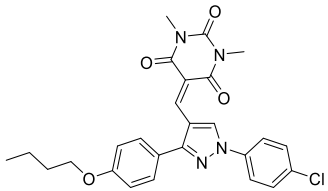 5-((3-(4-butoxyphenyl)-1-(4-chlorophenyl)-1H-pyrazol-4-yl)methylene)-1,3-dimethylpyrimidine-2,4,6(1H,3H,5H)-trione	^{1}H NMR (400 MHz, dmso) δ 9.76 (s, 1H), 8.23 (s, 1H), 7.96 (d, *J* = 8.7 Hz, 2H), 7.64 (d, *J* = 8.8 Hz, 2H), 7.51 (d, *J* = 8.5 Hz, 2H), 7.12 (d, *J* = 8.5 Hz, 2H), 4.07 (t, *J* = 6.4 Hz, 2H), 3.26 (s, 3H), 3.21 (s, 3H), 1.93 – 1.61 (m, 2H), 1.61 – 1.37 (m, 2H), 0.96 (t, *J* = 7.4 Hz, 3H).	^{13}C NMR (101 MHz, dmso) δ 162.73, 161.67, 160.19, 158.53, 151.47, 144.91, 137.72, 134.74, 132.58, 131.26, 130.24, 122.99, 121.67, 115.75, 115.29, 109.98, 67.81, 31.14, 28.96, 28.38, 19.18, 14.14.

py41	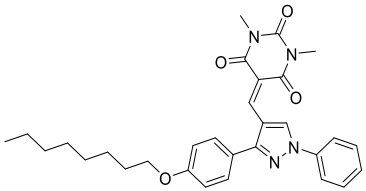 1,3-dimethyl-5-((3-(4-(octyloxy)phenyl)-1-phenyl-1H-pyrazol-4-yl)methylene)pyrimidine-2,4,6(1H,3H,5H)-trione	^{1}H NMR (400 MHz, dmso) δ 9.78 (s, 1H), 8.27 (s, 1H), 7.93 (d, *J* = 7.7 Hz, 2H), 7.60 (t, *J* = 7.9 Hz, 2H), 7.52 (d, *J* = 8.7 Hz, 2H), 7.47 (d, *J* = 7.4 Hz, 1H), 7.12 (d, *J* = 8.7 Hz, 2H), 4.06 (t, *J* = 6.5 Hz, 2H), 3.26 (s, 3H), 3.21 (s, 3H), 1.88 – 1.66 (m, 2H), 1.43 (d, *J* = 7.7 Hz, 2H), 1.39 – 1.20 (m, 8H), 0.87 (t, *J* = 6.7 Hz, 3H).	^{13}C NMR (101 MHz, dmso) δ 162.79, 161.73, 160.15, 158.48, 151.50, 145.16, 138.95, 134.70, 131.27, 130.34, 128.47, 123.17, 120.06, 115.60, 115.30, 114.19, 68.11, 31.68, 29.18, 29.11, 29.08, 28.95, 28.38, 25.96, 22.53, 14.40.
py42	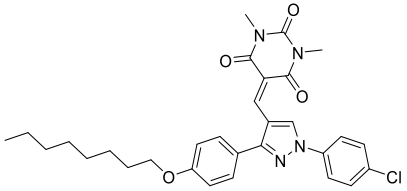 5-((1-(4-chlorophenyl)-3-(4-(octyloxy)phenyl)-1H-pyrazol-4-yl)methylene)-1,3-dimethylpyrimidine-2,4,6(1H,3H,5H)-trione	^{1}H NMR (400 MHz, dmso) δ 9.77 (s, 1H), 8.24 (s, 1H), 8.05 – 7.85 (m, 2H), 7.76 – 7.58 (m, 2H), 7.51 (d, *J* = 8.6 Hz, 2H), 7.12 (d, *J* = 8.7 Hz, 2H), 4.06 (t, *J* = 6.5 Hz, 2H), 3.26 (s, 3H), 3.21 (s, 3H), 1.88 – 1.66 (m, 2H), 1.51 – 1.39 (m, 2H), 1.39 – 1.20 (m, 8H), 0.87 (t, *J* = 6.8 Hz, 3H).	^{13}C NMR (101 MHz, dmso) δ 162.73, 161.67, 160.18, 158.52, 151.47, 144.92, 137.73, 134.73, 132.59, 131.25, 130.24, 122.99, 121.67, 115.75, 115.29, 114.42, 68.12, 67.63, 31.68, 29.18, 29.11, 28.95, 28.38, 25.96, 22.53, 14.40.
py43	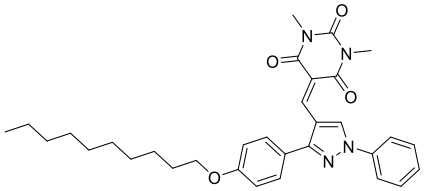 5-((3-(4-(decyloxy)phenyl)-1-phenyl-1H-pyrazol-4-yl)methylene)-1,3-	^{1}H NMR (400 MHz, dmso) δ 9.75 (s, 1H), 8.24 (s, 1H), 7.98 – 7.81 (m, 2H), 7.51 (ddd, *J* = 26.9, 18.0, 7.5 Hz, 5H), 7.09 (d, *J* = 8.7 Hz, 2H), 4.03 (t, *J* = 6.5 Hz, 2H), 3.23 (s, 3H), 3.18 (s, 3H), 1.90 – 1.63 (m, 2H), 1.40 (d, *J* = 8.1 Hz, 2H), 1.26 (t, *J* = 15.2 Hz, 12H), 0.82 (t, *J* = 6.9 Hz, 3H).	^{13}C NMR (101 MHz, dmso) δ 164.39, 162.79, 161.75, 160.15, 151.50, 145.16, 144.59, 140.16, 138.95, 131.27, 130.34, 129.85, 128.46, 120.06, 115.60, 115.30, 95.46, 68.11, 31.73, 29.46, 29.40, 29.21, 29.14, 29.08, 28.38, 25.94, 22.53, 14.39.

	dimethylpyrimidine-2,4,6(1H,3H,5H)-trione		
py44	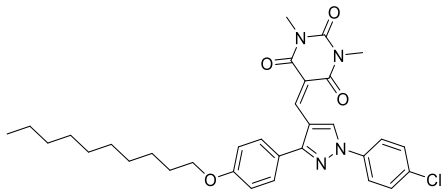 5-((1-(4-chlorophenyl)-3-(4-(decyloxy)phenyl)-1H-pyrazol-4-yl)methylene)-1,3-dimethylpyrimidine-2,4,6(1H,3H,5H)-trione	^{1}H NMR (400 MHz, dmso) δ 9.77 (s, 1H), 8.24 (s, 1H), 8.07 – 7.87 (m, 2H), 7.72 – 7.58 (m, 2H), 7.51 (d, *J* = 8.7 Hz, 2H), 7.12 (d, *J* = 8.7 Hz, 2H), 4.06 (t, *J* = 6.4 Hz, 2H), 3.27 (d, *J* = 4.8 Hz, 3H), 3.21 (s, 3H), 1.92 – 1.63 (m, 2H), 1.50 – 1.39 (m, 2H), 1.29 (t, *J* = 15.2 Hz, 12H), 0.86 (t, *J* = 6.8 Hz, 3H).	^{13}C NMR (101 MHz, dmso) δ 164.32, 162.73, 161.68, 160.18, 151.47, 144.92, 137.73, 134.74, 132.59, 131.25, 130.24, 123.00, 121.67, 115.75, 115.29, 109.99, 68.12, 31.73, 29.46, 29.40, 29.21, 29.14, 29.08, 28.95, 28.38, 25.94, 22.53, 14.39.
py45	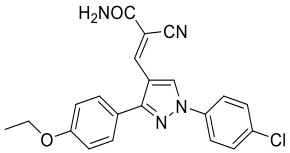 (E)-ethyl 3-(1-(4-chlorophenyl)-3-(4-ethoxyphenyl)-1H-pyrazol-4-yl)-2-cyanoacrylate	^{1}H NMR (400 MHz, dmso) δ 9.14 (s, 1H), 8.21 – 7.83 (m, 4H), 7.83 – 7.43 (m, 5H), 7.10 (d, *J* = 8.6 Hz, 2H), 4.11 (d, *J* = 6.9 Hz, 2H), 1.36 (t, *J* = 6.1 Hz, 3H).	^{13}C NMR (101 MHz, dmso) δ 162.88, 159.81, 154.88, 142.00, 137.91, 132.31, 130.61, 130.17, 129.54, 123.35, 121.54, 117.29, 115.30, 114.96, 105.14, 63.68, 15.06.
py46	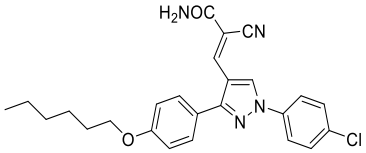 (E)-ethyl 3-(1-(4-chlorophenyl)-3-(4-(hexyloxy)phenyl)-1H-pyrazol-4-yl)-2-	^{1}H NMR (400 MHz, dmso) δ 9.13 (s, 1H), 8.00 (s, 1H), 7.96 (d, *J* = 8.4 Hz, 2H), 7.89 (s, 1H), 7.70 (s, 1H), 7.64 (d, *J* = 8.5 Hz, 2H), 7.55 (d, *J* = 8.1 Hz, 2H), 7.10 (d, *J* = 8.2 Hz, 2H), 4.03 (s, 2H), 1.73 (s, 2H), 1.43 (s, 2H), 1.32 (s, 4H), 0.88 (s, 3H).	^{13}C NMR (101 MHz, dmso) δ 162.87, 159.98, 154.89, 142.01, 137.90, 132.31, 130.59, 130.17, 129.52, 123.33, 121.52, 117.30, 115.33, 114.95, 105.11, 68.06, 31.43, 29.04, 25.62, 22.52, 14.36.

	cyanoacrylate		
py47	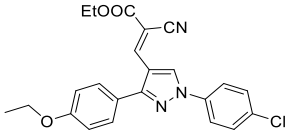 (E)-3-(1-(4-chlorophenyl)-3-(4-ethoxyphenyl)-1H-pyrazol-4-yl)-2-cyanoacrylamide	^{1}H NMR (400 MHz, dmso) δ 9.18 (s, 1H), 8.10 (s, 1H), 7.97 (d, *J* = 7.4 Hz, 2H), 7.66 (d, *J* = 7.6 Hz, 2H), 7.56 (d, *J* = 7.6 Hz, 2H), 7.11 (d, *J* = 7.6 Hz, 2H), 4.29 (d, *J* = 6.8 Hz, 2H), 4.11 (d, *J* = 6.5 Hz, 2H), 1.37 (d, *J* = 5.8 Hz, 3H), 1.28 (t, *J* = 6.5 Hz, 3H).	^{13}C NMR (101 MHz, dmso) δ 162.42, 160.01, 156.80, 155.69, 146.13, 137.73, 132.66, 130.73, 130.21, 122.93, 121.80, 116.37, 115.37, 114.79, 100.36, 63.73, 62.60, 15.04, 14.45.
py48	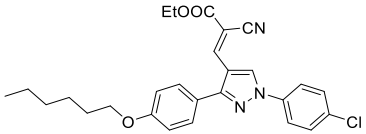 (E)-3-(1-(4-chlorophenyl)-3-(4-(hexyloxy)phenyl)-1H-pyrazol-4-yl)-2-cyanoacrylamide	^{1}H NMR (400 MHz, dmso) δ 9.18 (s, 1H), 8.10 (s, 1H), 7.97 (d, *J* = 7.9 Hz, 2H), 7.66 (d, *J* = 7.8 Hz, 2H), 7.55 (d, *J* = 7.6 Hz, 2H), 7.12 (d, *J* = 7.7 Hz, 2H), 4.29 (d, *J* = 6.7 Hz, 2H), 4.05 (s, 2H), 1.74 (s, 2H), 1.50 – 1.19 (m, 9H), 0.88 (s, 3H).	^{13}C NMR (101 MHz, dmso) δ 162.42, 160.17, 155.69, 146.13, 137.73, 132.66, 130.72, 130.21, 122.91, 121.80, 116.38, 115.41, 114.79, 109.99, 100.37, 68.09, 62.61, 31.43, 29.02, 25.61, 22.52, 14.45, 14.37.
py49	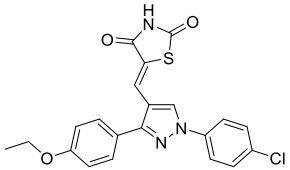 (Z)-5-((1-(4-chlorophenyl)-3-(4-ethoxyphenyl)-1H-pyrazol-4-yl)methylene)thiazolidine-2,4-dione	^{1}H NMR (400 MHz, dmso) δ 12.53 (s, 1H), 8.68 (s, 1H), 8.04 (d, *J* = 8.6 Hz, 2H), 7.78 – 7.41 (m, 5H), 7.09 (d, *J* = 8.4 Hz, 2H), 4.11 (d, *J* = 6.8 Hz, 2H), 1.37 (t, *J* = 6.8 Hz, 3H).	^{13}C NMR (101 MHz, dmso) δ 167.96, 167.54, 159.65, 154.06, 138.02, 131.87, 130.41, 129.90, 128.39, 123.70, 123.05, 122.44, 121.30, 116.00, 115.26, 63.66, 15.06.

py50	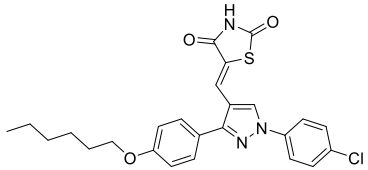 (Z)-5-((1-(4-chlorophenyl)-3-(4-(hexyloxy)phenyl)-1H-pyrazol-4-yl)methylene)thiazolidine-2,4-dione	^{1}H NMR (400 MHz, dmso) δ 12.54 (s, 1H), 8.69 (s, 1H), 8.06 (d, *J* = 8.7 Hz, 2H), 7.70 – 7.41 (m, 5H), 7.10 (d, *J* = 8.5 Hz, 2H), 4.04 (t, *J* = 6.2 Hz, 2H), 1.86 – 1.63 (m, 2H), 1.44 (s, 2H), 1.33 (s, 4H), 0.89 (s, 3H).	^{13}C NMR (101 MHz, dmso) δ 168.00, 159.82, 154.08, 140.67, 140.06, 138.04, 134.92, 132.33, 131.88, 130.41, 129.92, 128.43, 123.69, 122.43, 121.33, 116.02, 115.31, 68.05, 31.43, 29.05, 25.62, 22.52, 14.37.
py51	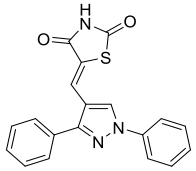 (Z)-5-((1,3-diphenyl-1H-pyrazol-4-yl)methylene)thiazolidine-2,4-dione	^{1}H NMR (400 MHz, dmso) δ 12.54 (s, 1H), 8.69 (s, 1H), 8.01 (d, *J* = 7.8 Hz, 2H), 7.70 – 7.31 (m, 10H).	^{13}C NMR (101 MHz, dmso) δ 167.91, 167.49, 154.00, 139.19, 131.76, 130.04, 129.44, 129.38, 129.11, 128.43, 127.90, 123.06, 122.47, 119.80, 115.92.
py52	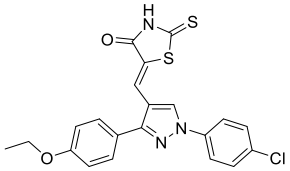 (Z)-5-((1-(4-chlorophenyl)-3-(4-ethoxyphenyl)-1H-pyrazol-4-yl)methylene)-2-thioxothiazolidin-4-one	^{1}H NMR (400 MHz, dmso) δ 13.72 (s, 1H), 8.67 (s, 1H), 8.05 (d, *J* = 8.7 Hz, 2H), 7.58 (d, *J* = 8.7 Hz, 2H), 7.52 (d, *J* = 8.5 Hz, 2H), 7.34 (s, 1H), 7.07 (d, *J* = 8.5 Hz, 2H), 4.35 – 3.87 (m, 2H), 1.36 (t, *J* = 6.8 Hz, 3H).	^{13}C NMR (101 MHz, dmso) δ 195.45, 169.46, 159.70, 154.31, 137.89, 131.96, 130.46, 129.84, 128.75, 124.69, 123.51, 122.18, 121.28, 116.13, 115.24, 63.66, 15.06.

py53	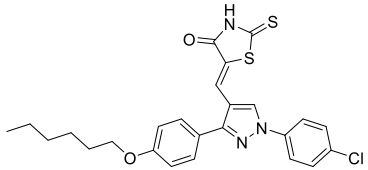 (Z)-5-((1-(4-chlorophenyl)-3-(4-(hexyloxy)phenyl)-1H-pyrazol-4-yl)methylene)-2-thioxothiazolidin-4-one	^{1}H NMR (400 MHz, dmso) δ 13.73 (s, 1H), 8.70 (s, 1H), 8.06 (d, *J* = 8.8 Hz, 2H), 7.70 – 7.43 (m, 4H), 7.35 (s, 1H), 7.08 (d, *J* = 8.5 Hz, 2H), 4.03 (t, *J* = 6.2 Hz, 2H), 1.83 – 1.57 (m, 2H), 1.56 – 1.21 (m, 6H), 0.88 (s, 3H).	^{13}C NMR (101 MHz, dmso) δ 195.46, 169.46, 159.88, 154.34, 137.91, 131.97, 130.46, 129.86, 128.81, 124.71, 123.50, 122.21, 121.31, 116.14, 115.29, 68.04, 31.45, 29.06, 25.63, 22.53, 14.37.
py54	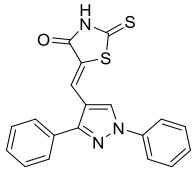 (Z)-5-((1,3-diphenyl-1H-pyrazol-4-yl)methylene)-2-thioxothiazolidin-4-one	^{1}H NMR (400 MHz, dmso) δ 13.75 (s, 1H), 8.75 (s, 1H), 8.13 – 7.96 (m, 2H), 7.68 – 7.53 (m, 8H), 7.46 – 7.37 (m, 2H).	^{13}C NMR (101 MHz, dmso) δ 195.52, 169.52, 154.30, 139.12, 131.61, 130.02, 129.54, 129.41, 129.19, 128.91, 127.99, 124.86, 122.20, 119.86, 116.10.
py55	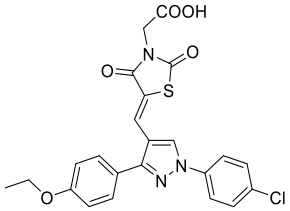 (Z)-2-(5-((1-(4-chlorophenyl)-3-(4-ethoxyphenyl)-1H-pyrazol-4-yl)methylene)-2,4-dioxothiazolidin-3-yl)acetic acid	^{1}H NMR (400 MHz, dmso) δ 13.47 (s, 1H), 8.76 (s, 1H), 8.05 (d, *J* = 8.7 Hz, 2H), 7.68 (s, 1H), 7.57 (dd, *J* = 26.7, 8.6 Hz, 4H), 7.09 (d, *J* = 8.6 Hz, 2H), 4.35 (s, 2H), 4.10 (q, *J* = 6.9 Hz, 2H), 1.36 (t, *J* = 6.9 Hz, 3H).	^{13}C NMR (101 MHz, dmso) δ 168.00, 166.61, 164.74, 159.29, 153.83, 137.53, 131.57, 130.03, 129.48, 128.35, 124.12, 123.13, 120.93, 119.57, 115.31, 114.84, 63.24, 42.37, 14.63.

py56	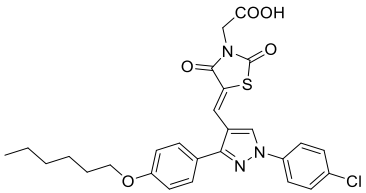 (Z)-2-(5-((1-(4-chlorophenyl)-3-(4-(hexyloxy)phenyl)-1H-pyrazol-4-yl)methylene)-2,4-dioxothiazolidin-3-yl)acetic acid	^{1}H NMR (400 MHz, dmso) δ 8.78 (s, 1H), 8.06 (d, *J* = 8.8 Hz, 2H), 7.69 (s, 1H), 7.63 (s, 1H), 7.61 – 7.47 (m, 3H), 7.09 (d, *J* = 8.7 Hz, 2H), 4.36 (s, 2H), 4.03 (t, *J* = 6.5 Hz, 2H), 1.82 – 1.64 (m, 2H), 1.48 – 1.28 (m, 6H), 0.88 (t, *J* = 6.8 Hz, 3H).	^{13}C NMR (101 MHz, dmso) δ 168.01, 166.62, 164.75, 159.47, 153.86, 137.55, 131.59, 130.04, 129.50, 128.40, 124.15, 123.13, 120.97, 119.59, 115.32, 114.90, 67.64, 42.34, 31.03, 28.63, 25.21, 22.11, 13.95.

Table I-3. Structures, Names, ^{1}H NMR and ^{13}C NMR data for hydrazide derivatives (Chapter 5)

No.	**structures**	**NMR**	
		^{1}H NMR	**^{13}C NMR**
zh01	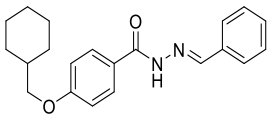 (E)-N'-benzylidene-4-(cyclohexylmethoxy) benzohydrazide	^{1}H NMR (400 MHz, dmso) δ 11.70 (s, 1H), 8.41 (s, 1H), 7.86 (d, *J* = 8.6 Hz, 2H), 7.69 (d, *J* = 6.4 Hz, 2H), 7.42 (d, *J* = 7.3 Hz, 3H), 7.01 (d, *J* = 8.6 Hz, 2H), 3.82 (d, *J* = 6.2 Hz, 2H), 1.90 – 1.50 (m, 6H), 1.34 – 0.82 (m, 5H).	^{13}C NMR (101 MHz, dmso) δ 162.90, 162.02, 147.49, 134.88, 130.36, 129.95, 129.26, 127.41, 125.57, 114.57, 73.32, 37.44, 29.62, 26.45, 25.67.
zh02	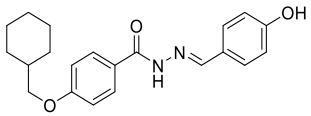 (E)-4-(cyclohexylmethoxy) -N'-(4-	^{1}H NMR (400 MHz, dmso) δ 11.50 (s, 1H), 9.90 (s, 1H), 8.30 (s, 1H), 7.84 (d, *J* = 7.5 Hz, 2H), 7.51 (d, *J* = 7.9 Hz, 2H), 6.99 (d, *J* = 7.9 Hz, 2H), 6.80 (d, *J* = 7.8 Hz, 2H), 3.81 (d, *J* = 6.0 Hz, 2H),	^{13}C NMR (101 MHz, dmso) δ 162.66, 161.87, 159.71, 147.84, 129.82, 129.16, 125.85, 125.81, 116.10, 114.51, 73.30, 37.44, 29.62, 26.45, 25.68.

	hydroxybenzylidene) benzohydrazide	1.85 – 1.52 (m, 6H), 1.30 – 0.86 (m, 5H).	
zh03	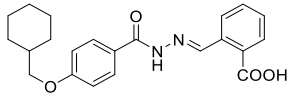 (E)-2-((2-(4-(cyclohexylmethoxy) benzoyl) hydrazono)methyl) benzoic acid	^{1}H NMR (400 MHz, dmso) δ 13.31 (s, 1H), 11.91 (s, 1H), 9.14 (s, 1H), 8.03 (d, *J* = 7.5 Hz, 1H), 7.96 – 7.74 (m, 3H), 7.60 (t, *J* = 7.3 Hz, 1H), 7.48 (t, *J* = 7.4 Hz, 1H), 7.00 (d, *J* = 8.7 Hz, 2H), 3.82 (d, *J* = 6.2 Hz, 2H), 1.94 – 1.50 (m, 6H), 1.32 – 0.92 (m, 5H).	^{13}C NMR (101 MHz, dmso) δ 168.55, 163.02, 162.06, 146.20, 135.18, 132.36, 131.02, 130.70, 130.07, 129.85, 126.98, 125.47, 114.50, 73.32, 37.45, 29.62, 26.45, 25.67.
zh04	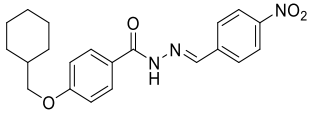 (E)-4-(cyclohexylmethoxy) -N'-(4-nitrobenzylidene) benzohydrazide	^{1}H NMR (400 MHz, dmso) δ 12.02 (s, 1H), 8.53 (s, 1H), 8.29 (d, *J* = 7.8 Hz, 2H), 7.97 (d, *J* = 6.1 Hz, 2H), 7.91 (d, *J* = 7.4 Hz, 2H), 7.05 (d, *J* = 7.9 Hz, 2H), 3.85 (d, *J* = 4.3 Hz, 2H), 1.99 – 1.44 (m, 6H), 1.15 (m, 5H).	^{13}C NMR (101 MHz, dmso) δ 163.13, 162.24, 148.12, 144.90, 141.25, 130.13, 128.28, 125.21, 124.49, 114.61, 73.35, 37.44, 29.61, 26.44, 25.67.
zh05	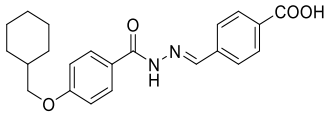 (E)-4-((2-(4-(cyclohexylmethoxy) benzoyl) hydrazono)methyl) benzoic acid	^{1}H NMR (400 MHz, dmso) δ 12.72 (s, 1H), 11.84 (s, 1H), 8.46 (s, 1H), 8.05 – 7.90 (m, 2H), 7.90 – 7.43 (m, 3H), 6.97 (t, *J* = 18.8 Hz, 2H), 3.74 (dd, *J* = 6.2 Hz, 2H), 1.92 – 1.41 (m, 6H), 1.41 – 0.68 (m, 5H).	^{13}C NMR (101 MHz, dmso) δ 167.33, 163.03, 162.13, 146.23, 138.96, 131.95, 130.19, 130.04, 127.38, 125.41, 114.57, 73.33, 40.54, 40.33, 40.12, 39.92, 39.71, 39.50, 39.29, 37.44, 29.60, 26.44, 25.67.
zh06	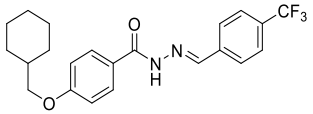 (E)-4-(cyclohexylmethoxy) -N'-(4-(trifluoromethyl) benzylidene)	^{1}H NMR (400 MHz, dmso) δ 11.90 (s, 1H), 8.48 (s, 1H), 7.97 – 7.71 (m, 5H), 7.02 (d, *J* = 8.5 Hz, 2H), 3.83 (d, *J* = 6.1 Hz, 2H), 2.01 – 1.47 (m, 6H), 1.39 – 0.84 (m, 5H).	^{13}C NMR (101 MHz, dmso) δ 163.09, 162.17, 145.66, 138.88, 130.07, 127.96, 126.17, 126.13, 125.34, 123.20, 114.62, 73.34, 37.44, 29.61, 26.45, 25.67.

	benzohydrazide		
zh07	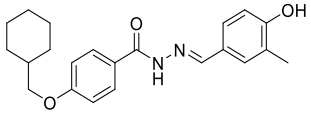 (E)-4-(cyclohexylmethoxy) -N'-(4-hydroxy-3-methylbenzylidene) benzohydrazide	^{1}H NMR (400 MHz, dmso) δ 11.46 (s, 1H), 9.80 (s, 2H), 8.25 (s, 1H), 7.84 (d, *J* = 8.4 Hz, 2H), 7.42 (s, 1H), 7.31 (d, *J* = 7.9 Hz, 1H), 7.00 (d, *J* = 8.5 Hz, 2H), 6.80 (d, *J* = 8.2 Hz, 1H), 3.82 (d, *J* = 6.1 Hz, 2H), 2.12 (s, 3H), 1.92 – 1.48 (m, 6H), 1.35 – 0.84 (m, 5H).	^{13}C NMR (101 MHz, dmso) δ 162.62, 161.85, 157.92, 147.97, 129.82, 129.71, 126.84, 125.85, 125.66, 124.87, 115.22, 114.51, 73.30, 68.37, 37.45, 29.62, 26.46, 25.76, 25.68, 16.36.
zh08	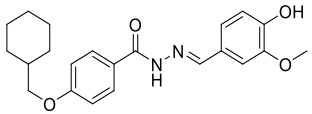 (E)-4-(cyclohexylmethoxy)-N'-(4-hydroxy-3-methoxybenzylidene) benzohydrazide	^{1}H NMR (400 MHz, dmso) δ 11.51 (s, 1H), 9.51 (s, 1H), 8.29 (s, 1H), 7.84 (d, *J* = 8.6 Hz, 2H), 7.27 (s, 1H), 7.01 (t, *J* = 10.5 Hz, 3H), 6.80 (d, *J* = 8.0 Hz, 1H), 3.87 – 3.62 (m, 5H), 1.90 – 1.47 (m, 6H), 1.32 – 0.81 (m, 5H).	^{13}C NMR (101 MHz, dmso) δ 162.67, 161.88, 149.26, 148.43, 148.07, 129.83, 126.27, 122.43, 115.82, 114.53, 109.20, 73.30, 55.93, 37.44, 29.62, 26.45, 25.68, 19.00.
zh09	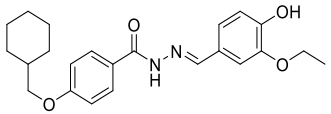 (E)-4-(cyclohexylmethoxy)-N'-(3-ethoxy-4-hydroxybenzylidene) benzohydrazide	^{1}H NMR (400 MHz, dmso) δ 11.50 (s, 1H), 9.40 (s, 1H), 8.29 (s, 1H), 7.85 (d, *J* = 8.8 Hz, 2H), 7.25 (s, 1H), 7.01 (dd, *J* = 16.7, 8.4 Hz, 3H), 6.82 (d, *J* = 8.1 Hz, 1H), 4.02 (q, *J* = 6.8 Hz, 2H), 3.81 (d, *J* = 6.2 Hz, 2H), 1.94 – 1.47 (m, 6H), 1.32 (t, *J* = 6.9 Hz, 3H), 1.24 – 0.84 (m, 5H).	^{13}C NMR (101 MHz, dmso) δ 162.72, 161.89, 149.54, 148.16, 147.59, 129.83, 126.29, 125.87, 122.35, 115.95, 114.52, 110.70, 73.32, 64.29, 37.45, 29.62, 26.45, 25.67, 15.16.
zh10	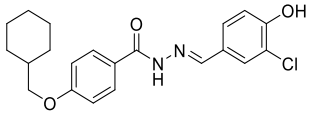 (E)-N'-(3-chloro-4-hydroxybenzylidene)-4-	^{1}H NMR (400 MHz, dmso) δ 11.63 (s, 1H), 10.69 (s, 1H), 8.27 (s, 1H), 7.84 (d, *J* = 8.3 Hz, 2H), 7.66 (s, 1H), 7.48 (d, *J* = 8.0 Hz, 1H), 7.00 (d, *J* = 8.4 Hz, 3H), 3.82 (d, *J* = 6.1 Hz, 2H), 1.79 – 1.57 (m, 6H), 1.24 – 0.96 (m, 5H).	^{13}C NMR (101 MHz, dmso) δ 162.78, 161.96, 155.13, 146.29, 129.89, 128.64, 127.56, 127.17, 125.63, 120.68, 117.27, 114.54, 109.99, 73.31, 37.44, 29.62, 26.45, 25.67.

	(cyclohexylmethoxy) benzohydrazide		
zh11	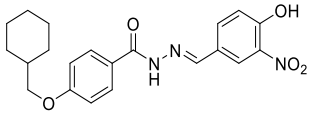 (E)-4-(cyclohexylmethoxy)-N'-(4-hydroxy-3-nitrobenzylidene) benzohydrazide	^{1}H NMR (400 MHz, dmso) δ 11.75 (s, 1H), 11.45 (s, 1H), 8.36 (s, 1H), 8.15 (s, 1H), 7.86 (t, *J* = 9.6 Hz, 3H), 7.18 (d, *J* = 8.7 Hz, 1H), 7.01 (d, *J* = 7.9 Hz, 2H), 3.82 (d, *J* = 6.1 Hz, 2H), 1.90 – 1.45 (m, 6H), 1.32 – 0.82 (m, 5H).	^{13}C NMR (101 MHz, dmso) δ 162.88, 162.04, 153.60, 145.37, 137.51, 133.26, 129.97, 126.41, 125.49, 124.24, 120.07, 114.56, 73.31, 37.43, 29.61, 26.45, 25.67.
zh12	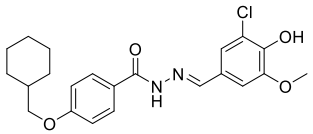 (E)-N'-(3-chloro-4-hydroxy-5-methoxybenzylidene)-4-(cyclohexylmethoxy) benzohydrazide	^{1}H NMR (400 MHz, dmso) δ 11.66 (s, 1H), 9.93 (s, 1H), 8.27 (s, 1H), 7.85 (d, *J* = 8.7 Hz, 2H), 7.24 (s, 2H), 7.01 (d, *J* = 8.7 Hz, 2H), 3.86 (s, 3H), 3.82 (d, *J* = 6.2 Hz, 2H), 1.85 – 1.50 (m, 6H), 1.30 – 0.94 (m, 5H).	^{13}C NMR (101 MHz, dmso) δ 162.81, 161.98, 149.33, 146.57, 145.01, 129.92, 126.53, 125.64, 121.89, 120.38, 114.55, 107.90, 73.31, 56.63, 37.44, 29.62, 26.45, 25.68.
zh13	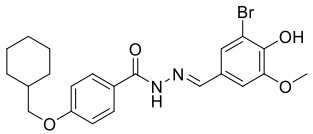 (E)-N'-(3-bromo-4-hydroxy-5-methoxybenzylidene)-4-(cyclohexylmethoxy) benzohydrazide	^{1}H NMR (400 MHz, dmso) δ 11.64 (s, 1H), 9.93 (s, 1H), 8.27 (s, 1H), 7.85 (d, *J* = 8.7 Hz, 2H), 7.37 (s, 1H), 7.28 (s, 1H), 7.00 (d, *J* = 8.7 Hz, 2H), 3.86 (s, 3H), 3.81 (d, *J* = 6.2 Hz, 2H), 1.92 – 1.48 (m, 6H), 1.32 – 0.88 (m, 5H).	^{13}C NMR (101 MHz, dmso) δ 162.84, 161.98, 149.05, 146.46, 146.06, 129.91, 127.25, 125.70, 124.64, 114.55, 109.77, 108.60, 73.33, 56.65, 37.44, 29.62, 26.45, 25.67.

zh14	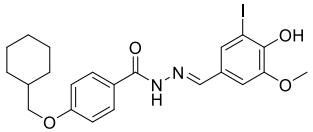 (E)-4-(cyclohexylmethoxy)-N'-(4-hydroxy-3-iodo-5-methoxybenzylidene) benzohydrazide	^{1}H NMR (400 MHz, dmso) δ 11.61 (s, 1H), 9.98 (s, 1H), 8.24 (s, 1H), 7.84 (d, *J* = 8.7 Hz, 2H), 7.55 (s, 1H), 7.28 (s, 1H), 7.00 (d, *J* = 8.7 Hz, 2H), 3.84 (s, 3H), 3.82 (d, *J* = 6.3 Hz, 2H), 1.83 – 1.54 (m, 6H), 1.28 – 0.92 (m, 5H).	^{13}C NMR (101 MHz, dmso) δ 162.83, 161.97, 148.58, 147.71, 146.37, 130.35, 129.90, 128.22, 125.72, 114.56, 109.45, 84.88, 73.33, 56.54, 37.45, 29.62, 26.45, 25.67.
zh15	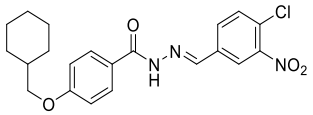 (E)-N'-(4-chloro-3-nitrobenzylidene)-4-(cyclohexylmethoxy) benzohydrazide	^{1}H NMR (400 MHz, dmso) δ 12.01 (s, 1H), 8.48 (s, 1H), 8.36 (s, 1H), 8.03 (d, *J* = 7.6 Hz, 1H), 7.90 (d, *J* = 8.1 Hz, 2H), 7.84 (d, *J* = 8.3 Hz, 1H), 7.05 (d, *J* = 8.4 Hz, 2H), 3.85 (d, *J* = 5.9 Hz, 2H), 1.99 – 1.48 (m, 6H), 1.39 – 0.81 (m, 5H).	^{13}C NMR (101 MHz, dmso) δ 163.10, 162.21, 148.33, 143.92, 135.60, 132.60, 131.84, 130.12, 125.96, 125.19, 123.83, 114.60, 73.34, 37.43, 29.61, 26.45, 25.67.
zh16	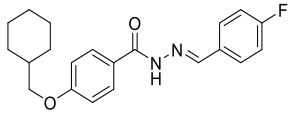 (E)-4-(cyclohexylmethoxy)-N'-(4-fluorobenzylidene) benzohydrazide	^{1}H NMR (400 MHz, dmso) δ 11.72 (s, 1H), 8.40 (s, 1H), 7.86 (d, *J* = 8.5 Hz, 2H), 7.79 – 7.69 (m, 2H), 7.26 (t, *J* = 8.7 Hz, 2H), 7.01 (d, *J* = 8.6 Hz, 2H), 3.82 (d, *J* = 6.2 Hz, 2H), 1.92 – 1.52 (m, 6H), 1.32 – 0.88 (m, 5H).	^{13}C NMR (101 MHz, dmso) δ 162.90, 162.03, 146.34, 131.51, 131.08, 129.94, 129.59, 129.51, 125.52, 116.62, 116.43, 116.21, 114.57, 73.31, 37.43, 29.61, 26.45, 25.67.
zh17	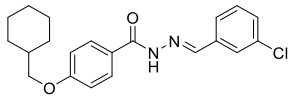	^{1}H NMR (400 MHz, dmso) δ 11.83 (s, 1H), 8.39 (s, 1H), 7.87 (d, *J* = 8.4 Hz, 2H), 7.74 (s, 1H), 7.64 (s, 1H), 7.45 (d, *J* = 4.3 Hz, 2H), 7.01 (d, *J* =	^{13}C NMR (101 MHz, dmso) δ 163.02, 162.12, 145.73, 137.16, 134.06, 131.17, 130.02, 126.58, 126.14, 125.39, 114.59,

	(E)-N'-(3-chlorobenzylidene)-4-(cyclohexylmethoxy) benzohydrazide	8.6 Hz, 2H), 3.82 (d, *J* = 6.2 Hz, 2H), 1.85 – 1.48 (m, 6H), 1.26 – 0.94 (m, 5H).	73.33, 37.44, 29.61, 26.45, 25.67.
zh18	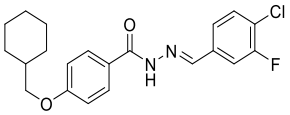 (E)-N'-(4-chloro-3-fluorobenzylidene)-4-(cyclohexylmethoxy) benzohydrazide	^{1}H NMR (400 MHz, dmso) δ 11.88 (s, 1H), 8.39 (s, 1H), 7.86 (d, *J* = 8.5 Hz, 2H), 7.76 – 7.43 (m, 3H), 7.01 (d, *J* = 8.8 Hz, 2H), 3.82 (d, *J* = 6.3 Hz, 2H), 1.99 – 1.45 (m, 6H), 1.37 – 0.72 (m, 5H).	^{13}C NMR (101 MHz, dmso) δ 163.01, 162.15, 159.08, 156.63, 144.99, 136.34, 136.27, 131.56, 130.04, 125.31, 124.48, 121.11, 115.03, 114.81, 114.58, 73.33, 37.43, 29.61, 26.45, 25.67.
zh19	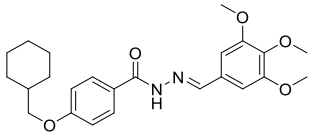 (E)-4-(cyclohexylmethoxy)-N'-(3,4,5-trimethoxybenzylidene) benzohydrazide	^{1}H NMR (400 MHz, dmso) δ 11.70 (s, 1H), 8.35 (s, 1H), 7.86 (d, *J* = 8.6 Hz, 2H), 7.09 – 6.83 (m, 4H), 3.80 (s, 6H), 3.67 (s, 2H), 1.90 – 1.47 (m, 6H), 1.32 – 0.73 (m, 5H).	^{13}C NMR (101 MHz, dmso) δ 162.92, 162.00, 153.60, 147.54, 139.44, 130.42, 129.95, 125.64, 114.57, 104.54, 73.32, 60.53, 56.33, 37.43, 29.61, 26.45, 25.67.
zh20	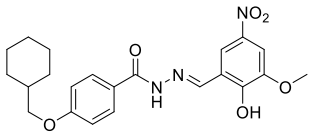 (E)-4-(cyclohexylmethoxy)-N'-(2-hydroxy-3-methoxy-5-nitrobenzylidene) benzohydrazide	^{1}H NMR (400 MHz, dmso) δ 12.14 (s, 2H), 8.69 (s, 1H), 8.22 (s, 1H), 7.89 (d, *J* = 8.2 Hz, 2H), 7.75 (s, 1H), 7.03 (d, *J* = 8.3 Hz, 2H), 3.92 (s, 3H), 3.83 (d, *J* = 6.1 Hz, 2H), 1.94 – 1.47 (m, 6H), 1.35 – 0.73 (m, 5H).	^{13}C NMR (101 MHz, dmso) δ 162.83, 162.31, 153.25, 148.54, 144.65, 139.92, 130.11, 124.76, 119.52, 116.57, 114.68, 107.50, 73.36, 56.84, 37.43, 29.61, 26.45, 25.67.

zh21	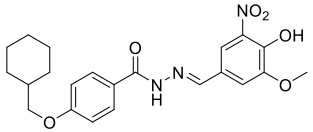 (E)-4-(cyclohexylmethoxy)-N'-(4-hydroxy-3-methoxy-5-nitrobenzylidene) benzohydrazide	^{1}H NMR (400 MHz, dmso) δ 11.78 (s, 1H), 10.91 (s, 1H), 8.35 (s, 1H), 7.86 (d, *J* = 8.7 Hz, 2H), 7.72 (s, 1H), 7.55 (s, 1H), 7.01 (d, *J* = 8.7 Hz, 2H), 3.92 (s, 3H), 3.82 (d, *J* = 6.2 Hz, 2H), 1.90 – 1.54 (m, 6H), 1.32 – 0.88 (m, 5H).	^{13}C NMR (101 MHz, dmso) δ 162.92, 162.04, 150.20, 145.75, 144.37, 137.58, 129.98, 125.64, 125.51, 116.27, 114.57, 112.41, 109.99, 73.32, 57.06, 37.43, 29.61, 26.45, 25.67.
zh22	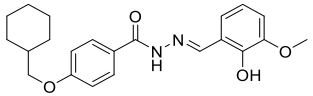 (E)-4-(cyclohexylmethoxy)-N'-(2-hydroxy-3-methoxybenzylidene) benzohydrazide	^{1}H NMR (400 MHz, dmso) δ 11.94 (s, 1H), 11.07 (s, 1H), 8.59 (s, 1H), 7.88 (d, *J* = 8.6 Hz, 2H), 7.18 – 6.95 (m, 4H), 6.83 (t, *J* = 7.9 Hz, 1H), 3.83 (d, *J* = 6.2 Hz, 2H), 3.78 (s, 3H), 1.89 – 1.48 (m, 6H), 1.37 – 0.82 (m, 5H).	^{13}C NMR (101 MHz, dmso) δ 162.57, 162.20, 148.33, 148.07, 147.55, 129.99, 124.97, 121.32, 119.40, 119.33, 114.66, 114.09, 73.35, 56.21, 37.44, 29.61, 26.45, 25.67.
zh23	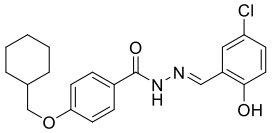 (E)-N'-(5-chloro-2-hydroxybenzylidene)-4-(cyclohexylmethoxy) benzohydrazide	^{1}H NMR (400 MHz, dmso) δ 12.05 (s, 1H), 11.35 (s, 1H), 8.56 (s, 1H), 7.89 (d, *J* = 6.5 Hz, 2H), 7.62 (s, 1H), 7.43 – 7.18 (m, 1H), 7.12 – 6.94 (m, 2H), 6.92 (dd, *J* = 8.7, 2.7 Hz, 1H), 3.82 (dd, *J* = 5.9, 2.8 Hz, 2H), 1.90 – 1.48 (m, 6H), 1.41 – 0.90 (m, 5H).	^{13}C NMR (101 MHz, dmso) δ 162.73, 162.26, 156.43, 145.71, 131.00, 130.06, 128.12, 124.84, 123.33, 121.13, 118.62, 114.64, 73.34, 37.43, 29.61, 26.44, 25.67.

zh24	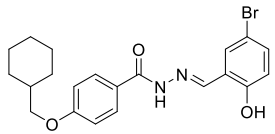 (E)-N'-(5-bromo-2-hydroxybenzylidene)-4-(cyclohexylmethoxy) benzohydrazide	^{1}H NMR (400 MHz, dmso) δ 12.05 (s, 1H), 11.35 (s, 1H), 8.56 (s, 1H), 7.88 (d, *J* = 8.5 Hz, 2H), 7.74 (s, 1H), 7.39 (dd, *J* = 8.7, 2.1 Hz, 1H), 7.02 (d, *J* = 8.7 Hz, 2H), 6.87 (d, *J* = 8.7 Hz, 1H), 3.82 (d, *J* = 6.2 Hz, 2H), 1.98 – 1.50 (m, 6H), 1.35 – 0.88 (m, 5H).	^{13}C NMR (101 MHz, dmso) δ 162.73, 162.25, 156.82, 145.51, 133.81, 130.94, 130.06, 124.85, 121.76, 119.08, 114.65, 110.81, 73.34, 37.43, 29.61, 26.45, 25.67.
zh25	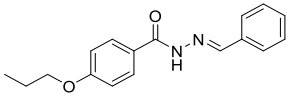 (E)-N'-benzylidene-4-propoxybenzohydrazide	^{1}H NMR (400 MHz, dmso) δ 11.70 (s, 1H), 8.41 (s, 1H), 7.87 (d, *J* = 8.7 Hz, 2H), 7.69 (d, *J* = 6.4 Hz, 2H), 7.42 (d, *J* = 7.3 Hz, 3H), 7.02 (d, *J* = 8.7 Hz, 2H), 3.97 (t, *J* = 6.6 Hz, 2H), 1.72 (dd, *J* = 14.1, 6.9 Hz, 2H), 0.95 (t, *J* = 7.4 Hz, 3H).	^{13}C NMR (101 MHz, dmso) δ 162.93, 161.88, 147.50, 134.87, 130.37, 129.96, 129.27, 127.41, 125.62, 114.56, 69.62, 22.38, 10.79.
zh26	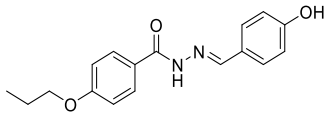 (E)-N'-(4-hydroxybenzylidene)-4-propoxybenzohydrazide	^{1}H NMR (400 MHz, dmso) δ 11.51 (s, 1H), 9.90 (s, 1H), 8.30 (s, 1H), 7.85 (d, *J* = 7.0 Hz, 2H), 7.51 (d, *J* = 7.4 Hz, 2H), 7.00 (d, *J* = 7.3 Hz, 2H), 6.80 (d, *J* = 7.2 Hz, 2H), 3.95 (dd, *J* = 8.5, 4.3 Hz, 2H), 1.71 (d, *J* = 6.9 Hz, 2H), 0.94 (t, *J* = 7.4 Hz, 3H).	^{13}C NMR (101 MHz, dmso) δ 162.70, 161.74, 159.71, 147.86, 129.84, 129.17, 125.84, 116.10, 114.49, 69.58, 22.38, 10.79.
zh27	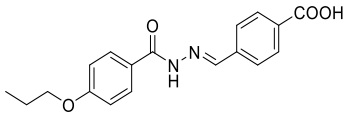 (E)-4-((2-(4-propoxybenzoyl) hydrazono) methyl) benzoic acid	^{1}H NMR (400 MHz, dmso) δ 13.07 (s, 1H), 11.86 (s, 1H), 8.46 (s, 1H), 7.97 (d, *J* = 7.9 Hz, 2H), 7.88 (d, *J* = 8.5 Hz, 2H), 7.80 (d, *J* = 7.7 Hz, 2H), 7.02 (d, *J* = 8.7 Hz, 2H), 3.97 (t, *J* = 6.5 Hz, 2H), 1.71 (dd, *J* = 14.0, 7.0 Hz, 2H), 0.95 (t, *J* = 7.4	^{13}C NMR (101 MHz, dmso) δ 167.35, 163.04, 161.99, 161.48, 146.23, 138.94, 137.89, 133.47, 131.95, 130.21, 130.06, 128.95, 127.41, 125.43, 114.57, 69.63, 22.37, 10.78.

		Hz, 3H).	
zh28	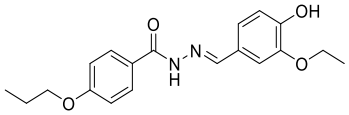 (E)-N'-(3-chloro-4-hydroxybenzylidene)-4-propoxybenzohydrazide	^{1}H NMR (400 MHz, dmso) δ 11.51 (s, 1H), 9.44 (s, 1H), 8.28 (s, 1H), 7.84 (d, *J* = 8.6 Hz, 2H), 7.25 (s, 1H), 7.01 (t, *J* = 9.5 Hz, 3H), 6.81 (d, *J* = 8.1 Hz, 1H), 4.03 (dd, *J* = 13.6, 6.7 Hz, 2H), 3.96 (t, *J* = 6.5 Hz, 2H), 1.71 (dd, *J* = 14.0, 6.9 Hz, 2H), 1.33 (t, *J* = 6.8 Hz, 3H), 0.95 (t, *J* = 7.4 Hz, 3H).	^{13}C NMR (101 MHz, dmso) δ 162.69, 161.74, 149.49, 148.10, 147.58, 129.84, 126.24, 125.86, 122.34, 115.91, 114.50, 110.55, 69.59, 64.23, 22.38, 15.17, 10.79.
zh29	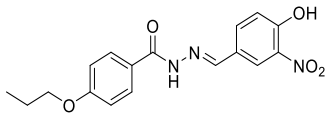 (E)-N'-(4-hydroxy-3-nitrobenzylidene)-4-propoxybenzohydrazide	^{1}H NMR (400 MHz, dmso) δ 11.75 (s, 1H), 11.48 (s, 1H), 8.34 (d, *J* = 8.0 Hz, 1H), 8.15 (s, 1H), 7.85 (d, *J* = 6.7 Hz, 3H), 7.17 (d, *J* = 10.9 Hz, 1H), 7.01 (d, *J* = 6.5 Hz, 2H), 3.97 (dd, *J* = 6.3, 3.5 Hz, 2H), 1.71 (dd, *J* = 11.2, 6.8 Hz, 2H), 0.95 (t, *J* = 7.3, 3.0 Hz, 3H).	^{13}C NMR (101 MHz, dmso) δ 161.90, 160.24, 153.61, 145.38, 137.50, 133.26, 129.97, 126.39, 125.54, 124.24, 120.08, 114.54, 69.61, 22.37, 10.78.
zh30	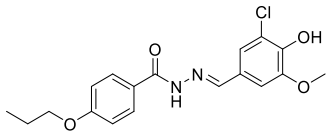 (E)-N'-(3-chloro-4-hydroxy-5-methoxybenzylidene)-4-propoxybenzohydrazide	^{1}H NMR (400 MHz, dmso) δ 11.64 (s, 1H), 9.88 (s, 1H), 8.28 (s, 1H), 7.85 (d, *J* = 7.7 Hz, 2H), 7.24 (s, 2H), 7.01 (d, *J* = 7.9 Hz, 2H), 3.97 (t, *J* = 6.1 Hz, 2H), 3.86 (s, 3H), 1.72 (dd, *J* = 13.6, 6.9 Hz, 2H), 0.95 (t, *J* = 7.3 Hz, 3H).	^{13}C NMR (101 MHz, dmso) δ 162.85, 161.84, 149.36, 146.61, 145.03, 129.92, 126.56, 125.74, 121.87, 120.42, 114.53, 108.01, 69.63, 56.65, 22.38, 10.77.

zh31	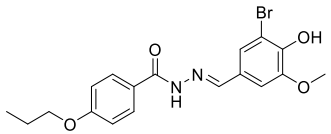 (E)-N'-(3-bromo-4-hydroxy-5-methoxybenzylidene)-4-propoxybenzohydrazide	^{1}H NMR (400 MHz, dmso) δ 11.67 (s, 1H), 9.97 (s, 1H), 8.26 (s, 1H), 7.85 (d, *J* = 8.8 Hz, 2H), 7.38 (s, 1H), 7.28 (s, 1H), 7.01 (d, *J* = 8.8 Hz, 2H), 3.97 (t, *J* = 6.6 Hz, 2H), 3.86 (s, 3H), 1.71 (dd, *J* = 14.1, 6.9 Hz, 2H), 0.95 (t, *J* = 7.4 Hz, 3H).	^{13}C NMR (101 MHz, dmso) δ 162.84, 161.83, 149.02, 146.45, 146.03, 129.93, 127.21, 125.68, 124.66, 114.52, 109.74, 108.50, 69.61, 56.63, 22.37, 10.79.
zh32	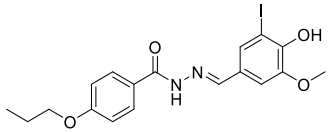 (E)-N'-(4-hydroxy-3-iodo-5-methoxybenzylidene)-4-propoxybenzohydrazide	^{1}H NMR (400 MHz, dmso) δ 11.65 (s, 1H), 10.03 (s, 1H), 8.24 (s, 1H), 7.84 (d, *J* = 8.8 Hz, 2H), 7.55 (s, 1H), 7.28 (s, 1H), 7.01 (d, *J* = 8.8 Hz, 2H), 3.97 (t, *J* = 6.6 Hz, 2H), 3.84 (s, 3H), 1.71 (d, *J* = 7.3 Hz, 2H), 0.95 (t, *J* = 7.4 Hz, 3H).	^{13}C NMR (101 MHz, dmso) δ 162.83, 161.82, 148.56, 147.67, 146.34, 130.37, 129.92, 128.17, 125.69, 114.52, 109.34, 84.90, 69.61, 56.51, 22.37, 10.79.
zh33	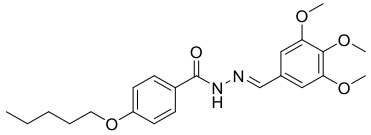 (E)-4-(pentyloxy)-N'-(3,4,5-trimethoxybenzylidene) benzohydrazide	^{1}H NMR (400 MHz, dmso) δ 11.69 (s, 1H), 8.35 (s, 1H), 7.86 (d, *J* = 7.5 Hz, 2H), 7.18 – 6.77 (m, 4H), 4.00 (t, *J* = 5.7 Hz, 2H), 3.80 (s, 6H), 3.67 (s, 3H), 1.92 – 1.54 (m, 2H), 1.54 – 1.19 (m, 4H), 0.86 (t, *J* = 6.2 Hz, 3H).	^{13}C NMR (101 MHz, dmso) δ 162.96, 161.87, 153.60, 147.57, 139.49, 130.42, 129.94, 125.70, 114.53, 104.57, 68.14, 60.52, 56.33, 28.69, 28.09, 22.32, 14.34.
zh34	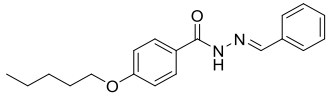	^{1}H NMR (400 MHz, dmso) δ 11.74 (s, 1H), 8.45 (s, 1H), 7.90 (d, *J* = 8.6 Hz, 2H), 7.72 (d, *J* = 6.4 Hz, 2H), 7.45 (d, *J* = 7.3 Hz, 3H), 7.05 (d, *J* = 8.7	^{13}C NMR (101 MHz, dmso) δ 162.91, 161.89, 147.48, 134.88, 130.35, 129.96, 129.26, 127.41, 125.61, 114.54, 68.14,

	(E)-N'-benzylidene-4-(pentyloxy) benzohydrazide	Hz, 2H), 4.04 (t, *J* = 6.5 Hz, 2H), 1.84 – 1.57 (m, 2H), 1.53 – 1.24 (m, 4H), 0.90 (t, *J* = 7.0 Hz, 3H).	28.70, 28.09, 22.33, 14.37.
zh35	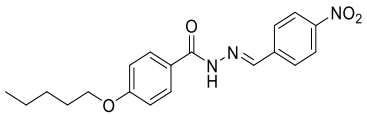 (E)-N'-(4-nitrobenzylidene)-4-(pentyloxy) benzohydrazide	^{1}H NMR (400 MHz, dmso) δ 12.01 (s, 1H), 8.52 (s, 1H), 8.28 (d, *J* = 8.5 Hz, 2H), 7.94 (dd, *J* = 20.3, 7.7 Hz, 4H), 7.05 (d, *J* = 8.6 Hz, 2H), 4.03 (t, *J* = 6.4 Hz, 2H), 1.92 – 1.57 (m, 2H), 1.48 – 1.23 (m, 4H), 0.89 (t, *J* = 6.8 Hz, 3H).	^{13}C NMR (101 MHz, dmso) δ 163.16, 162.09, 148.11, 144.89, 141.24, 130.13, 128.27, 125.24, 124.47, 114.57, 68.17, 28.69, 28.08, 22.32, 14.33.
zh36	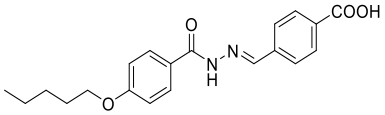 (E)-4-((2-(4-(pentyloxy) benzoyl) hydrazono)methyl) benzoic acid	^{1}H NMR (400 MHz, dmso) δ 13.04 (s, 1H), 11.86 (s, 1H), 8.46 (s, 1H), 7.98 (d, *J* = 8.0 Hz, 2H), 7.88 (d, *J* = 8.4 Hz, 2H), 7.80 (d, *J* = 7.5 Hz, 2H), 7.01 (d, *J* = 8.6 Hz, 2H), 3.99 (t, *J* = 6.5 Hz, 2H), 1.81 – 1.56 (m, 2H), 1.56 – 1.12 (m, 4H), 0.85 (t, *J* = 6.9 Hz, 3H).	^{13}C NMR (101 MHz, dmso) δ 167.35, 163.04, 162.00, 146.22, 138.95, 131.94, 130.21, 130.05, 127.40, 125.41, 114.56, 68.14, 28.70, 28.08, 22.33, 14.35.
zh37	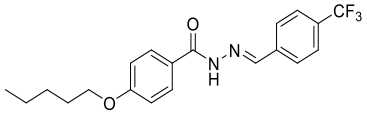 (E)-4-(pentyloxy)-N'-(4-(trifluoromethyl) benzylidene) benzohydrazide	^{1}H NMR (400 MHz, dmso) δ 11.94 (s, 1H), 8.51 (s, 1H), 8.03 – 7.85 (m, 4H), 7.80 (d, *J* = 8.0 Hz, 2H), 7.05 (d, *J* = 8.6 Hz, 2H), 4.03 (t, *J* = 6.5 Hz, 2H), 1.93 – 1.68 (m, 2H), 1.50 – 1.24 (m, 4H), 0.89 (t, *J* = 6.8 Hz, 3H).	^{13}C NMR (101 MHz, dmso) δ 163.15, 162.01, 145.63, 138.91, 130.06, 129.74, 127.93, 126.13, 126.09, 126.05, 125.89, 125.44, 123.19, 114.55, 68.14, 28.69, 28.08, 22.32, 14.33.
zh38	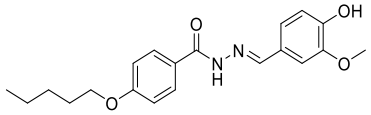 (E)-N'-(4-hydroxy-3-methoxybenzylidene)-4-	^{1}H NMR (400 MHz, dmso) δ 11.52 (s, 1H), 9.52 (s, 1H), 8.30 (s, 1H), 7.85 (d, *J* = 8.7 Hz, 2H), 7.27 (s, 1H), 7.09 – 6.94 (m, 3H), 6.80 (d, *J* = 8.1 Hz, 1H), 4.00 (t, *J* = 6.5 Hz, 2H), 3.79 (s, 3H), 1.87 – 1.56 (m, 2H), 1.48 – 1.21 (m, 4H), 0.86 (t,	^{13}C NMR (101 MHz, dmso) δ 162.70, 161.75, 149.27, 148.43, 148.09, 129.84, 126.27, 125.85, 122.45, 115.82, 114.50, 109.19, 68.11, 55.93, 28.70, 28.09, 22.33, 14.37.

	(pentyloxy) benzohydrazide	J = 6.9 Hz, 3H).	
zh39	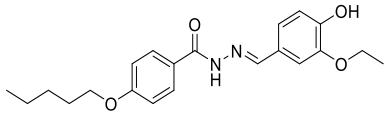 (E)-N'-(3-ethoxy-4-hydroxybenzylidene)-4-(pentyloxy) benzohydrazide	^{1}H NMR (400 MHz, dmso) δ 11.50 (s, 1H), 9.42 (s, 1H), 8.28 (s, 1H), 7.84 (d, J = 8.5 Hz, 2H), 7.25 (s, 1H), 7.14 – 6.90 (m, 3H), 6.81 (d, J = 7.9 Hz, 1H), 4.01 (dd, J = 14.4, 7.6 Hz, 4H), 1.89 – 1.52 (m, 2H), 1.52 – 1.15 (m, 6H), 0.86 (t, J = 6.8 Hz, 3H).	^{13}C NMR (101 MHz, dmso) δ 162.70, 161.74, 149.50, 148.12, 147.59, 129.83, 126.26, 125.88, 122.33, 115.93, 114.50, 110.62, 68.12, 64.26, 28.70, 28.09, 22.32, 15.17, 14.35.
zh40	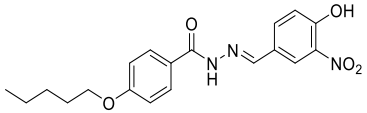 (E)-N'-(4-hydroxy-3-nitrobenzylidene)-4-(pentyloxy) benzohydrazide	^{1}H NMR (400 MHz, dmso) δ 11.80 (s, 1H), 11.49 (s, 1H), 8.40 (s, 1H), 8.19 (s, 1H), 7.91 (t, J = 9.5 Hz, 3H), 7.22 (d, J = 8.7 Hz, 1H), 7.05 (d, J = 8.3 Hz, 2H), 4.04 (t, J = 6.4 Hz, 2H), 1.87 – 1.61 (m, 2H), 1.50 – 1.25 (m, 4H), 0.90 (t, J = 6.7 Hz, 3H).	^{13}C NMR (101 MHz, dmso) δ 162.90, 161.91, 153.59, 145.38, 137.51, 133.26, 129.97, 126.40, 125.52, 124.24, 120.08, 114.54, 68.14, 28.69, 28.09, 22.33, 14.37.
zh41	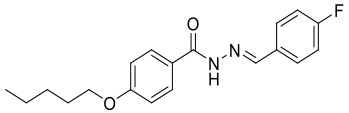 (E)-N'-(4-fluorobenzylidene)-4-(pentyloxy) benzohydrazide	^{1}H NMR (400 MHz, dmso) δ 11.72 (s, 2H), 8.41 (s, 1H), 7.86 (d, J = 8.4 Hz, 2H), 7.74 (d, J = 5.5 Hz, 2H), 7.26 (t, J = 8.6 Hz, 2H), 7.01 (d, J = 8.5 Hz, 2H), 4.00 (t, J = 6.5 Hz, 2H), 1.87 – 1.57 (m, 2H), 1.50 – 1.14 (m, 4H), 0.86 (t, J = 6.9 Hz, 3H).	^{13}C NMR (101 MHz, dmso) δ 164.67, 162.92, 162.20, 161.90, 146.34, 131.48, 129.95, 129.59, 129.50, 125.57, 116.43, 116.21, 114.54, 68.13, 28.70, 28.09, 22.32, 14.36.
zh42	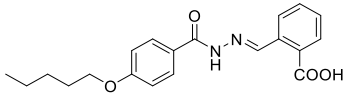 (E)-2-((2-(4-(pentyloxy)benzoyl)hydrazono) methyl) benzoic acid	^{1}H NMR (400 MHz, dmso) δ 13.34 (s, 1H), 11.96 (s, 1H), 9.18 (s, 1H), 8.07 (d, J = 7.6 Hz, 1H), 7.99 – 7.81 (m, 3H), 7.63 (t, J = 7.5 Hz, 1H), 7.51 (t, J = 7.4 Hz, 1H), 7.03 (d, J = 8.7 Hz, 2H), 4.03 (t, J = 6.5 Hz, 2H), 1.86 – 1.51 (m, 2H), 1.49 – 1.20 (m, 4H), 0.88 (t, J = 7.1 Hz, 3H).	^{13}C NMR (101 MHz, dmso) δ 168.55, 163.05, 161.93, 146.21, 135.21, 132.37, 130.97, 130.72, 130.08, 129.84, 127.00, 125.51, 114.47, 68.13, 28.70, 28.09, 22.32, 14.35.

zh43	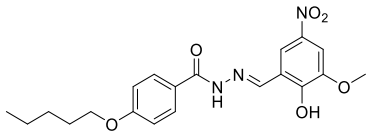 (E)-N'-(2-hydroxy-3-methoxy-5-nitrobenzylidene)-4-(pentyloxy) benzohydrazide	^{1}H NMR (400 MHz, dmso) δ 12.17 (s, 2H), 8.72 (s, 1H), 8.24 (s, 1H), 7.92 (d, *J* = 8.5 Hz, 2H), 7.77 (d, *J* = 2.2 Hz, 1H), 7.06 (d, *J* = 8.7 Hz, 2H), 4.04 (t, *J* = 6.5 Hz, 2H), 3.95 (s, 3H), 1.83 – 1.57 (m, 2H), 1.48 – 1.21 (m, 4H), 0.89 (t, *J* = 7.0 Hz, 3H).	^{13}C NMR (101 MHz, dmso) δ 162.82, 162.17, 153.25, 148.52, 144.63, 139.90, 130.11, 124.77, 119.49, 116.56, 114.63, 107.46, 68.18, 56.81, 28.69, 28.08, 22.33, 14.36.
zh44	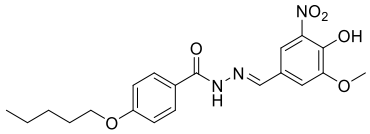 (E)-N'-(4-hydroxy-3-methoxy-5-nitrobenzylidene)-4-(pentyloxy) benzohydrazide	1H NMR (400 MHz, dmso) δ 11.82 (s, 1H), 10.92 (s, 1H), 8.38 (s, 1H), 7.89 (d, J = 8.6 Hz, 2H), 7.75 (s, 1H), 7.58 (s, 1H), 7.04 (d, J = 8.6 Hz, 2H), 4.03 (t, J = 6.5 Hz, 2H), 3.95 (s, 3H), 1.88 – 1.63 (m, 2H), 1.52 – 1.19 (m, 4H), 0.89 (t, J = 6.9 Hz, 3H).	^{13}C NMR (101 MHz, dmso) δ 162.94, 161.91, 150.20, 145.75, 144.39, 137.55, 129.99, 125.64, 125.55, 116.27, 114.53, 112.41, 68.14, 57.04, 28.69, 28.09, 22.33, 14.35.
zh45	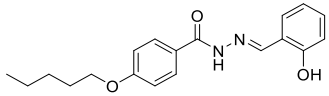 (E)-N'-(2-hydroxybenzylidene)-4-(pentyloxy) benzohydrazide	^{1}H NMR (400 MHz, dmso) δ 12.01 (s, 1H), 11.39 (s, 1H), 8.62 (s, 1H), 7.92 (d, *J* = 8.5 Hz, 2H), 7.52 (d, *J* = 7.6 Hz, 1H), 7.28 (d, *J* = 7.7 Hz, 1H), 7.06 (d, *J* = 8.3 Hz, 2H), 6.92 (t, *J* = 8.8 Hz, 2H), 4.04 (t, *J* = 6.4 Hz, 2H), 1.93 – 1.57 (m, 2H), 1.37 (td, *J* = 14.1, 6.7 Hz, 4H), 0.89 (t, *J* = 7.0 Hz, 3H).	^{13}C NMR (101 MHz, dmso) δ 162.61, 162.08, 157.86, 148.15, 131.63, 130.00, 124.95, 119.72, 119.11, 116.82, 114.63, 68.17, 28.70, 28.09, 22.33, 14.36.
zh46	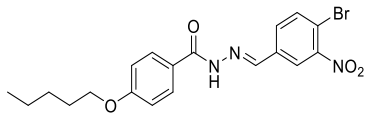 (E)-N'-(4-bromo-3-	^{1}H NMR (400 MHz, dmso) δ 11.99 (s, 1H), 8.42 (s, 1H), 8.27 (s, 1H), 7.90 (dd, *J* = 24.1, 8.1 Hz, 4H), 7.00 (d, *J* = 7.9 Hz, 2H), 3.98 (t, *J* = 6.4 Hz, 2H), 1.87 – 1.57 (m, 2H), 1.47 – 1.21 (m, 4H),	^{13}C NMR (101 MHz, dmso) δ 163.09, 162.08, 150.36, 143.98, 136.07, 135.63, 131.67, 130.12, 125.18, 123.67, 114.54, 114.23, 68.15, 28.70, 28.08, 22.34, 14.35.

	nitrobenzylidene)-4-(pentyloxy) benzohydrazide	0.85 (t, *J* = 6.5 Hz, 3H).	
zh47	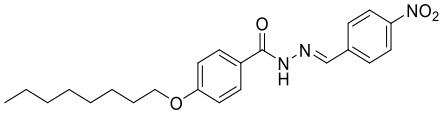 (E)-N'-(4-nitrobenzylidene)-4-(octyloxy) benzohydrazide	^{1}H NMR (400 MHz, dmso) δ 12.04 (s, 1H), 8.54 (s, 1H), 8.31 (d, *J* = 8.7 Hz, 2H), 7.99 (d, *J* = 7.9 Hz, 2H), 7.92 (d, *J* = 8.6 Hz, 2H), 7.07 (d, *J* = 8.8 Hz, 2H), 4.05 (t, *J* = 6.5 Hz, 2H), 1.89 – 1.61 (m, 2H), 1.41 (d, *J* = 7.6 Hz, 2H), 1.28 (d, *J* = 9.5 Hz, 8H), 0.86 (t, *J* = 6.7 Hz, 3H).	^{13}C NMR (101 MHz, dmso) δ 163.11, 162.11, 148.14, 144.95, 141.24, 130.14, 128.30, 125.23, 124.53, 114.61, 68.19, 31.68, 29.17, 29.11, 28.99, 25.91, 22.53, 14.42.
zh48	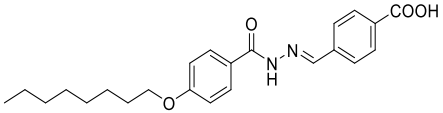 (E)-4-((2-(4-(octyloxy)benzoyl) hydrazono) methyl) benzoic acid	^{1}H NMR (400 MHz, dmso) δ 13.10 (s, 1H), 11.89 (s, 1H), 8.49 (s, 1H), 8.01 (d, *J* = 8.0 Hz, 2H), 7.91 (d, *J* = 8.5 Hz, 2H), 7.83 (d, *J* = 7.5 Hz, 2H), 7.05 (d, *J* = 8.7 Hz, 2H), 4.03 (t, *J* = 6.4 Hz, 2H), 1.86 – 1.59 (m, 2H), 1.48 – 1.36 (m, 2H), 1.36 – 1.16 (m, 8H), 0.85 (t, *J* = 6.6 Hz, 3H).	^{13}C NMR (101 MHz, dmso) δ 167.34, 163.02, 162.00, 146.21, 138.95, 131.95, 130.21, 130.05, 127.40, 125.41, 114.56, 68.16, 31.68, 29.18, 29.12, 29.00, 25.91, 22.53, 14.41.
zh49	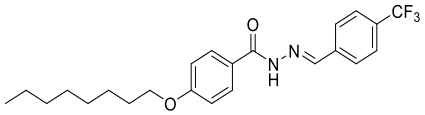 (E)-4-(octyloxy)-N'-(4-(trifluoromethyl) benzylidene) benzohydrazide	^{1}H NMR (400 MHz, dmso) δ 11.93 (s, 2H), 8.51 (s, 1H), 7.91 (d, *J* = 8.8 Hz, 4H), 7.81 (d, *J* = 7.9 Hz, 2H), 7.05 (d, *J* = 8.5 Hz, 2H), 4.04 (t, *J* = 6.3 Hz, 2H), 1.88 – 1.62 (m, 2H), 1.49 – 1.36 (m, 2H), 1.36 – 1.17 (m, 8H), 0.86 (s, 3H).	^{13}C NMR (101 MHz, dmso) δ 163.08, 162.02, 145.66, 138.89, 130.07, 129.77, 127.96, 126.17, 126.13, 125.37, 114.59, 68.17, 31.68, 29.17, 29.11, 29.00, 25.91, 22.53, 14.41.
zh50	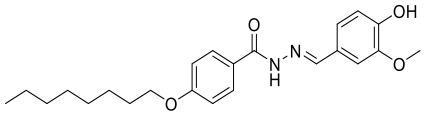 (E)-N'-(4-hydroxy-3-	^{1}H NMR (400 MHz, dmso) δ 11.55 (s, 1H), 9.55 (s, 1H), 8.33 (s, 1H), 7.88 (d, *J* = 8.7 Hz, 2H), 7.30 (s, 1H), 7.15 – 6.95 (m, 3H), 6.84 (d, *J* = 8.1 Hz, 1H), 4.03 (t, *J* = 6.5 Hz, 2H), 3.83 (s, 3H),	^{13}C NMR (101 MHz, dmso) δ 162.68, 161.75, 149.27, 148.43, 148.08, 129.84, 126.26, 125.84, 122.44, 115.82, 114.49, 109.19, 68.12, 55.93, 31.68, 29.18, 29.12,

	methoxybenzylidene)-4-(octyloxy) benzohydrazide	1.84 – 1.59 (m, 2H), 1.41 (s, 2H), 1.26 (s, 8H), 0.86 (t, *J* = 6.6 Hz, 3H).	29.01, 25.92, 22.54, 14.41.
zh51	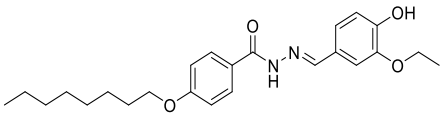 (E)-N'-(3-ethoxy-4-hydroxybenzylidene)-4-(octyloxy) benzohydrazide	^{1}H NMR (400 MHz, dmso) δ 11.54 (s, 1H), 9.46 (s, 1H), 8.31 (s, 1H), 7.88 (d, *J* = 8.6 Hz, 2H), 7.29 (s, 1H), 7.04 (t, *J* = 11.4 Hz, 3H), 6.85 (d, *J* = 8.0 Hz, 1H), 4.18 – 3.86 (m, 4H), 1.81 – 1.63 (m, 2H), 1.48 – 1.15 (m, 12H), 0.85 (d, *J* = 6.4 Hz, 3H).	^{13}C NMR (101 MHz, dmso) δ 162.70, 161.75, 149.50, 148.12, 147.59, 129.83, 126.26, 125.85, 122.33, 115.93, 114.50, 110.63, 68.13, 64.26, 31.67, 29.16, 29.10, 29.00, 25.91, 22.52, 15.16, 14.39.
zh52	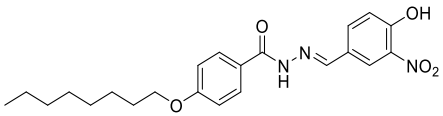 (E)-N'-(4-hydroxy-3-nitrobenzylidene)-4-(octyloxy) benzohydrazide	^{1}H NMR (400 MHz, dmso) δ 11.79 (s, 1H), 11.50 (s, 1H), 8.39 (s, 1H), 8.19 (s, 1H), 7.90 (t, *J* = 9.6 Hz, 3H), 7.21 (d, *J* = 8.7 Hz, 1H), 7.04 (d, *J* = 8.4 Hz, 2H), 4.03 (t, *J* = 6.4 Hz, 2H), 1.83 – 1.65 (m, 2H), 1.52 – 1.14 (m, 10H), 0.86 (t, *J* = 6.4 Hz, 3H).	^{13}C NMR (101 MHz, dmso) δ 162.90, 161.91, 153.61, 145.37, 137.50, 133.26, 129.97, 126.40, 125.52, 124.24, 120.08, 114.54, 68.14, 31.68, 29.17, 29.11, 29.00, 25.91, 22.53, 14.41.
zh53	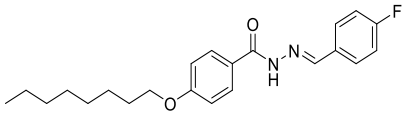 (E)-N'-(4-fluorobenzylidene)-4-(octyloxy) benzohydrazide	^{1}H NMR (400 MHz, dmso) δ 11.75 (s, 1H), 8.44 (s, 1H), 7.90 (d, *J* = 8.2 Hz, 2H), 7.78 (s, 2H), 7.29 (t, *J* = 8.5 Hz, 2H), 7.04 (d, *J* = 8.3 Hz, 2H), 4.03 (t, *J* = 6.3 Hz, 2H), 1.81 – 1.63 (m, 2H), 1.48 – 1.11 (m, 10H), 0.85 (d, *J* = 6.5 Hz, 3H).	^{13}C NMR (101 MHz, dmso) δ 164.67, 162.90, 162.20, 161.90, 146.32, 131.52, 129.94, 129.59, 129.50, 125.57, 116.42, 116.20, 114.53, 68.14, 31.68, 29.18, 29.12, 29.01, 25.92, 22.53, 14.40.
zh54	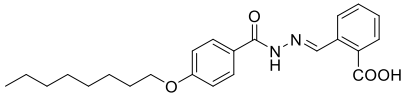 (E)-2-((2-(4-(octyloxy)benzoyl) hydrazono) methyl) benzoic acid	^{1}H NMR (400 MHz, dmso) δ 13.28 (s, 1H), 11.96 (s, 1H), 9.19 (s, 1H), 8.08 (d, *J* = 7.5 Hz, 1H), 7.92 (dd, *J* = 11.6, 8.5 Hz, 3H), 7.64 (t, *J* = 7.4 Hz, 1H), 7.52 (t, *J* = 7.5 Hz, 1H), 7.04 (d, *J* = 8.8 Hz, 2H), 4.03 (t, *J* = 6.5 Hz, 2H), 1.81 – 1.63 (m,	^{13}C NMR (101 MHz, dmso) δ 168.54, 163.03, 161.93, 146.20, 135.21, 132.37, 130.96, 130.71, 130.08, 129.84, 126.99, 125.51, 114.47, 68.14, 31.67, 29.17, 29.11, 29.01, 25.91, 22.52, 14.39.

		2H), 1.48 – 1.15 (m, 10H), 0.86 (t, *J* = 6.7 Hz, 3H).	
zh55	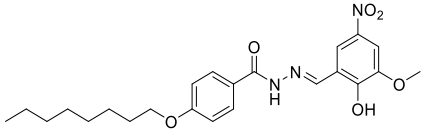 (E)-N'-(2-hydroxy-3-methoxy-5-nitrobenzylidene)-4-(octyloxy) benzohydrazide	^{1}H NMR (400 MHz, dmso) δ 12.15 (s, 2H), 8.69 (s, 1H), 8.23 (s, 1H), 7.89 (d, *J* = 8.4 Hz, 2H), 7.75 (d, *J* = 1.7 Hz, 1H), 7.03 (d, *J* = 8.5 Hz, 2H), 4.01 (t, *J* = 6.4 Hz, 2H), 3.92 (s, 3H), 1.85 – 1.61 (m, 2H), 1.47 – 1.34 (m, 2H), 1.34 – 1.10 (m, 8H), 0.83 (t, *J* = 6.4 Hz, 3H).	^{13}C NMR (101 MHz, dmso) δ 162.84, 162.18, 153.27, 148.54, 144.61, 139.90, 130.12, 124.78, 119.53, 116.53, 114.65, 107.48, 68.19, 56.83, 31.68, 29.17, 29.11, 28.99, 25.91, 22.53, 14.42.
zh56	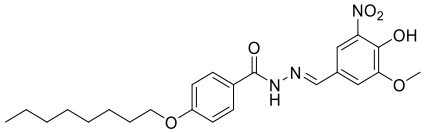 (E)-N'-(4-hydroxy-3-methoxy-5-nitrobenzylidene)-4-(octyloxy) benzohydrazide	^{1}H NMR (400 MHz, dmso) δ 11.82 (s, 1H), 10.90 (s, 1H), 8.39 (s, 1H), 7.89 (d, *J* = 8.7 Hz, 2H), 7.75 (s, 1H), 7.58 (s, 1H), 7.04 (d, *J* = 8.7 Hz, 2H), 4.03 (t, *J* = 6.5 Hz, 2H), 3.96 (s, 3H), 1.89 – 1.61 (m, 2H), 1.48 – 1.14 (m, 8H), 0.86 (t, *J* = 6.6 Hz, 2H).	^{13}C NMR (101 MHz, dmso) δ 162.93, 161.92, 150.20, 145.74, 144.39, 137.56, 129.98, 125.63, 125.54, 116.27, 114.53, 112.40, 68.15, 57.05, 31.68, 29.18, 29.12, 29.00, 25.91, 22.53, 14.41.
zh57	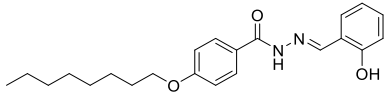 (E)-N'-(2-hydroxybenzylidene)-4-(octyloxy) benzohydrazide	^{1}H NMR (400 MHz, dmso) δ 11.98 (s, 1H), 11.36 (s, 1H), 8.58 (s, 1H), 7.88 (d, *J* = 8.6 Hz, 2H), 7.49 (d, *J* = 7.5 Hz, 1H), 7.25 (d, *J* = 7.3 Hz, 1H), 7.02 (d, *J* = 8.7 Hz, 2H), 6.89 (t, *J* = 8.5 Hz, 2H), 4.00 (t, *J* = 6.5 Hz, 2H), 1.77 – 1.56 (m, 2H), 1.43 – 1.12 (m, 10H), 0.82 (t, *J* = 6.7 Hz, 3H).	^{13}C NMR (101 MHz, dmso) δ 162.61, 162.08, 157.86, 148.15, 131.64, 130.00, 124.93, 119.72, 119.11, 116.82, 114.63, 68.17, 31.68, 29.17, 29.12, 29.00, 25.91, 22.53, 14.41.

zh58	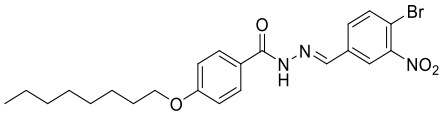 (E)-N'-(4-bromo-3-nitrobenzylidene)-4-(octyloxy) benzohydrazide	^{1}H NMR (400 MHz, dmso) δ 12.00 (s, 1H), 8.43 (s, 1H), 8.28 (s, 1H), 7.99 – 7.74 (m, 3H), 7.01 (d, *J* = 8.6 Hz, 2H), 4.00 (t, *J* = 6.4 Hz, 2H), 1.79 – 1.57 (m, 2H), 1.47 – 1.14 (m, 10H), 0.82 (t, *J* = 6.6 Hz, 2H).	^{13}C NMR (101 MHz, dmso) δ 163.10, 162.09, 150.42, 144.01, 136.07, 135.66, 131.66, 130.13, 125.19, 123.70, 114.58, 114.23, 68.18, 31.69, 29.18, 29.12, 28.99, 25.91, 22.54, 14.42.
zh59	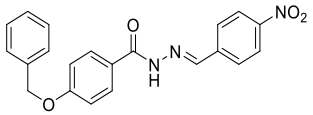 (E)-4-(benzyloxy)-N'-(4-nitrobenzylidene) benzohydrazide	^{1}H NMR (400 MHz, dmso) δ 12.05 (s, 1H), 8.54 (s, 1H), 8.30 (d, *J* = 8.5 Hz, 2H), 7.98 (d, *J* = 7.7 Hz, 2H), 7.93 (d, *J* = 8.4 Hz, 2H), 7.47 (d, *J* = 7.5 Hz, 2H), 7.41 (t, *J* = 7.4 Hz, 2H), 7.35 (d, *J* = 7.1 Hz, 1H), 7.16 (d, *J* = 8.6 Hz, 2H), 5.21 (s, 2H).	^{13}C NMR (101 MHz, dmso) δ 163.16, 161.70, 148.15, 145.01, 141.22, 137.00, 130.15, 128.92, 128.42, 128.30, 128.23, 125.66, 124.51, 115.03, 69.85.
zh60	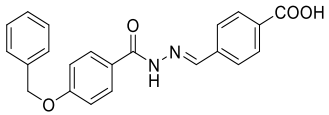 (E)-4-((2-(4-(benzyloxy) benzoyl) hydrazono) methyl) benzoic acid	^{1}H NMR (400 MHz, dmso) δ 12.97 (s, 1H), 11.91 (s, 1H), 8.49 (s, 1H), 8.01 (d, *J* = 8.1 Hz, 2H), 7.92 (d, *J* = 8.5 Hz, 2H), 7.84 (d, *J* = 7.8 Hz, 2H), 7.48 (d, *J* = 7.2 Hz, 2H), 7.41 (t, *J* = 7.4 Hz, 2H), 7.34 (t, *J* = 7.2 Hz, 1H), 7.15 (d, *J* = 8.7 Hz, 2H), 5.20 (s, 2H).	^{13}C NMR (101 MHz, dmso) δ 167.35, 163.04, 161.60, 146.30, 138.92, 137.02, 131.98, 130.22, 130.06, 128.91, 128.41, 128.24, 127.42, 125.84, 115.01, 69.83.
zh61	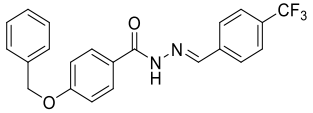 (E)-4-(benzyloxy)-N'-(4-(trifluoromethyl) benzylidene) benzohydrazide	^{1}H NMR (400 MHz, dmso) δ 11.95 (s, 1H), 8.53 (s, 1H), 7.94 (s, 4H), 7.79 (d, *J* = 6.9 Hz, 2H), 7.50 – 7.25 (m, 4H), 7.16 (d, *J* = 7.9 Hz, 2H), 5.20 (s, 2H).	^{13}C NMR (101 MHz, dmso) δ 163.14, 161.64, 145.76, 138.86, 137.01, 130.09, 129.82, 128.88, 128.37, 128.18, 127.95, 126.10, 125.84, 123.17, 114.99, 69.84.

zh62	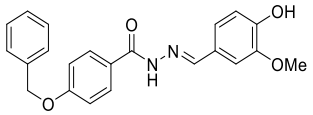 (E)-4-(benzyloxy)-N'-(4-hydroxy-3-methoxybenzylidene) benzohydrazide	^{1}H NMR (400 MHz, dmso) δ 11.59 (s, 1H), 9.57 (s, 1H), 8.33 (s, 1H), 7.90 (d, *J* = 8.8 Hz, 2H), 7.56 – 7.25 (m, 6H), 7.23 – 6.98 (m, 3H), 6.85 (d, *J* = 8.1 Hz, 1H), 5.20 (s, 2H), 3.83 (s, 3H).	^{13}C NMR (101 MHz, dmso) δ 162.75, 161.35, 149.30, 148.45, 148.20, 137.05, 129.87, 128.91, 128.39, 128.21, 126.25, 122.51, 115.83, 114.94, 109.20, 69.79, 55.92.
zh63	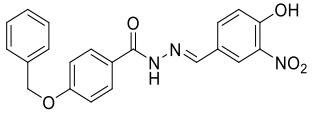 (E)-4-(benzyloxy)-N'-(4-hydroxy-3-nitrobenzylidene) benzohydrazide	^{1}H NMR (400 MHz, dmso) δ 11.77 (s, 1H), 11.41 (s, 1H), 8.36 (s, 1H), 8.16 (s, 1H), 7.87 (t, *J* = 7.4 Hz, 3H), 7.37 (m, 5H), 7.18 (d, *J* = 8.7 Hz, 1H), 7.11 (d, *J* = 8.6 Hz, 2H), 5.17 (s, 2H).	^{13}C NMR (101 MHz, dmso) δ 162.90, 161.50, 153.63, 145.45, 137.51, 137.03, 133.27, 129.98, 128.91, 128.41, 128.23, 126.37, 125.94, 124.28, 120.09, 114.97, 69.81.
zh64	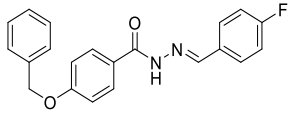 (E)-4-(benzyloxy)-N'-(4-fluorobenzylidene) benzohydrazide	^{1}H NMR (400 MHz, dmso) δ 11.77 (s, 1H), 8.44 (s, 1H), 7.91 (d, *J* = 8.5 Hz, 2H), 7.85 – 7.70 (m, 2H), 7.47 (d, *J* = 7.1 Hz, 2H), 7.41 (t, *J* = 7.3 Hz, 2H), 7.35 (d, *J* = 7.1 Hz, 1H), 7.30 (t, *J* = 8.8 Hz, 2H), 7.15 (d, *J* = 8.6 Hz, 2H), 5.20 (s, 2H).	^{13}C NMR (101 MHz, dmso) δ 164.68, 162.92, 162.22, 161.49, 146.41, 137.04, 131.47, 129.96, 129.61, 129.53, 128.91, 128.40, 128.23, 126.00, 116.43, 116.22, 114.97, 69.81.
zh65	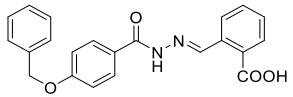 (E)-2-((2-(4-(benzyloxy)benzoyl) hydrazono) methyl) benzoic acid	^{1}H NMR (400 MHz, dmso) δ 13.31 (s, 1H), 11.93 (s, 1H), 9.15 (s, 1H), 8.04 (d, *J* = 7.6 Hz, 1H), 7.98 – 7.74 (m, 3H), 7.60 (d, *J* = 7.5 Hz, 1H), 7.53 – 7.26 (m, 6H), 7.11 (d, *J* = 8.8 Hz, 2H), 5.17 (s, 2H).	^{13}C NMR (101 MHz, dmso) δ 168.54, 163.05, 161.52, 146.30, 137.05, 135.18, 132.39, 130.99, 130.72, 130.09, 129.88, 128.91, 128.40, 128.23, 127.01, 125.94, 114.91, 69.83.

zh66	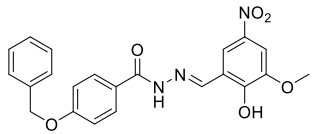 (E)-4-(benzyloxy)-N'-(2-hydroxy-3-methoxy-5-nitrobenzylidene) benzohydrazide	^{1}H NMR (400 MHz, dmso) δ 12.14 (s, 2H), 8.68 (s, 1H), 8.21 (s, 1H), 7.90 (d, *J* = 8.5 Hz, 2H), 7.73 (d, *J* = 2.2 Hz, 1H), 7.44 (d, *J* = 7.1 Hz, 2H), 7.37 (t, *J* = 7.3 Hz, 2H), 7.32 (d, *J* = 7.1 Hz, 1H), 7.12 (d, *J* = 8.7 Hz, 2H), 5.17 (s, 2H), 3.92 (s, 3H).	^{13}C NMR (101 MHz, dmso) δ 162.82, 161.77, 153.25, 148.52, 144.68, 139.88, 136.97, 130.12, 128.91, 128.42, 128.24, 125.20, 119.48, 116.55, 115.05, 107.45, 69.85, 56.80.
zh67	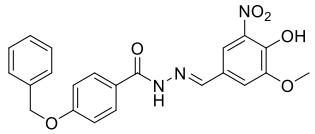 (E)-4-(benzyloxy)-N'-(4-hydroxy-3-methoxy-5-nitrobenzylidene) benzohydrazide	^{1}H NMR (400 MHz, dmso) δ 11.83 (s, 1H), 10.89 (s, 2H), 8.38 (s, 1H), 7.90 (d, *J* = 8.6 Hz, 2H), 7.75 (s, 1H), 7.58 (s, 1H), 7.47 (d, *J* = 7.4 Hz, 2H), 7.41 (t, *J* = 7.4 Hz, 2H), 7.35 (d, *J* = 7.0 Hz, 1H), 7.14 (d, *J* = 8.6 Hz, 2H), 5.20 (s, 2H), 3.95 (s, 3H).	^{13}C NMR (101 MHz, dmso) δ 162.94, 161.50, 150.20, 145.83, 144.41, 137.57, 137.03, 129.99, 128.91, 128.41, 128.22, 125.96, 125.60, 116.31, 114.97, 112.39, 69.80, 57.05.
zh68	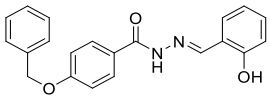 (E)-4-(benzyloxy)-N'-(2-hydroxybenzylidene) benzohydrazide	^{1}H NMR (400 MHz, dmso) δ 11.99 (s, 1H), 11.35 (s, 1H), 8.58 (s, 1H), 7.90 (d, *J* = 8.1 Hz, 2H), 7.50 (d, *J* = 7.5 Hz, 1H), 7.45 (d, *J* = 7.3 Hz, 1H), 7.38 (t, *J* = 7.2 Hz, 1H), 7.32 (d, *J* = 6.9 Hz, 1H), 7.25 (d, *J* = 7.7 Hz, 1H), 7.13 (d, *J* = 8.3 Hz, 2H), 6.90 (d, *J* = 8.7 Hz, 2H), 5.17 (s, 2H).	^{13}C NMR (101 MHz, dmso) δ 162.61, 161.67, 157.85, 148.18, 137.00, 131.67, 130.01, 128.92, 128.43, 128.26, 125.38, 119.74, 119.12, 116.83, 115.06, 69.85.
zh69	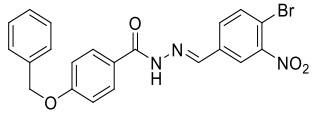 (E)-4-(benzyloxy)-N'-(4-bromo-3-	^{1}H NMR (400 MHz, dmso) δ 12.05 (s, 1H), 8.46 (s, 1H), 8.32 (s, 1H), 7.99 (d, *J* = 8.3 Hz, 1H), 7.96 – 7.82 (m, 3H), 7.48 (d, *J* = 8.0 Hz, 2H), 7.41 (t, *J* = 7.6 Hz, 2H), 7.38 – 7.29 (m, 1H), 7.15	^{13}C NMR (101 MHz, dmso) δ 163.11, 161.67, 150.43, 144.12, 136.99, 136.04, 135.66, 131.67, 130.13, 128.92, 128.42, 128.24, 125.62, 123.73, 115.02, 114.27,

	nitrobenzylidene) benzohydrazide	(d, J = 8.4 Hz, 2H), 5.20 (s, 2H).	69.83.
zh70	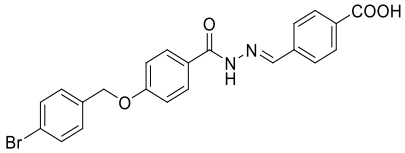 (E)-4-((2-(4-((4-bromobenzyl)oxy)benzoyl) hydrazono) methyl) benzoic acid	^{1}H NMR (400 MHz, dmso) δ 13.07 (s, 1H), 11.90 (s, 1H), 8.48 (s, 1H), 8.00 (d, J = 8.0 Hz, 2H), 7.91 (d, J = 8.5 Hz, 2H), 7.83 (d, J = 7.7 Hz, 2H), 7.60 (d, J = 8.3 Hz, 2H), 7.43 (d, J = 8.3 Hz, 2H), 7.14 (d, J = 8.7 Hz, 2H), 5.19 (s, 2H).	^{13}C NMR (101 MHz, dmso) δ 167.34, 163.00, 161.37, 146.32, 138.91, 136.51, 131.97, 131.84, 130.34, 130.22, 130.07, 127.43, 125.98, 121.53, 115.03, 68.99.
zh71	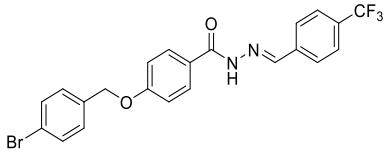 (E)-4-((4-bromobenzyl)oxy)-N'-(4-(trifluoromethyl)benzylidene) benzohydrazide	^{1}H NMR (400 MHz, dmso) δ 11.92 (s, 1H), 8.47 (s, 1H), 7.89 (d, J = 7.9 Hz, 3H), 7.78 (d, J = 8.0 Hz, 2H), 7.57 (d, J = 8.3 Hz, 1H), 7.40 (d, J = 8.3 Hz, 1H), 7.11 (d, J = 8.7 Hz, 1H), 5.16 (s, 2H).	^{13}C NMR (101 MHz, dmso) δ 163.06, 161.40, 145.76, 138.84, 136.50, 131.84, 130.33, 130.09, 127.98, 126.17, 126.13, 125.90, 123.19, 121.53, 115.03, 68.99.
zh72	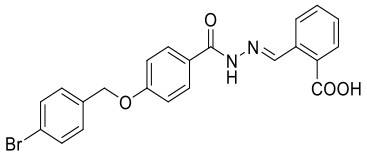 (E)-2-((2-(4-((4-bromobenzyl) oxy) benzoyl) hydrazono) methyl) benzoic acid	^{1}H NMR (400 MHz, dmso) δ 13.12 (s, 1H), 11.97 (s, 1H), 9.18 (s, 1H), 8.07 (d, J = 7.6 Hz, 1H), 8.00 – 7.82 (m, 3H), 7.71 – 7.56 (m, 3H), 7.52 (t, J = 7.4 Hz, 1H), 7.44 (d, J = 8.4 Hz, 2H), 7.13 (d, J = 8.8 Hz, 2H), 5.19 (s, 2H).	^{13}C NMR (101 MHz, dmso) δ 168.54, 163.01, 161.29, 146.32, 136.55, 135.16, 132.39, 131.84, 130.99, 130.72, 130.32, 130.10, 129.88, 127.00, 126.07, 121.52, 114.93, 68.99.

zh73	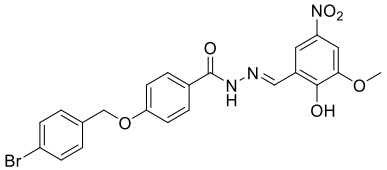 (E)-4-((4-bromobenzyl)oxy)-N'-(2-hydroxy-3-methoxy-5-nitrobenzylidene) benzohydrazide	^{1}H NMR (400 MHz, dmso) δ 12.18 (s, 1H), 12.06 (s, 1H), 8.72 (s, 1H), 8.26 (d, *J* = 1.8 Hz, 1H), 7.94 (d, *J* = 8.5 Hz, 2H), 7.78 (d, *J* = 2.2 Hz, 1H), 7.61 (d, *J* = 8.2 Hz, 2H), 7.44 (d, *J* = 8.2 Hz, 2H), 7.15 (d, *J* = 8.6 Hz, 2H), 5.19 (s, 2H), 3.96 (s, 3H).	^{13}C NMR (101 MHz, dmso) δ 162.81, 161.55, 153.26, 148.54, 144.66, 139.90, 136.48, 131.84, 130.35, 130.14, 125.36, 121.55, 119.53, 116.51, 115.09, 107.50, 69.02, 56.83.
zh74	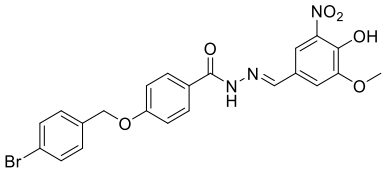 (E)-4-((4-bromobenzyl)oxy)-N'-(4-hydroxy-3-methoxy-5-nitrobenzylidene) benzohydrazide	^{1}H NMR (400 MHz, dmso) δ 11.83 (s, 1H), 10.93 (s, 1H), 8.38 (s, 1H), 7.90 (d, *J* = 8.6 Hz, 2H), 7.75 (s, 1H), 7.60 (t, *J* = 7.2 Hz, 3H), 7.43 (d, *J* = 8.2 Hz, 2H), 7.14 (d, *J* = 8.6 Hz, 2H), 5.19 (s, 2H), 3.95 (s, 3H).	^{13}C NMR (101 MHz, dmso) δ 162.90, 161.27, 150.20, 145.85, 144.40, 137.58, 136.53, 131.84, 130.32, 130.00, 126.10, 125.59, 121.52, 116.31, 115.00, 112.39, 68.96, 57.06.
zh75	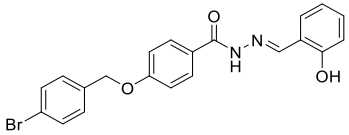 (E)-4-((4-bromobenzyl)oxy)-N'-(2-hydroxybenzylidene) benzohydrazide	^{1}H NMR (400 MHz, dmso) δ 12.02 (s, 1H), 11.37 (s, 1H), 8.62 (s, 1H), 7.93 (d, *J* = 8.6 Hz, 2H), 7.61 (d, *J* = 8.4 Hz, 2H), 7.53 (d, *J* = 7.2 Hz, 1H), 7.44 (d, *J* = 8.3 Hz, 2H), 7.30 (t, *J* = 7.7 Hz, 1H), 7.15 (d, *J* = 8.7 Hz, 2H), 6.99 – 6.85 (m, 2H), 5.19 (s, 2H).	^{13}C NMR (101 MHz, dmso) δ 162.58, 161.45, 157.85, 148.19, 136.49, 131.84, 131.68, 130.35, 130.03, 129.97, 125.52, 121.55, 119.74, 119.11, 116.83, 115.08, 69.01.

zh76	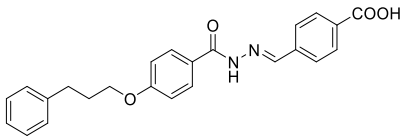 (E)-4-((2-(4-(3-phenylpropoxy) benzoyl) hydrazono) methyl) benzoic acid	^{1}H NMR (400 MHz, dmso) δ 13.10 (s, 1H), 11.90 (s, 1H), 8.49 (s, 1H), 8.01 (d, *J* = 8.1 Hz, 2H), 7.91 (d, *J* = 8.6 Hz, 2H), 7.84 (d, *J* = 7.6 Hz, 2H), 7.35 – 7.13 (m, 5H), 7.07 (d, *J* = 8.7 Hz, 2H), 4.05 (t, *J* = 6.3 Hz, 2H), 2.75 (t, *J* = 7.6 Hz, 2H), 2.17 – 1.90 (m, 2H).	^{13}C NMR (101 MHz, dmso) δ 167.35, 163.05, 161.92, 146.23, 141.70, 138.94, 131.96, 130.22, 130.08, 128.79, 127.42, 126.31, 125.56, 114.62, 67.38, 31.83, 30.70.
zh77	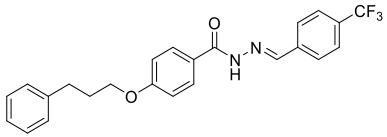 (E)-4-(3-phenylpropoxy)-N'-(4-(trifluoromethyl) benzylidene) benzohydrazide	^{1}H NMR (400 MHz, dmso) δ 11.95 (s, 1H), 8.51 (s, 1H), 7.93 (t, *J* = 8.4 Hz, 3H), 7.81 (d, *J* = 8.1 Hz, 2H), 7.35 – 7.12 (m, 4H), 7.07 (d, *J* = 8.7 Hz, 2H), 4.05 (t, *J* = 6.3 Hz, 2H), 2.90 – 2.61 (m, 2H), 2.19 – 1.86 (m, 2H).	^{13}C NMR (101 MHz, dmso) δ 163.10, 161.95, 145.68, 141.70, 138.87, 130.10, 128.79, 128.78, 127.97, 126.31, 126.17, 126.13, 125.90, 125.50, 123.20, 114.63, 67.39, 31.83, 30.69.
zh78	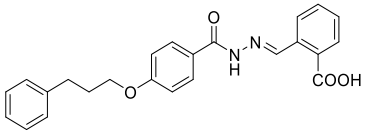 (E)-2-((2-(4-(3-phenylpropoxy) benzoyl) hydrazono) methyl) benzoic acid	^{1}H NMR (400 MHz, dmso) δ 13.35 (s, 1H), 11.97 (s, 1H), 9.19 (s, 1H), 8.08 (d, *J* = 7.5 Hz, 1H), 7.92 (dd, *J* = 13.2, 8.3 Hz, 2H), 7.64 (t, *J* = 7.5 Hz, 1H), 7.52 (t, *J* = 7.5 Hz, 1H), 7.36 – 7.13 (m, 3H), 7.05 (d, *J* = 8.7 Hz, 1H), 4.05 (t, *J* = 6.3 Hz, 1H), 2.85 – 2.63 (m, 1H), 2.23 – 1.90 (m, 1H).	^{13}C NMR (101 MHz, dmso) δ 168.55, 163.07, 161.84, 146.23, 141.71, 135.20, 132.39, 130.98, 130.72, 130.11, 129.86, 128.78, 127.00, 126.30, 125.65, 114.52, 67.37, 31.84, 30.71.

zh79	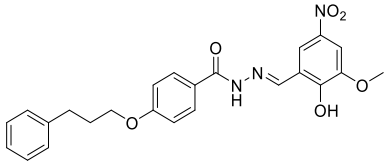 (E)-N'-(2-hydroxy-3-methoxy-5-nitrobenzylidene)-4-(3-phenylpropoxy) benzohydrazide	^{1}H NMR (400 MHz, dmso) δ 12.18 (s, 2H), 8.73 (s, 1H), 8.26 (s, 1H), 7.93 (d, *J* = 8.4 Hz, 2H), 7.78 (d, *J* = 1.8 Hz, 1H), 7.29 (t, *J* = 7.3 Hz, 2H), 7.24 (d, *J* = 7.2 Hz, 2H), 7.19 (t, *J* = 7.2 Hz, 1H), 7.07 (d, *J* = 8.6 Hz, 2H), 4.05 (t, *J* = 6.2 Hz, 2H), 3.96 (s, 3H), 2.75 (t, *J* = 7.6 Hz, 2H), 2.14 – 1.95 (m, 2H).	^{13}C NMR (101 MHz, dmso) δ 162.84, 162.09, 153.25, 148.53, 144.62, 141.70, 139.90, 130.15, 128.79, 128.78, 126.31, 124.92, 119.53, 116.53, 114.68, 107.48, 67.42, 56.83, 31.83, 30.69.
zh80	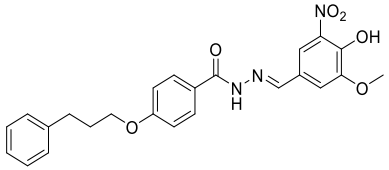 (E)-N'-(4-hydroxy-3-methoxy-5-nitrobenzylidene)-4-(3-phenylpropoxy) benzohydrazide	^{1}H NMR (400 MHz, dmso) δ 11.83 (s, 1H), 10.93 (s, 1H), 8.39 (s, 1H), 7.90 (d, *J* = 8.7 Hz, 2H), 7.75 (s, 1H), 7.58 (s, 1H), 7.34 – 7.14 (m, 5H), 7.05 (d, *J* = 8.7 Hz, 2H), 4.04 (t, *J* = 6.3 Hz, 2H), 3.95 (s, 3H), 2.75 (t, *J* = 7.7 Hz, 2H), 2.10 – 1.83 (m, 2H).	^{13}C NMR (101 MHz, dmso) δ 162.96, 161.83, 150.19, 145.78, 144.40, 141.70, 137.55, 130.02, 128.78, 126.30, 125.68, 125.63, 116.30, 114.57, 112.39, 67.36, 57.04, 31.83, 30.69.
zh81	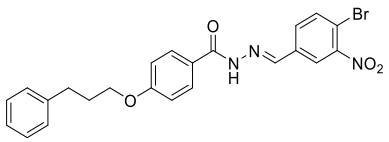 (E)-N'-(4-bromo-3-nitrobenzylidene)-4-(3-phenylpropoxy) benzohydrazide	^{1}H NMR (400 MHz, dmso) δ 12.05 (s, 1H), 8.47 (s, 1H), 8.32 (s, 1H), 8.04 – 7.84 (m, 3H), 7.36 – 7.14 (m, 4H), 7.07 (d, *J* = 8.2 Hz, 2H), 4.05 (t, *J* = 6.1 Hz, 2H), 2.75 (t, *J* = 7.5 Hz, 2H), 2.05 (dd, *J* = 13.9, 6.7 Hz, 2H).	^{13}C NMR (101 MHz, dmso) δ 163.19, 161.98, 160.19, 150.43, 144.02, 141.70, 136.10, 135.65, 131.65, 130.16, 128.78, 126.31, 125.43, 123.69, 114.62, 114.20, 67.40, 31.83, 30.69.
zh82	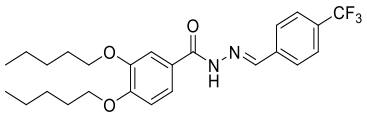	^{1}H NMR (400 MHz, dmso) δ 11.88 (s, 1H), 8.53 (s, 1H), 7.94 (d, *J* = 7.4 Hz, 2H), 7.82 (d, *J* = 8.1 Hz, 2H), 7.56 (d, *J* = 8.6 Hz, 1H), 7.50 (d, *J* = 1.7	^{13}C NMR (101 MHz, dmso) δ 163.11, 152.19, 148.40, 145.74, 138.87, 130.10, 127.96, 126.15, 125.50, 121.75, 113.20,

	(E)-3,4-bis(pentyloxy)-N'-(4-(trifluoromethyl)benzylidene) benzohydrazide	Hz, 1H), 7.09 (d, *J* = 8.5 Hz, 1H), 4.03 (q, *J* = 6.0 Hz, 4H), 1.83 – 1.61 (m, 4H), 1.52 – 1.23 (m, 8H), 0.90 (t, *J* = 7.0 Hz, 6H).	112.81, 68.97, 68.69, 28.87, 28.74, 28.22, 28.19, 22.32, 14.40.
zh83	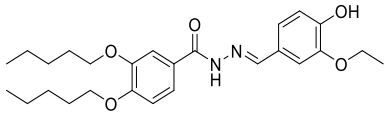 (E)-N'-(3-ethoxy-4-hydroxybenzylidene)-3,4-bis(pentyloxy) benzohydrazide	^{1}H NMR (400 MHz, dmso) δ 11.48 (s, 2H), 9.44 (s, 1H), 8.34 (s, 1H), 7.56 – 7.45 (m, 2H), 7.28 (s, 1H), 7.06 (d, *J* = 8.3 Hz, 2H), 6.85 (d, *J* = 8.1 Hz, 1H), 4.22 – 3.84 (m, 7H), 1.88 – 1.56 (m, 5H), 1.48 – 1.21 (m, 11H), 0.90 (t, *J* = 6.9 Hz, 6H).	^{13}C NMR (101 MHz, dmso) δ 162.72, 149.55, 148.25, 147.58, 126.26, 122.31, 121.55, 118.08, 115.97, 113.28, 112.93, 110.79, 69.04, 68.73, 64.31, 28.89, 28.76, 28.22, 28.18, 22.31, 15.17, 14.37.
zh84	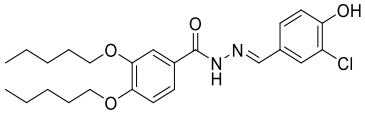 (E)-N'-(3-chloro-4-hydroxybenzylidene)-3,4-bis(pentyloxy) benzohydrazide	^{1}H NMR (400 MHz, dmso) δ 11.62 (s, 2H), 10.73 (s, 1H), 8.33 (s, 1H), 7.70 (s, 1H), 7.58 – 7.41 (m, 3H), 7.06 (t, *J* = 7.7 Hz, 2H), 4.17 – 3.91 (m, 4H), 1.85 – 1.61 (m, 4H), 1.54 – 1.21 (m, 8H), 0.90 (t, *J* = 7.0 Hz, 6H).	^{13}C NMR (101 MHz, dmso) δ 162.82, 155.11, 151.97, 148.37, 146.38, 128.64, 127.55, 127.19, 125.82, 121.56, 120.68, 117.26, 113.16, 112.79, 68.95, 68.67, 28.89, 28.75, 28.23, 28.19, 22.34, 22.33, 14.40.
zh85	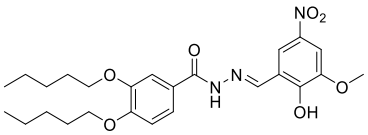 (E)-N'-(2-hydroxy-3-methoxy-5-nitrobenzylidene)-3,4-bis(pentyloxy) benzohydrazide	^{1}H NMR (400 MHz, dmso) δ 12.11 (s, 2H), 8.74 (s, 1H), 8.26 (s, 1H), 7.79 (d, *J* = 2.4 Hz, 1H), 7.57 (d, *J* = 8.1 Hz, 1H), 7.51 (s, 1H), 7.09 (d, *J* = 8.5 Hz, 1H), 4.03 (q, *J* = 6.1 Hz, 4H), 3.96 (s, 3H), 1.92 – 1.61 (m, 4H), 1.52 – 1.21 (m, 8H), 0.90 (t, *J* = 7.0 Hz, 6H).	^{13}C NMR (101 MHz, dmso) δ 162.89, 153.23, 152.34, 148.56, 148.42, 144.53, 139.92, 124.90, 121.83, 119.58, 116.43, 113.15, 112.82, 107.50, 68.96, 68.69, 56.84, 28.86, 28.73, 28.22, 28.18, 22.34, 22.32, 14.41.

zh86	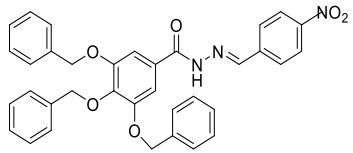 (E)-3,4,5-tris(benzyloxy)-N'-(4-nitrobenzylidene) benzohydrazide	^{1}H NMR (400 MHz, dmso) δ 11.79 (s, 1H), 11.51 (s, 1H), 8.44 (s, 1H), 8.21 (s, 1H), 7.94 (d, *J* = 8.1 Hz, 1H), 7.58 – 7.09 (m, 18H), 5.21 (s, 4H), 5.03 (s, 2H).	^{13}C NMR (101 MHz, dmso) δ 162.86, 153.75, 152.51, 146.13, 140.54, 137.81, 137.55, 137.19, 133.35, 128.89, 128.62, 128.51, 128.40, 128.33, 128.13, 126.23, 124.34, 120.13, 107.33, 74.71, 70.90.
zh87	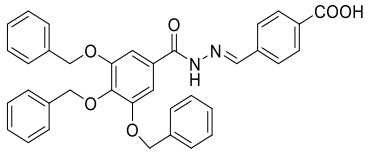 (E)-4-((2-(3,4,5-tris(benzyloxy) benzoyl) hydrazono) methyl) benzoic acid	^{1}H NMR (400 MHz, dmso) δ 13.13 (s, 1H), 11.93 (s, 1H), 8.56 (s, 1H), 8.04 (d, *J* = 7.5 Hz, 2H), 7.87 (d, *J* = 7.2 Hz, 2H), 7.61 – 7.01 (m, 17H), 5.22 (s, 4H), 5.04 (s, 2H).	^{13}C NMR (101 MHz, dmso) δ 167.36, 163.03, 152.55, 146.96, 140.66, 138.77, 137.82, 137.19, 132.18, 130.25, 128.89, 128.63, 128.51, 128.40, 128.32, 128.14, 127.52, 109.99, 107.41, 74.74, 70.93.
zh88	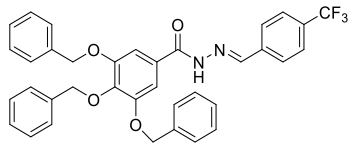 (E)-3,4,5-tris(benzyloxy)-N'-(4-(trifluoromethyl) benzylidene) benzohydrazide	^{1}H NMR (400 MHz, dmso) δ 11.94 (s, 1H), 8.56 (s, 1H), 7.96 (d, *J* = 7.7 Hz, 2H), 7.83 (d, *J* = 7.9 Hz, 2H), 7.61 – 7.17 (m, 16H), 5.22 (s, 4H), 5.04 (s, 2H).	^{13}C NMR (101 MHz, dmso) δ 163.05, 152.54, 146.39, 140.68, 138.71, 137.81, 137.19, 128.89, 128.78, 128.62, 128.51, 128.40, 128.33, 128.13, 128.07, 126.21, 126.17, 125.89, 123.18, 107.43, 74.73, 70.93.
zh89	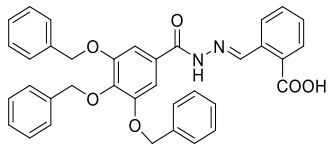	^{1}H NMR (400 MHz, dmso) δ 13.39 (s, 1H), 11.97 (s, 1H), 9.23 (s, 1H), 8.09 (d, *J* = 7.6 Hz, 1H), 7.92 (d, *J* = 7.7 Hz, 1H), 7.76 – 7.08 (m, 17H), 5.22 (s, 4H), 5.04 (s, 2H).	^{13}C NMR (101 MHz, dmso) δ 168.55, 163.02, 152.50, 146.80, 140.57, 137.84, 137.23, 135.10, 132.45, 131.03, 130.76, 130.04, 128.88, 128.62, 128.51, 128.39,

	(E)-2-((2-(3,4,5-tris(benzyloxy) benzoyl) hydrazono) methyl) benzoic acid		128.32, 128.15, 127.17, 107.46, 74.72, 70.93.
zh90	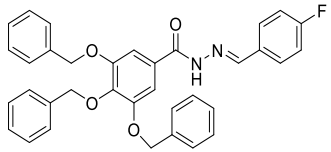 (E)-3,4,5-tris(benzyloxy)-N'-(4-fluorobenzylidene) benzohydrazide	^{1}H NMR (400 MHz, dmso) δ 11.77 (s, 1H), 8.49 (s, 1H), 7.94 – 7.73 (m, 2H), 7.60 – 7.14 (m, 19H), 5.22 (s, 4H), 5.04 (s, 2H).	^{13}C NMR (101 MHz, dmso) δ 164.79, 162.85, 162.33, 152.52, 147.06, 140.53, 137.82, 137.20, 131.36, 131.33, 129.72, 129.64, 128.97, 128.89, 128.62, 128.51, 128.40, 128.32, 128.13, 116.49, 116.27, 107.31, 74.72, 70.89.
zh91	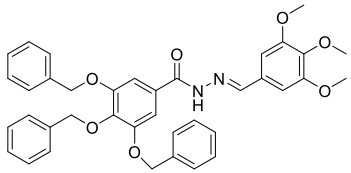 (E)-3,4,5-tris(benzyloxy)-N'-(3,4,5-trimethoxybenzylidene) benzohydrazide	^{1}H NMR (400 MHz, dmso) δ 11.72 (s, 1H), 8.43 (s, 1H), 7.40 (ddd, *J* = 50.0, 33.3, 5.9 Hz, 15H), 7.04 (s, 2H), 5.21 (s, 4H), 5.03 (s, 2H), 3.84 (s, 6H), 3.72 (s, 3H).	^{13}C NMR (101 MHz, dmso) δ 162.87, 153.64, 152.50, 148.39, 140.50, 139.67, 137.82, 137.20, 130.21, 129.09, 128.89, 128.63, 128.52, 128.40, 128.33, 128.12, 107.32, 104.71, 74.72, 70.89, 60.56, 56.38.

Appendix II. Calculated formula weight (F.W.), Calculated molecular weight for protonated compounds (MH)+, and experimental results by High Performance mass spectrum (HPMS) (Found)

Table II-1. Calculated F.W., $(MH)^+$ and HPMS of 2-cyano-3-phenylacrylic acid derivatives (Chapter 3)

V	Possible Protonated Structures	Calculated F.W.	Calculated $(MH)^+$	Found
v01	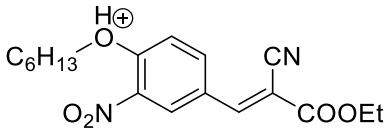 Chemical Formula: $C_{18}H_{23}N_2O_5^+$ Exact Mass: 347.1601 Molecular Weight: 347.3905	346.1529	347.1601	**347.1597**
v02	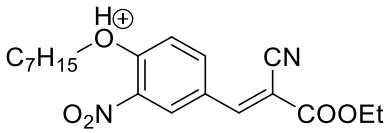 Chemical Formula: $C_{19}H_{25}N_2O_5^+$ Exact Mass: 361.1758 Molecular Weight: 361.4175	360.1685	361.1758	**361.1758**
v03	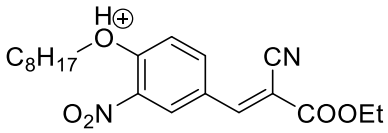 Chemical Formula: $C_{20}H_{27}N_2O_5^+$ Exact Mass: 375.1914 Molecular Weight: 375.4445	374.1842	375.1914	**375.1909**
v04	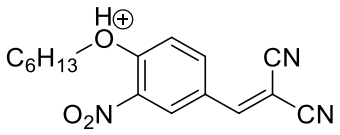 Chemical Formula: $C_{16}H_{18}N_3O_3^+$ Exact Mass: 300.1343 Molecular Weight: 300.3375	299.1270	300.1343	**300.1340**

v05	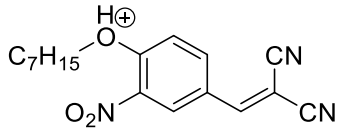 Chemical Formula: $C_{17}H_{20}N_3O_3^+$ Exact Mass: 314.1499 Molecular Weight: 314.3645	313.1426	314.1499	**314.1489**
v06	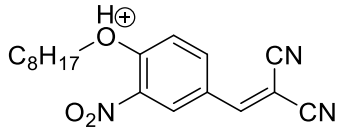 Chemical Formula: $C_{18}H_{22}N_3O_3^+$ Exact Mass: 328.1656 Molecular Weight: 328.3915	327.1583	328.1656	**328.1650**
v07	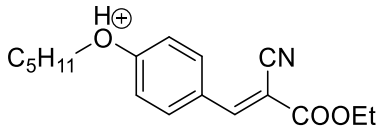 Chemical Formula: $C_{17}H_{22}NO_3^+$ Exact Mass: 288.1594 Molecular Weight: 288.3665	287.1521	288.1594	**288.1593**
v08	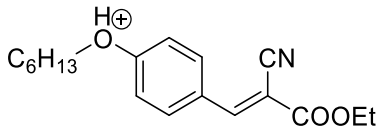 Chemical Formula: $C_{18}H_{24}NO_3^+$ Exact Mass: 302.1751 Molecular Weight: 302.3935	301.1678	302.1751	**302.1757**
v9	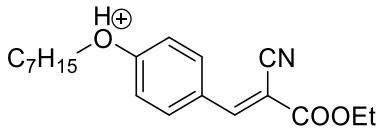 Chemical Formula: $C_{19}H_{26}NO_3^+$ Exact Mass: 316.1907 Molecular Weight: 316.4205	315.1834	316.1907	**316.1911**
v10	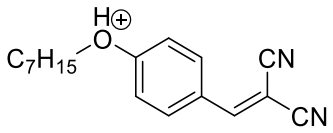 Chemical Formula: $C_{17}H_{21}N_2O^+$ Exact Mass: 269.1648 Molecular Weight: 269.3675	268.1576	269.1648	**269.1651**

v11	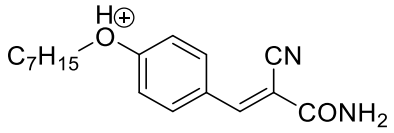 Chemical Formula: $C_{17}H_{23}N_2O_2^+$ Exact Mass: 287.1754 Molecular Weight: 287.3825	286.1681	287.1754	**287.1759**
v12	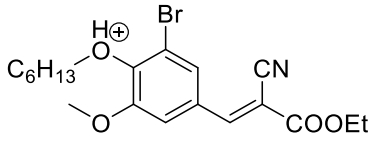 Chemical Formula: $C_{19}H_{25}BrNO_4^+$ Exact Mass: 410.0961 Molecular Weight: 411.3155	409.0889	410.0961	**410.0968**
v13	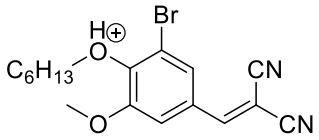 Chemical Formula: $C_{17}H_{20}BrN_2O_2^+$ Exact Mass: 363.0703 Molecular Weight: 364.2625	362.0630	363.0703	**363.0711**
v14	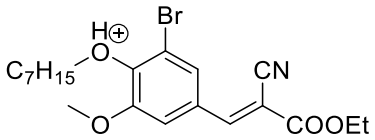 Chemical Formula: $C_{20}H_{27}BrNO_4^+$ Exact Mass: 424.1118 Molecular Weight: 425.3425	423.1040	424.1118	**424.1112**
v15	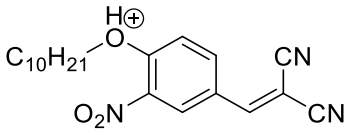 Chemical Formula: $C_{20}H_{26}N_3O_3^+$ Exact Mass: 356.1969 Molecular Weight: 356.4455	355.1890	356.1969	**356.1964**
v16	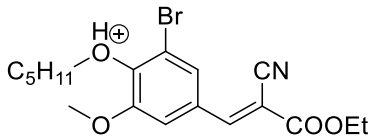 Chemical Formula: $C_{18}H_{23}BrNO_4^+$ Exact Mass: 396.0805 Molecular Weight: 397.2885	395.0732	396.0805	**396.0804**

v17	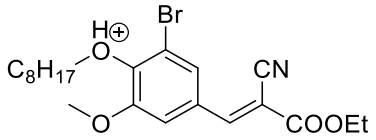 Chemical Formula: $C_{21}H_{29}BrNO_4^+$ Exact Mass: 438.1274 Molecular Weight: 439.3695	437.1202	438.1274	**438.1270**
v18	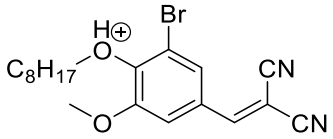 Chemical Formula: $C_{19}H_{24}BrN_2O_2^+$ Exact Mass: 391.1016 Molecular Weight: 392.3165	390.0943	391.1016	**391.1011**
v19	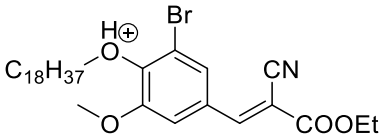 Chemical Formula: $C_{31}H_{49}BrNO_4^+$ Exact Mass: 578.2839 Molecular Weight: 579.6395	577.2767	578.2839	**578.2838**
v20	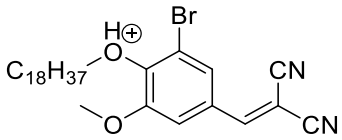 Chemical Formula: $C_{29}H_{44}BrN_2O_2^+$ Exact Mass: 531.2581 Molecular Weight: 532.5865	530.2508	531.2581	**531.2580**
v21	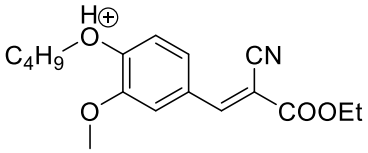 Chemical Formula: $C_{17}H_{22}NO_4^+$ Exact Mass: 304.1543 Molecular Weight: 304.3655	303.1471	304.1543	**304.1553**
v22	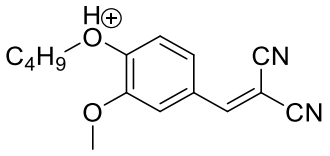 Chemical Formula: $C_{15}H_{17}N_2O_2^+$ Exact Mass: 257.1285 Molecular Weight: 257.3125	256.1212	257.1285	**257.1298**

v23	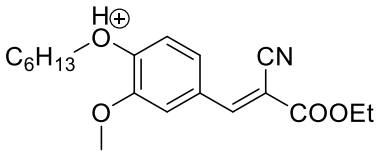 Chemical Formula: $C_{19}H_{26}NO_4^+$ Exact Mass: 332.1856 Molecular Weight: 332.4195	331.1784	332.1856	**332.1871**
v24	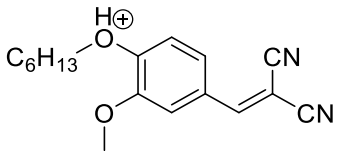 Chemical Formula: $C_{17}H_{21}N_2O_2^+$ Exact Mass: 285.1598 Molecular Weight: 285.3665	284.1525	285.1598	**285.1604**
v25	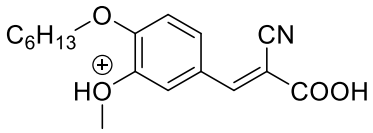 Chemical Formula: $C_{17}H_{22}NO_4^+$ Exact Mass: 304.1543 Molecular Weight: 304.3655	303.1471	304.1543	**304.1550**
v26	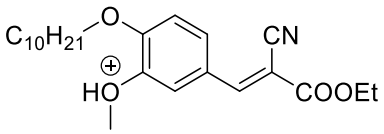 Chemical Formula: $C_{23}H_{34}NO_4^+$ Exact Mass: 388.2482 Molecular Weight: 388.5275	387.2410	388.2482	**388.2498**
v27	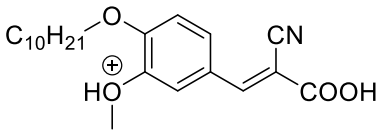 Chemical Formula: $C_{21}H_{30}NO_4^+$ Exact Mass: 360.2169 Molecular Weight: 360.4735	359.2097	360.2169	**360.2177**
v28	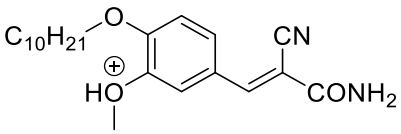 Chemical Formula: $C_{21}H_{31}N_2O_3^+$ Exact Mass: 359.2329 Molecular Weight: 359.4895	358.2256	359.2329	**359.2328**

v29	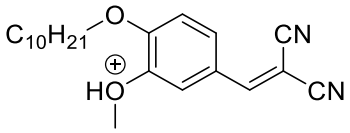 Chemical Formula: $C_{21}H_{29}N_2O_2^+$ Exact Mass: 341.2224 Molecular Weight: 341.4745	340.2151	341.2224	**341.2222**
v30	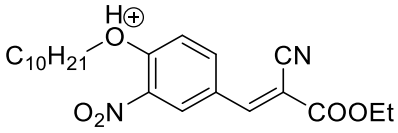 Chemical Formula: $C_{22}H_{31}N_2O_5^+$ Exact Mass: 403.2227 Molecular Weight: 403.4985	402.2155	403.2227	**403.2237**
v31	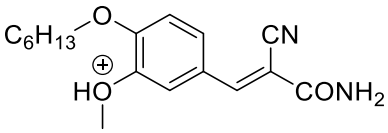 Chemical Formula: $C_{17}H_{23}N_2O_3^+$ Exact Mass: 303.1703 Molecular Weight: 303.3815	302.1630	303.1703	**303.1703**
v32	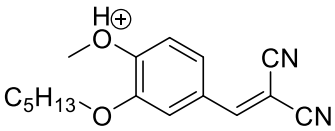 Chemical Formula: $C_{16}H_{21}N_2O_2^+$ Exact Mass: 273.1598 Molecular Weight: 273.3555	272.1525	273.1598	**273.1604**
v33	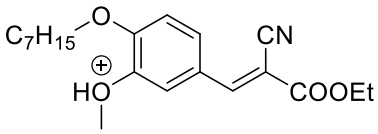 Chemical Formula: $C_{20}H_{28}NO_4^+$ Exact Mass: 346.2013 Molecular Weight: 346.4465	345.1940	346.2013	**346.2021**
v34	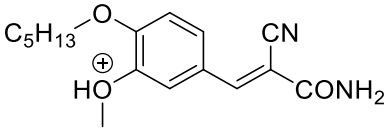 Chemical Formula: $C_{16}H_{23}N_2O_3^+$ Exact Mass: 291.1703 Molecular Weight: 291.3705	290.1630	291.1703	**291.1711**

v35	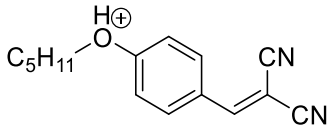 Chemical Formula: $C_{15}H_{17}N_2O^+$ Exact Mass: 241.1335 Molecular Weight: 241.3135	240.1263	241.1335	**241.1343**
v36	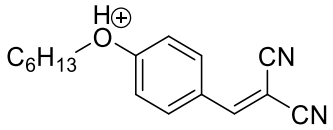 Chemical Formula: $C_{16}H_{19}N_2O^+$ Exact Mass: 255.1492 Molecular Weight: 255.3405	254.1419	255.1482	**255.1490**
v37	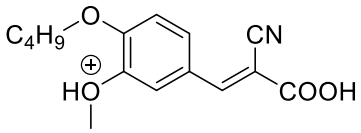 Chemical Formula: $C_{15}H_{18}NO_4^+$ Exact Mass: 276.1230 Molecular Weight: 276.3115	275.1158	276.1230	**276.1228**
v38	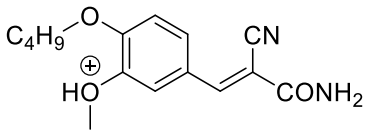 Chemical Formula: $C_{15}H_{19}N_2O_3^+$ Exact Mass: 275.1390 Molecular Weight: 275.3275	274.1317	275.1390	**275.1383**
v39	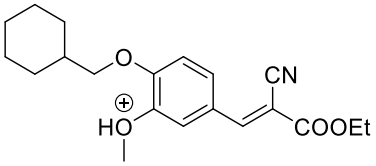 Chemical Formula: $C_{20}H_{26}NO_4^+$ Exact Mass: 344.1856 Molecular Weight: 344.4305	343.1784	344.1856	**344.1856**
v40	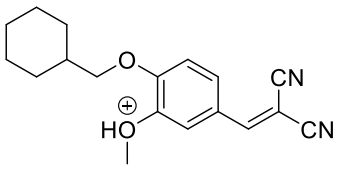 Chemical Formula: $C_{18}H_{21}N_2O_2^+$ Exact Mass: 297.1598 Molecular Weight: 297.3775	296.1525	297.1598	**297.1607**

v41	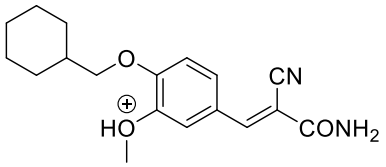 Chemical Formula: $C_{18}H_{23}N_2O_3^+$ Exact Mass: 315.1703 Molecular Weight: 315.3925	314.1630	315.1703	**315.1703**
v42	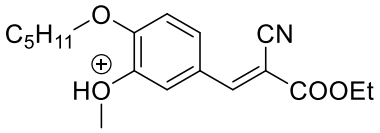 Chemical Formula: $C_{18}H_{24}NO_4^+$ Exact Mass: 318.1700 Molecular Weight: 318.3925	317.1627	318.1700	**318.1696**
v43	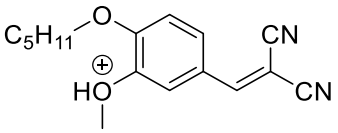 Chemical Formula: $C_{16}H_{19}N_2O_2^+$ Exact Mass: 271.1441 Molecular Weight: 271.3395	270.1368	271.1441	**271.1437**
v44	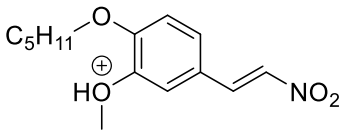 Chemical Formula: $C_{14}H_{20}NO_4^+$ Exact Mass: 266.1387 Molecular Weight: 266.3165	265.1314	266.1387	**266.1378**
v45	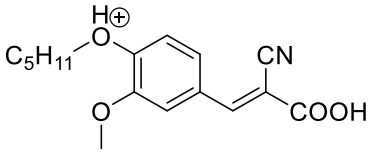 Chemical Formula: $C_{16}H_{20}NO_4^+$ Exact Mass: 290.1387 Molecular Weight: 290.3385	289.1314	290.1387	**290.1388**
v46	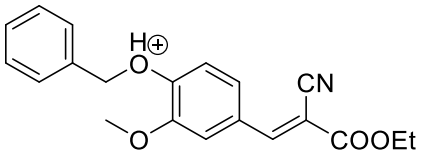 Chemical Formula: $C_{20}H_{20}NO_4^+$ Exact Mass: 338.1387 Molecular Weight: 338.3825	337.1314	338.1387	**338.1389**

v47	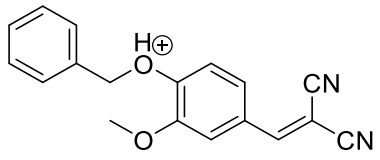 Chemical Formula: $C_{18}H_{15}N_2O_2^+$ Exact Mass: 291.1128 Molecular Weight: 291.3295	290.1055	291.1128	**291.1132**
v48	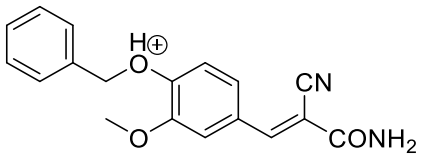 Chemical Formula: $C_{18}H_{17}N_2O_3^+$ Exact Mass: 309.1234 Molecular Weight: 309.3445	308.1161	309.1234	**309.1241**
v49	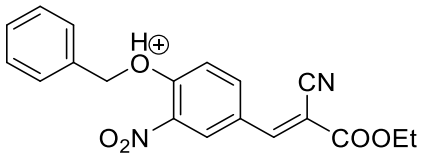 Chemical Formula: $C_{19}H_{17}N_2O_5^+$ Exact Mass: 353.1132 Molecular Weight: 353.3535	352.1059	353.1132	**353.1140**
v50	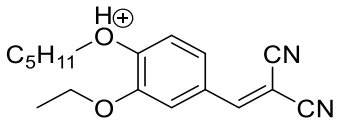 Chemical Formula: $C_{17}H_{21}N_2O_2^+$ Exact Mass: 285.1598 Molecular Weight: 285.3665	284.1525	285.1598	**285.1602**
v51	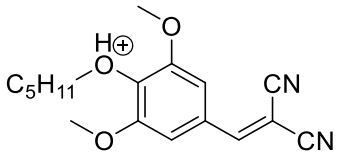 Chemical Formula: $C_{17}H_{21}N_2O_3^+$ Exact Mass: 301.1547 Molecular Weight: 301.3655	300.1474	301.1547	**301.1550**
v52	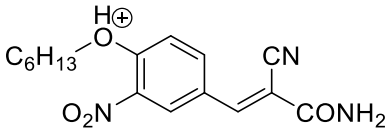 Chemical Formula: $C_{16}H_{20}N_3O_4^+$ Exact Mass: 318.1448 Molecular Weight: 318.3525	317.1376	318.1448	**318.1454**

v53	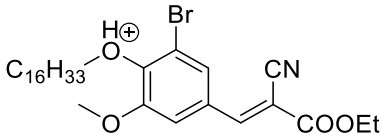 Chemical Formula: $C_{29}H_{45}BrNO_4^+$ Exact Mass: 550.2526 Molecular Weight: 551.5855	549.2454	550.2526	**550.2512**
v54	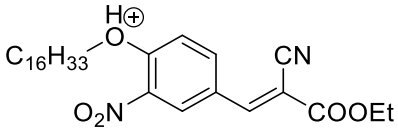 Chemical Formula: $C_{28}H_{43}N_2O_5^+$ Exact Mass: 487.3166 Molecular Weight: 487.6605	486.3094	487.3166	**487.3164**
v55	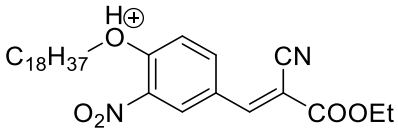 Chemical Formula: $C_{30}H_{47}N_2O_5^+$ Exact Mass: 515.3479 Molecular Weight: 515.7145	514.3407	515.3479	**515.3479**
v56	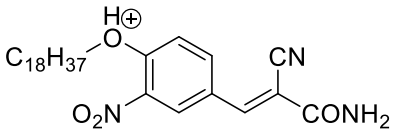 Chemical Formula: $C_{28}H_{44}N_3O_4^+$ Exact Mass: 486.3326 Molecular Weight: 486.6765	485.3254	486.3326	**486.3233**
v57	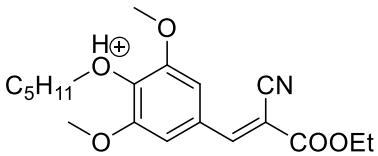 Chemical Formula: $C_{19}H_{26}NO_5^+$ Exact Mass: 348.1805 Molecular Weight: 348.4185	347.1733	348.1805	**348.1811**
v58	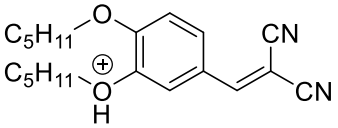 Chemical Formula: $C_{20}H_{27}N_2O_2^+$ Exact Mass: 327.2067 Molecular Weight: 327.4475	326.1994	327.2067	**327.2065**

Table II-2. Calculated F.W., $(MH)^+$ and HPMS of 1, 3-Diphenylpyrazole derivatives (Chapter 4)

	Structures of Pyrazole compounds.	Calculated F.W.	Calculated $(MH)^+$	Found
py01	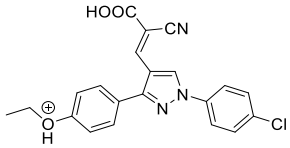 Chemical Formula: $C_{21}H_{17}ClN_3O_3^+$ Exact Mass: 394.0953 Molecular Weight: 394.8345	393.0880	394.0953	**394.0926**
py02	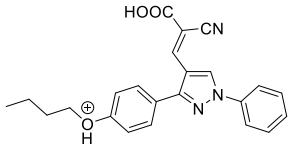 Chemical Formula: $C_{23}H_{22}N_3O_3^+$ Exact Mass: 388.1656 Molecular Weight: 388.4465	387.1583	388.1656	**388.1641**
py03	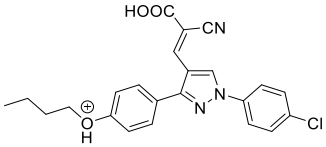 Chemical Formula: $C_{23}H_{21}ClN_3O_3^+$ Exact Mass: 422.1266 Molecular Weight: 422.8885	421.1193	422.1266	**422.1235**
py04	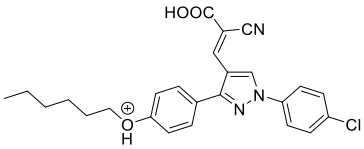 Chemical Formula: $C_{25}H_{25}ClN_3O_3^+$ Exact Mass: 450.1579 Molecular Weight: 450.9425	449.1506	450.1579	**450.1558**
py05	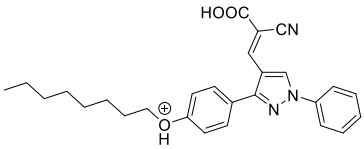 Chemical Formula: $C_{27}H_{30}N_3O_3^+$ Exact Mass: 444.2282 Molecular Weight: 444.5545	443.2209	444.2282	**444.2252**
py06	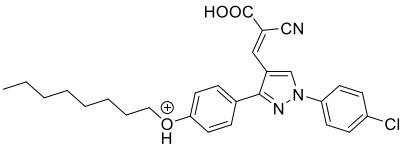 Chemical Formula: $C_{27}H_{29}ClN_3O_3^+$ Exact Mass: 478.1892 Molecular Weight: 478.9965	477.1819	478.1892	**478.1861**

py07	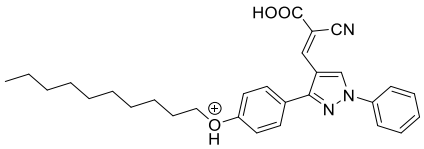 Chemical Formula: $C_{29}H_{34}N_3O_3^+$ Exact Mass: 472.2595 Molecular Weight: 472.6085	471.2522	472.2595	**472.2576**
py08	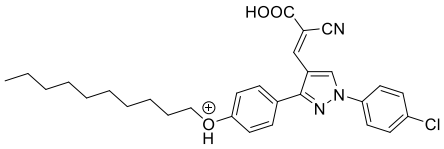 Chemical Formula: $C_{29}H_{33}ClN_3O_3^+$ Exact Mass: 506.2205 Molecular Weight: 507.0505	505.2132	506.2205	**506.2177**
py09	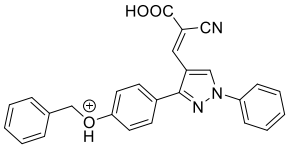 Chemical Formula: $C_{26}H_{20}N_3O_3^+$ Exact Mass: 422.1499 Molecular Weight: 422.4635	421.1426	422.1499	**422.1486**
py10	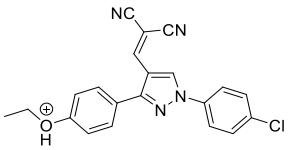 Chemical Formula: $C_{21}H_{16}ClN_4O^+$ Exact Mass: 375.1007 Molecular Weight: 375.8355	374.0934	375.1007	**377.0881**
py11	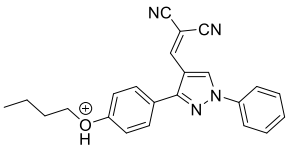 Chemical Formula: $C_{23}H_{21}N_4O^+$ Exact Mass: 369.1710 Molecular Weight: 369.4475	368.1637	369.1710	**369.1681**
py12	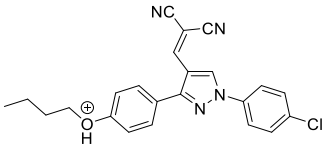 Chemical Formula: $C_{23}H_{20}ClN_4O^+$ Exact Mass: 403.1320 Molecular Weight: 403.8895	402.1427	403.1320	**403.1326**
py13	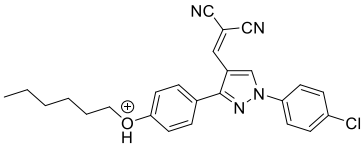 Chemical Formula: $C_{25}H_{24}ClN_4O^+$ Exact Mass: 431.1633 Molecular Weight: 431.9435	430.1560	431.1633	**431.1640**

py14	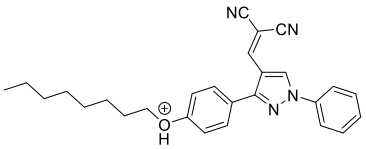 Chemical Formula: $C_{27}H_{29}N_4O^+$ Exact Mass: 425.2336 Molecular Weight: 425.5555	424.2263	425.2336	**425.2339**
py15	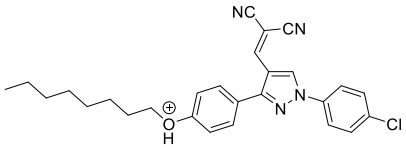 Chemical Formula: $C_{27}H_{28}ClN_4O^+$ Exact Mass: 459.1946 Molecular Weight: 459.9975	458.1873	459.1946	**459.1956**
py16	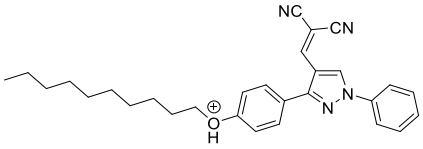 Chemical Formula: $C_{29}H_{33}N_4O^+$ Exact Mass: 453.2649 Molecular Weight: 453.6095	452.2576	453.2649	**453.2655**
py17	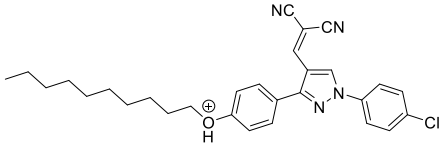 Chemical Formula: $C_{29}H_{32}ClN_4O^+$ Exact Mass: 487.2259 Molecular Weight: 488.0515	486.2186	487.2259	**487.2265**
py18	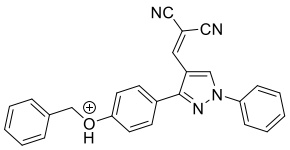 Chemical Formula: $C_{26}H_{19}N_4O^+$ Exact Mass: 403.1553 Molecular Weight: 403.4645	402.1481	403.1553	**403.1553**
py19	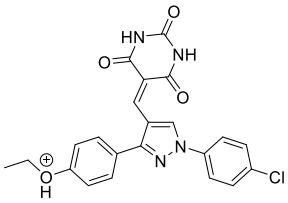 Chemical Formula: $C_{22}H_{18}ClN_4O_4^+$ Exact Mass: 437.1011 Molecular Weight: 437.8595	436.0938	437.1011	**437.1001**

py20	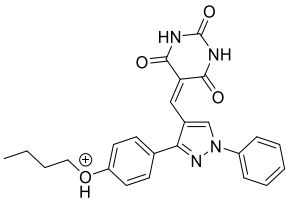 Chemical Formula: $C_{24}H_{23}N_4O_4^+$ Exact Mass: 431.1714 Molecular Weight: 431.4715	430.1641	431.1714	**431.1715**
py21	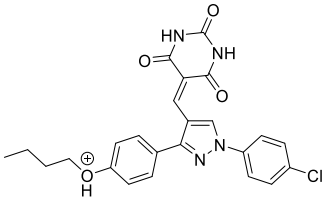 Chemical Formula: $C_{24}H_{22}ClN_4O_4^+$ Exact Mass: 465.1324 Molecular Weight: 465.9135	464.1251	465.1324	**465.1315**
py22	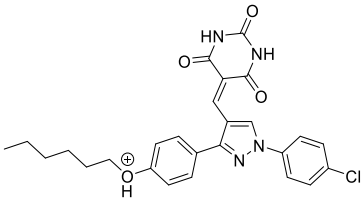 Chemical Formula: $C_{26}H_{26}ClN_4O_4^+$ Exact Mass: 493.1637 Molecular Weight: 493.9675	492.1564	439.1637	**439.1632**
py23	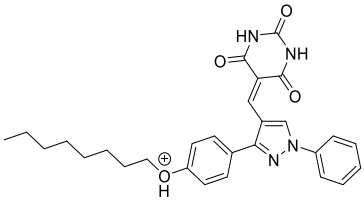 Chemical Formula: $C_{28}H_{31}N_4O_4^+$ Exact Mass: 487.2340 Molecular Weight: 487.5795	486.2267	487.2340	**487.2333**
py24	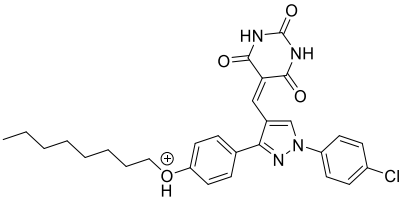 Chemical Formula: $C_{28}H_{30}ClN_4O_4^+$ Exact Mass: 521.1950 Molecular Weight: 522.0215	520.1877	521.1950	**521.1949**
py25	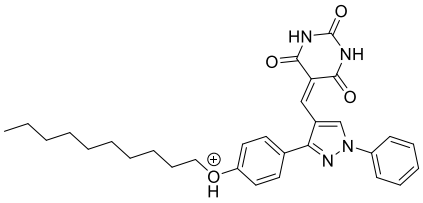 Chemical Formula: $C_{30}H_{35}N_4O_4^+$ Exact Mass: 515.2653 Molecular Weight: 515.6335	514.2580	515.2653	**515.2645**

py26	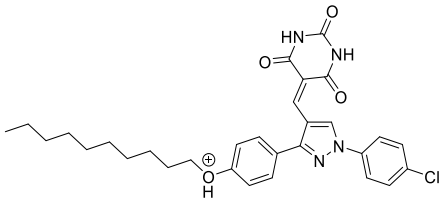 Chemical Formula: $C_{30}H_{34}ClN_4O_4^+$ Exact Mass: 549.2263 Molecular Weight: 550.0755	548.2190	549.2263	**549.2259**
py27	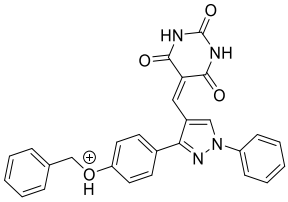 Chemical Formula: $C_{27}H_{21}N_4O_4^+$ Exact Mass: 465.1557 Molecular Weight: 465.4885	464.1485	465.1557	**465.1553**
py28	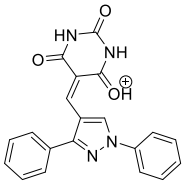 Chemical Formula: $C_{20}H_{15}N_4O_3^+$ Exact Mass: 359.1139 Molecular Weight: 359.3645	358.1066	359.1139	**359.1134**
py29	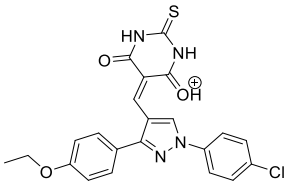 Chemical Formula: $C_{22}H_{18}ClN_4O_3S^+$ Exact Mass: 453.0783 Molecular Weight: 453.9205	452.0710	453.0783	**453.0781**
py30	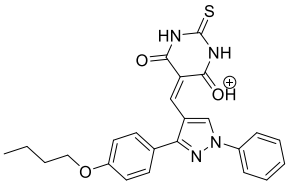 Chemical Formula: $C_{24}H_{23}N_4O_3S^+$ Exact Mass: 447.1485 Molecular Weight: 447.5325	446.1413	447.1485	**447.1478**
py31	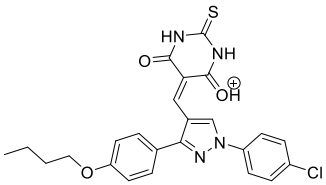 Chemical Formula: $C_{24}H_{22}ClN_4O_3S^+$ Exact Mass: 481.1096 Molecular Weight: 481.9745	480.1023	481.1096	**481.1095**

py32	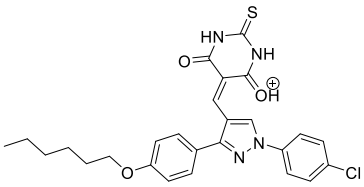 Chemical Formula: $C_{26}H_{26}ClN_4O_3S^+$ Exact Mass: 509.1409 Molecular Weight: 510.0285	508.1336	509.1409	**509.1403**
py33	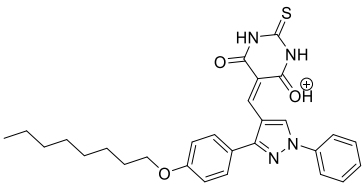 Chemical Formula: $C_{28}H_{31}N_4O_3S^+$ Exact Mass: 503.2111 Molecular Weight: 503.6405	502.2039	503.2111	**503.2107**
py34	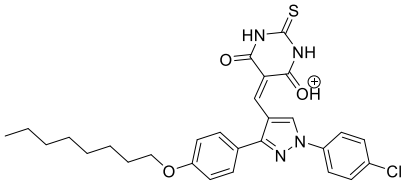 Chemical Formula: $C_{28}H_{30}ClN_4O_3S^+$ Exact Mass: 537.1722 Molecular Weight: 538.0825	536.1649	537.1722	**537.1714**
py35	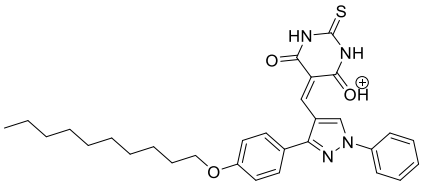 Chemical Formula: $C_{30}H_{35}N_4O_3S^+$ Exact Mass: 531.2424 Molecular Weight: 531.6945	530.2352	531.2424	**531.2419**
py36	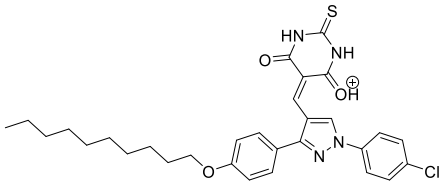 Chemical Formula: $C_{30}H_{34}ClN_4O_3S^+$ Exact Mass: 565.2035 Molecular Weight: 566.1365	564.1962	565.2035	**565.2029**
py37	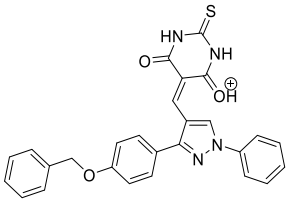 Chemical Formula: $C_{27}H_{21}N_4O_3S^+$ Exact Mass: 481.1329 Molecular Weight: 481.5495	480.1256	481.1329	**481.1339**

py38	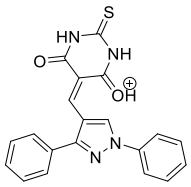 Chemical Formula: $C_{20}H_{15}N_4O_2S^+$ Exact Mass: 375.0910 Molecular Weight: 375.4255	374.0837	375.0910	**379.0907**
py39	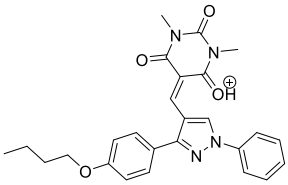 Chemical Formula: $C_{26}H_{27}N_4O_4^+$ Exact Mass: 459.2027 Molecular Weight: 459.5255	458.1954	459.2027	**459.2026**
py40	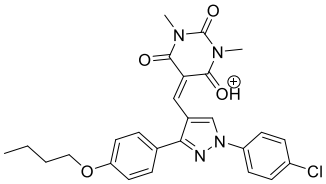 Chemical Formula: $C_{26}H_{26}ClN_4O_4^+$ Exact Mass: 493.1637 Molecular Weight: 493.9675	492.1564	493.1637	**493.1651**
py41	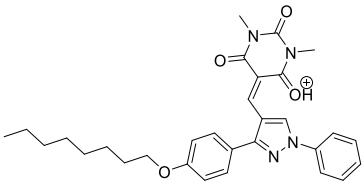 Chemical Formula: $C_{30}H_{35}N_4O_4^+$ Exact Mass: 515.2653 Molecular Weight: 515.6335	514.2580	515.2653	**515.2655**
py42	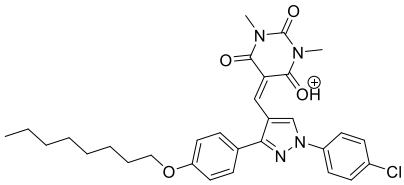 Chemical Formula: $C_{30}H_{34}ClN_4O_4^+$ Exact Mass: 549.2263 Molecular Weight: 550.0755	548.2190	549.2263	**549.2252**
py43	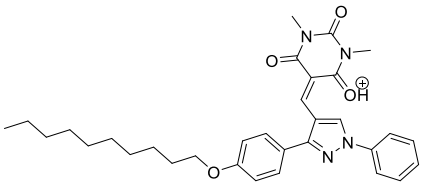 Chemical Formula: $C_{32}H_{39}N_4O_4^+$ Exact Mass: 543.2966 Molecular Weight: 543.6875	542.2893	543.2966	**543.2964**

py44	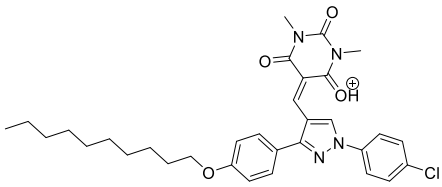 Chemical Formula: $C_{32}H_{38}ClN_4O_4^+$ Exact Mass: 577.2576 Molecular Weight: 578.1295	576.2503	577.2576	**577.2578**
py45	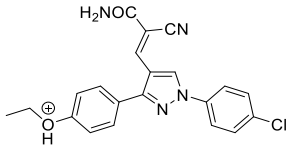 Chemical Formula: $C_{21}H_{18}ClN_4O_2^+$ Exact Mass: 393.1113 Molecular Weight: 393.8505	392.1040	393.1113	**393.1117**
py46	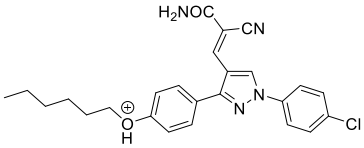 Chemical Formula: $C_{25}H_{26}ClN_4O_2^+$ Exact Mass: 449.1739 Molecular Weight: 449.9585	448.1666	449.1739	**449.1740**
py47	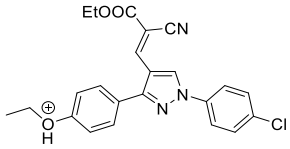 Chemical Formula: $C_{23}H_{21}ClN_3O_3^+$ Exact Mass: 422.1266 Molecular Weight: 422.8885	421.1193	422.1266	**422.1269**
py48	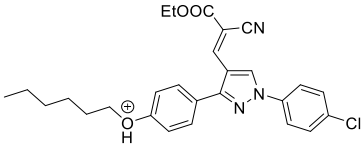 Chemical Formula: $C_{27}H_{29}ClN_3O_3^+$ Exact Mass: 478.1892 Molecular Weight: 478.9965	477.1819	478.1892	**478.1889**
py49	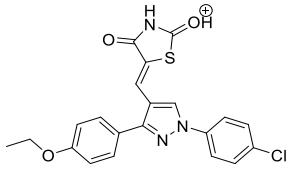 Chemical Formula: $C_{21}H_{17}ClN_3O_3S^+$ Exact Mass: 426.0674 Molecular Weight: 426.8945	425.0601	426.0674	**426.0674**

py50	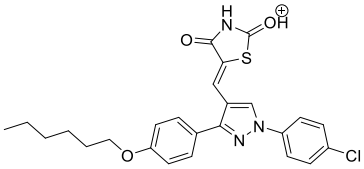 Chemical Formula: $C_{25}H_{25}ClN_3O_3S^+$ Exact Mass: 482.1300 Molecular Weight: 483.0025	481.1227	482.1300	**482.1303**
py51	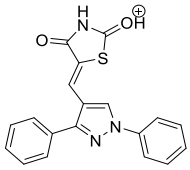 Chemical Formula: $C_{19}H_{14}N_3O_2S^+$ Exact Mass: 348.0801 Molecular Weight: 348.3995	347.0728	348.0801	**348.0803**
py52	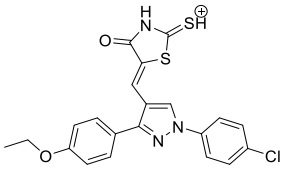 Chemical Formula: $C_{21}H_{17}ClN_3O_2S_2^+$ Exact Mass: 442.0445 Molecular Weight: 442.9555	441.0372	442.0445	**442.0448**
py53	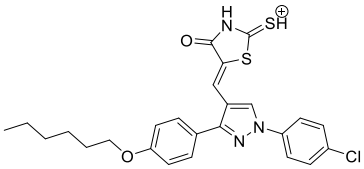 Chemical Formula: $C_{25}H_{25}ClN_3O_2S_2^+$ Exact Mass: 498.1071 Molecular Weight: 499.0635	497.0998	498.1071	**498.1072**
py54	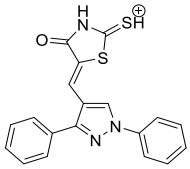 Chemical Formula: $C_{19}H_{14}N_3OS_2^+$ Exact Mass: 364.0573 Molecular Weight: 364.4605	363.0500	364.0573	**364.0579**
py55	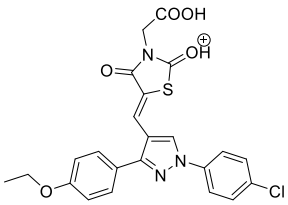 Chemical Formula: $C_{23}H_{19}ClN_3O_5S^+$ Exact Mass: 484.0728 Molecular Weight: 484.9305	483.0656	484.0728	**484.0728**

py56	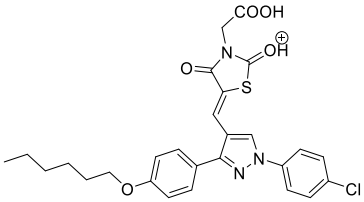 Chemical Formula: $C_{27}H_{27}ClN_3O_5S^+$ Exact Mass: 540.1354 Molecular Weight: 541.0385	539.1282	540.1354	**540.1352**

Table II-3. Calculated F.W., $(MH)^+$ and HPMS of hydrazide derivatives. (Chapter 5)

No.	Hydrazide structures	Calculated F.W.	Calculated (MH)+	Found
zh01	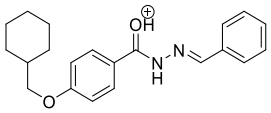 Chemical Formula: $C_{21}H_{25}N_2O_2^+$ Exact Mass: 337.1911 Molecular Weight: 337.4425	336.1383	337.1911	**337.1913**
zh02	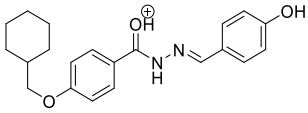 Chemical Formula: $C_{21}H_{25}N_2O_3^+$ Exact Mass: 353.1860 Molecular Weight: 353.4415	352.1787	353.1860	**353.1863**
zh03	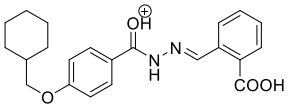 Chemical Formula: $C_{22}H_{25}N_2O_4^+$ Exact Mass: 381.1809 Molecular Weight: 381.4515	380.1736	381.1809	**381.1805**
zh04	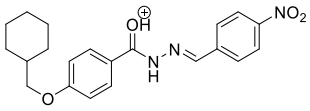 Chemical Formula: $C_{21}H_{24}N_3O_4^+$ Exact Mass: 382.1761 Molecular Weight: 382.4395	381.1689	382.1761	**382.1759**
zh05	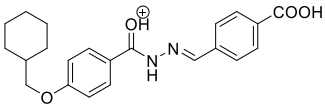 Chemical Formula: $C_{22}H_{25}N_2O_4^+$ Exact Mass: 381.1809 Molecular Weight: 381.4515	380.1736	381.1809	**381.1804**

zh06	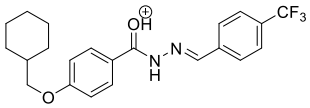 Chemical Formula: $C_{22}H_{24}F_3N_2O_2^+$ Exact Mass: 405.1784 Molecular Weight: 405.4407	404.1712	405.1784	**405.1781**
zh07	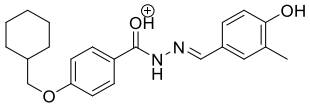 Chemical Formula: $C_{22}H_{27}N_2O_3^+$ Exact Mass: 367.2016 Molecular Weight: 367.4685	366.1943	367.2016	**367.2012**
zh08	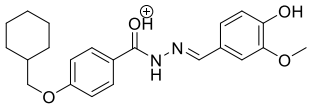 Chemical Formula: $C_{22}H_{27}N_2O_4^+$ Exact Mass: 383.1965 Molecular Weight: 383.4675	382.1893	383.1965	**383.1953**
zh09	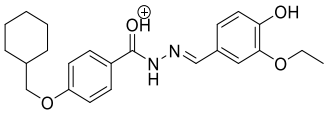 Chemical Formula: $C_{23}H_{29}N_2O_4^+$ Exact Mass: 397.2122 Molecular Weight: 397.4945	396.2046	397.2122	**397.2115**
zh10	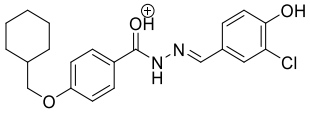 Chemical Formula: $C_{21}H_{24}ClN_2O_3^+$ Exact Mass: 387.1470 Molecular Weight: 387.8835	386.1397	387.1470	**387.1462**
zh11	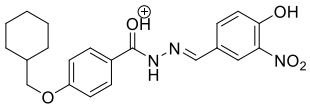 Chemical Formula: $C_{21}H_{24}N_3O_5^+$ Exact Mass: 398.1710 Molecular Weight: 398.4385	397.1638	398.1710	**398.1710**
zh12	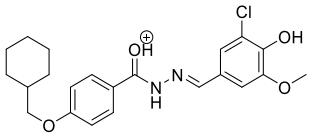 Chemical Formula: $C_{22}H_{26}ClN_2O_4^+$ Exact Mass: 417.1576 Molecular Weight: 417.9095	416.1503	417.1576	**417.1574**
zh13	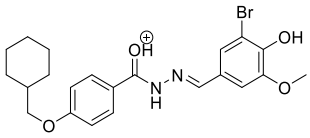 Chemical Formula: $C_{22}H_{26}BrN_2O_4^+$ Exact Mass: 461.1070 Molecular Weight: 462.3635	460.0998	461.1070	**461.1068**

zh14	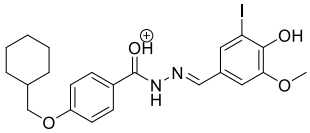 Chemical Formula: $C_{22}H_{26}IN_2O_4^+$ Exact Mass: 509.0932 Molecular Weight: 509.3639	508.0859	509.0932	**509.0928**
zh15	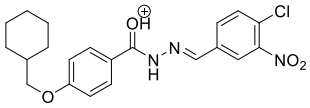 Chemical Formula: $C_{21}H_{23}ClN_3O_4^+$ Exact Mass: 416.1372 Molecular Weight: 416.8815	445.1299	416.1372	**416.1360**
zh16	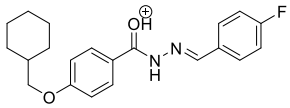 Chemical Formula: $C_{21}H_{24}FN_2O_2^+$ Exact Mass: 355.1816 Molecular Weight: 355.4329	345.1744	355.1816	**355.1816**
zh17	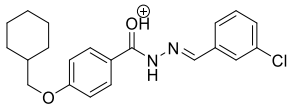 Chemical Formula: $C_{21}H_{24}ClN_2O_2^+$ Exact Mass: 371.1521 Molecular Weight: 371.8845	370.1448	371.1521	**371.1521**
zh18	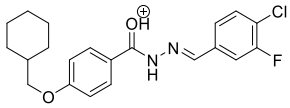 Chemical Formula: $C_{21}H_{23}ClFN_2O_2^+$ Exact Mass: 389.1427 Molecular Weight: 389.8749	388.1354	389.1427	**389.1425**
zh19	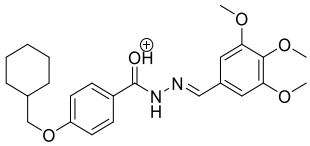 Chemical Formula: $C_{24}H_{31}N_2O_5^+$ Exact Mass: 427.2227 Molecular Weight: 427.5205	426.2155	427.2227	**427.2223**
zh20	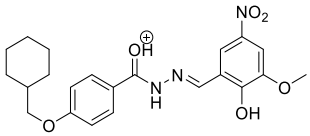 Chemical Formula: $C_{22}H_{26}N_3O_6^+$ Exact Mass: 428.1816 Molecular Weight: 428.4645	427.1743	428.1816	**428.1817**

zh21	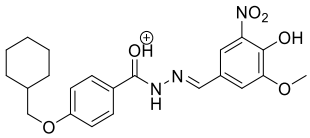 Chemical Formula: $C_{22}H_{26}N_3O_6^+$ Exact Mass: 428.1816 Molecular Weight: 428.4645	427.1743	428.1816	**428.1614**
zh22	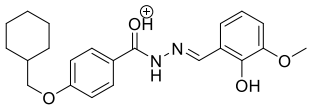 Chemical Formula: $C_{22}H_{27}N_2O_4^+$ Exact Mass: 383.1965 Molecular Weight: 383.4675	382.1893	383.1965	**383.1963**
zh23	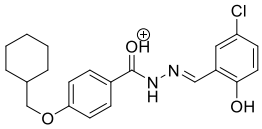 Chemical Formula: $C_{21}H_{24}ClN_2O_3^+$ Exact Mass: 387.1470 Molecular Weight: 387.8835	386.1397	387.1470	**387.1471**
zh24	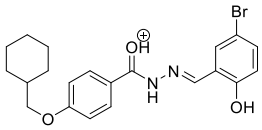 Chemical Formula: $C_{21}H_{24}BrN_2O_3^+$ Exact Mass: 431.0965 Molecular Weight: 432.3375	430.0892	431.0965	**431.0961**
zh25	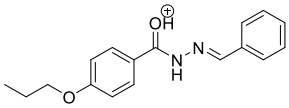 Chemical Formula: $C_{17}H_{19}N_2O_2^+$ Exact Mass: 283.1441 Molecular Weight: 283.3505	282.1368	283.1441	**283.1441**
zh26	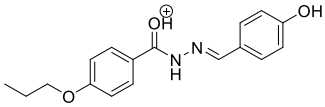 Chemical Formula: $C_{17}H_{19}N_2O_3^+$ Exact Mass: 299.1390 Molecular Weight: 299.3495	298.1317	299.1390	**299.1390**
zh27	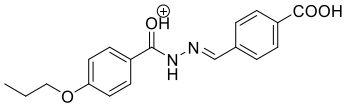 Chemical Formula: $C_{18}H_{19}N_2O_4^+$ Exact Mass: 327.1339 Molecular Weight: 327.3595	326.1267	327.1339	**327.1339**
zh28	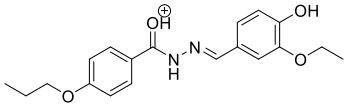 Chemical Formula: $C_{19}H_{23}N_2O_4^+$ Exact Mass: 343.1652 Molecular Weight: 343.4025	342.1580	343.1652	**343.1644**

zh29	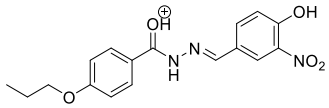 Chemical Formula: $C_{17}H_{18}N_3O_5^+$ Exact Mass: 344.1241 Molecular Weight: 344.3465	343.1168	344.1241	**344.1230**
zh30	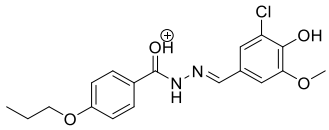 Chemical Formula: $C_{18}H_{20}ClN_2O_4^+$ Exact Mass: 363.1106 Molecular Weight: 363.8175	362.1033	363.1106	**363.1096**
zh31	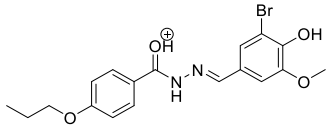 Chemical Formula: $C_{18}H_{20}BrN_2O_4^+$ Exact Mass: 407.0601 Molecular Weight: 408.2715	406.0528	407.0601	**407.0584**
zh32	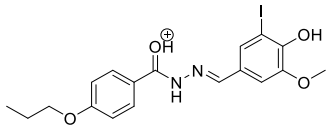 Chemical Formula: $C_{18}H_{20}IN_2O_4^+$ Exact Mass: 455.0462 Molecular Weight: 455.2719	454.0390	455.0462	**455.0451**
zh33	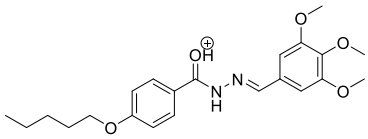 Chemical Formula: $C_{22}H_{29}N_2O_5^+$ Exact Mass: 401.2071 Molecular Weight: 401.4825	400.1998	401.2071	**401.2068**
zh34	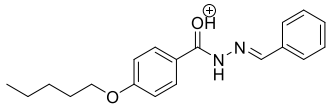 Chemical Formula: $C_{19}H_{23}N_2O_2^+$ Exact Mass: 311.1754 Molecular Weight: 311.4045	310.1681	311.1754	**311.1745**
zh35	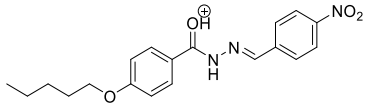 Chemical Formula: $C_{19}H_{22}N_3O_4^+$ Exact Mass: 356.1605 Molecular Weight: 356.4015	355.1532	356.1605	**356.1596**
zh36	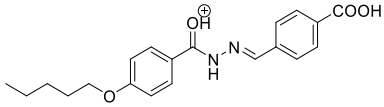 Chemical Formula: $C_{20}H_{23}N_2O_4^+$ Exact Mass: 355.1652 Molecular Weight: 355.4135	354.1580	355.1652	**355.1655**

zh37	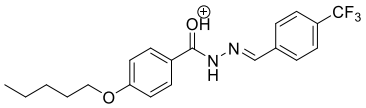 Chemical Formula: $C_{20}H_{22}F_3N_2O_2^+$ Exact Mass: 379.1628 Molecular Weight: 379.4027	378.1555	379.1628	**379.1623**
zh38	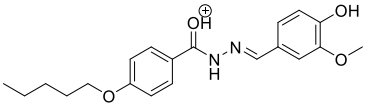 Chemical Formula: $C_{20}H_{25}N_2O_4^+$ Exact Mass: 357.1809 Molecular Weight: 357.4295	356.1736	357.1809	**357.1811**
zh39	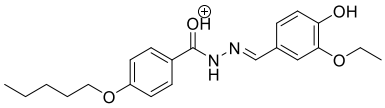 Chemical Formula: $C_{21}H_{27}N_2O_4^+$ Exact Mass: 371.1965 Molecular Weight: 371.4565	370.1893	371.1965	**371.1965**
zh40	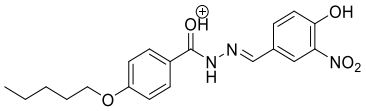 Chemical Formula: $C_{19}H_{22}N_3O_5^+$ Exact Mass: 372.1554 Molecular Weight: 372.4005	371.1481	372.1554	**372.1553**
zh41	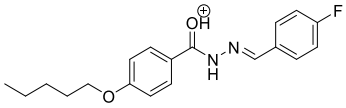 Chemical Formula: $C_{19}H_{22}FN_2O_2^+$ Exact Mass: 329.1660 Molecular Weight: 329.3949	328.1587	329.1660	**329.1656**
zh42	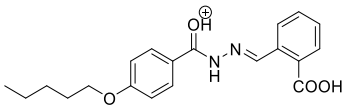 Chemical Formula: $C_{20}H_{23}N_2O_4^+$ Exact Mass: 355.1652 Molecular Weight: 355.4135	354.1580	355.1652	**355.1654**
zh43	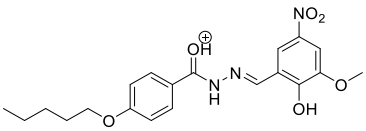 Chemical Formula: $C_{20}H_{24}N_3O_6^+$ Exact Mass: 402.1660 Molecular Weight: 402.4265	401.1587	402.1660	**402.1655**
zh44	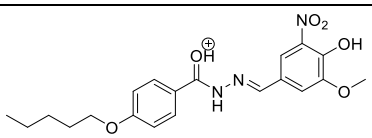 Chemical Formula: $C_{20}H_{24}N_3O_6^+$ Exact Mass: 402.1660 Molecular Weight: 402.4265	401.1587	402.1660	**402.1655**

zh45	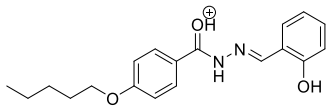 Chemical Formula: $C_{19}H_{23}N_2O_3^+$ Exact Mass: 327.1703 Molecular Weight: 327.4035	326.1630	327.1703	**327.1701**
zh46	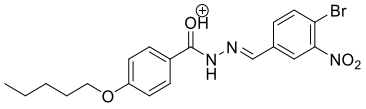 Chemical Formula: $C_{19}H_{21}BrN_3O_4^+$ Exact Mass: 434.0710 Molecular Weight: 435.2975	433.0637	434.0710	**434.0704**
zh47	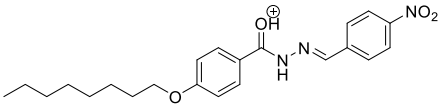 Chemical Formula: $C_{22}H_{28}N_3O_4^+$ Exact Mass: 398.2074 Molecular Weight: 398.4825	397.2002	398.2074	**398.2070**
zh48	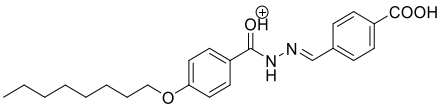 Chemical Formula: $C_{23}H_{29}N_2O_4^+$ Exact Mass: 397.2122 Molecular Weight: 397.4945	396.2049	397.2122	**397.2123**
zh49	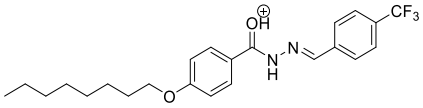 Chemical Formula: $C_{23}H_{28}F_3N_2O_2^+$ Exact Mass: 421.2097 Molecular Weight: 421.4837	420.2025	421.2097	**421.2095**
zh50	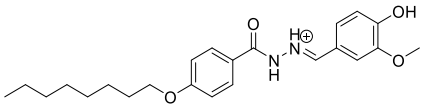 Chemical Formula: $C_{23}H_{31}N_2O_4^+$ Exact Mass: 399.2278 Molecular Weight: 399.5105	398.2206	399.2278	**399.2274**
zh51	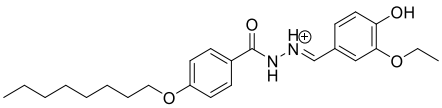 Chemical Formula: $C_{24}H_{33}N_2O_4^+$ Exact Mass: 413.2435 Molecular Weight: 413.5375	412.2362	413.2435	**413.2436**
zh52	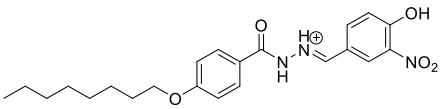 Chemical Formula: $C_{22}H_{28}N_3O_5^+$ Exact Mass: 414.2023 Molecular Weight: 414.4815	413.1951	414.2023	**414.2023**

zh53	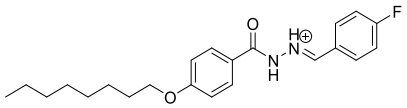 Chemical Formula: $C_{22}H_{28}FN_2O_2^+$ Exact Mass: 371.2129 Molecular Weight: 371.4759	370.2057	371.2129	**371.2130**
zh54	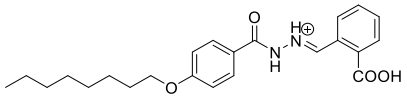 Chemical Formula: $C_{23}H_{29}N_2O_4^+$ Exact Mass: 397.2122 Molecular Weight: 397.4945	396.2049	397.2122	**397.2121**
zh55	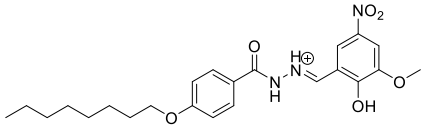 Chemical Formula: $C_{23}H_{30}N_3O_6^+$ Exact Mass: 444.2129 Molecular Weight: 444.5075	443.2056	444.2129	**444.2130**
zh56	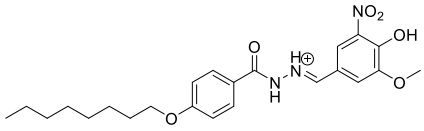 Chemical Formula: $C_{23}H_{30}N_3O_6^+$ Exact Mass: 444.2129 Molecular Weight: 444.5075	443.2056	444.2129	**444.2130**
zh57	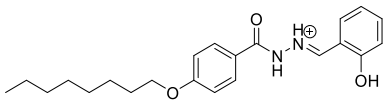 Chemical Formula: $C_{22}H_{29}N_2O_3^+$ Exact Mass: 369.2173 Molecular Weight: 369.4845	368.2100	369.2173	**369.2178**
zh58	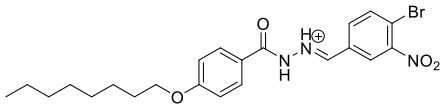 Chemical Formula: $C_{22}H_{27}BrN_3O_4^+$ Exact Mass: 476.1179 Molecular Weight: 477.3785	475.1107	476.1179	**476.1194**
zh59	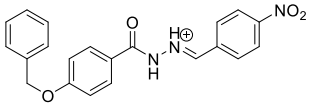 Chemical Formula: $C_{21}H_{18}N_3O_4^+$ Exact Mass: 376.1292 Molecular Weight: 376.3915	375.1219	376.1292	**376.1300**
zh60	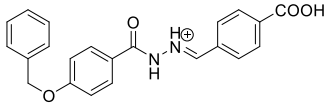 Chemical Formula: $C_{22}H_{19}N_2O_4^+$ Exact Mass: 375.1339 Molecular Weight: 375.4035	374.1267	375.1339	**375.1348**

zh61	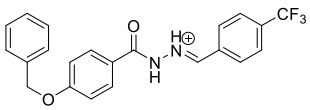 Chemical Formula: $C_{22}H_{18}F_3N_2O_2^+$ Exact Mass: 399.1315 Molecular Weight: 399.3927	398.1242	399.1315	**399.1518**
zh62	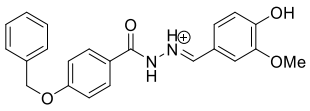 Chemical Formula: $C_{22}H_{21}N_2O_4^+$ Exact Mass: 377.1496 Molecular Weight: 377.4195	376.1423	377.1496	**377.1496**
zh63	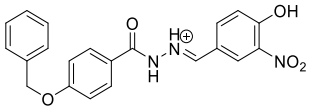 Chemical Formula: $C_{21}H_{18}N_3O_5^+$ Exact Mass: 392.1241 Molecular Weight: 392.3905	391.1168	392.1241	**392.1238**
zh64	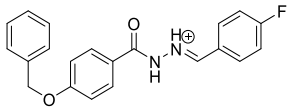 Chemical Formula: $C_{21}H_{18}FN_2O_2^+$ Exact Mass: 349.1347 Molecular Weight: 349.3849	348.1274	349.1347	**349.1344**
zh65	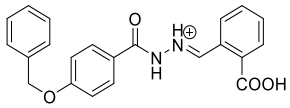 Chemical Formula: $C_{22}H_{19}N_2O_4^+$ Exact Mass: 375.1339 Molecular Weight: 375.4035	374.1267	375.1339	**375.1339**
zh66	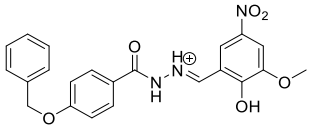 Chemical Formula: $C_{22}H_{20}N_3O_6^+$ Exact Mass: 422.1347 Molecular Weight: 422.4165	421.1274	422.1347	**422.1346**
zh67	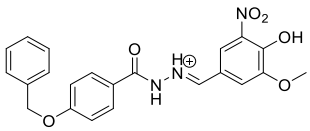 Chemical Formula: $C_{22}H_{20}N_3O_6^+$ Exact Mass: 422.1347 Molecular Weight: 422.4165	421.1274	422.1347	**422.1346**
zh68	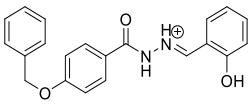 Chemical Formula: $C_{21}H_{19}N_2O_3^+$ Exact Mass: 347.1390 Molecular Weight: 347.3935	346.1317	347.1390	**347.1394**

zh69	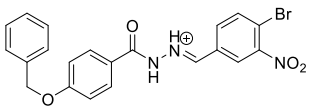 Chemical Formula: $C_{21}H_{17}BrN_3O_4^+$ Exact Mass: 454.0397 Molecular Weight: 455.2875	453.0324	454.0397	**454.0394**
zh70	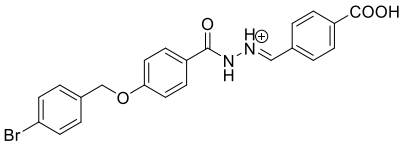 Chemical Formula: $C_{22}H_{18}BrN_2O_4^+$ Exact Mass: 453.0444 Molecular Weight: 454.2995	452.0372	453.0444	**453.0442**
zh71	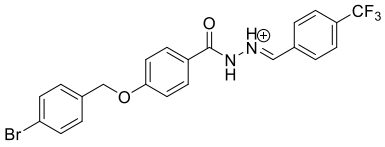 Chemical Formula: $C_{22}H_{17}BrF_3N_2O_2^+$ Exact Mass: 477.0420 Molecular Weight: 478.2887	476.0347	477.0420	**477.0428**
zh72	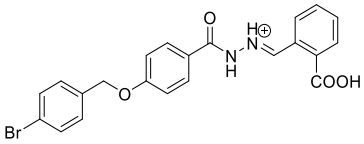 Chemical Formula: $C_{22}H_{18}BrN_2O_4^+$ Exact Mass: 453.0444 Molecular Weight: 454.2995	452.0372	453.0444	**453.0463**
zh73	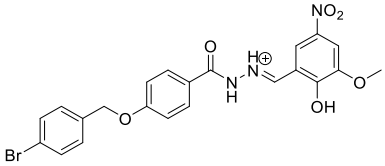 Chemical Formula: $C_{22}H_{19}BrN_3O_6^+$ Exact Mass: 500.0452 Molecular Weight: 501.3125	499.0379	500.0452	**500.0466**
zh74	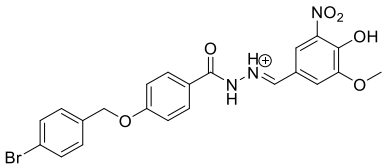 Chemical Formula: $C_{22}H_{19}BrN_3O_6^+$ Exact Mass: 500.0452 Molecular Weight: 501.3125	499.0379	500.0452	**500.0472**
zh75	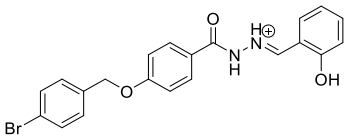 Chemical Formula: $C_{21}H_{18}BrN_2O_3^+$ Exact Mass: 425.0495 Molecular Weight: 426.2895	424.0423	425.0495	**425.0509**

zh76	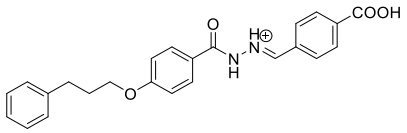 Chemical Formula: $C_{24}H_{23}N_2O_4^+$ Exact Mass: 403.1652 Molecular Weight: 403.4575	402.1580	403.1652	**403.1657**
zh77	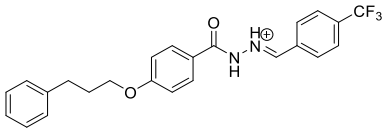 Chemical Formula: $C_{24}H_{22}F_3N_2O_2^+$ Exact Mass: 427.1628 Molecular Weight: 427.4467	426.1555	427.1628	**427.1637**
zh78	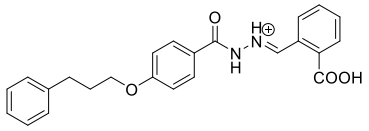 Chemical Formula: $C_{24}H_{23}N_2O_4^+$ Exact Mass: 403.1652 Molecular Weight: 403.4575	402.1580	403.1652	**403.1659**
zh79	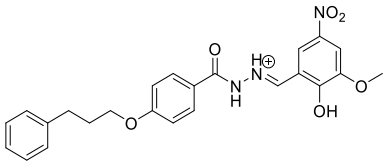 Chemical Formula: $C_{24}H_{24}N_3O_6^+$ Exact Mass: 450.1660 Molecular Weight: 450.4705	449.1587	450.1660	**450.1673**
zh80	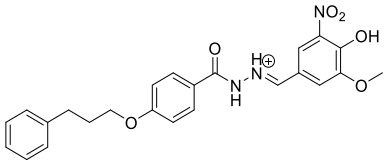 Chemical Formula: $C_{24}H_{24}N_3O_6^+$ Exact Mass: 450.1660 Molecular Weight: 450.4705	449.1587	450.1660	**450.1670**
zh81	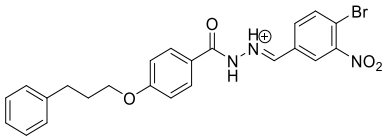 Chemical Formula: $C_{23}H_{21}BrN_3O_4^+$ Exact Mass: 482.0710 Molecular Weight: 483.3415	481.0637	482.0710	**482.0707**
zh82	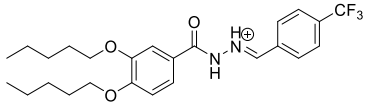 Chemical Formula: $C_{25}H_{32}F_3N_2O_3^+$ Exact Mass: 465.2360 Molecular Weight: 465.5367	464.2287	465.2360	**465.2360**

zh83	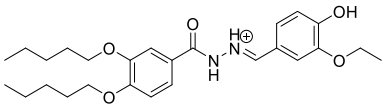 Chemical Formula: $C_{26}H_{37}N_2O_5^+$ Exact Mass: 457.2697 Molecular Weight: 457.5905	456.2624	457.2697	**457.2700**
zh84	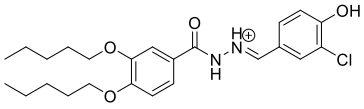 Chemical Formula: $C_{24}H_{32}ClN_2O_4^+$ Exact Mass: 447.2045 Molecular Weight: 447.9795	446.1972	447.2045	**447.2046**
zh85	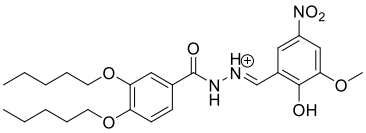 Chemical Formula: $C_{25}H_{34}N_3O_7^+$ Exact Mass: 488.2391 Molecular Weight: 488.5605	487.2319	488.2391	**604.2069**
zh86	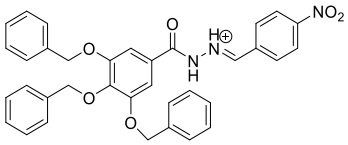 Chemical Formula: $C_{35}H_{30}N_3O_6^+$ Exact Mass: 588.2129 Molecular Weight: 588.6395	587.2056	588.2129	**604.2077**
zh87	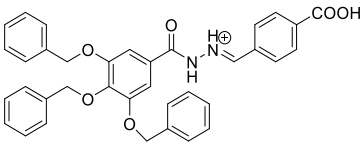 Chemical Formula: $C_{36}H_{31}N_2O_6^+$ Exact Mass: 587.2177 Molecular Weight: 587.6515	586.2104	587.2177	**587.2176**
zh88	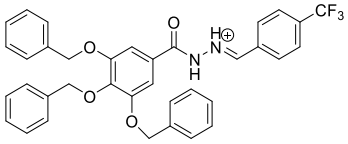 Chemical Formula: $C_{36}H_{30}F_3N_2O_4^+$ Exact Mass: 611.2152 Molecular Weight: 611.6407	610.2079	611.2152	**611.2150**
zh89	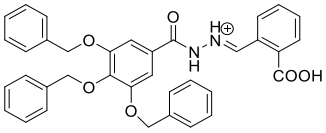 Chemical Formula: $C_{36}H_{31}N_2O_6^+$ Exact Mass: 587.2177 Molecular Weight: 587.6515	586.2104	587.2177	**587.2178**

zh90	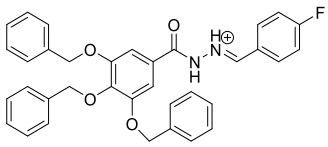 Chemical Formula: $C_{35}H_{30}FN_2O_4^+$ Exact Mass: 561.2184 Molecular Weight: 561.6329	560.2111	561.2184	**561.2184**
zh91	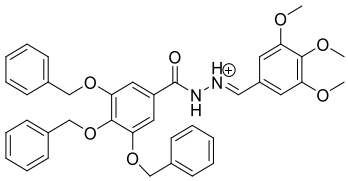 Chemical Formula: $C_{38}H_{37}N_2O_7^+$ Exact Mass: 633.2595 Molecular Weight: 633.7205	632.2523	633.2595	**633.2590**

Vita

Ziyuan Zhou

Education

Doctor of Philosophy (Candidate) in Pharmaceutical Sciences 2013-2017

College of Pharmacy, University of Kentucky Lexington, KY, USA

Master of Science in Pesticide Sciences 2011-2013

College of Science, China Agricultural University (中国农业大学) Beijing, China

Bachelor of Science in Applied Chemistry 2007-2011

Department of Chemistry, Zhengzhou University (郑州大学) Zhengzhou, China

Certificate & Graduate Certificates

National Computer Ranking Examination Certificate – Grade 2 in Visual Basic 2010

Graduate Certificate in Applied Statistics, Department of Statistics, College of Art and Sciences, University of Kentucky - Lexington, KY, USA 2016

Graduate Certificate in Biostatistics, Department of Biostatistics, College of Public Health, University of Kentucky - Lexington, KY, USA 2017

Professionals

Research Assistant, College of Pharmacy, University of Kentucky, KY (2013 - 2017)

Memberships

American Chemical Society (ACS) (2017-Now)

American Association of Pharmaceutical Scientists (AAPS) (2014-Now)

Travel Supports and Conference Abstracts

2017 – Travel Support, University of Kentucky, College of Pharmacy. Abstracts: "Computational Design, Synthesis and Characterization of Novel mPGES-1 Inhibitors" &

"Clinical Potential of a Cocaine Hydrolase for Drug Overdose: A study of Gender Differences" Drug Discovery and Development Colloquium (DDDC) 2017, Little Rock, Arkansas

2017 – Travel Support, University of Kentucky, Graduate School and College of Pharmacy. Abstract: "Computational Design, Synthesis and Characterization of Novel mPGES-1 Inhibitors" 253rd ACS national meeting, 2017, San Francisco, California

2015 – Travel Support, University of Kentucky, Graduate School and College of Pharmacy. Abstract: "Design and synthesis hydrazide derivatives as a novel structure class of selective human mPGES-1 inhibitors" AAPS 2015, Orlando, Florida

2014 – Travel Support, University of Kentucky, Graduate School and College of Pharmacy. Abstract: "Design and synthesis 1, 3-Diphenylpyrazole derivatives as human mPGES-1 inhibitors" AAPS 2014, San Diego, California

Publications

2017

Ziyuan Zhou, Yaxia Yuan, Shuo Zhou, Kai Ding, Fang Zheng, and Chang-Guo Zhan* "Selective Inhibitors of Human mPGES-1 from Structure-Based Computational Screening", *Bioorg. Med. Chem. Lett.* 27 (2017): 3739-3743.

Wang, Xiachang, Yinan Zhang, Larissa V. Ponomareva, Qingchao Qiu, Ryan Woodcock, Sherif I. Elshahawi, Xiabin Chen, **Ziyuan Zhou**, Bruce E. Hatcher, James C. Hower, Chang-Guo Zhan, Sean Parkin, Madan K. Kharel, S. Randal Voss, Khaled A. Shaaban and Jon S. Thorson* "Mccrearamycins a-D, Geldanamycin-Derived Cyclopentenone Macrolactams from an Eastern Kentucky Abandoned Coal Mine Microbe", *Angew. Chem., Int. Ed.* 56 (2017): 2994-2998.

Chen Xiabin, Xirong Zheng, Kai Ding, **Ziyuan Zhou**, Chang-Guo Zhan* and Fang Zheng. "A Quantitative LC-MS/MS Method for Simultaneous Determination of Cocaine and Its Metabolites in Whole Blood", *J. Pharm. Biomed. Anal.* 134, (2017): 243-251.

Zhou Shuo, **Ziyuan Zhou**, Yaxia Yuan and Chang-Guo Zhan* "Novel mPGES-1 Inhibitors Identified from Structure-Based Virtual Screening Based on New Acting Mechanism", 253rd ACS National Meeting & Exposition, San Francisco, CA, United States, April 2017, MEDI-179.

Ziyuan Zhou, Kai Ding, Shuo Zhou, Yaxia Yuan, Fang Zheng and Chang-Guo Zhan* "Computational Design, Synthesis and Characterization of Novel mPGES-1 Inhibitors", 253rd ACS National Meeting & Exposition, San Francisco, CA, United States, April, 2017, MEDI-260.

Ding, Kai, **Ziyuan Zhou**, Yaxia Yuan, Fang Zheng and Chang-Guo Zhan* "Rational Design, Synthesis, and in Vitro Evaluation of mPGES-1 Inhibitors as Next-Generation of Anti-Inflammatory Drugs", 253rd ACS National Meeting & Exposition, San Francisco, CA, United States, April 2017, MEDI-104.

Ting Zhang, Xirong Zheng, **Ziyuan Zhou**, Xiabin Chen, Fang Zheng and Chang-Guo Zhan* "Clinical Potential of an Enzyme-based Novel Therapy for Drug Overdose", *Scientific Report*, submitted (in revision).

Kai Ding#, **Ziyuan Zhou#**, Shuo Zhou, Shurong Hou, Yaxia Yuan, Shuo Zhou, Xirong Zheng, Charles Loftin, Fang Zheng, and Chang-Guo Zhan* "Design, Synthesis and Evaluation of Benzylidenebarbituric Acid Derivatives as Potent and Selective Inhibitors against Both Human and Mouse mPGES-1", in preparation (# Co-first authors)

Ziyuan Zhou, Kai Ding, Yaxia Yuan, Shuo Zhou, Shurong Hou, Yao Chen, Fang Zheng, and Chang-Guo Zhan* "Design, synthesis and characterization of hydrazide derivatives as a novel class of selective human mPGES-1 inhibitors", in preparation.

Ziyuan Zhou, Shuo Zhou, Kai Ding, Yaxia Yuan, Shurong Hou, Fang Zheng and Chang-Guo Zhan* "Synthesis and SAR of 2-cyano-3-phenylacrylic acid derivatives as human and mouse mPGES-1 dual inhibitors", in preparation.

Xirong Zheng#, **Ziyuan Zhou#**, Ting Zhang, Zhengyu Jin, Xiabin Chen, Jing Deng, Fang Zheng and Chang-Guo Zhan* "Clinical Potential of a Cocaine Hydrolase for Drug Overdose: A study of Gender Differences", in preparation (# Co-first authors)

Ziyuan Zhou#, Kai Ding#, Shuo Zhou, Yaxia Yuan, Shurong Hou, Kyungbo Kim, Fang Zheng and Chang-Guo Zhan* "5-(1,3-diphenyl-1H-pyrazol-4-yl) methylene) pyrimidine- 2,4,6 (1H,3H,5H) - trione and related derivatives as novel inhibitors against human and mouse mPGES-1 enzymes", in preparation (# Co-first authors)

2016

Chen, Xiabin, Xirong Zheng, Max Zhan, **Ziyuan Zhou**, Chang-Guo Zhan* and Fang Zheng. "Metabolic Enzymes of Cocaine Metabolite Benzoylecgonine", *ACS Chem. Biol.* 11 (2016): 2186-2194.

Chen, Xiabin, Xirong Zheng, **Ziyuan Zhou**, Chang-Guo Zhan* and Fang Zheng. "Effects of a Cocaine Hydrolase Engineered from Human Butyrylcholinesterase on Metabolic Profile of Cocaine in Rats", *Chem Biol Interact* 259 (2016): 104-109.

Li, Yue, Fangfang Li, Yanyan Zhu, Xue Li, **Ziyuan Zhou**, Chunmei Liu, Wenjing Zhang and Mingsheng Tang* "DFT Study on Reaction Mechanisms of Cyclic Dipeptide Generation", *Struct. Chem.* 27 (2016): 1165-1173

Before 2016

Yuan, Xiaoyong, Lu Zhang, Xiaoqiang Han, **Ziyuan Zhou**, Shijie Du, Chuan Wan, Dongyan Yang and Zhaohai Qin* "Synthesis and Fungicidal Activity of the Strobilurins Containing 1,3,4-Thiodiazole Ring", *Youji Huaxue* 34 (2014): 170-177.

Han, Xiaoqiang, **Ziyuan Zhou**, Chuan Wan, Yumei Xiao and Zhaohai Qin* "Co(Acac)2-Catalyzed Allylic and Benzylic Oxidation by Tert-Butyl Hydroperoxide", *Synthesis* 45 (2013): 615-620.

Qin, Zhaohai*, Yongqiang Ma, Yihui Zhou, Yong Xu, Changqing Jia, **Ziyuan Zhou** and Dongyan Yang. "Process for Synthesis of Nitroaminoguanidine Derivative", CN 102863360 A. 2013.